Specific Calcium and Abscisic Acid Regulation of Anion Channels in *Arabidopsis* Guard Cells

Dissertation

der Mathematisch-Naturwissenschaftlichen Fakultät

der Eberhard Karls Universität Tübingen

zur Erlangung des Grades eines

Doktors der Naturwissenschaften

(Dr. rer. nat.)

vorgelegt von

Benjamin Brandt

aus Würzburg

Tübingen

2014

Gedruckt mit Genehmigung der Mathematisch-Naturwissenschaftlichen Fakultät der Eberhard Karls Universität Tübingen

Tag der mündlichen Qualifikation: 07.10.2014

Dekan: Prof. Dr. Prof. Dr. Wolfgang Rosenstiel

1. Berichterstatter Prof. Dr. Klaus Harter

2. Berichterstatter Prof. Dr. Julian I. Schroeder, University of California, San Diego, USA

3. Berichterstatter Prof. Dr. Stephan Clemens, Universität Bayreuth

Danksagung:

Im Folgenden will ich den Personen danken, die durch Ihre Unterstützung diese Arbeit erst möglich gemacht haben:

Prof. Julian I. Schroeder für die interessante Themenstellung, Möglichkeit in seinem Labor meine Forschung zu betreiben, lehrreiche and anspruchsvolle Aufgaben, und seine Hilfe in vielen Dingen.

Prof. Klaus Harter für die Bereitschaft sich als Betreuer meiner Doktorarbeit zur Verfügung zu stellen und seine Unterstützung in vielen organisatorischen Angelegenheiten.

Den Studenten Dennis Brodsky, Desiree Nguyen, Thomas Belknap, and Taiming Yong. für eine tolle Zusammenarbeit und Ihre Hilfe in allen Projekten.

Dem ganzen Schroeder Labor, vor allem Shintaro Munemasa, Fernando Aleman, Rainer Waadt, Hans-Henning Kunz, Feliz Hauser, and Aaron Stephan für die hervorragende Zusammenarbeit und auch die Stunden neben der Arbeit.

Meiner Familie, Freunden, und Freundin, die mich immer unterstützten und einen sehr großen Anteil an dieser Arbeit haben.

Erklärung

Hiermit erkläre ich, dass ich die vorliegende Dissertation selbständig angefertigt habe. Es wurden nur die in der Arbeit ausdrücklich benannten Quellen und Hilfsmittel benutzt. Wörtlich oder sinngemäß übernommenes Gedankengut habe ich als solches kenntlich gemacht.

Ort, Datum

Unterschrift

1 Summary/Zusammenfassung

Knowledge of the molecular mechanisms mediating responses of plants to drought conditions are of highest significance in times of a rapidly growing world population accompanied with an increasingly scarce supply of fresh water. Plant guard cells represent a single cell type controlling evaporative water loss and uptake of CO_2 and are subject to intensive research. The plant hormone abscisic acid (ABA) accumulates in leaves during drought stress and leads to stomatal closure, representing a crucial protective mechanism to prevent excessive water loss. Within the last >15 years many aspects and proteins involved in this ABA-dependent closing mechanism have been determined resulting in guard cells being a model cell type for signal transduction research in plants. The gene for the S-type anion channel, *SLAC1*, of which activation is an essential step in fast stomatal closure, has been identified. Several proteins are phosphorylating and activating SLAC1 with free cytosolic Ca^{2+} playing an important role here. This activation is inhibited by protein phosphatases. In the presence of ABA these phosphatase are negatively regulated mediated by ABA-receptor proteins. However, many mechanistic details are still unknown. For example, whether the above mentioned protein components are sufficient for a functional reconstitution of the signal transduction pathway is not known. Moreover, the mechanism explaining how Ca^{2+}-signaling specificity is achieved and how Ca^{2+}-dependent and Ca^{2+}-independent signaling branches are functionally linked is still unclear.

In this work, besides the calcium dependent protein kinases (CPKs) already known to be involved in guard cell S-type anion activation mediated by SLAC1, two novel CPKs, CPK5 and CPK6, were identified to activate SLAC1. A quadruple knock out mutant including CPK5 and CPK6 was established and patch clamp analysis revealed that ABA- and Ca^{2+}-dependent S-type anion current activation is abrogated in this mutant. Several aspects of CPK6-mediated SLAC1 activation, including identification of the phosphorylated residue responsible for the activation, kinase and channel phosphorylation affinities, the Ca^{2+}-dependency of CPK6 activity, the regulatory role of PP2C phosphatases, and the functional reconstitution of the entire signal transduction pathway are presented. Furthermore, biochemical, genetic, and cell biology tools were used to reveal the molecular mechanism of how specificity in Ca^{2+}- and ABA-dependent signal transduction mediated by PP2C phosphatases is achieved. Also, the presented results suggest that the functional dependence of Ca^{2+}-dependent and Ca^{2+}-independent ABA signaling branches is due to differential phosphorylation of SLAC1, synergistically integrating these two branches of ABA signal transduction. These results help to understand the tight control of ABA-dependent stomatal closure, a mechanism essential for plant survival during drought conditions.

In Zeiten einer stark wachsenden Weltbevölkerung bei gleichzeitiger Süswasserknappheit, ist das Verständnis von Mechanismen die erklären, wie Pflanzen sich vor Austrocknung schützen, von höchstem Interesse. Pflanzliche Schließzellen, welche Spaltöffnungen umschließen, sind verantwortlich für die Regulation der Aufnahme von CO_2 bei gleichzeitigem Verlust von Wasser und werden deshalb intensiv erforscht. Unter Trockenstress reichert sich das Pflanzenhormon Abscisinsäure (ABA) in Blättern an und führt zu dem Schluss der Spaltöffnung, um Pflanzung vor übermäßigen Verlust von Wasser zu schützen. Innerhalb der letzten >15 Jahre wurden viele Aspekte und Proteine, die eine wichtige Rolle im ABA-induzierten Schluss der Spaltöffnung spielen, identifiziert, weshalb sich Schließzellen zu einem Modellzelltyp für pflanzliche Signaltransduktionsforschung entwickelten. Das Gen des S-typ Anionkanals, *SLAC1*, der eine sehr wichtige Rolle im schnellen Schluss der Stomata spielt, wurde identifiziert. SLAC1 wird von mehreren Kinase phosphoryliert und aktiviert. Zytosolische Kalziumerhöhungen sind während dieser Aktivierung sehr wichtig. Diese Aktivierung wiederum wird negativ durch Protein Phosphatasen reguliert, welche durch ABA, in Kombination mit ABA Rezeptorproteinen, inhibiert werden. Viele mechanistische Details sind aber bis heute aber noch nicht verstanden. Der Mechanismus, wie spezifische Antworten auf eine zytosolische Kalziumerhöhung erreicht werden, ist noch nicht bekannt. Außerdem ist noch unklar, wie der Ca^{2+}-abhängige und der Ca^{2+}-unabhängigen Zweig der S-typ Anionenkanal Aktivierung interagieren.

Neben den schon bekannten Kalzium abhängigen Proteinkinasen (CPKs), wird in dieser Arbeit gezeigt, dass zwei weitere CPKs, CPK5 und CPK6, SLAC1 aktivieren und phosphorylieren. Patch clamp Experimente einer vierfach Mutante, in der die Transkription von vier CPKs, einschließlich CPK5 und CPK6, verhindert ist, zeigt dass ABA und Ca^{2+} Applikation nicht mehr zu der Aktivierung von S-Typ Anionenkanälen führt. Mechanistische details der CPK Aktivierung von SLAC1 einschließlich der Identifikation einer funktionell wichtigen phosphorylierten Aminosäure, die Affinität der Phosphorylierung von SLAC1 durch mehrere Kinasen, die Ca^{2+}-Abhängigkeit der CPK6 Aktivität, die regulatorische Funktion der Protein Phosphatasen, und eine Rekonstitution des gesamten ABA Signaltransduktionswegs werden in dieser Arbeit präsentiert. Unter Berücksichtigung dieser Resultate und unter Benutzung biochemischer, zellbiologischer und genetischer Methoden konnte ein Mechanismus gefunden werden, der erklärt wie zytosolische Ca^{2+} Erhöhungen zu einer spezifischen Antwort innerhalb des ABA-abhängigen Schlusses der Spaltöffnung führen. Außerdem deuten Ergebnisse darauf hin, dass die Interaktion der Ca^{2+}-abhängigen und -unabhängigen S-Typ Anionenkanal Aktivierung darauf beruht, dass SLAC1 differentiell von Kinasen dieser Zweige phosphoryliert und synergistisch aktiviert wird.

2 List of publications/Liste der Publikationen

Accepted publications/Akzeptierte Publikationen:

Hubbard, K. E., R. S.Siegel, G.Valerio, **B. Brandt** and J. I. Schroeder (2012). "Abscisic acid and CO_2 signalling via calcium sensitivity priming in guard cells, new CDPK mutant phenotypes and a method for improved resolution of stomatal stimulus–response analyses." Annals of Botany **109**(1): 5-17.

Contribution/Eigenanteil: 10%

Brandt, B., D. E. Brodsky, S. Xue, J. Negi, K. Iba, J. Kangasjärvi, M. Ghassemian, A. B. Stephan, H. Hu and J. I. Schroeder. (2012). "Reconstitution of abscisic acid activation of SLAC1 anion channel by CPK6 and OST1 kinases and branched ABI1 PP2C phosphatase action." Proceedings of the National Academy of Sciences **109**(26): 10593-10598.

Contribution/Eigenanteil: 55%

Laanemets, K., **B. Brandt**, J. Li, E. Merilo, Y.-F. Wang, M. M. Keshwani, S. S. Taylor, H. Kollist and J. I. Schroeder (2013). "Calcium-Dependent and -Independent Stomatal Signaling Network and Compensatory Feedback Control of Stomatal Opening via Ca^{2+} Sensitivity Priming." Plant Physiology.

Contribution/Eigenanteil: 30%

Submitted publications/Eingereichte Publikationen:

Brandt, B., S. Munemasa, C. Wang, D. Nguyen, T. Belknap, F. Aleman, J. I. Schroeder (2014). “Calcium Specificity Mechanism within ABA-dependent Signal Transduction in *Arabidopsis thaliana*.” submitted

Contribution/Eigenanteil: 60%

Waadt, R., B. Manalansan, N. Rauniyar, C. Waadt, D.A. Nusinow, S. Munemasa, **B. Brandt**, S. A. Kay, H. H. Kunz, A. Delong, J. R. Yates, J. I. Schroeder, “Identification of OST1-interacting proteins reveals SnRK2-type protein kinase homo- and heterodimerisation and interactions with PP2A-type phosphatases.” Submitted

(not discussed in this work)

Contribution/Eigenanteil: 10%

3 Introduction

3.1 Water as a limiting factor of crop production

The world's population is estimated to grow up to 9.6 billion people in 2050 and by then the world's food production is estimated to be required to increase up to 60% to feed the world population (Undesa, 2012, FAO, 2012) but already presently for around 870 million people food availability is limited resulting in undernourishment (FAO, 2013). Worldwide, agriculture uses more than 70% of fresh water with more than 90% in the least developed countries, even though agriculture occupies only 11% of the land surface (FAO, 2011).The global water consumption of agriculture is estimated to increase by ~20% by 2050 given that no improvements are made (WWAP, 2012). Many regions of the world are already facing severe drought conditions and global warming is predicted to further decrease the supply of fresh water (IPCC 2008). Understanding the mechanisms of how plants utilize water and how plants adapt to drought conditions will contribute to securing world nutrition. Plants lose between 70-90% of their water through macroscopic pores called stomata which are introduced in the next chapter. To understand the regulation of the aperture of this pore accompanied by water loss might help to improve plants to prevent excessive water loss and thus be more resistant to conditions with limited water availability.

3.2 Guard cells as "gate keepers" regulating water loss and CO_2 uptake

3.2.1 Occurrence and Anatomy

In the mesophyll of plant leaves, the majority of photosynthetic fixation of atmospheric CO_2, or the conversion of light energy into chemical energy, takes place. This stored chemical energy can be used for all crucial processes in plants and represents the major mechanism for biomass production. The adaxial and abaxial waxy layer on the leaf surfaces known as cuticle renders leaf surfaces almost impenetrable for gases (Boyer et al., 1997). To enable the uptake of atmospheric CO_2 into the leaf to be used for photosynthesis, plants possess specialized cells termed guard cells. Guard cells can be found on all aerial parts of plants but mostly accumulate in the abaxial epidermis of leaves. One pair of guard cells form a pore called stoma which represents an opening connecting the atmosphere with the intercellular space of the spongy mesophyll in leaves (Figure 1). Open stomata and CO_2 uptake leads to evaporation of water which drives translocation of xylem sap supplemented

with macro and micro nutrients as well as other molecules from root to shoot, a process crucial for plant survival. Therefore, evolution of stomata in plants represents a key evolutionary adaption important for the survival of plants on land (John A. Raven, 2002). Stomatal apertures are required for CO_2 uptake and nutrient translocation, but can also be detrimental due to excessive water loss in the form of water vapor and formation of pathogen entry sites (Melotto et al., 2006) and hence must be tightly controlled.

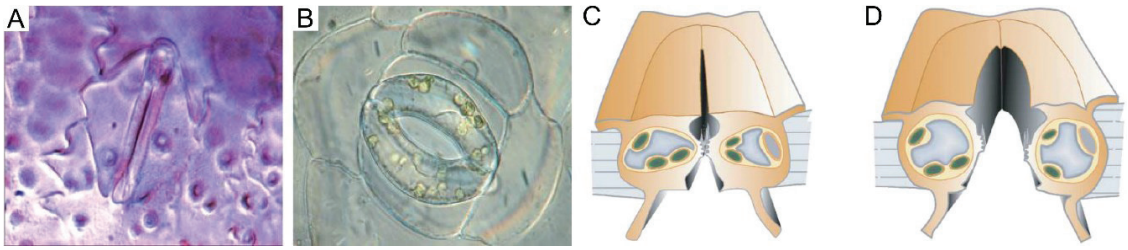

Figure 1: **Dumb-bell- and kidney-shaped stomata and schematic cartoon of turgor pressure-dependent stomatal movements.**
(A) Grass species possess dumb-bell-shaped stomata while **(B)** kidney-shaped stomata are common amongst all other species. **(C)** In the state of low turgore pressure the specialized cell wall architecture leads to closed stomatal pores while **(D)** high turgor pressure renders the pore open. (Source of figure: Adapted from Hetherington et al., 2003 (Panel A+B), M. Rob G. Roelfsema et al., 2005 (Panel C+B))

Guard cells forming stomata, dumb-bell or kidney-shaped, possess thickened cell walls with a specialized structure (Figure 1). This structure allows the stomatal pore between the guard cells to be either open or closed and therefore serves as a valve permitting or denying gas exchange. Guard cells of open stomata are turgescent which is achieved by the accumulation of osmotically active substances, including organic acids and ions (Figure 1D) (Kim et al., 2010). To close stomata, these osmotically active substances have to be removed from the cell. The stimuli and mechanisms underlying the control of turgor pressure in guard cells and therefore stomatal movements are explained in the following chapters.

3.2.2 Stomatal movements

3.2.2.1 Stomatal opening

At the onset of daylight the photosynthetic activity and the need for CO_2 of most plants is increasing and has to be supplied by the atmospheric air. Consequently, decreased cytosolic CO_2 concentrations (C_i) and light serve as stomatal opening stimuli enabling the uptake of CO_2 through the stomatal pores. Two blue light photoreceptors, PHOTOTROPIN 1 and 2 (PHOT1 and PHOT2), have been identified to sense the blue light fraction of the daylight and to mediate the blue light induced stomatal opening response. Here, blue light

is perceived by PHOT1 and PHOT2 and leads to auto-phosphorylation of the cytosolic kinase domains (Kinoshita et al., 2001, Kinoshita et al., 2003, Inoue et al., 2008). Subsequently, the recently identified kinase BLUE LIGHT SIGNALING 1 (BLUS1) is phosphorylated by PHOT1 which represents an important step in blue light induced

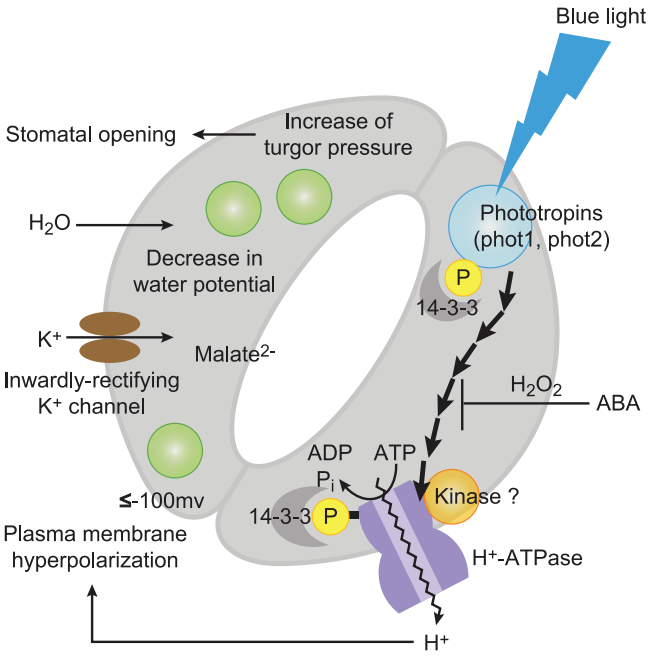

Figure 2: **Simplified cartoon depicturing blue light-induced stomatal opening mechanisms.**
Blue light is perceived by the phototropin blue light receptors. A mulit-step signlaing cascade including BLUS1 kinase and 14-3-3 proteins lead to the activation of the plasma membrane H^+-ATPase. H^+-ATPase mediated active H^+-transport hyperpolarizes the plasma membrane which leads to the influx of K^+ via K_{in} ion channels. Together with the formation of Malate^{2-} the accumulation of K^+ ions is triggering water influx thereby increasing turgor preasure resulting in stomatal opening. (Source of figure: Shimazaki et al., 2007)

stomatal closure (Takemiya et al., 2013). Down-stream multistep signaling mechanisms subsequently trigger the phosphorylation and activation of the plasma membrane localized and ATP-driven proton pump (H^+-ATPase; Figure 2; Assmann et al., 1985, Kinoshita et al., 2001, Shimazaki et al., 2007). An unknown serine/threonine kinase, different from PHOT1 and PHOT2, is phosphorylating a threonine residue in the C-terminal auto-inhibitory region of the H^+-ATPase (Shimazaki et al., 2007). This creates a binding site for 14-3-3 scaffolding proteins and 14-3-3 protein binding results in the translocation of the auto-inhibitory domain, thereby activating the H^+-ATPase (Shimazaki et al., 2007). The molecular nature of the signal transduction pathway downstream of BLUS1 and upstream of the H^+-ATPase is not

well understood and subject to intensive research. Besides the above mentioned protein components, Okadaic acid and calyculin A sensitive phosphatases as well Calcium have been implicated to be involved in this signal transduction mechanism (Shimazaki et al., 2007). The H^+-ATPase mediated proton extrusion results in the hyperpolarization of the plasma membrane (Figure 2; Assmann et al., 1985). This hyperpolarization of the plasma membrane in turn leads to the activation of inward-rectifying K^+-channels (K_{in}), such as POTASSIUM CHANNEL IN ARABIDOPSIS THALIANA 1 (KAT1), POTASSIUM CHANNEL IN ARABIDOPSIS THALIANA 2 (KAT2), ARABIDOPSIS K^+ TRANSPORTER 1, 2, and 3 (AKT1, AKT2, and AKT3) which mediate K^+ influx into the cell (Figure 2; Shimazaki et al., 2007, Kollist et al., 2014). The accumulation of positively charged ions (K^+) requires the generation of negatively charged counter ions such as $Malate^{2-}$ and anions including Cl^- and NO_3^- which are taken up or produced by several mechanisms (Kollist et al., 2014). To avoid cellular toxicity due to high cytosolic ion concentrations, the majority of these ions and malate are stored in the vacuole and are transported across the tonoplast by various transporters and ion channels (Kollist et al., 2014). A decrease in C_i and red light have also been associated to be stomatal opening stimuli (Shimazaki et al., 2007).

The accumulation of osmotically active substances leads to a decrease in the cellular water potential. Differences in water potentials between the intracellular space in guard cells and the apoplast induces an influx of water into to the guard cells resulting in increased turgor pressure. This increase in turgor together with the above mentioned specialized cell wall structure results in opening of the stomatal pore.

3.2.2.2 Stomatal closing

To conserve water and to protect the plant while taking up sufficient amount of CO_2, stomata close in response to biotic and abiotic stresses including pathogen attack, cold stress, heat stress, low humidity, salt stress, darkness, ozone, and low CO_2 levels.

3.2.2.2.1 The abiotic stress hormone abscisic acid in guard cells

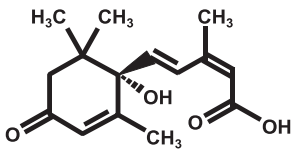

Figure 3: Chemical structure of S-(+)-abscisic acid.

Several of the above mentioned abiotic stresses result in elevated concentrations of the sesquiterpenoid plant hormone abscisic acid (ABA; (2Z,4E)-5-[(1S)-1-hydroxy-2,6,6-trimethyl-4-oxocyclohex-2-en-1-yl]-3-methylpenta-2,4-dienoic acid; Figure 3) in guard cells, or leaves in general. Plants began utilizing ABA as drought stress hormone during land colonization (Hauser et al., 2011). Measuring ABA levels by enzyme-amplified immunosorbent assay (ELISA) and Förster resonance energy transfer (FRET)-based optogenetic nanosensors showed that ABA concentrations in guard cells increased already

15 min after the onset of low humidity (Harris et al., 1991, Waadt et al., 2014). When subjected to drought conditions, plant leaf ABA concentrations were increased up to 30-fold (Harris et al., 1988, Harris et al., 1991, Ikegami et al., 2009). Unstressed guard cell ABA concentration was estimated to a value of ~ 500 nM which is increasing to ~15 µM under stress conditions (Harris et al., 1988, Harris et al., 1991, Waadt et al., 2014).

Soil drought stress is sensed in roots and two non-mutually exclusive mechanisms have been postulated to explain how the drought signal leads to ABA accumulation in the shoot of the plants: 1. During drought conditions ABA is synthesized in the roots and then transported towards the shoot via the xylem (Sauter et al., 2001, Wilkinson et al., 2002). 2. After sensing drought conditions, a hydraulic signal is transported to the shoot which triggers ABA synthesis (Christmann et al., 2005, Christmann et al., 2007, Ikegami et al., 2009). 2.5 hours after subjecting *Arabidopsis thaliana* roots to drought stress, ABA levels in the leaves were increased (Ikegami et al., 2009). The recent development of optogenetic FRET-based nanosensors (Jones et al., 2014, Waadt et al., 2014) will help to determine the details of time-resolved kinetics of ABA-transport and accumulation. ABA accumulation in guard cells leads to closure of the stomatal pore. The molecular mechanisms underlying this drought protection mechanism are explained in the following.

3.2.2.2.2 Mechanism of Ca^{2+}- and ABA-dependent stomatal closure

The perception of ABA by guard cells leads to cytosolic Ca^{2+} ($[Ca^{2+}]_{cyt}$) increase (McAinsh et al., 1990, Schroeder et al., 1990, Grabov et al., 1998, Allen et al., 1999, Staxén et al., 1999, MacRobbie, 2000, Marten et al., 2007, Hubbard et al., 2012). Also, ABA triggers formation of reactive oxygen species (ROS) which leads to the activation Ca^{2+}-permeable plasma membrane localized channels (I_{ca}), thus contributing to high $[Ca^{2+}]_{cyt}$ levels (Pei et al., 2000, Murata et al., 2001). *Arabidopsis* mutant guard cells lacking the ROS producing NADP(H) oxidases RESPIRATORY BURST OXIDASE PROTEIN D and F (RbohD and RbohF) are impaired in ABA-dependent ROS production, cytosolic Ca^{2+}-transients, and additionally display decreased stomatal closure in response to ABA demonstrating the important role of ROS and subsequent Ca^{2+}-elevations in stomatal closure (Kwak et al., 2003). A recent study revealed that RbohF activity is Ca^{2+}-activated and dependent on phosphorylation suggesting a positive feedback loop (Kimura et al., 2012). Multiple studies reported that Ca^{2+} is required for stomatal closure (De Silva et al., 1985, Schwartz, 1985, McAinsh et al., 1990, Grabov et al., 1998, MacRobbie, 2000). The frequency of cytosolic Ca^{2+} transients has been shown to be important for the long term, so called "Ca^{2+}-programmed" closure of guard cells, while short term or fast reactive closure, meaning that stomata re-open after ~ 60 min, is independent of the frequency (Allen et al., 2001). Another

study, however, indicated that ABA-induced stomatal closure is independent of cytosolic Ca^{2+}-elevations but requires resting Ca^{2+} levels (Levchenko et al., 2005). Quantitative analyses of ABA-induced stomatal closure in conditions, which abolish cytosolic Ca^{2+}-elevations (but hold $[Ca^{2+}]_{cyt}$ at resting levels), have shown that ~70% of ABA-triggered stomatal closure is dependent on cytosolic Ca^{2+}-elevations (Siegel et al., 2009). Surprisingly, intracellular Ca^{2+} has also been reported to play a role in stomatal opening in response to several stimuli (Irving et al., 1992, Shimazaki et al., 1992, Curvetto et al., 1994, Shimazaki et al., 1997, Cousson et al., 1998, Young et al., 2006) and additionally long term $[Ca^{2+}]_{cyt}$ monitoring has shown that cytosolic Ca^{2+} transients even occur without stimulus (Grabov et al., 1998, Allen et al., 1999, Staxén et al., 1999, Klüsener et al., 2002, Young et al., 2006). These results raise the question of how molecular mechanisms in guard cells discriminate between $[Ca^{2+}]_{cyt}$ being a signal for stomatal opening or for stomatal closure.

Elevated $[Ca^{2+}]_{cyt}$ results in the activation of slow-activating sustained (S-type) and rapid-transient (R-type) anion channels (Schroeder et al., 1989, Hedrich et al., 1990, Mori et al., 2006, Vahisalu et al., 2008, Siegel et al., 2009, Chen et al., 2010, Meyer et al., 2010). However, detailed analyses have shown that elevated $[Ca^{2+}]_{cyt}$ only triggers S-type anion currents when guard cells were pre-exposed to several stomatal closing stimuli including high external Ca^{2+}, CO_2, and ABA (Allen et al., 2002, Siegel et al., 2009, Chen et al., 2010, Xue et al., 2011). Besides anion channel regulation, high $[Ca^{2+}]_{cyt}$ leads to the inhibition of K_{in} preventing the influx of K^+ into the guard cells (Schroeder et al., 1989, Kelly et al., 1995, Grabov et al., 1999, Kwak et al., 2001). Moreover, Ca^{2+}-dependent inhibition of the H^+-ATPase (Schroeder et al., 1989, Kinoshita et al., 1995) prevents the re-polarization of the plasma membrane impairing the re-opening of the guard cells. The S- and R-type anion channels mediate the extrusion of negatively charged anions (A^-), which results in the de-polarization of the plasma membrane triggering the activity of voltage gated outward-rectifying K^+-channels (K_{out}) such as GATED OUTWARDLY-RECTIFYING K^+ CHANNEL (GORK) driving the efflux of K^+ (Schroeder et al., 1987, Ache et al., 2000, Becker et al., 2003, Hosy et al., 2003). The majority of these ions as well as $Malate^{2-}$ are stored in the vacuole during stomatal opening and are released into the cytosol by the action of ion channels and transporters (Kollist et al., 2014). The reduced cellular A^- and K^+ content triggers water efflux which results in the loss of turgor pressure and ultimately in the closure of the stomatal pore.

3.2.2.2.2.1 Anion channels in ABA-dependent stomatal closure

The gene encoding a major S-type anion current mediating anion channel, *SLOW ANION CHANNEL ASSOCIATED 1* (*SLAC1*), has recently been identified by employing screens measuring ozone induced stomatal closure and leaf temperatures in response to

CO_2 (Negi et al., 2008, Vahisalu et al., 2008). SLAC1 is expressed in guard cells, localized to the plasma membrane, and anion selective with a high conductivity for NO_3^- and Cl^- (Negi et al., 2008, Geiger et al., 2009). In *slac1* knock out lines ABA-dependent and Ca^{2+}-induced S-type anion currents as well as stomatal closure are abrogated (Vahisalu et al., 2008), clearly showing the importance of this channel in the fast reactive closure of stomata. A structural homology model based on a bacterial homologue, HiTehA, predicts SLAC1 to consist of 10 transmembrane helices which surround the ion conducting pore (Chen et al., 2010). Homology structure guided analyses of point mutated SLAC1 versions expressed in *Xenopus* oocytes pinpointed a bulky Phenylalanine (F450) residue to block the pore and to be removed during channel activation (Chen et al., 2010). Besides SLAC1, a closely related anion channel, SLAC1 HOMOLOGUE 3 (SLAH3), has been reported to be important for NO_3^- anion transport in guard cells (Geiger et al., 2011). SLAH3, when expressed under the *SLAC1* promoter, is able to rescue the *slac1* CO_2-phenotype (Negi et al., 2008). However, the importance of SLAH3 in ABA-dependent stomatal closure remains unclear.

Just recently, a channel mediating R-type anion currents, ALUMINUM-ACTIVATED MALATE TRANSPORTER 12 (ALMT12) or QUICKLY-ACTIVATING ANION CHANNEL 1 (QUAC1), has been identified (Meyer et al., 2010). QUAC1 is highly expressed in guard cells, localized to the plasma membrane and possesses a high conductivity for $malate^{2-}$ (Meyer et al., 2010). Plants, in which the *QUAC1* gene is knocked out, display impaired guard cell R-type anion currents and decreased ABA-dependent stomatal closure (Meyer et al., 2010), potentially due to impaired $Malate^{2-}$ efflux.

Early patch-clamp studies revealed that ABA-dependent S-type anion current activation requires ATP and is inhibited in the presence of the Serine/Threonine kinase inhibitor K252a, suggesting the involvement of Serine/Threonine protein kinases (Schmidt et al., 1995, Allen et al., 1999). It was also indicated that ABA-triggered stomatal closure is mediated by Ca^{2+}-dependent and Ca^{2+}-independent pathways which depend on each other quantitatively (Siegel et al., 2009). After the discovery of the SLAC1, subsequent studies showed that SLAC1 is activated by Ca^{2+}-independent SNF1-RELATED KINASE 2s (SnRK2s), most importantly SnRK2.6/OPEN STOMATA 1 (OST1), and Ca^{2+}-DEPENDENT PROTEIN KINASES 21 and 23 (CPK23 and CPK21) in *Xenopus* oocytes (Geiger et al., 2009, Lee et al., 2009, Geiger et al., 2010). *In vitro* kinase assays showed that OST1, CPK21, and CPK23 phosphorylate the N-terminal (amino acids 1-186; SLAC1-NT), but not the C-terminal (SLAC1-CT) cytosolic domain of SLAC1. Phospho-site mapping of OST1-phosphorylated SLAC1-NT revealed that the residues S59, S86, S113, and S120 are phosphorylated by OST1 *in vitro* (Vahisalu et al., 2010). Serine 120 has been shown to be

important for OST1, but not for CPK23, activation of SLAC1 in oocytes (Geiger et al., 2009, Geiger et al., 2010). SLAC1 activation by OST1 or CPK23 is inhibited in the presence of the clade A protein phosphatase 2Cs (PP2Cs; see chapter 2.2.2.2.2.4) ABA-INSENSITIVE 1 and 2 (ABI1 and ABI2) in oocytes (Geiger et al., 2009, Geiger et al., 2010) while OST1 activation is inhibited by co-expression of PROTEIN PHOSPHATASE 2CA (PP2CA) in *Xenopus* oocytes (Lee et al., 2009). *In vitro*, the trans-phosphorylation of the SLAC1-NT by OST1, CPK21 or CPK23 is inhibited in the presence of ABI1 (Geiger et al., 2010). However, the exact mechanism of this inhibition is not known. Moreover, SLAC1-NT phosphorylation by OST1 in inhibited in the presence of PP2CA *in vitro* (Lee et al., 2009). Additionally, co-expression of OST1 in *Xenopus* oocytes activates QUAC1 in $Malate^{2-}$ containing media (Imes et al., 2013).

3.2.2.2.2.2 SnRK2 protein kinases in ABA-dependent stomatal closure

The *Arabidopsis* genome encodes for 10 SnRK2 kinases (Hrabak et al., 2003). OST1/SnRK2.6 has been identified in a thermal imaging screen to be crucial for stomatal closure (Merlot et al., 2002, Mustilli et al., 2002). OST1/SnRK2.6 as well as SnRK2.2 and SnRK2.3 have been reported to be activated by ABA while 9 SnRKs were activated by salt and osmotic stress (Mustilli et al., 2002, Yoshida et al., 2002, Boudsocq et al., 2004, Yoshida et al., 2006, Boudsocq et al., 2007, Fujii et al., 2007, Fujii et al., 2009, Nakashima et al., 2009, Umezawa et al., 2009). While OST1 represents the major SnRK responsible for ABA-dependent stomatal phenotypes (Merlot et al., 2002, Mustilli et al., 2002, Yoshida et al., 2002, Geiger et al., 2009, Imes et al., 2013, Merilo et al., 2013) the ABA-activated SnRK2.2 and SnRK2.3 appear to be important in other ABA related mechanisms such as root growth and seedling establishment (Fujii et al., 2007, Fujii et al., 2009, Fujita et al., 2009, Nakashima et al., 2009). Single *ost1* plants show stronger water loss when compared to wild type plants and this effect is increased in plants in which additionally *SnRK2.2* and *SnRK2.3* genes are disrupted (Fujita et al., 2009). Consistent with the SLAC1 activation by OST1 in *Xenopus* oocytes disrupting the expression of the OST1 gene in the *Arabidopsis* Col0 ecotype leads to an impaired ABA-activation of S-type anion currents in guard cells (Geiger et al., 2009) resulting in the ABA-hyposensitive stomatal phenotypes mentioned above. The additive effect of SnRKs in water loss could be explained by the ability of SnRK2.2 and SnRK2.3 to moderately activate SLAC1 in *Xenopus* oocytes (Fujita et al., 2009, Geiger et al., 2009). Another explanation could be that all ABA-activated SnRKs play an important role in the control of stress responsive gene expression (Umezawa et al., 2004, Fujii et al., 2007, Fujii et al., 2009, Fujita et al., 2009, Nakashima et al., 2009) which might indirectly influence drought adaption mechanisms. Moreover, OST1 has been shown to phosphorylate RbohF *in vitro* and to activate RbohD and RbohF in a heterologous

expression system (Sirichandra et al., 2009, Kimura et al., 2012) potentially regulating cytosolic Ca^{2+} levels during ABA-signaling. Consequently, *ost1* mutant plants are impaired in ABA-dependent ROS production and stomatal closure (Mustilli et al., 2002). Recently the regulatory role of OST1 in the regulation of the guard cell R-type anion channel QUAC1 has been reported (Imes et al., 2013) adding yet another regulatory role of OST1 in stomatal closure. Here, patch clamp studies have shown strongly decreased R-type anion currents in *ost1* mutant guard cells comparable to R-type anion currents in *abi1-1* guard cells (Imes et al., 2013). Additionally, OST1 phosphorylates the K_{in} channel KAT1 (Sato et al., 2009) and in the Ler accession of *Arabidopsis thaliana ost1* guard cells are impaired in ABA-dependent K_{in} channel inhibition (Acharya et al., 2013).

The molecular mechanism of the ABA-dependent regulation of SnRK activity has been subject to intensive research and is well understood. The protein kinase activity of SnRK2 kinases is dependent on the phosphorylation of the activation loop (T-loop) and the presence of the DI-domain/SnRK2-box (Belin et al., 2006, Boudsocq et al., 2007). The DI-domain is required for the stabilization of the kinase domain of SnRK2s and has been linked to ABA-independent regulation mechanisms (Belin et al., 2006, Yoshida et al., 2006, Yunta et al., 2011). ABA-dependent SnRK2 regulation has been shown to be mediated by the interaction of PP2Cs (Chapter 1.2.2.2.2.4) with the DII-domain of SnRK2s leading to the de-phosphorylation of residues in the activation loop of SnRK2s thus rendering the kinases inactive (Yoshida et al., 2006, Umezawa et al., 2009). The phosphorylation of the SnRK2 activation loop is mediated by auto- and auto-(trans)-phosphorylation events (Belin et al., 2006, Ng et al., 2011), however, trans-phosphorylation of the SnRKs activation loop by staurosporine-independent upstream kinases has also been discussed (Boudsocq et al., 2007).

3.2.2.2.2.3 Calcium dependent protein kinases (CPKs) in ABA-dependent stomatal closure

Besides other calcium sensing proteins such as CALMODULIN (CaM), CALMODULIN LIKE (CML), and CALCINEURIN B-LIKE (CBL) plants possess a unique class of Ca^{2+} sensing protein kinases, CPKs. Unlike the other above mentioned Ca^{2+}-binding proteins one CPK molecule senses Ca^{2+} and additionally possesses an enzymatic activity transducing the Ca^{2+}-signal into the post-translational modification of down-stream targets. There are 34 *CPK* genes in the *Arabidopsis* genome clustering into 4 subgroups (Boudsocq et al., 2012). CPK proteins consist of a variable N-terminal domain, a conserved kinase domain, and a conserved C-terminal domain termed CPK activation domain (CAD). The

variable N-terminal domain of CPK has been shown to be involved in substrate recognition (Ito et al., 2010). It also is the site of myristoylation or palmitoylation for several CPKs, resulting in many CPKs being membrane localized (Boudsocq et al., 2012). The CAD contains a pseudo-substrate domain followed by a 4 EF-hands containing so called Calmodulin-like domain. Biochemical and structural studies showed that without calcium the CAD is folded on top of the catalytic cleft of the kinase domain which is stabilized by the pseudo-substrate domain binding to the catalytic cleft. Upon binding of Ca^{2+} the CAD is translocated to the backside of the protein which renders the catalytic cleft accessible to the substrate thus leading to the activation of the CPK (Liese et al., 2013). However, some CPKs possess degenerated EF-hands potentially impaired in Ca^{2+}-binding and therefore Ca^{2+}-activation. Detailed biochemical analyses studying Ca^{2+}-dependent CPK activities of 14 CPKs expressed *in planta* revealed that subgroup 3 CPKs and also CPK25 are not activated by Ca^{2+} (Boudsocq et al., 2012). Moreover, CPK23 isolated from bacteria has been reported to be only weakly activated by Ca^{2+} while CPK21 activity is strongly Ca^{2+}-dependent (Geiger et al., 2010). CPKs auto-phosphorylating themselves and are additionally trans-phosphorylated by upstream kinases, but the functional importance of these post-translational modifications are still not clear (Liese et al., 2013). As mentioned above, CPK activation of SLAC1 is inhibited in the presence of the phosphatases ABI1 and ABI2 (Geiger et al., 2010), but the exact mechanism of this negative regulation has yet to be determined.

When the genes of *CPK4*, *CPK10*, and *CPK11* are disrupted the mutant plants exhibit enhanced drought sensitive and impaired stomatal closure phenotypes (Zhu et al., 2007, Zou et al., 2010). For *cpk4* and *cpk11* these phenotypes can be explained by the involvement of these CPKs in the regulation of ABA-dependent gene expression (Zhu et al., 2007). *CPK3* and *CPK6* single knock out plants are impaired in Ca^{2+}- and ABA-dependent guard S-type anion current activation and with stronger phenotypes in the *cpk3cpk6* double knock-out mutant (Mori et al., 2006). Furthermore, in *cpk3cpk6* double mutant plants Ca^{2+}-activated stomatal closure is impaired (Mori et al., 2006). *cpk23* plants exhibit decreased Ca^{2+}-activated S-type anion current activities (Geiger et al., 2010). Surprisingly however, the *cpk23* mutant plant exhibits enhanced drought resistance phenotypes (Ma et al., 2007) which might be due to transcriptional changes of several other proteins involved in the regulation of S-type anion currents (Geiger et al., 2010). Moreover, whole plant mechanisms independent of the regulation of stomatal apertures in *cpk23* might be involved. CPK5, a close homologue to CPK6, has been reported to phosphorylate the NADP(H) oxidase RbohD and in *cpk5* knock out plants bacterial elicitor triggered ROS production is impaired (Dubiella et al., 2013). In addition, c*pk3* and *cpk6* single as well as double knock out mutants are impaired in ABA-dependent I_{ca} channel regulation (Mori et

al., 2006). However, studies placing the CPK23 homologue in the Ler accession, GROWTH CONTROLLED BY ABSCISIC ACID 2 (GCA2), downstream of the ROS production (Pei et al., 2000) and the discovery that ABA-dependent I_{ca} channel activation is independent of the Serine-Threonine kinase inhibitor K252a (Mori et al., 2006) suggests that ABA-activated and CPK-mediated I_{ca} channel regulation mechanism might be independent of Rboh phosphorylation events. The detailed role of CPK-mediated and ABA-dependent I_{ca} regulation has still to be determined. CPK3 and CPK6 are, similar to OST1, involved in R-type anion channel regulation in *Arabidopsis* guard cells demonstrated by decreased R-type anion channel activity in *cpk3cpk6* mutant guard cells (Mori et al., 2006). In general, all reported stomatal phenotypes of *cpk* knock-out mutants reported so far (Mori et al., 2006, Zhu et al., 2007, Geiger et al., 2010, Zou et al., 2010, Hubbard et al., 2012) are intermediate in comparison to *ost1* plant phenotypes which might be due to functional redundancy of CPKs.

3.2.2.2.2.4 Clade A PP2C phosphatases in ABA-dependent stomatal closure

The clade A of PP2Cs consist of 9 members in *Arabidopsis* and many of them have been described to play a role as negative regulators within ABA-related responses including seed germination and vegetative growth (Fuchs et al., 2013). In guard cells, the dominant negative mutations of ABI1 and ABI2, *abi1-1* and *abi2-1*, exhibit impaired ABA-induced I_{ca} Ca^{2+}-channel activation, cytosolic Ca^{2+}-increases, and stomatal closure (Allen et al., 1999, Merlot et al., 2001, Murata et al., 2001). In *abi1-1* and *abi2-1* mutant guard cells ABA-activated S-type anion currents are impaired (Pei et al., 1997) and also R-type anion currents are decreased in *abi1-1* guard cells (Imes et al., 2013). These results are in agreement with *abi1-1* and *abi2-1* plants displaying a higher steady state stomatal conductance, increased water loss and for *abi1-1* stomatal closure is insensitive to ABA (Pei et al., 1997, Yoshida et al., 2006, Merilo et al., 2013). Structural and biochemical analyses revealed that the point mutations in the *abi1-1* and *abi2-1* mutant proteins prohibit the interaction of the mutant PP2C with ABA-bound receptors (Melcher et al., 2009, Miyazono et al., 2009, Yin et al., 2009), hence rendering the phosphatase constitutively active independent of the presence of ABA. No reports on ABA-related stomatal phenotypes of single knock-out mutants are available which might be due to the functional redundancy of these protein phosphatases. A T-DNA insertion mutant in the PP2C genes *ABI1*, *HYPERSENSITIVE TO ABA 1* (*HAB1)*, and *PP2CA* (*abi1-2/hab1-1/ppc2ca-1*) mutant displayed a lower steady-state stomatal conductance in gas exchange measurements when compared to the wild type (Merilo et al., 2013).

3.2.2.2.2.5 ABA receptors in ABA-dependent stomatal closure

Two independent approaches, a chemical-genetic screen and a protein-protein interaction screen, led to the identification of cytosolic ABA receptors PYRABACTIN RESISTANCE 1/PYR1-LIKE /REGULATORY COMPONENT OF ABA RECEPTOR (PYR/PYL/RCAR) (Ma et al., 2009, Park et al., 2009), a protein family with 14 members. ABA perception is achieved by direct binding of the hormone in a hydrophobic pocket which triggers a conformational change leading to the translocation of two β-loops which lock the ABA molecule within the binding pocket, and are therefore termed “gate” and “latch” (Melcher et al., 2009). This conformational change creates a binding site for PP2Cs blocking the active site, thus inhibiting the phosphatase activity (Ma et al., 2009, Melcher et al., 2009, Park et al., 2009). Protein-protein interaction screens revealed that the ABA receptors interact with specific PP2Cs creating an interaction network with many different combinations. *In vitro* ABA-binding affinities of PYR/PYL/RCAR proteins vary and greatly increase in the presence of PP2Cs dependent on the combination (Ma et al., 2009, Santiago et al., 2009, Szostkiewicz et al., 2010, Hao et al., 2011, Miyakawa et al., 2013, Fuchs et al., 2014) which allows fine-tuned responses to cytosolic ABA concentration changes. However, some ABA receptors interact with and inhibit PP2Cs even without ABA, which requires the PYR/PYL/RCAR proteins to be monomeric (Hao et al., 2011). In plants where the expression of 4 *PYR/PYL/RCAR* genes was disrupted (*pyr1/pyl1/pyl2/pyl4*), ABA-induced anion current activation as well as K_{in}-inhibition were abrogated (Wang et al., 2013). Mutant plants lacking PYR/PYL/RCAR proteins display an ABA-hyposensitive stomatal closure phenotype and increased stomatal apertures (Gonzalez-Guzman et al., 2012). Gas exchange experiments demonstrate increased steady-state stomatal conductance for *PYR/PYL/RCAR* null mutant plants which intensifies with increasing numbers of knocked-out ABA-receptors (Gonzalez-Guzman et al., 2012, Merilo et al., 2013). This effect could be explained by the fact that some monomeric ABA-receptor interact with and inhibit PP2Cs even without ABA and in their absence the basal inhibition of PP2Cs is impaired.

3.2.2.2.2.6 Summary and model of ABA- and Ca^{2+}-dependent stomatal closure

The above described results lead to the following simplified model of ABA- and Ca^{2+}-dependent stomatal closure (Figure 4).

1: In the presence of the phytohormone ABA, the cytosolic ABA-receptors (RCAR/PYR/PYL) form a complex with PP2Cs which leads to the inhibition of the protein phosphatase activity.

2: PP2Cs represent a major negative regulator within this signaling network and fulfill multiple roles in ABA signaling. When ABA is present, PP2Cs are inhibited, which results in the following cellular events in guard cells:

3: The inhibition of the positive regulator kinase OST1 is released which results in both phosphorylation and activation of the NADPH oxidases Rbohs. Rboh proteins catalyze the formation of apoplastic ROS such as H_2O_2 and $O_2^{\cdot -}$ which trigger the elevation of cytosolic Ca^{2+} mediated by plasma membrane localized Ca^{2+}-permeable ion channels.

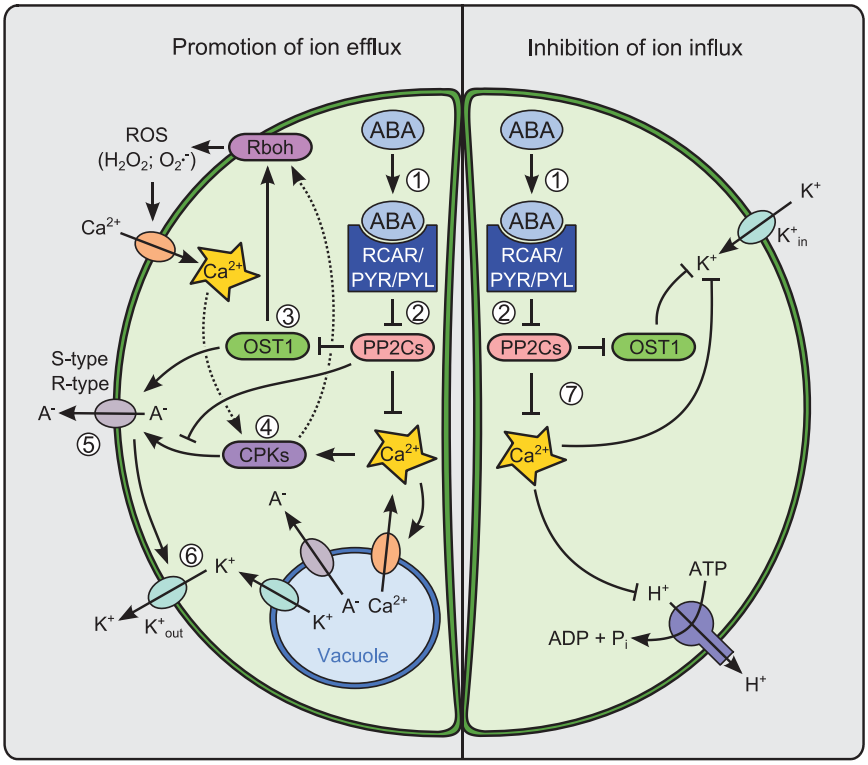

Figure 4: **Schematic model of ABA- and Ca^{2+}-dependent stomatal closure**

Multi-component signaling including second messengers and protein components ensure a tight and specific regulation of stomatal closure. (Illustration created by the author)

4: This cytosolic Ca^{2+} elevation, supported by Ca^{2+}-promoted release of Ca^{2+} stored in organelles, including the vacuole, leads to the activation of CPKs. CPKs are also involved in the ABA-activation of Rboh proteins further promoting Ca^{2+} influx into the cytosol.

5. Both OST1 and CPK kinases phosphorylate and thereby activate plasma membrane localized anion channels leading to efflux of anions (A^-). This process can be inhibited directly by PP2C phosphatases in the absence of ABA. Two types of anion channels are activated: the slow (S-type) and rapid (R-type) anion channels.

6. Anion efflux leads to depolarization of the plasma membrane which drives K^+ efflux mediated by outward-rectifying potassium (K^+_{out}) channels. The majority of A^- and K^+ in a plant cell are stored in the vacuole and are released into the cytosol via Ca^{2+}-activated K^+ channels and anion release transporters present in the tonoplast. The efflux of ions (A^- and K^+) causes loss of turgor pressure of guard cells which results in stomatal closure.

7. To prevent the counteracting accumulation of ions during stomatal closure, ABA and RCAR/PYR/PYL mediated PP2C inhibition results in the blocking of mechanisms mediating the accumulation of ions (for stomatal opening), such as plasma membrane H^+-ATPases activity and inward rectifying K^+ (K^+_{in}) channels.

This signaling network provides the basis for robust stomatal ABA-signaling, a signal transduction cascade crucial for drought adaption and therefore plant survival. However, there are still many unknown aspects and unraveling them will greatly improve our understanding of ABA- and Ca^{2+}-dependent signal transduction in guard cells. In the next chapter I will list the open questions I wanted to address in this work.

4 Objectives of this work

Guard cells are crucial cell types for drought adaption mechanisms and plant survival under water-limited conditions. Several aspects of the Ca^{2+}- and ABA-dependent signal transduction pathway in guard cells are known (Figure 4), however there are still many open questions. To determine the details of that mechanisms would greatly improve the understanding of drought adaption mechanisms in plants. Additionally, as many different stimuli induce Ca^{2+}-transients in guard cells this cell type is ideal to study specificity mechanisms in Ca^{2+}-signaling events.

In this work, the following questions were asked:

1. As CPK single or double knock out mutants displayed only intermediate phenotypes in S-type anion current activation the question whether more CPKs are involved in SLAC1 activation and whether higher order knock out mutants lead to completely abrogated S-type anion current activation arose. Furthermore, a detailed characterization of CPKs and the activation and phosphorylation of SLAC1 by these protein kinases was a goal of this work.

2. Many proteins of the ABA-signaling core resulting in SLAC1 activation have been identified, however a functional reconstitution of this signaling pathway has not yet been achieved. Whether the identified proteins within Ca^{2+}-dependent and Ca^{2+}-independent ABA-signaling are sufficient, or whether more proteins are involved is a question addressed in this work.

3. As mentioned above, Ca^{2+} has been reported to play an important role in stomatal closing and also in stomatal opening raising the question of how specificity in Ca^{2+}-signaling in guard cell can be achieved. The presence of ABA primes Ca^{2+}-sensors to be susceptible to elevated $[Ca^{2+}]_{cyt}$ thus enabling a specific Ca^{2+}-response. Unraveling the molecular mechanisms of this Ca^{2+}-sensitivity mechanism taking results from questions 1 and 2 into account was another goal of this work.

4. Ca^{2+}-dependent and Ca^{2+}-independent ABA-signaling in guard cell depend on each other quantitatively. However, the molecular mechanism of these interaction is not known and has been subject to research presented in this work.

5 Results and discussion

5.1 Identification and characterization of novel CPKs involved in SLAC1-mediated S-type anion current activation and stomatal closure

Hubbard, K. E., R. S. Siegel, G. Valerio, B. Brandt and J. I. Schroeder (2012). "Abscisic acid and CO_2 signalling via calcium sensitivity priming in guard cells, new CDPK mutant phenotypes and a method for improved resolution of stomatal stimulus–response analyses." Annals of Botany **109**(1): 5-17.

Brandt, B., D. E. Brodsky, S. Xue, J. Negi, K. Iba, J. Kangasjärvi, M. Ghassemian, A. B. Stephan, H. Hu and J. I. Schroeder (2012). "Reconstitution of abscisic acid activation of SLAC1 anion channel by CPK6 and OST1 kinases and branched ABI1 PP2C phosphatase action." Proceedings of the National Academy of Sciences **109**(26): 10593-10598.

Laanemets, K., B. Brandt, J. Li, E. Merilo, Y.-F. Wang, M. M. Keshwani, S. S. Taylor, H. Kollist and J. I. Schroeder (2013). "Calcium-Dependent and -Independent Stomatal Signaling Network and Compensatory Feedback Control of Stomatal Opening via Ca^{2+} Sensitivity Priming." Plant Physiology.

Brandt B., Munemasa S., Wang C., Nguyen D., Belknap T., Aleman F., Schroeder JI (2014). “Calcium Specificity Mechanism within ABA-dependent Signal Transduction in *Arabidopsis* thaliana.” submitted

Single and double knock out mutants of CPKs led to intermediate ABA-dependent stomatal closure and S-type anion current regulation phenotypes (Mori et al., 2006, Zhu et al., 2007, Zou et al., 2010, Hubbard et al., 2012), potentially due to functional redundancy of CPKs. *cpk3* and *cpk6* single and double mutant plants exhibit reduced ABA- and Ca^{2+}-activated S-type anion currents (Mori et al., 2006). Co-expression of CPK6 together with SLAC1 gave rise to macroscopic anion currents (Brandt et al., 2012). *In vitro* kinase assay revealed that CPK6 is phosphorylating the SLAC1-NT (Brandt et al., 2012). These results confirmed that the *in planta* S-type anion current phenotype (Mori et al., 2006) is due to the direct action of the kinase on SLAC1. Subsequent detailed biochemical analyses revealed that CPK6 phosphorylates the SLAC1-NT effectively and that CPK6 phosphorylates the SLAC1-NT residue Serine 59 (Brandt et al., 2012). When Serine 59 in the SLAC1 was substituted with a non-phophorylatable amino acid, Alanine, no CPK6-mediated SLAC1 activation could be seen in oocytes confirming the functional importance of SLAC1 Serine 59 phosphorylation during CPK6 activation of that channel (Brandt et al., 2012). CPK6 has been reported to be only weakly activated in a Ca^{2+}-dependent manner and possess a high core activity at low Ca^{2+}-concentrations (Scherzer et al., 2012). Detailed biochemical analyses, however, clearly showed the requirement of high free Ca^{2+} concentrations for SLAC1-NT phosphorylation and revealed a half maximal activation of CPK6 at a free Ca^{2+} concentration of ~ 500 nM using a synthetic peptide as the substrate (Brandt et al., 2012,

Laanemets et al., 2013). CPK6 possesses a core activity of ~15% of the maximal phosphorylation activity in these analyses (Laanemets et al., 2013). Electrophysiological experiments in oocytes did not show SLAC1 activation when co-expressed with CPK3 (Brandt et al., 2012), however a truncated and constitutively active version of CPK3 activated SLAC1 in oocytes (Scherzer et al., 2012). A close homologue of CPK6, CPK5, was identified to also activate SLAC1 in oocytes (Brandt et al., 2014). A mutant plant in which the expression of *CPK5*, *CPK6*, *CPK11*, and *CPK23* was disrupted (*cpk5/6/11/23*) was completely impaired in high external Ca^{2+}- and ABA-priming of anion current activation by elevated $[Ca^{2+}]_{cyt}$ (Brandt et al., 2014).

The presented and previous results show that several CPKs are able to fulfill the role of activating SLAC1/S-type anion currents which aids to the robustness of this crucial step of stomatal closure. However, knocking out 4 CPKs leads to completely abrogated ABA- and Ca^{2+}-activation of S-type anion currents (Brandt et al., 2014) suggesting that CPK-mediated S-type anion current activation requires a certain number of CPKs. SLAC1 Serine 120 has been reported to be important for activation of SLAC1 by OST1 while CPK23 activation of SLAC1 S120A was comparable to the wild type version of SLAC1 (Geiger et al., 2010). The requirement of Serine 59 for SLAC1 activation by CPK6 (Brandt et al., 2012) identifies a novel amino acid responsible for activation of SLAC1 by CPKs which might represent a novel mechanism of synergistic SLAC1 regulation by Ca^{2+}-dependent and Ca^{2+}-independent kinases (see chapter 4.2).

5.2 Molecular mechanism of Ca^{2+}-specificity and interdependence of the Ca^{2+}-dependent and Ca^{2+}-independent branches of ABA-signaling

Brandt, B., D. E. Brodsky, S. Xue, J. Negi, K. Iba, J. Kangasjärvi, M. Ghassemian, A. B. Stephan, H. Hu and J. I. Schroeder (2012). "Reconstitution of abscisic acid activation of SLAC1 anion channel by CPK6 and OST1 kinases and branched ABI1 PP2C phosphatase action." Proceedings of the National Academy of Sciences **109**(26): 10593-10598.

Brandt, B., S. Munemasa, C. Wang, D. Nguyen, T. Belknap, F. Aleman, J. I. Schroeder (2014). “Calcium Specificity Mechanism within ABA-dependent Signal Transduction in *Arabidopsis thaliana*.” submitted

Several components of the ABA-signaling core have been identified and the signal transduction pathway has been reconstituted in mesophyll protoplast with OST1 as the kinase using a stress activated promoter fused to a reporter gene (Fujii et al., 2009). This approach does not exclude the possibility of additional factors which are required for the

signal transduction pathway to be functional being present in the plant cells used. *In vitro*, ABA-pathway reconstitution resulting in SLAC1-NT phosphorylation including either OST1 of CPK23 was reported (Geiger et al., 2010). However, whether a functional *in vivo* reconstitution resulting in SLAC1 activity is possible was not known. Using *Xenopus* oocytes, ABA-dependent SLAC1 activation by signal transduction pathway reconstitution including either OST1 of CPK6 could be seen (Brandt et al., 2012). These results indicate the components reported so far are sufficient for a functional reconstitution of the ABA signaling pathway. Also, these analyses revealed that the inclusion of either the Ca^{2+}-independent protein kinase OST1 or the Ca^{2+}-dependent protein kinase CPK6 is sufficient for the ABA-activation of SLAC1 indicating a branched configuration of the signal transduction pathway.

The role of PP2Cs was assessed to investigate the molecular mechanism underlying the phenomenon that the presence of ABA and high external Ca^{2+} (Chapter 2.2.2.2.2) primes Ca^{2+}-sensors to be susceptible to cytosolic Ca^{2+} elevations. In quadruple PP2C knock out plants (*abi1-2/abi2-2/hab1-1/pp2ca-1*), elevating $[Ca^{2+}]_{cyt}$ triggered the activation of S-type anion currents even when guard cell were not pre-exposed to ABA (Brandt et al., 2014), underlining the important role of these PP2Cs within this Ca^{2+}-sensitivity mechanism. Detailed biochemical analyses revealed that PP2Cs do not directly regulate CPK activities, but inhibit CPK and also OST1 activation by directly removing phosphorylations added by these kinases to SLAC1 (Brandt et al., 2012, Brandt et al., 2014). These results suggest that “in the absence of the specific signal, ABA, Ca^{2+}-responsiveness is inhibited by PP2Cs, thereby preventing responses to unrelated Ca^{2+} elevations […] (Irving et al., 1992, Shimazaki et al., 1992, Curvetto et al., 1994, Cousson et al., 1998, Klüsener et al., 2002, Roelfsema et al., 2002, Young et al., 2006). As PP2Cs inhibit OST1 and also down-regulate SLAC1 directly, this network not only enables stimulus specific activation of SLAC1 via phosphorylation, but also provides a tight off switch via PP2C-catalyzed de-phosphorylation of SLAC1 […]. This mechanism could also prevent SLAC1 activation by CPK23, which exhibits a moderate Ca^{2+} sensitivity (Geiger et al., 2010). Moreover, as PP2Cs control Ca^{2+} signaling specificity downstream of the Ca^{2+} sensor […], CPKs could still be capable of fulfilling other signaling roles (Boudsocq et al., 2010, Munemasa et al., 2011, Dubiella et al., 2013, Gao et al., 2013).” (Brandt et al., 2014)

The ABA-signal transduction pathway resulting in SLAC1 activation was functionally reconstituted using either OST1 or CPK6 as kinase (Brandt et al., 2012), indicating that SLAC1 activation can be achieved either by the Ca^{2+}-dependent or the Ca^{2+}-independent branch of ABA signaling in oocytes. However, analyses of ABA-induced stomatal closure revealed that in conditions which abolish cytosolic Ca^{2+}-elevations, only ~30% of the stomatal closure could be seen (Siegel et al., 2009). Also, in *cpk5/6/11/23* and

snrk2.2/snrk2.3/ost1 mutant guard cells ABA-activation of S-type anion currents was abrogated (Brandt et al., 2014) showing that both the Ca^{2+}-dependent and the Ca^{2+}-independent branch of ABA signal transduction are required for S-type anion currents activation *in planta*. This interdependence could be due to a direct cross-regulation of OST1 and CPKs, however no direct interaction or cross-(trans)-phosphorylation between OST1 and CPK6 can be seen (Brandt et al., 2014). Electrophysiological experiments in oocytes revealed that in this system SLAC1 Serine 59 is required for the activation by CPK5, CPK6, and CPK23, but not for the activation by OST1 (Brandt et al., 2012, Brandt et al., 2014). That SLAC1 Serine 120 is crucial for the activation mediated by OST1 but not by CPK5, CPK6, and CPK23 (Geiger et al., 2009, Geiger et al., 2010, Brandt et al., 2014) suggests that the functional linkage of the Ca^{2+}-dependent and the Ca^{2+}-independent pathway is mediated by specific SLAC1 phosphorylation events. Co-expression of CPK6 and OST1 together with SLAC1 led to a synergistic activation of the anion channel (Brandt et al., 2014). However, experiments carried out in the heterologous system of *Xenopus* oocytes and *in vitro* experiments do not necessarily represent the situation in the plant as many parameters including protein abundances, localizations, and activities might be substantially different. Further research is needed to elucidate the detailed mechanism *in planta*.

"The control of ABA-triggered stomatal closure by parallel interdependent Ca^{2+}-dependent and –independent mechanisms can contribute to the robustness of this essential signaling network (Hetherington, 2001). Genome analyses have revealed the existence of more than 200 genes encoding for proteins containing Ca^{2+}-binding EF-hands (Day et al., 2002) with overlapping expression of many genes in the same cell type, including guard cells (Winter et al., 2007). The mechanism described here could represent a more general principle present in plants and possibly other eukaryotes contributing to Ca^{2+}-specificity within cellular signaling while also maintaining the availability of Ca^{2+}-sensors for distinct Ca^{2+}-dependent signaling outputs." (Brandt et al., 2014)

6 Abbreviations

A-	Anion
ABA	abscisic acid
ABI	ABA-INSENSITIVE
AKT1	ARABIDOPSIS K^+ TRANSPORTER 1
AKT2	ARABIDOPSIS K^+ TRANSPORTER 2
AKT3	ARABIDOPSIS K^+ TRANSPORTER 3
ALMT12	ALUMINUM-ACTIVATED MALATE TRANSPORTER 12
BLUS1	BLUE LIGHT SIGNALING 1
$[Ca^{2+}]_{cyt}$	cytosolic calcium concentration
CAD	CPK activation domain
CaM	CALMODULIN
CBL	CALCINEURIN B-LIKE
C_i	cytosolic CO_2 concentration
CML	CALMODULIN LIKE
CPK	Ca^{2+}-DEPENDENT PROTEIN KINASE
ELISA	enzyme-linked immunosorbent assay
FRET	Förster resonance energy transfer
GCA2	GROWTH CONTROLLED BY ABSCISSIC ACID 2
GORK	GATED OUTWARDLY-RECTIFYING K^+ CHANNEL
H^+-ATPase	ATP-driven proton pump
I_{ca}	Ca^{2+}-permeable plasma membrane localized channels
K_{in}	inward-rectifying K^+-channels
K_{out}	outward-rectifying K^+-channels
KAT1	POTASSIUM CHANNEL IN ARABIDOPSIS THALIANA 1
KAT2	POTASSIUM CHANNEL IN ARABIDOPSIS THALIANA 1
OST1	OPEN STOMATA 1
PHOT1	PHOTOTROPIN 1
PHOT2	PHOTOTROPIN 2
PP2C	clade A protein phosphatase 2C
PP2CA	PROTEIN PHOSPHATASE 2CA
PYR1	PYRABACTIN RESISTANCE 1
PYL	PYR1-LIKE
QUAC1	QUICKLY-ACTIVATING ANION CHANNEL 1
Rboh	RESPIRATORY BURST OXIDASE PROTEIN
RCAR	REGULATORY COMPONENT OF ABA RECEPTOR
ROS	reactive oxygen species
SLAC1	SLOW ANION CHANNEL ASSOCIATED 1
SLAC1-CT	C-terminal cytosolic domain of SLAC1
SLAC1-NT	N-terminal cytosolic domain of SLAC1
SLAH3	SLAC1 HOMOLOGUE 3
SnRK2	SNF1-RELATED KINASE 2

7 References

Acharya, B. R., B. W. Jeon, W. Zhang and S. M. Assmann (2013). "Open Stomata 1 (OST1) is limiting in abscisic acid responses of Arabidopsis guard cells." New Phytologist **200**(4): 1049–1063.

Ache, P., D. Becker, N. Ivashikina, P. Dietrich, M. R. G. Roelfsema and R. Hedrich (2000). "GORK, a delayed outward rectifier expressed in guard cells of *Arabidopsis thaliana*, is a K^+-selective, K^+-sensing ion channel." FEBS Letters **486**(2): 93-98.

Allen, G. J., S. P. Chu, C. L. Harrington, K. Schumacher, T. Hoffmann, Y. Y. Tang, E. Grill and J. I. Schroeder (2001). "A defined range of guard cell calcium oscillation parameters encodes stomatal movements." Nature **411**(6841): 1053-1057.

Allen, G. J., K. Kuchitsu, S. P. Chu, Y. Murata and J. I. Schroeder (1999). "Arabidopsis *abi1-1* and *abi2-1* Phosphatase Mutations Reduce Abscisic Acid–Induced Cytoplasmic Calcium Rises in Guard Cells." Plant Cell **11**(9): 1785-1798.

Allen, G. J., J. M. Kwak, S. P. Chu, J. Llopis, R. Y. Tsien, J. F. Harper and J. I. Schroeder (1999). "Cameleon calcium indicator reports cytoplasmic calcium dynamics in *Arabidopsis* guard cells." Plant Journal **19**(6): 735-747.

Allen, G. J., Y. Murata, S. P. Chu, M. Nafisi and J. I. Schroeder (2002). "Hypersensitivity of Abscisic Acid–Induced Cytosolic Calcium Increases in the *Arabidopsis* Farnesyltransferase Mutant *era1-2*." Plant Cell **14**(7): 1649-1662.

Assmann, S. M., L. Simoncini and J. I. Schroeder (1985). "Blue light activates electrogenic ion pumping in guard cell protoplasts of *Vicia faba*." Nature **318**(6043): 285-287.

Becker, D., S. Hoth, P. Ache, S. Wenkel, M. R. G. Roelfsema, O. Meyerhoff, W. Hartung and R. Hedrich (2003). "Regulation of the ABA-sensitive Arabidopsis potassium channel gene GORK in response to water stress." FEBS Letters **554**(1-2): 119-126.

Belin, C., P.-O. de Franco, C. Bourbousse, S. Chaignepain, J.-M. Schmitter, A. Vavasseur, J. Giraudat, H. Barbier-Brygoo and S. Thomine (2006). "Identification of Features Regulating OST1 Kinase Activity and OST1 Function in Guard Cells." Plant Physiol. **141**(4): 1316-1327.

Boudsocq, M., H. Barbier-Brygoo and C. Laurière (2004). "Identification of Nine Sucrose Nonfermenting 1-related Protein Kinases 2 Activated by Hyperosmotic and Saline Stresses in *Arabidopsis thaliana*." Journal of Biological Chemistry **279**(40): 41758-41766.

Boudsocq, M., M.-J. Droillard, H. Barbier-Brygoo and C. Laurière (2007). "Different phosphorylation mechanisms are involved in the activation of sucrose non-fermenting 1 related protein kinases 2 by osmotic stresses and abscisic acid." Plant Molecular Biology **63**(4): 491-503.

Boudsocq, M., M.-J. Droillard, L. Regad and C. Lauriere (2012). "Characterization of Arabidopsis calcium-dependent protein kinases: activated or not by calcium?" Biochemical Journal **447**: 291-299.

Boudsocq, M. and J. Sheen (2012). "CDPKs in immune and stress signaling." Trends in Plant Science **18**(1): 30-40.

Boudsocq, M., M. R. Willmann, M. McCormack, H. Lee, L. Shan, P. He, J. Bush, S.-H. Cheng and J. Sheen (2010). "Differential innate immune signalling via Ca^{2+} sensor protein kinases." Nature **464**(7287): 418-422.

Boyer, J. S., S. C. Wong and G. D. Farquhar (1997). "CO_2 and Water Vapor Exchange across Leaf Cuticle (Epidermis) at Various Water Potentials." Plant Physiology **114**(1): 185-191.

Brandt, B., D. E. Brodsky, S. Xue, J. Negi, K. Iba, J. Kangasjärvi, M. Ghassemian, A. B. Stephan, H. Hu and J. I. Schroeder (2012). "Reconstitution of abscisic acid activation of SLAC1 anion channel by CPK6 and OST1 kinases and branched ABI1 PP2C phosphatase action." Proceedings of the National Academy of Sciences **109**(26): 10593-10598.

Brandt, B., S. Munemasa, C. Wang, D. Nguyen, T. Belknap, F. Aleman, J. I. Schroeder (2014). “Calcium Specificity Mechanism within ABA-dependent Signal Transduction in *Arabidopsis thaliana*.” submitted

Chen, Y.-h., L. Hu, M. Punta, R. Bruni, B. Hillerich, B. Kloss, B. Rost, J. Love, S. A. Siegelbaum and W. A. Hendrickson (2010). "Homologue structure of the SLAC1 anion channel for closing stomata in leaves." Nature **467**(7319): 1074-1080.

Chen, Z. H., A. Hills, C. K. Lim and M. R. Blatt (2010). "Dynamic regulation of guard cell anion channels by cytosolic free Ca^{2+} concentration and protein phosphorylation." Plant Journal **61**(5): 816-825.

Christmann, A., T. Hoffmann, I. Teplova, E. Grill and A. Muller (2005). "Generation of Active Pools of Abscisic Acid Revealed by *In Vivo* Imaging of Water-Stressed *Arabidopsis*." Plant Physiology **137**(1): 209-219.

Christmann, A., E. W. Weiler, E. Steudle and E. Grill (2007). "A hydraulic signal in root-to-shoot signalling of water shortage." The Plant Journal **52**(1): 167-174.

Cousson, A. and A. Vavasseur (1998). "Putative involvement of cytosolic Ca^{2+} and GTP-binding proteins in cyclic-GMP-mediated induction of stomatal opening by auxin in *Commelina communis L*." Planta **206**(2): 308-314.

Curvetto, N., L. Darjania and S. Delmastro (1994). "Effect of 2 cAMP analogs on stomatal opening in *Vicia Faba*. Possible relationship with cytosolic calcium-concentration." Plant Physiology and Biochemistry **32**(3): 365-372.

Day, I. S., V. S. Reddy, G. S. Ali and A. S. N. Reddy (2002). "Analysis of EF-hand-containing proteins in *Arabidopsis*." Genome Biology **3**(10): research0056.0051–research0056.0024.

De Silva, D. L. R., R. C. Cox, A. M. Hetherington and T. A. Mansfield (1985). "Suggested Involvement of Calcium and Calmodulin in the Responses of Stomata to Abscisic Acid." New Phytologist **101**(4): 555-563.

Dubiella, U., H. Seybold, G. Durian, E. Komander, R. Lassig, C.-P. Witte, W. X. Schulze and T. Romeis (2013). "Calcium-dependent protein kinase/NADPH oxidase activation circuit is required for rapid defense signal propagation." Proceedings of the National Academy of Sciences **110**(21): 8744-8749.

FAO (Food and Agriculture Organization of the United Nations). 2011. The State of the World’s Land and Water Resources: Managing Systems at Risk. London/Rome, Earthscan/FAO.

FAO (Food and Agriculture Organization of the United Nations). 2012. World Agriculture Towards 2030/2050: The 2012 Revision. N. Alexandratos and J. Bruinsma, ESA Working paper No. 12-03. Rome, FAO.

FAO (Food and Agriculture Organization of the United Nations). 2013. FAO World Hunger Map. Rome, FAO.

Fuchs, S., E. Grill, I. Meskiene and A. Schweighofer (2013). "Type 2C protein phosphatases in plants." FEBS Journal **280**(2): 681-693.

Fuchs, S., S. V. Tischer, C. Wunschel, A. Christmann and E. Grill (2014). "Abscisic acid sensor RCAR7/PYL13, specific regulator of protein phosphatase coreceptors." Proceedings of the National Academy of Sciences **111**(15): 5741-5746.

Fujii, H., V. Chinnusamy, A. Rodrigues, S. Rubio, R. Antoni, S.-Y. Park, S. R. Cutler, J. Sheen, P. L. Rodriguez and J.-K. Zhu (2009). "*In vitro* reconstitution of an abscisic acid signalling pathway." Nature **462**(7273): 660-664.

Fujii, H., P. E. Verslues and J.-K. Zhu (2007). "Identification of Two Protein Kinases Required for Abscisic Acid Regulation of Seed Germination, Root Growth, and Gene Expression in *Arabidopsis*." Plant Cell **19**(2): 485-494.

Fujii, H. and J.-K. Zhu (2009). "Arabidopsis mutant deficient in 3 abscisic acid-activated protein kinases reveals critical roles in growth, reproduction, and stress." Proceedings of the National Academy of Sciences **106**(20): 8380-8385.

Fujita, Y., K. Nakashima, T. Yoshida, T. Katagiri, S. Kidokoro, N. Kanamori, T. Umezawa, M. Fujita, K. Maruyama, K. Ishiyama, M. Kobayashi, S. Nakasone, K. Yamada, T. Ito, K. Shinozaki and K.

Yamaguchi-Shinozaki (2009). "Three SnRK2 Protein Kinases are the Main Positive Regulators of Abscisic Acid Signaling in Response to Water Stress in Arabidopsis." Plant Cell Physiol. **50**(12): 2123-2132.

Gao, X., X. Chen, W. Lin, S. Chen, D. Lu, Y. Niu, L. Li, C. Cheng, M. McCormack, J. Sheen, L. Shan and P. He (2013). "Bifurcation of *Arabidopsis* NLR Immune Signaling via Ca^{2+}-Dependent Protein Kinases." PLoS Pathogen **9**(1): e1003127.

Geiger, D., T. Maierhofer, K. A. S. AL-Rasheid, S. Scherzer, P. Mumm, A. Liese, P. Ache, C. Wellmann, I. Marten, E. Grill, T. Romeis and R. Hedrich (2011). "Stomatal Closure by Fast Abscisic Acid Signaling Is Mediated by the Guard Cell Anion Channel SLAH3 and the Receptor RCAR1." Science Signaling **4**(173): ra32.

Geiger, D., S. Scherzer, P. Mumm, I. Marten, P. Ache, S. Matschi, A. Liese, C. Wellmann, K. A. S. Al-Rasheid, E. Grill, T. Romeis and R. Hedrich (2010). "Guard cell anion channel SLAC1 is regulated by CDPK protein kinases with distinct Ca^{2+} affinities." Proceedings of the National Academy of Sciences **107**: 8023–8028.

Geiger, D., S. Scherzer, P. Mumm, A. Stange, I. Marten, H. Bauer, P. Ache, S. Matschi, A. Liese, K. A. S. Al-Rasheid, T. Romeis and R. Hedrich (2009). "Activity of guard cell anion channel SLAC1 is controlled by drought-stress signaling kinase-phosphatase pair." Proceedings of the National Academy of Sciences **106**(50): 21425-21430.

Gonzalez-Guzman, M., G. A. Pizzio, R. Antoni, F. Vera-Sirera, E. Merilo, G. W. Bassel, M. A. Fernández, M. J. Holdsworth, M. A. Perez-Amador, H. Kollist and P. L. Rodriguez (2012). "Arabidopsis PYR/PYL/RCAR Receptors Play a Major Role in Quantitative Regulation of Stomatal Aperture and Transcriptional Response to Abscisic Acid." The Plant Cell Online **24**(6): 2483-2496.

Grabov, A. and M. R. Blatt (1998). "Membrane voltage initiates Ca^{2+} waves and potentiates Ca^{2+} increases with abscisic acid in stomatal guard cells." Proceedings of the National Academy of Sciences **95**(8): 4778-4783.

Grabov, A. and M. R. Blatt (1999). "A Steep Dependence of Inward-Rectifying Potassium Channels on Cytosolic Free Calcium Concentration Increase Evoked by Hyperpolarization in Guard Cells." Plant Physiol. **119**(1): 277-288.

Hao, Q., P. Yin, W. Li, L. Wang, C. Yan, Z. Lin, Jim Z. Wu, J. Wang, S. F. Yan and N. Yan (2011). "The Molecular Basis of ABA-Independent Inhibition of PP2Cs by a Subclass of PYL Proteins." Molecular Cell **42**(5): 662-672.

Harris, M. J. and W. H. Outlaw (1991). "Rapid Adjustment of Guard-Cell Abscisic Acid Levels to Current Leaf-Water Status." Plant Physiology **95**(1): 171-173.

Harris, M. J., W. H. Outlaw, R. Mertens and E. W. Weiler (1988). "Water-stress-induced changes in the abscisic acid content of guard cells and other cells of Vicia faba L. leaves as determined by enzyme-amplified immunoassay." Proceedings of the National Academy of Sciences **85**(8): 2584-2588.

Hauser, F., R. Waadt and Julian I. Schroeder (2011). "Evolution of Abscisic Acid Synthesis and Signaling Mechanisms." Current Biology **21**(9): R346-R355.

Hedrich, R., H. Busch and K. Raschke (1990). "Ca^{2+} and nucleotide dependent regulation of voltage dependent anion channels in the plasma membrane of guard cells." Embo Journal **9**(12): 3889-3892.

Hetherington, A. M. (2001). "Guard Cell Signaling." Cell **107**(6): 711-714.

Hetherington, A. M. and F. I. Woodward (2003). "The role of stomata in sensing and driving environmental change." Nature **424**(6951): 901-908.

Hosy, E., A. Vavasseur, K. Mouline, I. Dreyer, F. Gaymard, F. Poree, J. Boucherez, A. Lebaudy, D. Bouchez, A.-A. Very, T. Simonneau, J.-B. Thibaud and H. Sentenac (2003). "The Arabidopsis outward K^+ channel GORK is involved in regulation of stomatal movements and plant transpiration." Proceedings of the National Academy of Sciences **100**(9): 5549-5554.

Hrabak, E. M., C. W. M. Chan, M. Gribskov, J. F. Harper, J. H. Choi, N. Halford, J. Kudla, S. Luan, H. G. Nimmo, M. R. Sussman, M. Thomas, K. Walker-Simmons, J.-K. Zhu and A. C. Harmon

(2003). "The Arabidopsis CDPK-SnRK Superfamily of Protein Kinases." Plant Physiol. **132**(2): 666-680.

Hubbard, K. E., R. S. Siegel, G. Valerio, B. Brandt and J. I. Schroeder (2012). "Abscisic acid and CO_2 signalling via calcium sensitivity priming in guard cells, new CDPK mutant phenotypes and a method for improved resolution of stomatal stimulus–response analyses." Annals of Botany **109**(1): 5-17.

Ikegami, K., M. Okamoto, M. Seo and T. Koshiba (2009). "Activation of abscisic acid biosynthesis in the leaves of Arabidopsis thaliana in response to water deficit." Journal of Plant Research **122**(2): 235-243.

Imes, D., P. Mumm, J. Böhm, K. A. S. Al-Rasheid, I. Marten, D. Geiger and R. Hedrich (2013). "Open STomata Kinase OST1 controls R-type anion channel QUAC1 in Arabidopsis guard cells." Plant Journal **34**(3): 372-382.

Inoue, S.-i., T. Kinoshita, M. Matsumoto, K. I. Nakayama, M. Doi and K.-i. Shimazaki (2008). "Blue light-induced autophosphorylation of phototropin is a primary step for signaling." Proceedings of the National Academy of Sciences **105**(14): 5626-5631.

IPCC (Intergovernmental Panel on Climate Change). 2008. Climate Change and Water. Technical Paper VI. B.C. Bates, Z.W., Kundzewicz, S. Wu and J.P. Palutikof (eds). Geneva, IPCC Secretariat.

Irving, H. R., C. A. Gehring and R. W. Parish (1992). "Changes in cytosolic pH and calcium of guard cells precede stomatal movements." Proceedings of the National Academy of Sciences **89**(5): 1790-1794.

Ito, T., M. Nakata, J. Fukazawa, S. Ishida and Y. Takahashi (2010). "Alteration of Substrate Specificity: The Variable N-Terminal Domain of Tobacco Ca^{2+}-Dependent Protein Kinase Is Important for Substrate Recognition." Plant Cell **22**(5): 1592-1604.

John A. Raven (2002). "Selection pressures on stomatal evolution." New Phytologist **153**(3): 371-386.

Jones, A. M., J. A. H. Danielson, S. N. ManojKumar, V. Lanquar, G. Grossmann and W. B. Frommer (2014). "Abscisic acid dynamics in roots detected with genetically encoded FRET sensors." Elife **3**.

Kelly, W. B., J. E. Esser and J. I. Schroeder (1995). "Effects Of Cytosolic Calcium And Limited, Possible Dual, Effects Of G-Protein Modulators On Guard-Cell Inward Potassium Channels." Plant Journal **8**(4): 479-489.

Kim, T.-H., M. Böhmer, H. Hu, N. Nishimura and J. I. Schroeder (2010). "Guard Cell Signal Transduction Network: Advances in Understanding Abscisic Acid, CO_2, and Ca^{2+} Signaling." Annual Review of Plant Biology **61**(1).

Kimura, S., H. Kaya, T. Kawarazaki, G. Hiraoka, E. Senzaki, M. Michikawa and K. Kuchitsu (2012). "Protein phosphorylation is a prerequisite for the Ca2+-dependent activation of Arabidopsis NADPH oxidases and may function as a trigger for the positive feedback regulation of Ca2+ and reactive oxygen species." Biochimica et Biophysica Acta (BBA) - Molecular Cell Research **1823**(2): 398-405.

Kinoshita, T., M. Doi, N. Suetsugu, T. Kagawa, M. Wada and K. Shimazaki (2001). "phot1 and phot2 mediate blue light regulation of stomatal opening." Nature **414**(6864): 656-660.

Kinoshita, T., T. Emi, M. Tominaga, K. Sakamoto, A. Shigenaga, M. Doi and K.-i. Shimazaki (2003). "Blue-Light- and Phosphorylation-Dependent Binding of a 14-3-3 Protein to Phototropins in Stomatal Guard Cells of Broad Bean." Plant Physiology **133**(4): 1453-1463.

Kinoshita, T., M. Nishimura and K. Shimazaki (1995). "Cytosolic Concentration of Ca2+ Regulates the Plasma Membrane H+-ATPase in Guard Cells of Fava Bean." Plant Cell **7**(8): 1333-1342.

Klüsener, B., J. J. Young, Y. Murata, G. J. Allen, I. C. Mori, V. Hugouvieux and J. I. Schroeder (2002). "Convergence of Calcium Signaling Pathways of Pathogenic Elicitors and Abscisic Acid in Arabidopsis Guard Cells." Plant Physiology **130**(4): 2152-2163.

Kollist, H., M. Nuhkat and M. R. G. Roelfsema (2014). "Closing gaps: linking elements that control stomatal movement." New Phytologist **203**(1): 44-62.

Kwak, J. M., I. C. Mori, Z. M. Pei, N. Leonhardt, M. A. Torres, J. L. Dangl, R. E. Bloom, S. Bodde, J. D. G. Jones and J. I. Schroeder (2003). "NADPH oxidase AtrbohD and AtrbohF genes function in ROS-dependent ABA signaling in Arabidopsis." Embo Journal **22**(11): 2623-2633.

Kwak, J. M., Y. Murata, V. M. Baizabal-Aguirre, J. Merrill, M. Wang, A. Kemper, S. D. Hawke, G. Tallman and J. I. Schroeder (2001). "Dominant Negative Guard Cell K^+ Channel Mutants Reduce Inward-Rectifying K^+ Currents and Light-Induced Stomatal Opening in Arabidopsis." Plant Physiology **127**(2): 473-485.

Laanemets, K., B. Brandt, J. Li, E. Merilo, Y.-F. Wang, M. M. Keshwani, S. S. Taylor, H. Kollist and J. I. Schroeder (2013). "Calcium-Dependent and -Independent Stomatal Signaling Network and Compensatory Feedback Control of Stomatal Opening via Ca^{2+} Sensitivity Priming." Plant Physiology **163**(2): 504-513.

Lee, S. C., W. Lan, B. B. Buchanan and S. Luan (2009). "A protein kinase-phosphatase pair interacts with an ion channel to regulate ABA signaling in plant guard cells." Proceedings of the National Academy of Sciences **106**(50): 21419-21424.

Levchenko, V., K. R. Konrad, P. Dietrich, M. R. G. Roelfsema and R. Hedrich (2005). "Cytosolic abscisic acid activates guard cell anion channels without preceding Ca^{2+} signals." Proceedings of the National Academy of Sciences **102**(11): 4203-4208.

Liese, A. and T. Romeis (2013). "Biochemical regulation of in vivo function of plant calcium-dependent protein kinases (CDPK)." Biochimica et Biophysica Acta (BBA) - Molecular Cell Research **1833**(7): 1582-1589.

M. Rob G. Roelfsema and Rainer Hedrich (2005). "In the light of stomatal opening: new insights into 'the Watergate'." New Phytologist **167**(3): 665-691.

Ma, S.-Y. and W.-H. Wu (2007). "AtCPK23 functions in Arabidopsis responses to drought and salt stresses." Plant Molecular Biology **65**(4): 511-518.

Ma, Y., I. Szostkiewicz, A. Korte, D. Moes, Y. Yang, A. Christmann and E. Grill (2009). "Regulators of PP2C Phosphatase Activity Function as Abscisic Acid Sensors." Science **324**(5930): 1064-1068.

MacRobbie, E. A. C. (2000). "ABA activates multiple Ca^{2+} fluxes in stomatal guard cells, triggering vacuolar $K^+(Rb^+)$ release." Proceedings of the National Academy of Sciences **97**(22): 12361-12368.

Marten, H., K. R. Konrad, P. Dietrich, M. R. G. Roelfsema and R. Hedrich (2007). "Ca^{2+}-dependent and -independent abscisic acid activation of plasma membrane anion channels in guard cells of Nicotiana tabacum." Plant Physiology **143**: 28-37.

McAinsh, M. R., C. Brownlee and A. M. Hetherington (1990). "Abscisic acid-induced elevation of guard cell cytosolic Ca^{2+} precedes stomatal closure." Nature **343**(6254): 186-188.

Melcher, K., L.-M. Ng, X. E. Zhou, F.-F. Soon, Y. Xu, K. M. Suino-Powell, S.-Y. Park, J. J. Weiner, H. Fujii, V. Chinnusamy, A. Kovach, J. Li, Y. Wang, J. Li, F. C. Peterson, D. R. Jensen, E.-L. Yong, B. F. Volkman, S. R. Cutler, J.-K. Zhu and H. E. Xu (2009). "A gate-latch-lock mechanism for hormone signalling by abscisic acid receptors." Nature **462**(7273): 602-608.

Melotto, M., W. Underwood, J. Koczan, K. Nomura and S. Y. He (2006). "Plant Stomata Function in Innate Immunity against Bacterial Invasion." Cell **126**(5): 969-980.

Merilo, E., K. Laanemets, H. Hu, S. Xue, L. Jakobson, I. Tulva, M. Gonzalez-Guzman, P. L. Rodriguez, J. I. Schroeder, M. Brosche and H. Kollist (2013). "PYR/RCAR Receptors Contribute to Ozone-, Reduced Air Humidity-, Darkness- and CO_2-Induced Stomatal Regulation." Plant Physiology.

Merlot, S., F. Gosti, D. Guerrier, A. Vavasseur and J. Giraudat (2001). "The ABI1 and ABI2 protein phosphatases 2C act in a negative feedback regulatory loop of the abscisic acid signalling pathway." The Plant Journal **25**(3): 295-303.

Merlot, S., A. C. Mustilli, B. Genty, H. North, V. Lefebvre, B. Sotta, A. Vavasseur and J. Giraudat (2002). "Use of infrared thermal imaging to isolate Arabidopsis mutants defective in stomatal regulation." Plant Journal **30**(5): 601-609.

Meyer, S., P. Mumm, D. Imes, A. Endler, B. Weder, K. A. Al-Rasheid, D. Geiger, I. Marten, E. Martinoia and R. Hedrich (2010). "AtALMT12 represents an R-type anion channel required for stomatal movement in Arabidopsis guard cells." The Plant Journal **63**(6): 1054–1062.

Miyakawa, T., Y. Fujita, K. Yamaguchi-Shinozaki and M. Tanokura (2013). "Structure and function of abscisic acid receptors." Trends in Plant Science **18**(5): 259-266.

Miyazono, K.-i., T. Miyakawa, Y. Sawano, K. Kubota, H.-J. Kang, A. Asano, Y. Miyauchi, M. Takahashi, Y. Zhi, Y. Fujita, T. Yoshida, K.-S. Kodaira, K. Yamaguchi-Shinozaki and M. Tanokura (2009). "Structural basis of abscisic acid signalling." Nature **462**(7273): 609-614.

Mori, I. C., Y. Murata, Y. Yang, S. Munemasa, Y.-F. Wang, S. Andreoli, H. Tiriac, J. M. Alonso, J. F. Harper, J. R. Ecker, J. M. Kwak and J. I. Schroeder (2006). "CDPKs CPK6 and CPK3 Function in ABA Regulation of Guard Cell S-Type Anion- and Ca^{2+}- Permeable Channels and Stomatal Closure." PLoS Biology **4**(10): e327.

Munemasa, S., M. A. Hossain, Y. Nakamura, I. C. Mori and Y. Murata (2011). "The Arabidopsis Calcium-Dependent Protein Kinase, CPK6, Functions as a Positive Regulator of Methyl Jasmonate Signaling in Guard Cells." Plant Physiology **155**(1): 553-561.

Murata, Y., Z.-M. Pei, I. C. Mori and J. Schroeder (2001). "Abscisic Acid Activation of Plasma Membrane Ca^{2+} Channels in Guard Cells Requires Cytosolic NAD(P)H and Is Differentially Disrupted Upstream and Downstream of Reactive Oxygen Species Production in *abi1-1* and *abi2-1* Protein Phosphatase 2C Mutants." Plant Cell **13**(11): 2513-2523.

Mustilli, A.-C., S. Merlot, A. Vavasseur, F. Fenzi and J. Giraudat (2002). "Arabidopsis OST1 Protein Kinase Mediates the Regulation of Stomatal Aperture by Abscisic Acid and Acts Upstream of Reactive Oxygen Species Production." Plant Cell **14**(12): 3089-3099.

Nakashima, K., Y. Fujita, N. Kanamori, T. Katagiri, T. Umezawa, S. Kidokoro, K. Maruyama, T. Yoshida, K. Ishiyama, M. Kobayashi, K. Shinozaki and K. Yamaguchi-Shinozaki (2009). "Three Arabidopsis SnRK2 Protein Kinases, SRK2D/SnRK2.2, SRK2E/SnRK2.6/OST1 and SRK2I/SnRK2.3, Involved in ABA Signaling are Essential for the Control of Seed Development and Dormancy." Plant Cell Physiology **50**(7): 1345-1363.

Negi, J., O. Matsuda, T. Nagasawa, Y. Oba, H. Takahashi, M. Kawai-Yamada, H. Uchimiya, M. Hashimoto and K. Iba (2008). "CO_2 regulator SLAC1 and its homologues are essential for anion homeostasis in plant cells." Nature **452**(7186): 483-486.

Ng, L.-M., F.-F. Soon, X. E. Zhou, G. M. West, A. Kovach, K. M. Suino-Powell, M. J. Chalmers, J. Li, E.-L. Yong, J.-K. Zhu, P. R. Griffin, K. Melcher and H. E. Xu (2011). "Structural basis for basal activity and autoactivation of abscisic acid (ABA) signaling SnRK2 kinases." Proceedings of the National Academy of Sciences **108**(52): 21259-21264.

Park, S.-Y., P. Fung, N. Nishimura, D. R. Jensen, H. Fujii, Y. Zhao, S. Lumba, J. Santiago, A. Rodrigues, T.-f. F. Chow, S. E. Alfred, D. Bonetta, R. Finkelstein, N. J. Provart, D. Desveaux, P. L. Rodriguez, P. McCourt, J.-K. Zhu, J. I. Schroeder, B. F. Volkman and S. R. Cutler (2009). "Abscisic Acid Inhibits Type 2C Protein Phosphatases via the PYR/PYL Family of START Proteins." Science **324**(5930): 1068-1071.

Pei, Z.-M., Y. Murata, G. Benning, S. Thomine, B. Klusener, G. J. Allen, E. Grill and J. I. Schroeder (2000). "Calcium channels activated by hydrogen peroxide mediate abscisic acid signalling in guard cells." Nature **406**(6797): 731-734.

Pei, Z. M., K. Kuchitsu, J. M. Ward, M. Schwarz and J. I. Schroeder (1997). "Differential Abscisic Acid Regulation of Guard Cell Slow Anion Channels in Arabidopsis Wild-Type and *abi1* and *abi2* Mutants." Plant Cell **9**(3): 409-423.

Roelfsema, M. R. G., S. Hanstein, H. H. Felle and R. Hedrich (2002). "CO_2 provides an intermediate link in the red light response of guard cells." Plant Journal **32**(1): 65-75.

Santiago, J., A. Rodrigues, A. Saez, S. Rubio, R. Antoni, F. Dupeux, S.-Y. Park, J. A. Márquez, S. R. Cutler and P. L. Rodriguez (2009). "Modulation of drought resistance by the abscisic acid receptor PYL5 through inhibition of clade A PP2Cs." The Plant Journal **60**(4): 575-588.

Sato, A., Y. Sato, Y. Fukao, M. Fujiwara, T. Umezawa, K. Shinozaki, T. Hibi, M. Taniguchi, H. Miyake, D. B. Goto and N. Uozumi (2009). "Threonine at position 306 of the KAT1 potassium channel is essential for channel activity and is a target site for ABA-activated SnRK2/OST1/SnRK2.6 protein kinase." Biochemical Journal **424**: 439-448.

Sauter, A., W. J. Davies and W. Hartung (2001). "The long-distance abscisic acid signal in the droughted plant: the fate of the hormone on its way from root to shoot." Journal of Experimental Botany **52**(363): 1991-1997.

Scherzer, S., T. Maierhofer, K. A. S. Al-Rasheid, D. Geiger and R. Hedrich (2012). "Multiple Calcium-Dependent Kinases Modulate ABA-Activated Guard Cell Anion Channels." Molecular Plant.

Schmidt, C., I. Schelle, Y. J. Liao and J. I. Schroeder (1995). "Strong regulation of slow anion channels and abscisic acid signaling in guard cells by phosphorylation and dephosphorylation events." Proceedings of the National Academy of Sciences of the United States of America **92**(21): 9535-9539.

Schroeder, J. I. and S. Hagiwara (1989). "Cytosolic calcium regulates ion channels in the plasma membrane of Vicia faba guard cells." Nature **338**(6214): 427-430.

Schroeder, J. I. and S. Hagiwara (1990). "Repetitive Increases In Cytosolic Ca^{2+} Of Guard-Cells By Abscisic-Acid Activation Of Nonselective Ca^{2+} Permeable Channels." Proceedings of the National Academy of Sciences **87**(23): 9305-9309.

Schroeder, J. I., K. Raschke and E. Neher (1987). "Voltage Dependence Of K^+ Channels In Guard-Cell Protoplasts." Proceedings of the National Academy of Sciences **84**(12): 4108-4112.

Schwartz, A. (1985). "Role of Ca^{2+} and EGTA on Stomatal Movements in Commelina communis L." Plant Physiology **79**(4): 1003-1005.

Shimazaki, K.-i., M. Doi, S. M. Assmann and T. Kinoshita (2007). "Light Regulation of Stomatal Movement." Annual Review of Plant Biology **58**(1): 219-247.

Shimazaki, K.-i., T. Kinoshita and M. Nishimura (1992). "Involvement of Calmodulin and Calmodulin-Dependent Myosin Light Chain Kinase in Blue Light-Dependent H+ Pumping by Guard Cell Protoplasts from Vicia faba L." Plant Physiology **99**(4): 1416-1421.

Shimazaki, K.-i., M. Tominaga and A. Shigenaga (1997). "Inhibition of the Stomatal Blue Light Response by Verapamil at High Concentration." Plant and Cell Physiology **38**(6): 747-750.

Siegel, R. S., S. Xue, Y. Murata, Y. Yang, N. Nishimura, A. Wang and J. I. Schroeder (2009). "Calcium elevation-dependent and attenuated resting calcium-dependent abscisic acid induction of stomatal closure and abscisic acid-induced enhancement of calcium sensitivities of S-type anion and inward-rectifying K^+ channels in Arabidopsis guard cells." The Plant Journal **59**(2): 207-220.

Sirichandra, C., D. Gu, H.-C. Hu, M. Davanture, S. Lee, M. Djaoui, B. Valot, M. Zivy, J. Leung, S. Merlot and J. M. Kwak (2009). "Phosphorylation of the Arabidopsis AtrbohF NADPH oxidase by OST1 protein kinase." FEBS Letters **583**(18): 2982-2986.

Staxén, I., C. Pical, L. T. Montgomery, J. E. Gray, A. M. Hetherington and M. R. McAinsh (1999). "Abscisic acid induces oscillations in guard-cell cytosolic free calcium that involve phosphoinositide-specific phospholipase C." Proceedings of the National Academy of Sciences **96**(4): 1779-1784.

Szostkiewicz, I., K. Richter, M. Kepka, S. Demmel, Y. Ma, A. Korte, F. F. Assaad, A. Christmann and E. Grill (2010). "Closely related receptor complexes differ in their ABA selectivity and sensitivity." The Plant Journal **61**(1): 25-35.

Takemiya, A., N. Sugiyama, H. Fujimoto, T. Tsutsumi, S. Yamauchi, A. Hiyama, Y. Tada, J. M. Christie and K.-i. Shimazaki (2013). "Phosphorylation of BLUS1 kinase by phototropins is a primary step in stomatal opening." Nature Communications **4**.

Umezawa, T., N. Sugiyama, M. Mizoguchi, S. Hayashi, F. Myouga, K. Yamaguchi-Shinozaki, Y. Ishihama, T. Hirayama and K. Shinozaki (2009). "Type 2C protein phosphatases directly regulate abscisic acid-activated protein kinases in *Arabidopsis*." Proceedings of the National Academy of Sciences **106**(41): 17588-17593.

Umezawa, T., R. Yoshida, K. Maruyama, K. Yamaguchi-Shinozaki and K. Shinozaki (2004). "SRK2C, a SNF1-related protein kinase 2, improves drought tolerance by controlling stress-responsive gene expression in Arabidopsis thaliana." Proceedings of the National Academy of Sciences **101**(49): 17306-17311.

UNDESA (United Nations Department of Economic and Social Affairs). 2012. World Urbanization Prospects, The 2011 Revision: Highlights. New York, UN

Vahisalu, T., H. Kollist, Y.-F. Wang, N. Nishimura, W.-Y. Chan, G. Valerio, A. Lamminmaki, M. Brosche, H. Moldau, R. Desikan, J. I. Schroeder and J. Kangasjarvi (2008). "SLAC1 is required for plant guard cell S-type anion channel function in stomatal signalling." Nature **452**(7186): 487-491.

Vahisalu, T., I. Puzõrjova, M. Brosché, E. Valk, M. Lepiku, H. Moldau, P. Pechter, Y.-S. Wang, O. Lindgren, J. Salojärvi, M. Loog, J. Kangasjärvi and H. Kollist (2010). "Ozone-triggered rapid stomatal response involves the production of reactive oxygen species, and is controlled by SLAC1 and OST1." The Plant Journal **62**(3): 442-453.

Waadt, R., K. Hitomi, N. Nishimura, C. Hitomi, S. R. Adams, E. D. Getzoff and J. I. Schroeder (2014). "FRET-based reporters for the direct visualization of abscisic acid concentration changes and distribution in Arabidopsis." Elife **3**.

Wang, Y., Z.-H. Chen, B. Zhang, A. Hills and M. R. Blatt (2013). "PYR/PYL/RCAR Abscisic Acid Receptors Regulate K^+ and Cl^- Channels through Reactive Oxygen Species-Mediated Activation of Ca^{2+} Channels at the Plasma Membrane of Intact Arabidopsis Guard Cells." Plant Physiology **163**(2): 566-577.

Wilkinson, S. and W. J. Davies (2002). "ABA-based chemical signalling: the co-ordination of responses to stress in plants." Plant, Cell & Environment **25**(2): 195-210.

Winter, D., B. Vinegar, H. Nahal, R. Ammar, G. V. Wilson and N. J. Provart (2007). "An “Electronic Fluorescent Pictograph” Browser for Exploring and Analyzing Large-Scale Biological Data Sets." PLoS ONE **2**(8): e718.

Xue, S., H. Hu, A. Ries, E. Merilo, H. Kollist and J. I. Schroeder (2011). "Central functions of bicarbonate in S-type anion channel activation and OST1 protein kinase in CO_2 signal transduction in guard cell." EMBO J **30**(8): 1645-1658.

Yin, P., H. Fan, Q. Hao, X. Yuan, D. Wu, Y. Pang, C. Yan, W. Li, J. Wang and N. Yan (2009). "Structural insights into the mechanism of abscisic acid signaling by PYL proteins." Nat Struct Mol Biol. **16**(12): 1230-1236.

Yoshida, R., T. Hobo, K. Ichimura, T. Mizoguchi, F. Takahashi, J. Aronso, J. R. Ecker and K. Shinozaki (2002). "ABA-Activated SnRK2 Protein Kinase is Required for Dehydration Stress Signaling in Arabidopsis." Plant Cell Physiology **43**(12): 1473-1483.

Yoshida, R., T. Umezawa, T. Mizoguchi, S. Takahashi, F. Takahashi and K. Shinozaki (2006). "The Regulatory Domain of SRK2E/OST1/SnRK2.6 Interacts with ABI1 and Integrates Abscisic Acid (ABA) and Osmotic Stress Signals Controlling Stomatal Closure in Arabidopsis." Journal of Biological Chemistry **281**(8): 5310-5318.

Young, J. J., S. Mehta, M. Israelsson, J. Godoski, E. Grill and J. I. Schroeder (2006). "CO_2 signaling in guard cells: Calcium sensitivity response modulation, a Ca^{2+}-independent phase, and CO_2 insensitivity of the *gca2* mutant." Proceedings of the National Academy of Sciences **103**(19): 7506-7511.

Yunta, C., M. Martínez-Ripoll, J.-K. Zhu and A. Albert (2011). "The Structure of Arabidopsis thaliana OST1 Provides Insights into the Kinase Regulation Mechanism in Response to Osmotic Stress." Journal of Molecular Biology **414**(1): 135-144.

Zhu, S.-Y., X.-C. Yu, X.-J. Wang, R. Zhao, Y. Li, R.-C. Fan, Y. Shang, S.-Y. Du, X.-F. Wang, F.-Q. Wu, Y.-H. Xu, X.-Y. Zhang and D.-P. Zhang (2007). "Two Calcium-Dependent Protein Kinases, CPK4 and CPK11, Regulate Abscisic Acid Signal Transduction in Arabidopsis." Plant Cell **19**(10): 3019-3036.

Zou, J.-J., F.-J. Wei, C. Wang, J.-J. Wu, D. Ratnasekera, W.-X. Liu and W.-H. Wu (2010). "Arabidopsis Calcium-Dependent Protein Kinase CPK10 Functions in Abscisic Acid- and Ca2+-Mediated Stomatal Regulation in Response to Drought Stress." Plant Physiology **154**(3): 1232-1243.

Abscisic acid and CO2 signalling via calcium sensitivity priming in guard cells, new CDPK mutant phenotypes and a method for improved resolution of stomatal stimulus–response analyses

Katharine E. Hubbard, Robert S. Siegel, Gabriel Valerio, Benjamin Brandt and Julian I. Schroeder

Cell and Developmental Biology Section, Division of Biological Sciences, University of California, San Diego,9500 Gilman Drive, La Jolla, CA 92093-0116, USA

Background Stomatal guard cells are the regulators of gas exchange between plants and the atmosphere. Ca^{2+}-dependent and Ca^{2+}independent mechanisms function in these responses. Key stomatal regulation mechanisms, including plasma membrane and vacuolar ion channels have been identified and are regulated by the free cytosolic Ca^{2+} concentration ($[Ca^{2+}]_{cyt}$).

Scope Here we show that CO_2-induced stomatal closing is strongly impaired under conditions that prevent intra-cellular Ca^{2+} elevations. Moreover, Ca^{2+} oscillation-induced stomatal closing is partially impaired in knock-out mutations in several guard cell-expressed Ca^{2+}-dependent protein kinases (CDPKs) here, including the *cpk4cpk11* double and *cpk10* mutants; however, abscisic acid-regulated stomatal movements remain relatively intact in the *cpk4cpk11* and *cpk10* mutants. We further discuss diverse studies of Ca^{2+} signalling in guard cells, discuss apparent peculiarities, and pose novel open questions. The recently proposed Ca^{2+} sensitivity priming model could account for many of the findings in the field. Recent research shows that the stomatal closing stimuli abscisic acid and CO_2 enhance the sensitivity of stomatal closing mechanisms to intracellular Ca^{2+}, which has been termed 'calcium sensitivity priming'. The genome of the reference plant Arabidopsis thaliana encodes for over 250 Ca^{2+}-sensing proteins, giving rise to the question, how can specificity in Ca^{2+} responses be achieved? Calcium sensitivity priming could provide a key mechanism contributing to specificity in eukaryotic Ca^{2+} signal transduction, a topic of central interest in cell signalling research. In this article we further propose an individual stomatal tracking method for improved analyses of stimulus-regulated stomatal movements in Arabidopsis guard cells that reduces noise and increases fidelity in stimulus-regulated stomatal aperture responses (Box 1). This method is recommended for stomatal response research, in parallel to previously adopted blind analyses, due to the relatively small and diverse sizes of stomatal apertures in the reference plant Arabidopsis thaliana.

Key words: Stomata, ABA, guard cell, Ca^{2+}, CDPK, calcium sensitivity priming, carbon dioxide, Arabidopsis thaliana.

INTRODUCTION

Stomatal guard cells play a critical role in the regulation of plant gas exchange and water use efficiency (Kim et al., 2010). Several key physiological stimuli regulate stomatal aperture, including abscisic acid (ABA), CO_2 and pathogenic elicitors (Raschke et al., 1988; Pandey et al., 2007; Joshi-Saha et al., 2010; Kim et al., 2011). One signalling com-ponent that links these diverse stimuli is the cytosolic free-calcium concentration ($[Ca^{2+}]_{cyt}$), which induces stomatal closure (DeSilva et al., 1985; Gilroy et al., 1990; McAinsh et al., 1990; Webb et al., 1996; Grabov and Blatt, 1998; Allen et al., 1999a; Staxen et al., 1999; Kluesener et al., 2002; Young et al., 2006). Several independent mechanisms have been identified that are activated by $[Ca^{2+}]_{cyt}$ in guard cells, and contribute to ABA-induced stomatal closing, including $[Ca^{2+}]_{cyt}$ activation of S-type anion channels (Schroeder and Hagiwara, 1989; Mori et al., 2006; Vahisalu et al., 2008; Siegel et al., 2009; Chen et al., 2010), $[Ca^{2+}]_{cyt}$ activation of R-type anion channels (Hedrich et al., 1990; Meyer et al., 2010), $[Ca^{2+}]_{cyt}$ down-regulation of plasma membrane proton pumps (Kinoshita et al., 1995), $[Ca^{2+}]_{cyt}$ down-regulation of K^+ influx channels (Schroeder and Hagiwara, 1989; Kelly et al., 1995; Grabov and Blatt, 1997; Kwak et al., 2001) and Ca^{2+}-activation of vacuolar K^+ release (VK) channels (Ward and Schroeder, 1994; Allen and Sanders, 1996; Gobert et al., 2007). These studies and subsequent studies have identified mechanisms through which plasma membrane and tonoplast ion channels and ATPases function as key mediators in a network that controls stomatal closing and inhibits stomatal opening (reviewed in MacRobbie, 1998; Schroeder et al., 2001; Pandey et al., 2007). The importance of $[Ca^{2+}]_{cyt}$, relative to Ca^{2+}-elevation-independent control of stomatal closure has recently been quantified in Arabidopsis showing that the Ca^{2+}-dependent response is responsible for approx. 70 % of the ABA response (Siegel et al., 2009). This research is consist-ent with previous studies that demonstrated a requirement for Ca^{2+} in ABA-induced closure (DeSilva et al., 1985; Schwartz, 1985; McAinsh et al., 1990; Grabov and Blatt, 1998; MacRobbie, 2000). Recent ABA signalling models (Cutler et al., 2010; Hubbard et al., 2010; Melcher et al., 2010) have not yet incorporated a clear role for $[Ca^{2+}]_{cyt}$. $[Ca^{2+}]_{cyt}$ elevation-independent ABA-induced stomatal closure accounted for approx. 30 % of the response (Siegel et al., 2009). Ca^{2+}-independent signalling mechanisms function in ABA-and CO_2-induced stomatal closing and have been reviewed in depth elsewhere (Levchenko et al., 2005; Israelsson et al., 2006; Sirichandra et al., 2009; Kim et al., 2010; Hubbard et al., 2010; Raghavendra et al., 2010). In this study, we examine and review studies that have identified and analysed Ca^{2+}-dependent stomatal closure and provide an overview of the mechanisms that have been established during $[Ca^{2+}]_{cyt}$ signalling in guard cells, and consider models of how specificity and plasticity in Ca^{2+}-signalling networks may be achieved.

DYNAMICS IN 'RESTING' $[Ca^{2+}]_{cyt}$ AND SPONTANEOUS Ca^{2+} TRANSIENTS

Due to the cytotoxicity of large Ca^{2+} concentrations inside cells and diverse Ca^{2+}-binding proteins expressed in cells, the free cytosolic Ca^{2+} concentration is maintained within the 150 nM range in unstimulated cells through the action of Ca^{2+}-ATPases and Ca^{2+}–H^+ ion exchangers at the plasma membrane and membranes of internal stores. However, a number of studies have described fluctuations in $[Ca^{2+}]_{cyt}$ in guard cells, which had not yet been challenged with ABA or known stimuli (with the caveat that Ca^{2+} imaging experiments are performed under specific conditions which may inadvertently include physiological stimuli). For example, in Vicia faba guard cells, spontaneous increases in $[Ca^{2+}]_{cyt}$ were observed before the application of ABA (Grabov and Blatt, 1998). Similarly, spontaneous transients were noted in a subset of unstimulated Commelina communis cells (Staxen et al., 1999), and spontaneous $[Ca^{2+}]_{cyt}$ transients were observed in Arabidopsis guard cells expressing the non-invasive FRET reporter Yellow Cameleon with no exposure to ABA (Allen et al., 1999b; Kluesener et al., 2002). As with stimulus-induced $[Ca^{2+}]_{cyt}$ increases (see below), spontaneous $[Ca^{2+}]_{cyt}$ transients are not necessarily synchronized between guard cells of the same pair (Allen et al., 1999b). It is possible that $[Ca^{2+}]_{cyt}$ increases happen not at the level of the cell but at the level of $[Ca^{2+}]_{cyt}$ microdomains, as observed in mammalian tissue (Berridge, 2006). This may contribute to the highly stochastic nature of spontaneous $[Ca^{2+}]_{cyt}$ transients. Spontaneous Ca^{2+} transients

have also been observed in guard cells of intact leaves of Arabidopsis plants (Yang et al., 2008). These Ca^{2+} transients can be inhibited by loading cells with high concentrations of Ca^{2+} chelators including the Ca^{2+} chelating reporter fura-2 and its derivative BAPTA (Young et al., 2006). Interestingly, these spontaneous Ca^{2+} transients can be inhibited by removal of extracellular Ca^{2+} or by buffering the extracellular free Ca^{2+} concentration to 200 nM (Young et al., 2006; Siegel et al., 2009) and can be dampened or removed by more positive (depolarized) mem-brane potentials in guard cells (Grabov and Blatt, 1998; Staxen et al., 1999; Kluesener et al., 2002; Young et al., 2006). Spontaneous $[Ca^{2+}]_{cyt}$ transients have been observed in guard cells from several species and using different $[Ca^{2+}]_{cyt}$ imaging techniques indicating that spontaneous transients in $[Ca^{2+}]_{cyt}$ are a conserved feature of guard cell $[Ca^{2+}]_{cyt}$ dynamics that are sensitive to external Ca^{2+} and cytoplasmically loaded Ca^{2+} buffer concentrations. While the nature and function of spontaneous Ca^{2+} transients is currently poorly understood, it is likely that they include a contribution from Ca^{2+}-permeable cation channels in the plasma membrane that are activated at increasingly negative (hyperpolarized) membrane voltages (Aharon et al., 1998; Hamilton et al., 2000; Pei et al., 2000). Driving mem-brane voltage to more negative (hyperpolarized) membrane potentials increased the amplitude of $[Ca^{2+}]_{cyt}$ transients (Grabov and Blatt, 1998) and increases the open probability of Ca^{2+}-permeable cation channels in the plasma membrane of guard cells (Hamilton et al., 2000; Pei et al., 2000). Consistent with these findings, the proportion of guard cells with transients and the frequency of transients is dependent on the incubation buffer used. Low $[K^+]_{ext}$ (0·1 mM) results in more negative (hyperpolarized) membrane potentials and concomitant rapid transients in the majority of cells, while high $[K^+]_{ext}$ (100 mM) causes more positive (depolarized) membrane potentials and abolishes the Ca^{2+} transients (Kluesener et al., 2002). That some cells exhibit spontaneous transients while others in the same epidermal preparation have constant resting $[Ca^{2+}]_{cyt}$ levels may reflect a contribution from variation in the membrane potentials of the population of cells, with only those passing a certain threshold of negative voltages exhibiting spontaneous transients.

CO_2-INDUCED STOMATAL CLOSING IS STRONGLY IMPAIRED IN THE ABSENCE OF Ca^{2+} ELEVATIONS

The significance of $[Ca^{2+}]_{cyt}$-dependent ABA-induced stomatal closure, relative to Ca^{2+}-elevation-independent control of stomatal closure, has recently been quantified in Arabidopsis using the above described approaches that inhibit spontaneous and ABA-induced $[Ca^{2+}]_{cyt}$ increases. Guard cells where increases in $[Ca^{2+}]_{cyt}$ were prevented using the Ca^{2+}-chelator BAPTA showed only 30 % of the ABA-induced stomatal closure response compared with guard cells where $[Ca^{2+}]_{cyt}$ was allowed to increase (Siegel et al., 2009). Under the same experimental conditions that inhibit $[Ca^{2+}]_{cyt}$ elevations (i.e. in the presence of BAPTA, buffering free Ca^{2+} concentration in the extracellular medium to 200 nM; Siegel et al., 2009), we analysed stomatal closing induced by elevation in the CO_2 concentration here. Interestingly, under these conditions, CO_2-induced stomatal closing was strongly inhibited (Fig. 1B), whereas addition of 50 μM Ca^{2+} to the bath medium was sufficient to ensure a robust CO_2-induced stomatal closing response (Fig. 1A). Thus CO_2-induced stomatal closing is strongly Ca^{2+} dependent in Arabidopsis, consistent with pre-vious findings in Commelina guard cells (Schwartz, 1985; Webb et al., 1996). The Ca^{2+} requirement for CO_2-induced stomatal closing (Fig. 1) is particularly interesting because recent research has revealed that the Ca^{2+}-independent protein kinase, OST1, is required for CO_2-induced stomatal closure in Arabidopsis (Xue et al., 2011). These data indicate that present models strictly separating Ca^{2+}-dependent and Ca^{2+}-independent stomatal closing may be oversimplified, and that these mechanisms may interact in an unknown manner and will require further research.

STIMULUS-INDUCED CHANGES IN $[Ca^{2+}]_{cyt}$

Several distinct stimuli are known to cause an increase in guard cell $[Ca^{2+}]_{cyt}$, including cold (Allen et al., 2000; Wood et al., 2000), extracellular Ca^{2+} ($[Ca^{2+}]_{ext}$) (McAinsh et al., 1995), ABA (McAinsh et al., 1990; Schroeder and Hagiwara, 1990; Grabov and Blatt, 1998; Allen et al., 1999a, b; Staxen et al., 1999; MacRobbie, 2000; Jung et al., 2002; Marten et al., 2007), CO_2 (Webb et al., 1996; Young et al., 2006) and certain pathogenic elicitors (Klusener et al., 2002). In cells that show constant resting Ca^{2+} levels, upon application of a given stimulus, $[Ca^{2+}]_{cyt}$ can increase from approx. 100 –150 nM to ≥350 nM. The pattern of $[Ca^{2+}]_{cyt}$ increases is related to the stimulus applied and the buffer in which cells are incubated. For example, for cells incubated in a high $[K^+]$ buffer (50 mM) a cold shock results in a single large transient (Fig. 2A), whereas exposure to high $[Ca^{2+}]_{ext}$ induces $[Ca^{2+}]_{cyt}$ oscillations (Fig. 2B). Physiological stimuli can also alter the pattern of spon-taneous $[Ca^{2+}]_{cyt}$ transients; for example, transfer from a low to a high $[CO_2]$ buffer reduces the rate of spontaneous Ca^{2+} transients in wild-type Arabidopsis (Landsberg erecta) guard cells (Young et al., 2006). This elevated CO_2-induced dam-pening of Ca^{2+} transients was proposed to occur due to depolarization of the guard cell plasma membrane mediated by CO_2 signalling (Young et al., 2006). Both types of responses (stimulation and dampening) have been associated with exposure of cells to ABA, with some studies showing ABA-induced $[Ca^{2+}]_{cyt}$ transients (Schroeder and Hagiwara, 1990; Grabov and Blatt, 1998; Allen et al., 1999a, 2000, 2002; Staxen et al., 1999; Islam et al., 2010). However, in cells that exhibit spontaneous Ca^{2+} transients, prior to ABA application, ABA-dependent dampening and slowing of spon-taneous $[Ca^{2+}]_{cyt}$ transients was found (Grabov and Blatt, 1998; Staxen et al., 1999; Klusener et al., 2002). A number of studies have noted a variety of ABA-induced responses ranging from repetitive oscillations to no measureable ABA-dependent change in $[Ca^{2+}]_{cyt}$ (Schroeder and Hagiwara, 1990; Gilroy et al., 1991; Allen et al., 1999a; Hugouvieux et al., 2001; Jung et al., 2002; Kwak et al., 2002, 2003; Levchenko et al., 2005). These studies and data in Fig. 2 indicate that amongst a population of guard cells different microenvironments or signalling states may exist resulting in either lack of ABA-induced $[Ca^{2+}]_{cyt}$ increases (Fig. 2C) or ABA-induced $[Ca^{2+}]_{cyt}$ increases (Fig. 2D, E). Note that plants analysed in Fig. 2C–D were grown at high humidity, and were misted daily with water, similar to pre-vious reports (Allen et al., 1999a; see methods in the figure captions). Daily misting of plant leaves with water may serve to reduce endogenous ABA levels in guard cells, and appears to enhance mechanisms mediating ABA-induced $[Ca^{2+}]_{cyt}$ elevations. Mechanistically, evidence suggests that $[Ca^{2+}]_{cyt}$ increases induced by separate stimuli are likely generated by a different combination of mechanisms. $[Ca^{2+}]_{cyt}$ oscillations recorded in response to $[Ca^{2+}]_{ext}$, cold and ABA have distinct patterns (Allen et al., 2000), indicating their generation is differently regulated. To generate a specific $[Ca^{2+}]_{cyt}$ pattern, such as a repetitive oscillation, requires the co-ordinated action of both Ca^{2+} influx channels and active Ca^{2+} efflux transporters. Sorting out the specific genes encoding candidate Ca^{2+}-permeable ion channels and efflux transporters that mediate specific $[Ca^{2+}]_{cyt}$ patterns will require further research. This question is likely to be complicated by the circumstances that (a) large families of candidate Ca^{2+}-permeable ion channels exist in plants with overlapping gene functions (Lacombe et al., 2001; Kaplan et al., 2007) and (b) more than one Ca^{2+} channel type is likely to contribute to any given stimulus-induced Ca^{2+} elevation pattern.

$[Ca^{2+}]_{cyt}$ -REACTIVE MECHANISMS

There are a large number of $[Ca^{2+}]_{cyt}$-dependent mechanisms that have been described within the guard-cell signalling network, most of which function in mediation of stomatal closing, leading to the proposal that $[Ca^{2+}]_{cyt}$ functions as a ‘hub’ within the stomatal signalling network (Hetherington and Woodward, 2003). The diversity of $[Ca^{2+}]_{cyt}$-dependent processes is illustrated by the large number (approx. 250) of proteins containing Ca^{2+}-binding ‘EF-hand’ motifs encoded within the Arabidopsis thaliana genome (Day et al., 2002). This is likely to be an underestimate of the total number of Ca^{2+}-binding proteins present, as some proteins such as the 14-3-3 protein GF14 have been described as Ca^{2+}-binding (Lu et al., 1994; Athwal and Huber, 2002) but do not contain an EF hand (Day et al., 2002). EF-hand-containing proteins include

several families of signalling components commonly referred to as Ca^{2+}-sensors which include calmo-dulins (CaM) and CaM-like (CML) proteins, calcineurin-B-like (CBL) proteins and Ca^{2+}-dependent protein kinases (CPKs); these protein families have been extensively reviewed elsewhere (Dodd et al., 2010; Kudla et al., 2010) and so will not be discussed in detail here. Moreover, additional 'target proteins' including ion channels contain EF-hand(s), and can be directly regulated by $[Ca^{2+}]_{cyt}$. For example, the K^+- and Ca^{2+}-permeable two-pore channel 1 (TPC1) protein which encodes the slow vacuolar (SV) channel (Peiter et al., 2005) contains two EF hands and is Ca^{2+} activated (Hedrich and Neher, 1987; Pei et al., 1999). The literature might in a few cases over-interpret findings as mainly supporting a model in which only unique stimulus-specific patterns in $[Ca^{2+}]_{cyt}$ elevations, rather than Ca^{2+} elevations above thresholds in concentrations and durations, are required in plant cells for Ca^{2+} to elicit an output. (We have avoided the attractive term 'Ca^{2+} signature' in our previous studies, as this can have several definitions. Nevertheless, further research in plant model cell systems is needed to elucidate the underlying cell-signalling and bio-chemical mechanisms, which would represent important breakthroughs in plant Ca^{2+} signalling.) Experimental impo-sition of $[Ca^{2+}]_{cyt}$ transients through repetitive buffer swap experiments showed that any Ca^{2+} elevation above a threshold value could trigger a rapid 'Ca^{2+}-reactive' stomatal closing response [see supplemental data for Allen et al. (2001)]. Thus the Ca -reactive stomatal closing response was shown to be largely independent of the $[Ca^{2+}]_{cyt}$ elevation frequency, number or duration of transients (Allen et al., 2001). Nevertheless, the rate and the final degree of Ca^{2+}-reactive stomatal closing depends on the number and integrated amplitude of Ca^{2+} elevations, which per se could also be modelled by a threshold-type mechanism. S-type anion channels in the plasma membrane of guard cells play a central role in controlling stomatal closure (Schroeder and Hagiwara, 1989; Schroeder, 1995). The rapid Ca -reactive phase of stomatal closing in response to imposed Ca^{2+} transients is reduced in the Ca^{2+}-dependent protein kinase double mutant *cpk3cpk6* (Mori et al., 2006; see Fig. 4A). Moreover, mutations that disrupt the gene encoding the S-type anion channel, SLAC1 (Negi et al., 2008; Vahisalu et al., 2008), show a dramatically impaired Ca^{2+}-reactive stomatal closure (Vahisalu et al., 2008). These findings are consistent with the model that Ca^{2+}-dependent protein kinases activate S-type anion chan-nels, thus mediating stomatal closing (Mori et al., 2006; Geiger et al., 2010). In contrast to Ca^{2+}-reactive stomatal closing, imposed Ca^{2+} oscillations of particular frequencies and durations resulted in inhibition of stomatal re-opening, after Ca^{2+} transients had been terminated (Allen et al., 2001; Li et al., 2004). This latter Ca^{2+}-dependent inhibition of stomatal re-opening has been coined long-term 'Ca^{2+}-programmed' stomatal closure (Allen et al., 2001; Yang et al., 2003; Li et al., 2004). The gca2 mutant exhibits more 'spiky' Ca^{2+} oscillations during ABA and elevated CO_2 exposures and gca2 exhibits impaired stomatal closure responses (Allen et al., 2001; Young et al., 2006). In the gca2 mutant, experimental imposition of strong Ca^{2+} oscillations restored 65 % of stomatal closure compared with wild-type guard cells (Allen et al., 2001). Further research suggested that the increased rate of $[Ca^{2+}]_{cyt}$ transi-ents observed in gca2 mutant guard cells (Allen et al., 2001) could result from the more negative (hyperpolarized) mem-brane potential of this mutant (Young et al., 2006). Indeed membrane potential hyperpolarization enhances the rate of $[Ca^{2+}]_{cyt}$ transients in guard cells, as discussed earlier (Grabov and Blatt, 1998; Kluesener et al., 2002).

CALCIUM SENSITIVITY PRIMING

Given that both spontaneous transients and stimulus-specific changes in $[Ca^{2+}]_{cyt}$ have been reported in guard cells, the question remains; how are guard cells able to respond in a Ca^{2+}-dependent manner? In other words why can Ca^{2+} alter, for example, anion channel activity in response to the appropriate stimulus, but not in response to spontaneous Ca^{2+} transients? There is increasing evidence to suggest that the prior conditions that guard cells have experienced modu-late the sensitivity of the signalling network to increases in $[Ca^{2+}]_{cyt}$, thus determining the final response of the cell. For example, $[Ca^{2+}]_{cyt}$-induced activation of the S-type anion channels was found not to occur in Arabidopsis guard cells under non-stimulated conditions (see fig. 3 in Allen et al., 2002). Exposure to high extracellular Ca^{2+} concentrations, and even after a

subsequent return to more physiological extra-cellular Ca^{2+} levels, was found to alter the signalling state of guard cells, such that $[Ca^{2+}]_{cyt}$ activation of anion channels was restored (Allen et al., 2002; Mori et al., 2006; Suh et al., 2007). These data along with the resolution of spon-taneous Ca^{2+} transients in guard cells provided first evidence that the $[Ca^{2+}]_{cyt}$ sensitivity of stomatal closing mechanisms can be up- and down-regulated (i.e. primed or de-primed). Ensuing studies showed that $[Ca^{2+}]_{cyt}$-activation of S-type anion channels is primed by pre-exposure of guard cells to ABA (Siegel et al., 2009; Chen et al., 2010). Similarly, K^+-influx channels in Arabidopsis guard cells are rendered more $[Ca^{2+}]_{cyt}$ sensitive by pre-exposure of guard cells to ABA as well (Siegel et al., 2009). These findings and Ca^{2+} imaging studies led to the proposal of the 'Ca^{2+}-sensitivity priming' hypothesis (Young et al., 2006; Siegel et al., 2009), which postulates that a given physiological stimulus renders a component(s) of the signalling network more $[Ca^{2+}]_{cyt}$ responsive (Fig. 3). Thus, for example, in the primed state a lower amplitude Ca^{2+} transient would cause a stronger activation of anion channels (Chen et al., 2010). This model resolves some of the potential paradoxes found in the literature. An important question for Ca^{2+} sensitivity priming remains, whether ABA or CO_2 can sensitize guard cells to typical base-line resting $[Ca^{2+}]_{cyt}$ concentrations of 150 nM in vivo. Some circumstantial evidence exists that this may be the case. For example, in Vicia faba and other species, guard cells have been previously shown to exhibit ABA-induced Ca^{2+} increases in only a minority of guard cells (Schroeder and Hagiwara, 1990; Gilroy et al., 1991; McAinsh et al., 1992). Furthermore, loading the Ca^{2+} reporter fura-2 into Vicia faba guard cells was shown to enable ABA-induced stomatal closing at resting $[Ca^{2+}]_{cyt}$ levels in the absence of measurable $[Ca^{2+}]_{cyt}$ elevations (Levchenko et al., 2005). However, in the same experiments loading a higher concentration of the fura-2-analogous Ca^{2+} chelator BAPTA into guard cells reduced resting Ca^{2+} levels to below typical baseline levels and then inhibited ABA-induced stomatal closing (Levchenko et al., 2005). Thus, ABA may enhance (prime) the sensitivity of stomatal closing mechanisms even to resting Ca^{2+} levels. This gives rise to the question whether Ca^{2+}-independent signalling in vivo (Fig. 2C) is truly Ca^{2+} independent. More research is needed to investigate this question.

There are many potential (non-mutually exclusive) mechanisms through which Ca^{2+}-sensitivity priming may occur, including post-translational modification of signalling proteins, sub-cellular re-localization, protein–protein interactions, coincidence detection of Ca^{2+} and a second parallel signal, interaction of parallel Ca^{2+}-dependent and -independent signalling pathways and transcriptional reprogramming (for reviews and discussion of putative mechanisms, see Hubbard et al., 2010; Kim et al., 2010). These events may occur at the level of the Ca^{2+}-sensors, but may potentially play a role at any point of the signalling network downstream of or parallel to $[Ca^{2+}]_{cyt}$ responses. Recent research has shown that elevation of the intracellular CO_2 and bicarbonate concentrations in Arabidopsis guard cell protoplasts rapidly enhances the ability of $[Ca^{2+}]_{cyt}$ to activate S-type anion channels, within approx. 3–5 min of whole-cell patch clamp initiation (Xue et al., 2011). These findings demonstrate that Ca^{2+}-sensitivity priming can occur rapidly in guard cells, and may therefore not underlie a slower transcriptional regulation mechanism (Xue et al., 2011). The Ca^{2+}-dependent protein kinase CPK1 of Mesembryanthemum crystallinum is dynamically re-localized within cells depending on growth conditions; upon transfer to low humidity the kinase moves from the plasma membrane to soluble and nuclear cell fractions, where it is presumably able to activate downstream signalling processes (Chehab et al., 2004). Further research is needed to elucidate the unknown biochemical and cell biological mechanisms by which the stomatal closing stimuli CO_2 and ABA enhance the sensitivity of Ca^{2+}-dependent stomatal closing (Young et al., 2006; Siegel et al., 2009; Chen et al., 2010; Xue et al., 2011).

MODULAR BASIS OF $[Ca^{2+}]_{cyt}$ SIGNALLING

Plants contain a diverse array of proteins associated with Ca^{2+} signalling. For $[Ca^{2+}]_{cyt}$-signals to be generated and interpreted with specificity, a specific subset of these com-ponents must be employed at a given time and location. The concept of the 'signalosome' has previously been pro-posed for mammalian Ca^{2+} signalling (Berridge et al., 2003), and is equally applicable for plant systems, particularly given the

large number of Ca^{2+}-binding site-containing proteins encoded in plant genomes. The components of the signalosome may be tissue-, cell- or subcellular location-dependent, and may also vary with time, either in response to endogenous cues such as those provided by the circadian clock, or in response to particular stimuli. On a technical level, variation in growth conditions, age and physiological conditions of individual plants may influence the composition of the guard cell signalosome and therefore the sensitivity of stomata to different stimuli. Evidence for specific control of subcellular location of Ca^{2+}-signalling components has been elegantly demonstrated through transient expression analysis for the CBL –CIPK network, where particular CBL –CIPK pairs are restricted to defined sub-cellular locations (Waadt et al., 2008; Batistic et al., 2010). CIPK14 is located at the tonoplast when in complex with CBL2 or CBL3, but is found at the plasma mem-brane when co-expressed with CBL8 (Batistic et al., 2010). It would therefore be predicted for the intact plant that expression of the individual Ca^{2+}-sensor would affect down-stream signalling specificity.

ANALYSIS OF Ca^{2+}-DEPENDENT PROTEIN KINASE FUNCTIONS IN STOMATAL REGULATION

Microarray analysis provides evidence that Ca^{2+}-signalling components are expressed in guard cells, e.g. CPK3, 6, 4, 10 and 11. Additional CPKs are expressed in guard cells, whereas CPK2, 18 and 34 (for example) are only very weakly expressed in this cell type (Leonhardt et al., 2004; Mori et al., 2006; Zhu et al., 2007; Yang et al., 2008; Zou et al., 2010). Interestingly, most of the above-mentioned Ca^{2+}-dependent protein kinases have been reported to contribute to ABA-induced stomatal closing (Mori et al., 2006; Zhu et al., 2007; Zou et al., 2010). Here, we show that individual mutants in these same genes show partial insensitivities in the rapid Ca^{2+}-reactive stomatal closing response, as shown for the *cpk3cpk6*, *cpk10*, *cpk4cpk11* and *cpk7cpk8cpk32* mutants (Fig. 4; Valerio, 2007). However, mutants in these Ca^{2+}-dependent protein kinases (CDPKs), including *cpk10*, and even *cpk4cpk11* double-mutant stomata and *cpk7cpk8cpk32* triple-mutant stomata did not show a clear ABA-insensitive phenotype in our analyses of ABA-induced stomatal closing (Fig. 5) and ABA-inhibition of stomatal opening (Fig. 6; Valerio, 2007). These findings with a *cpk4cpk11* double mutant (Figs 5 and 7; Valerio, 2007) do not correlate with a very strong ABA insensitivity reported for *cpk4cpk11* (Zhu et al., 2007). Note that the *cpk4* allele (*cpk4-2*; SALK_000685) in the double-mutant plants used for these experiments differs from the ones used in a previous study (Zhu et al., 2007; cpk4-1; SALK_081860), whereas the same *cpk11-2* allele was used. The T-DNA insertion of the *cpk4-2* allele analysed here was identified as lying in the 6th exon and RT-PCR analysis revealed that plants harbouring *cpk4-2* and *cpk11-2* alleles do not express mature transcripts (Fig. 7). These findings showing statistically functional ABA responses but slightly impaired Ca^{2+}-reactive stomatal closing responses in the analysed cpk mutants (Valerio, 2007; Figs 4–6) point to the hypothesis that combinations of these mutants may lead to a stronger ABA insensitivity, as found for the partial ABA insensitivity of *cpk3cpk6* double mutants (Mori et al., 2006). Furthermore, CPK23 is also expressed in guard cells, but functions genetically as a negative regulator in drought stress experiments as well as control of stomatal aperture (Ma and Wu, 2007). Contrary to the phenotype of *cpk23* mutants, CPK23 on the other hand activates the SLAC1 anion channel in Xenopus oocytes and S-type anion currents in guard cell protoplasts of *cpk23* mutants are reduced (Geiger et al., 2010). The in vivo mechanisms mediating these opposing responses will require further analysis. The closest homologue to CPK23, CPK21, can also mediate acti-vation of the SLAH3 anion channel and to a smaller extent SLAC1 anion channels in Xenopus oocytes (Geiger et al., 2011). SLAH3 shows a relative nitrate permeability similar to S-type anion currents in Vicia faba guard cells (Schmidt and Schroeder, 1994; Geiger et al., 2011). An aspect of signalosome models is that protein complexes are dynamically remodelled; and this could include a potentially $[Ca^{2+}]_{cyt}$-dependent remodelling (Berridge et al., 2003). For example, adding a continuous high extracellular Ca^{2+} concentration to Arabidopsis leaf epidermis causes $[Ca^{2+}]_{cyt}$ elevation (McAinsh et al., 1995; Allen et al., 1999a), but under the appropriate conditions does not cause stomatal closing, in spite of the $[Ca^{2+}]_{cyt}$ elevation, indicating a non-primed state (K. E. Hubbard et al., unpubl. res.). However, repetitively pulsing

extracellular Ca^{2+} to the same leaf epidermis causes a clear Ca^{2+}-reactive stomatal closing response (Allen et al., 2001; e.g. Fig. 4). These findings suggest that this later Ca^{2+} treatment of repetitive extracellular Ca^{2+} pulses causes a Ca^{2+}-primed state compared with simple continuous elevation in extracellular Ca^{2+}. Such remodelling can establish feedback mechanisms (Berridge et al., 2003). It is entirely possible that an analogous process contributes to $[Ca^{2+}]_{cyt}$ sensitivity priming in guard cell signalling. Many Arabidopsis genes are transcriptionally regulated in response to $[Ca^{2+}]_{cyt}$, which include transcripts associated with Ca^{2+}-signalling such as CML24/TCH2 (Braam, 1992; Kaplan et al., 2006) and CPK32 (Kaplan et al., 2006). Similarly, many Ca^{2+}-signalling components are regulated at the level of transcript abundance by ABA treatment (Hoth et al., 2002; Sa´nchez et al., 2004; Zeller et al., 2009). Therefore the potential exists for $[Ca^{2+}]_{cyt}$-dependent and conditional remodelling of the guard cell signalosome, which should be further investigated. Note, however, that CO_2/HCO_3-induced priming of Ca^{2+}-dependent activation of anion channels occurs within ,3 to 5 min in whole patch clamp experiments, demonstrating that relatively rapid events function in priming Ca^{2+}sensitivity (Xue et al., 2011). Similarly the repetitive Ca^{2+} pulse-induced Ca^{2+}-reactive stomatal closure is measurable within approx. 5 min of Ca^{2+} pulsing as resolved using tracking of individual stomatal apertures (see Box 1, overleaf).

CONCLUSIONS

Ca^{2+} functions as a second messenger in guard cell signalling and stomatal movements, as was originally described over 20 years ago (DeSilva et al., 1985; Schwartz, 1985; Schroeder and Hagiwara, 1989; McAinsh et al., 1990). The recently derived Ca^{2+}-sensitivity priming model and the concomitant signalosome model provide a mechanism for specificity in plant $[Ca^{2+}]_{cyt}$ signalling. Further research at the single-cell type specific level should shed light on the underlying molecular and protein-mediated Ca^{2+} signalling mechanisms. Guard cells provide a potent system to pursue combined single-cell time-resolved small molecule and protein imaging, electro-physiological ion-channel regulation, cell biological, and whole-leaf and -plant response analyses which undoubtedly will spring new surprises and lead to new levels of understanding of plant-cell signalling dynamics.

ACKNOWLEDGEMENTS

We thank Drs Shintaro Munemasa and Rainer Waadt for comments on an early draft of the manuscript. This research was supported by NIH (R01GM060396) and NSF (MCB0918220) and in part by Chemical Sciences, Geosciences, and Biosciences Division of the Office of Basic Energy Sciences at the US Department of Energy (DE-FG02-03ER15449) grants (J.I.S.). Data in the Box Figure are reproduced from Siegel et al. (2009) with per-mission from Wiley-Blackwell.

FIGURE 1

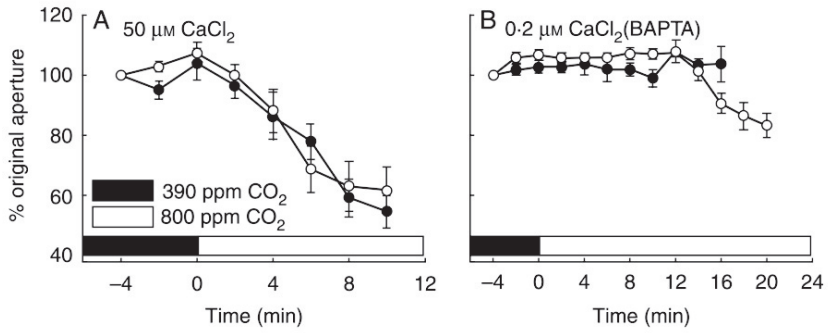

FIG. 1. CO_2-induced stomatal closing is strongly inhibited under conditions that prevent $[Ca^{2+}]_{cyt}$ elevations in guard cells. (A) Robust CO_2-induced stomatal closing was observed in response to CO_2 elevation with 50 mM Ca^{2+} added to the bathing medium (10 mM KCl, 7·5 mM iminodeactic acid, 10 mM MES, pH 6·2). Stomatal closing of individual stomata was tracked (see Box 1 for Methods) in response to elevations in the extracellular CO_2 concentration from ambient (approx. 390 ppm) to 800 ppm (added at time = 0) with 50 μM Ca^{2+} in the bathing medium. (B) Buffering the extracellular free Ca^{2+} concentration to a low level of 200 nM using the Ca^{2+} chelator BAPTA strongly inhibited CO_2-induced stomatal closing. Extracellular bathing media and free Ca^{2+} buffering to 200 nM was performed using identical solutions to those reported in Siegel et al. (2009). Experiments were conducted on 4- to 5-week-old plants according to the protocols described in (Siegel et al., 2009). CO_2-induced stomatal closing experiments were performed under identical Ca^{2+} solutions to those published for ABA-induced stomatal closing experiments with 200 nM free Ca^{2+} or 50 μM Ca^{2+} in the bath medium (Siegel et al., 2009). Two independent experiments are shown for each condition (open and closed symbols); errors are presented as +/- s.e. of the mean, n = 30.

FIGURE 2

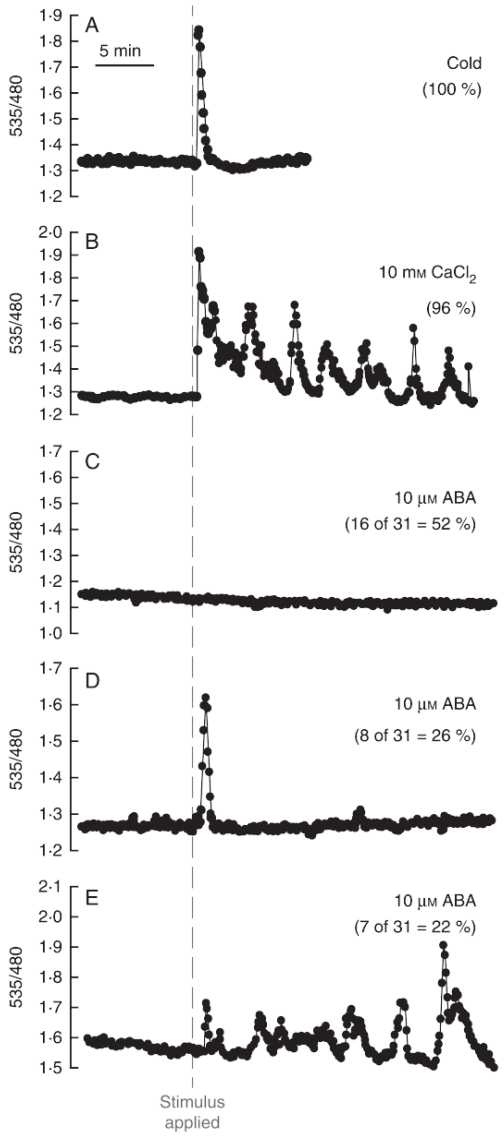

FIG. 2. Stimulus-induced increases in guard cell $[Ca^{2+}]_{cyt}$. Plants trans-formed with the FRET-based Ca^{2+} sensor YC3·6, targeted to guard cells with the pGC1 guard cell promoter, were imaged (Allen et al., 1999b). Cells were initially incubated in a stomatal-opening buffer and then after 10 min of recording were challenged with (A) a cold shock (4ºC; n = 15), (B) 10 mM external $CaCl_2$ (n = 26) or (C–E) 10 µM ABA (n = 31) as indicated. External $[Ca^{2+}]$ elevation induces oscillations in $[Ca^{2+}]_{cyt}$ consistent with previous studies (McAinsh et al., 1995; Allen et al., 2000). The response to ABA was variable, with some cells showing no changes in $[Ca^{2+}]_{cyt}$ and others exhibiting oscillations in $[Ca^{2+}]_{cyt}$ in response to ABA under the imposed conditions (Allen et al., 1999b; Hugouvieux et al., 2001; Jung et al., 2002; Kwak et al., 2003), as discussed in the text. All traces are expressed as the ratio of recorded fluorescence emitted at 535 nm divided by fluorescence emitted at 480 nm after excitation at 440 nm as described in Allen et al. (1999b). Daily misting of plants with water was used to reduce endogenous ABA concentrations and increased the percentage of guard cells that showed ABA-induced $[Ca^{2+}]_{cyt}$ elevation, as reported previously (Allen et al., 1999a,b). Epidermal peels were prepared from 3- to 5-week-old plants stably transformed with the cameleon construct according to the method described in Allen et al. (1999b). Samples were incubated in either a high-$[K^+]$ buffer (50 mM K^+, 10 mM MES-Tris, pH 6·2) for cold and the indicated $CaCl_2$ treatment (Fig. 2A, B) or stomatal-opening buffer (5 mM K^+, 50 µM $CaCl_2$, 10 mM MES-Tris, pH 6·2; ABA) for 3 h before imaging (C–E). Imaging was performed as described in Allen et al. (1999b). Cells were treated with either a cold shock (4ºC; n = 15), 10 mM $CaCl_2$ (n = 26) or 10 µM ABA (dis-solved in methanol). All traces were corrected for YFP bleaching through sub-traction of the overall gradual decline in fluorescence in each channel from each data point (Allen et al., 1999b; Kluesener et al., 2002).

FIGURE 3

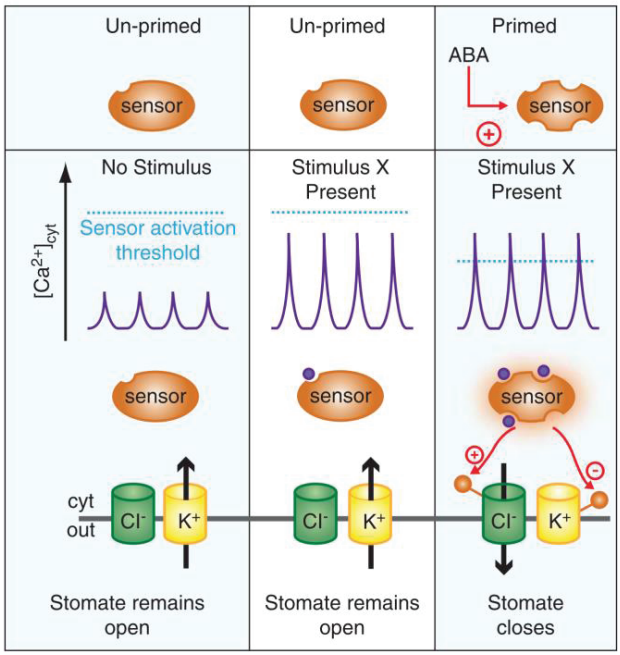

FIG. 3. Ca^{2+}-sensitivity priming. In the Ca^{2+}-sensitivity priming model, the response of a cell to a given stimulus depends on the conditions the cell has previously experienced. A generic model is presented, where the magnitude of Ca^{2+} increases and ABA-dependent priming combine to determine the eventual response (Siegel et al., 2009; Chen et al., 2010). Without a specific stimulus only spontaneous $[Ca^{2+}]_{cyt}$ transients occur. In the presence of a stimulus (X) the amplitude of transients increases, but in the un-primed state this is insufficient to trigger the downstream response (e.g. ion-channel acti-vation). A previously encountered condition (e.g. ABA) may modulate a Ca^{2+}-response pathway, making it more Ca^{2+} responsive or 'primed'. When stimulus X is perceived under the primed conditions the sensor is more Ca^{2+} responsive and therefore downstream responses are triggered. Note, however, that $[Ca^{2+}]_{cyt}$ sensitivity enhancement could theoretically occur at any point in the network downstream of or parallel to $[Ca^{2+}]_{cyt}$. See text for details.

FIGURE 4

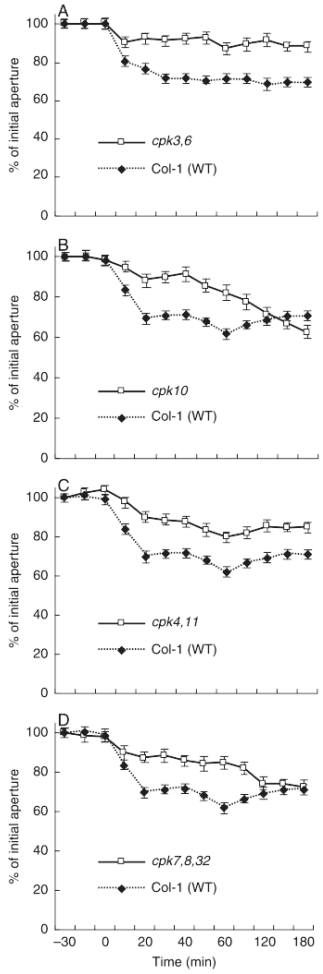

FIG. 4. Imposed Ca^{2+} oscillation-induced stomatal closure is impaired in *cpk3,cpk6, cpk10, cpk4,cpk11* and *cpk32,cpk7,cpk8* mutants compared with wild-type stomata. Samples were pre-incubated in depolarizing stomatal-opening buffer for 3 h (50 mM KCl and 10 mM MES-Tris at pH = 5.6). Stomatal apertures of individually tracked stomata (see Box 1) were measured periodically at the indicated times. Starting at time = 0 and for the first 40 min the sample was exposed to hyperpolarizing (1 m M KCl, 1 mM $CaCl_2$ and 10 mM MES-Tris at pH 5·6) solution four times for 5 min each (Allen et al., 2001; Mori et al., 2006). For experiments illustrated in Figs 4–6 plants were tented using transparent plastic wrap to maintain a high humidity (.95 %) to reduce endogenous ABA levels. After 2 weeks of growth, slits were cut in the plastic tent to allow enhanced air circulation. Twenty-four hours before each experiment, the old plastic was replaced with a new plastic wrap for a high humidity treatment. Stomatal movement analyses were performed following the imposed Ca^{2+} oscillation protocol and solutions described in Mori et al. (2006). The lower epidermis of Arabidopsis leaves was attached to glass cover slides using Hollister medical adhesive 9 to attach a leaf abaxial side down onto a coverslip. A razor blade was then used to carefully remove mesophyll layers of the leaf until only the epidermal layer remained. The coverslip was then incubated in 4 mL depolarizing buffer (50 mM KCl and 10 mM MES-Tris at pH 5·6) in a Petri dish (35 × 10 mm) for 3 h under white light (200 μE) to open stomata. The coverslip with epidermal layer attached was then sealed to a glass slide with a 2-cm hole drilled in the middle to create a 200 mL perfusion well. Depolarizing buffer was alternated with hyperpolarizing buffer (1 mM KCl, 1 mM $CaCl_2$, and 10 mm MES-Tris at pH 5·6) using a bath perfusion system. Four 5-min extracellular Ca^{2+} pulses were applied in 10-min intervals in the first 40 min, as described previously (Mori et al., 2006). In between each transient and after the final transient depolarizing buffer was continuously applied. Stomatal apertures were measured using an inverted microscope at ×40. Both mutant and wild-type plants could be placed side by side on one coverslip during a single exper-iment. Eight individual stomata per condition were measured and tracked using Scion Image Software. Experiments were repeated at least three times for each mutant and parallel wild-type controls. Seed sources were *cpk3-1 cpk6-1* (Mori et al., 2006), *cpk10* (Salk_032021) and *cpk32* (GABI 824E2). For information on *cpk4* and sources see Fig. 7. Experiments were per-formed single-blinded with the genotype identity unknown. Data are from Valerio (2007).

FIGURE 5

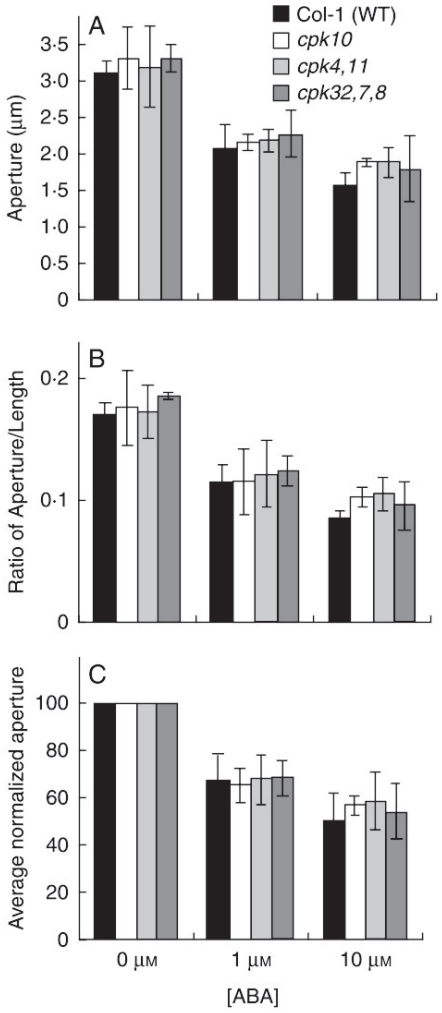

FIG. 5. ABA-induced stomatal closure was not dramatically impaired in *cpk10*, *cpk4cpk11* and *cpk32cpk7cpk8* compared with Col-1 wild type. Whole leaves were pre-incubated in stomatal-opening buffer (10 mM KCl, 7·5 mM iminodeac-tic acid, 10 mM MES, pH 6·2) for 2 h and then incubated for an additional hour with 0, 1 or 10 μM ABA. Stomatal aperture (A) and ratio (width : length) (B) were then measured. In (C) the average normalized stomatal apertures from (A) are shown. Experiments were performed double blind with both genotype and ABA concentration unknown; n = 3 experiments with 30 stomata analysed per condition in each experiment (90 stomatal apertures analysed per bar in the graphs). Error bars represent +/- s.e. of the mean relative to n = 3 experiments. Plants were grown at approx. 95 % humidity and were subjected to 24 h of high (.98 %) humidity prior to experimentation. ABA-dependent stomatal movement imaging analyses (Valerio, 2007) were performed following the pro-tocol from Kwak et al. (2002). Rosette leaves from 4- to 5-week-old plants were excised and the curvature of each leaf was gently inverted using a finger so that the abaxial side did not form any air pockets when floating on solution during incubation. Using forceps the whole leaf was placed with the abaxial side down in 4 mL of stomatal-opening buffer (10 mM KCl, 7·5 mM iminodeactic acid, 10 mM MES, pH 6·2) in a Petri dish (35 × 10 mm). Leaves were incubated in stomatal-opening buffer for 2 h under white light (200 μE). Then, the stomatal-opening buffer was removed via a pipette and replaced with 4 mL stomatal-opening buffer containing 0 μM, 1 μM or 10 μM ABA and the leaves were incubated under white light for one more hour. The abaxial epidermis of each leaf was peeled using forceps and placed on a glass coverslip with approx. 200 mL of the treatment buffer. Experiments were performed double-blinded. Both genotype identity and ABA concentrations were unknown to the experimenter. Data are from Valerio (2007).

FIGURE 6

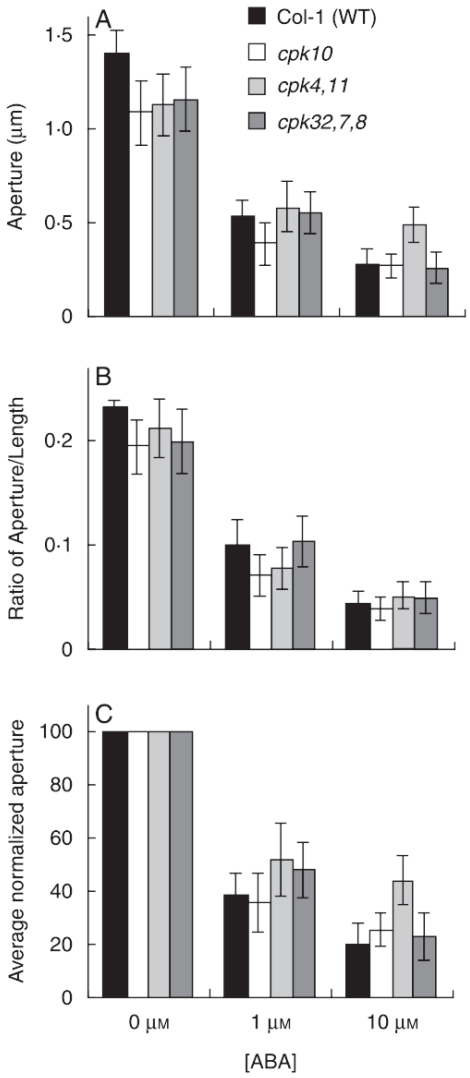

FIG. 6. ABA inhibition of stomatal opening is not affected in *cpk10*, *cpk4cpk11* and *cpk32cpk7cpk8* compared with Col-1 wild type. Stomatal apertures (A) and ratios (width : length) (B) were measured. In (C) the averages of normalized apertures are shown. Experiments were performed double blind with both genotype and ABA concentration unknown to the experimenter; n = 3 experiments with 30 stomata per condition per experiment (90 stomatal apertures analysed per bar in graph). Error bars represent + standard error of the mean for n = 3 experiments. For analyses of ABA inhibition of stomatal opening, plants were subjected for 24 h to darkness to reduce stomatal apertures. Whole leaves were then pre-incubated in stomatal-opening buffer with 0, 1 or 10 μM ABA concentrations for 2 h. The epidermis was then peeled off and attached onto a glass slide. Stomatal apertures were measured using a microscope at ×40. Thirty stomata per condition were measured in each epidermal peel using Scion Image Software. Data are from Valerio (2007).

FIGURE 7

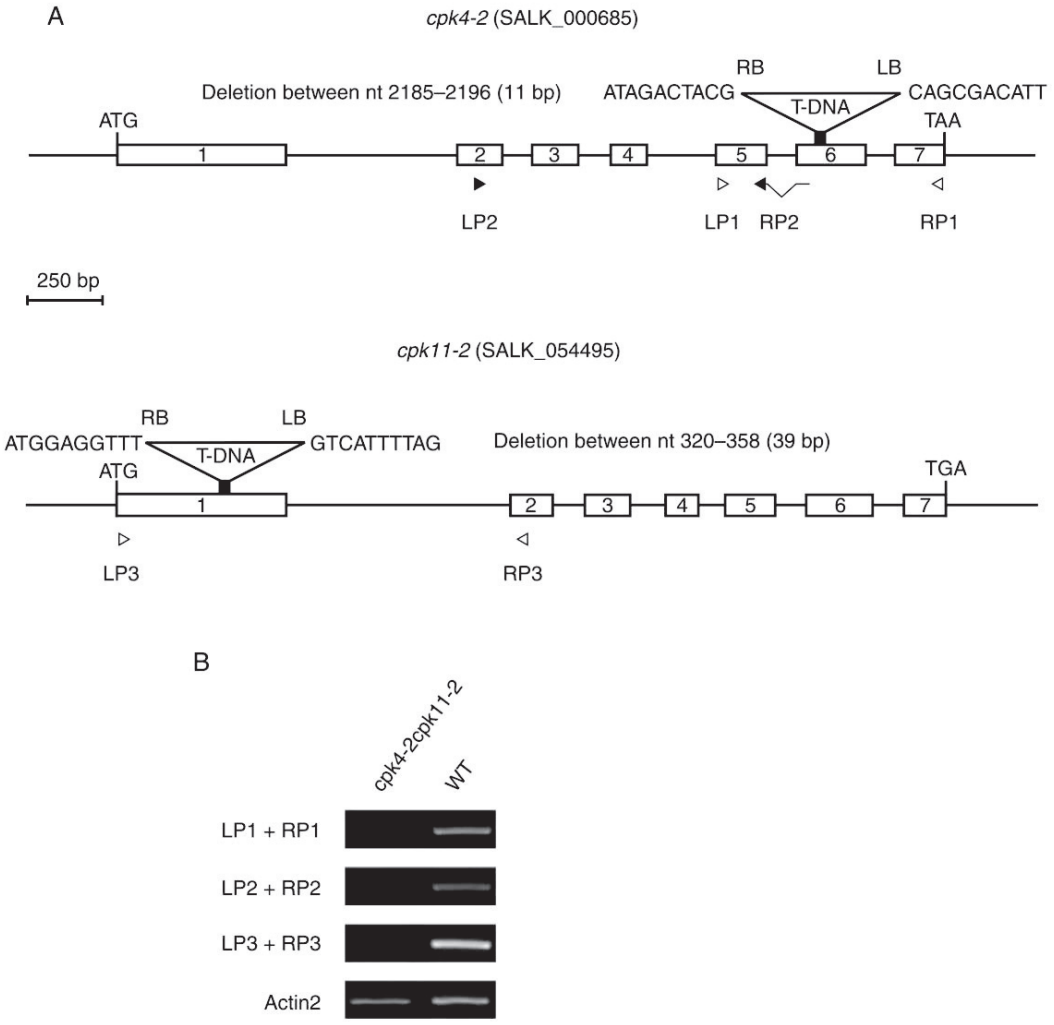

FIG. 7. Characterization *of cpk4-2 cpk11-2* mutant plants. (A) Cartoon showing genomic DNA of CPK4 and CPK11 and the T-DNA insertion sites of the corresponding mutant alleles. White boxes represent exons. Arrowheads show primer locations used for RT-PCR experiments shown in (B). The T-DNA insertion site of the *cpk4-2* allele was localized in the 6th exon at nucleotide 2184 after ATG by sequencing. In the *cpk4-2* mutant, 11 nucleotides (2185–2196) are deleted. The T-DNA insertion of *cpk11-2* in the first exon corresponds to that published by Zhu et al. (2007) and was confirmed. (B) RT-PCR analysis of complementary DNA prepared from mutant and wild-type plant RNA revealed that in both, *cpk4-2* and the *cpk11-2* mutant plants no transcripts were detected (35 PCR cycles). Loading control was Actin2 (23 PCR cycles).

BOX 1. IMPROVED RESOLUTION OF STIMULUS-INDUCED STOMATAL MOVEMENTS IN GUARD CELLS BY TRACKING OF INDIVIDUAL STOMATAL APERTURES

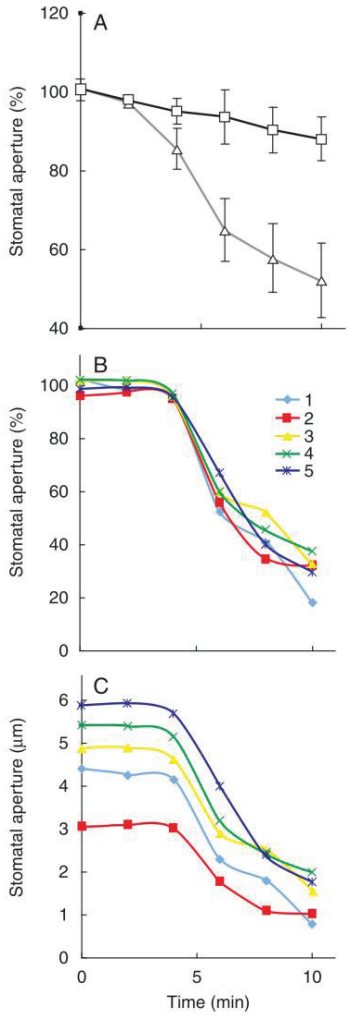

BOX FIG. 1. ABA-induced stomatal closing of individually tracked stomatal apertures. (A) Average individually tracked stomatal apertures in the presence of 50 µM Ca^{2+} (open triangles) and in the presence of 200 nM free Ca^{2+} (open squares) in the bath solution from three experiments are shown and were normalized to the stomatal apertures at time = 0. (B, C) ABA-induced stomatal closing in the presence of 50 µM Ca^{2+} in five individually tracked stomatal apertures. In (A; open triangles) normalized stomatal apertures of the same stomata depicted in (B) and (C) are shown. Methods used in these experiments tracking individual stomatal apertures are described in Siegel et al. (2009). ABA-induced stomatal closing experiments are reproduced from Siegel et al. (2009) with permission of the publisher.

Arabidopsis guard cells have become a prime model system for analysing signal transduction, since early research combining genetic and ion channel analyses in this system (Ichida et al., 1997; Pei et al., 1997, 1998; Roelfsema and Prins, 1997). Arabidopsis stomata are small relative to other stomatal model systems and stomatal apertures of various plant types including Arabidopsis are known to show variability in the size of individual stomatal complexes and also variability in the opening apertures of stomata of similar size in a given leaf (Gorton et al., 1988; Mott and Buckley, 2000; Mott and Peak, 2007). Thus stomatal aperture measurements are expected to show a clear degree of statistical variation. Use of blind experiments, in which the genotype and, when possible, the stimulus being applied to guard cells is unknown to the experimenter (Murata et al., 2001) has been employed by several laboratories, has become a standard in

the field and has aided in addressing the above limitations of the range of stomatal aperture sizes found under any given condition. Research in our laboratory has shown that a major additional improvement in experiments can be made, by adding imaging of the same individual stomatal apertures over time (Allen et al., 2001; Mori et al., 2006; Vahisalu et al., 2008; Siegel et al., 2009), while performing blind experiments. In such 'stomatal tracking' experiments the lower side of a leaf is attached to a glass coverslip in an extracellular incubation medium (Webb etal.,2001; Young etal.,2006). The mesophyll and upper leaf epidermis are removed surgically for better optical resolution of stomatal apertures in the intact lower leaf epidermis (Young et al., 2006). For stimulus-induced stomatal closing analyses, a field of well-opened stomata is located and images are captured (e.g. using Scion Image software) for later analyses and data storage. The bottom (dry side) of coverslips can be marked with colour marker pens to label grids in the regions where apertures where imaged, for finding these same stomata subsequently if needed. Images of the same stomatal apertures are taken over time and can be stored for later analyses of individual stomatal apertures and for deposition of image files. While this approach has been used as a standard for imposed Ca^{2+} oscillation studies (Allen et al., 2001; Mori et al., 2006; Vahisalu et al., 2008; Fig. 4), we have found that this method also substantially improves stomatal movement response analyses to any given stimulus (Siegel et al., 2009; see Figs 1 and 4 and, Box Fig. 1). For example, while individual stomata are known to have diverse apertures (e.g. Box Fig. 1C), the relative responses of wide open stomata and smaller stomatal apertures to ABA or to CO_2 were comparable (Fig. 1 and Box Fig. 1; Siegel et al., 2009). Note that this method has previously been proposed and used in Vicia faba (Gorton et al., 1988), for which stomata exhibit relatively weak ABA and CO_2 responses, compared with, for example, Arabidopsis. We propose that this simple image-capturing approach, together with blind analyses, be used as a standard for stomatal response research in arabidopsis. Our research experience with this method shows that this approach will aid in greatly improving resolution and robustness and in defining the functions of individual Ca^{2+}-independentandCa^{2+}-dependent components and mechanisms in stomatal response analyses.

LITERATURE CITED

Aharon GS, Gelli A, Snedden WA, Blumwald E. 1998. Activation of a plant plasma membrane Ca^{2+} channel by TGalpha1, a heterotrimeric G protein alpha-subunit homologue. FEBS Letters 424: 17–21.

Allen GJ, Sanders D. 1996. Control of ionic currents in guard cell vacuoles by cytosolic and luminal calcium. The Plant Journal 10: 1055– 1069.

Allen GJ, Kuchitsu K, Chu SP, Murata Y, Schroeder JI. 1999a.

Arabidopsis abi1-1 and abi2-1 phosphatase mutations reduce abscisic acid-induced cytoplasmic calcium rises in guard cells. The Plant Cell 11: 1785–1798.

Allen GJ, Kwak JM, Chu SP, et al. 1999b. Cameleon calcium indicator reports cytoplasmic calcium dynamics in Arabidopsis guard cells. The Plant Journal 19: 735–747.

Allen GJ, Chu SP, Schumacher K, et al. 2000. Alteration of stimulus-specific guard cell calcium oscillations and stomatal closing in Arabidopsis det3 mutant. Science 289: 2338–2342.

Allen GJ, Chu SP, Harrington CL, et al. 2001. A defined range of guard cell calcium oscillation parameters encodes stomatal movements. Nature 411: 1053–1057.

Allen GJ, Murata Y, Chu SP, Nafisi M, Schroeder JI. 2002.Hypersensitivity of abscisic acid-induced cytosolic calcium increases in the Arabidopsis farnesyltransferase mutant era1-2. The Plant Cell 14: 1649–1662.

Athwal G, Huber S. 2002. Divalent cations and polyamines bind to loop 8 of 14-3-3 proteins, modulating their interaction with phosphorylated nitrate reductase. The Plant Journal 29: 119–129.

Batistic˘ O, Waadt R, Steinhorst L, Held K, Kudla J. 2010. CBL-mediated targeting of CIPKs facilitates the decoding of calcium signals emanating from distinct cellular stores. The Plant Journal 61: 211–222.

Berridge MJ. 2006. Calcium microdomains: organization and function. Cell Calcium 40: 405–412.

Berridge MJ, Bootman MD, Roderick HL. 2003. Calcium signalling: dynamics, homeostasis and remodelling. Nature Reviews Molecular Cell Biology 4: 517–529.

Braam J. 1992. Regulated expression of the calmodulin-related TCH genes in cultured Arabidopsis cells: induction by calcium and heat shock. Proceedings of the National Academy of Sciences of the USA 89: 3213–3216.

Chehab EW, Patharkar OR, Hegeman AD, Taybi T, Cushman JC. 2004. Autophosphorylation and subcellular localization dynamics of a salt-and water deficit-induced calcium-dependent protein kinase from ice plant. Plant Physiology 135: 1430–1446.

Chen Z-H, Hills A, Lim CK, Blatt MR. 2010. Dynamic regulation of guard cell anion channels by cytosolic free Ca^{2+} concentration and protein phosphorylation. The Plant Journal 61: 816–825.

Cutler SR, Rodriguez PL, Finkelstein RR, Abrams SR. 2010. Abscisic acid: emergence of a core signaling network. Annual Review of Plant Biology 61: 651–679.

Day I, Reddy V, Shad Ali G, Reddy A. 2002. Analysis of EF-hand-containing proteins in Arabidopsis. Genome Biology 3: research0056˙1–re-search0056˙24. doi:10.1186/gb-2002-3-10-research0056.

DeSilva DLR, Cox RC, Hetherington AM, Mansfield TA. 1985. Synergism between calcium ions and abscisic acid in preventing stomatal opening. New Phytologist 100: 473–482.

Dodd AN, Kudla J, Sanders D. 2010. The language of calcium signalling. Annual Review of Plant Biology 61: 593–620.

Geiger D, Scherzer S, Mumm P, et al. 2010. Guard cell anion channel SLAC1 is regulated by CDPK protein kinases with distinct Ca^{2+} affi-nities. Proceedings of the National Academy of Sciences of the USA 107: 8023–8028.

Geiger D, Maierhofer T, Al-Rasheid KA, et al. 2011. Stomatal closure by fast abscisic acid signaling is mediated by the guard cell anion channel SLAH3 and the receptor RCAR1. Science Signaling 4: ra32. doi:10.1126/scisignal.2001346.

Gilroy S, Fricker MD, Read ND, Trewavas AJ. 1991. Role of calcium in signal transduction of commelina guard cells. The Plant Cell 3: 333–344.

Gilroy S, Read ND, Trewavas AJ. 1990. Elevation of cytoplasmic calcium by caged calcium or caged inositol trisphosphate initiates stomatal closure. Nature 346: 769–771.

Gobert A, Isayenkov S, Voelker C, Czempinski K, Maathuis FJ. 2007. The two-pore channel TPK1 gene encodes the vacuolar K^+ conductance and plays a role in K^+ homeostasis. Proceedings of the National Academy of Sciences of the USA 104: 10726–10731.

Gorton HL, Williams WE, Binns ME. 1988. Repeated measurements of aperture for individual stomates. Plant Physiology 89: 387–390.

Grabov A, Blatt MR. 1997. Parallel control of the inward-rectifier K^+ channel by cytosolic free Ca^{2+} and pH in Vicia guard cells. Planta 201: 84–95.

Grabov A, Blatt MR. 1998. Membrane voltage initiates Ca^{2+} waves and potentiates Ca^{2+} increases with abscisic acid in stomatal guard cells. Proceedings of the National Academy of Sciences of the USA 95: 4778–4783.

Hamilton DW, Hills A, Kohler B, Blatt MR. 2000. Ca^{2+} channels at the plasma membrane of stomatal guard cells are activated by hyperpolariz-ation and abscisic acid. Proceedings of the National Academy of Sciences of the USA 97: 4967–4972.

Hedrich R, Neher E. 1987. Cytoplasmic calcium regulates voltage-dependent ion channels in plant vacuoles. Nature 329: 833–836.

Hedrich R, Busche H, Raschke K. 1990. Ca^{2+} and nucleotide dependent regulation of voltage dependent anion channels in the plasma membrane of guard cells. EMBO Journal 9: 3889–3892.

Hetherington AM, Woodward FI. 2003. The role of stomata in sensing and driving environmental change. Nature 424: 901–908.

Hoth S, Morgante M, Sanchez J-P, Hanafey MK, Tingey SV, Chua N-H. 2002. Genome-wide gene expression profiling in Arabidopsis thaliana reveals new targets of abscisic acid and largely impaired gene regulation in the abi1-1 mutant. Journal of Cell Science 115: 4891–4900.

Hubbard KE, Nishimura N, Hitomi K, Getzoff ED, Schroeder JI. 2010. Early abscisic acid signal transduction mechanisms: newly discovered components and newly emerging questions. Genes & Development 24: 1695–1708.

Hugouvieux V, Kwak JM, Schroeder JI. 2001. An mRNA cap binding protein, ABH1, modulates early abscisic acid signal transduction in arabi-dopsis. Cell 106: 477–487.

Ichida AM, Pei ZM, Baizabal-Aguirre VM, Turner KJ, Schroeder JI. 1997. Expression of a Cs^+-resistant guard cell K^+ channel confers Cs^+-resistant, light-induced stomatal opening in transgenic arabidopsis. The Plant Cell 9: 1843–1857.

Islam MM, Hossain MA, Jannat R, et al. 2010. Cytosolic alkalization and cytosolic calcium oscillation in Arabidopsis guard cells response to ABA and MeJA. Plant and Cell Physiology 51: 1721–1730.

Israelsson M, Siegel RS, Young J, Hashimoto M, Iba K, Schroeder JI. 2006. Guard cell ABA and CO_2 signaling network updates and Ca^{2+} sensor priming hypothesis. Current Opinion in Plant Biology 9: 654–663.

Joshi-Saha A, Valon C, Leung J. 2011. Abscisic acid signal off the STARTing block. Molecular Plant 4: 562–80.

Jung JY, Kim YW, Kwak JM, et al. 2002. Phosphatidylinositol 3- and 4-phosphate are required for normal stomatal movements. The Plant Cell 14: 2399–2412.

Kaplan B, Davydov O, Knight H, et al. 2006. Rapid transcriptome changes induced by cytosolic Ca^{2+} transients reveal ABRE-related sequences as Ca^{2+}-responsive cis elements in Arabidopsis. The Plant Cell 18: 2733–2748.

Kaplan B, Sherman T, Fromm H. 2007. Cyclic nucleotide-gated channels in plants. FEBS Letters 581: 2237–2246.

Kelly WB, Esser JE, Schroeder JI. 1995. Effects of cytosolic calcium and limited, possible dual, effects of G protein modulators on guard cell inward potassium channels. The Plant Journal 8: 479–489.

Kim T-H, Bo¨hmer M, Hu H, Nishimura N, Schroeder JI. 2010. Guard cell signal transduction network: advances in understanding abscisic acid, CO_2, and Ca^{2+} signaling. Annual Review of Plant Biology 61: 561–591.

Kinoshita T, Nishimura M, Shimazaki K. 1995. Cytosolic concentration of Ca^{2+} rregulates the plasma membrane H^+-ATPase in guard cells of fava bean. The Plant Cell 7: 1333–1342.

Kluesener B, Young JJ, Murata Y, et al. 2002. Convergence of calcium sig-naling pathways of pathogenic elicitors and abscisic acid in arabidopsis guard cells. Plant Physiology 130: 2152–2163.

Kudla J, Batistic O, Hashimoto K. 2010. Calcium signals: the lead currency of plant information processing. The Plant Cell 22: 541–563.

Kwak JM, Murata Y, Baizabal-Aguirre VM, et al. 2001. Dominant negative guard cell K^+ channel mutants reduce inward-rectifying K^+ currents and light-induced stomatal opening in arabidopsis. Plant Physiology 127: 473–485.

Kwak JM, Moon J-H, Murata Y, et al. 2002. Disruption of a guard cell-expressed protein phosphatase 2A regulatory subunit, RCN1, confers abscisic acid insensitivity in arabidopsis. The Plant Cell 14: 2849–2861.

Kwak JM, Mori IC, Pei Z-M, et al. 2003. NADPH oxidase AtrbohD and AtrbohF genes function in ROS-dependent ABA signaling in Arabidopsis. EMBO Journal 22: 2623–2633.

Lacombe B, Becker D, Hedrich R, et al. 2001. The identity of plant gluta-mate receptors. Science 292: 1486–1487.

Leonhardt N, Kwak JM, Robert N, Waner D, Leonhardt G, Schroeder JI. 2004. Microarray expression analyses of arabidopsis guard cells and iso-lation of a recessive abscisic acid hypersensitive protein phosphatase 2C mutant. The Plant Cell 16: 596–615.

Levchenko V, Konrad KR, Dietrich P, Roelfsema MRG, Hedrich R. 2005. Cytosolic abscisic acid activates guard cell anion channels without pre-ceding Ca^{2+} signals. Proceedings of the National Academy of Sciences of the USA 102: 4203–4208.

Li Y, Wang G-X, Xin M, Yang H-M, Wu X-J, Li T. 2004. The parameters of guard cell calcium oscillation encode inhibition of stomatal opening in Vicia faba. Plant Science 166: 415–421.

Lu G, Sehnke PC, Ferl RJ. 1994. Phosphorylation and calcium binding prop-erties of an arabidopsis GF14 brain protein homolog. The Plant Cell 6: 501–510.

McAinsh MR, Brownlee C, Hetherington AM. 1990. Abscisic acid-induced elevation of guard-cell cytosolic Ca^{2+} precedes stomatal closure. Nature 343: 186–188.

McAinsh MR, Brownlee C, Hetherington AM. 1992. Visualizing changes in cytosolic-free Ca^{2+} during the response of stomatal guard cells to abscisic acid. The Plant Cell 4: 1113–1122.

McAinsh MR, Webb AAR, Staxen I, Taylor JE, Hetherington AM. 1995. Stimulus-induced oscillations in guard-cell cytosolic-free Ca^{2+}. Plant Physiology 108: 100–100.

Ma SY, Wu WH. 2007. AtCPK23 functions in Arabidopsis responses to drought and salt stresses. Plant Molecular Biology 65: 511–518.

MacRobbie EA. 1998. Signal transduction and ion channels in guard cells. Philosophical Transactions of the Royal Society of London Series B – Biological Sciences 353: 1475–1488.

MacRobbie EA. 2000. ABA activates multiple Ca(2+) fluxes in stomatal guard cells, triggering vacuolar K(+)(Rb(+)) release. Proceedings of the National Academy of Sciences of the USA 97: 12361–12368.

Marten H, Konrad KR, Dietrich P, Roelfsema MR, Hedrich R. 2007. Ca^{2+}-dependent and -independent abscisic acid activation of plasma membrane anion channels in guard cells of Nicotiana tabacum. Plant Physiology 143: 28–37.

Melcher K, Zhou XE, Xu HE. 2010. Thirsty plants and beyond: structural mechanisms of abscisic acid perception and signaling. Current Opinion in Structural Biology 20: 722–729.

Meyer S, Mumm P, Imes D, et al. 2010. AtALMT12 represents an R-type anion channel required for stomatal movement in Arabidopsis guard cells. The Plant Journal 63: 1054–1062.

Mori IC, Murata Y, Yang Y, et al. 2006. CDPKs CPK6 and CPK3 function in ABA regulation of guard cell S-type anion- and Ca^{2+}-permeable chan-nels and stomatal closure. PLoS Biology 4: e327. doi:10.1371/ journal.pbio.0040327.

Mott KA, Buckley TN. 2000. Patchy stomatal conductance: emergent collec-tive behaviour of stomata. Trends in Plant Science 5: 258–262.

Mott KA, Peak D. 2007. Stomatal patchiness and task-performing networks. Annals of Botany 99: 219–226.

Murata Y, Pei Z-M, Mori IC, Schroeder J. 2001. Abscisic acid activation of plasma membrane Ca^{2+} channels in guard cells requires cytosolic NAD(P)H and is differentially disrupted upstream and downstream of reactive oxygen species production in abi1-1 and abi2-1 protein phospha-tase 2C mutants. The Plant Cell 13: 2513–2523.

Negi J, Matsuda O, Nagasawa T, et al. 2008. CO_2 regulator SLAC1 and its homologues are essential for anion homeostasis in plant cells. Nature 452: 483–486.

Pandey S, Zhang W, Assmann SM. 2007. Roles of ion channels and transpor-ters in guard cell signal transduction. FEBS Letters 581: 2325–2336.

Pei ZM, Kuchitsu K, Ward JM, Schwarz M, Schroeder JI. 1997. Differential abscisic acid regulation of guard cell slow anion channels in arabidopsis wild-type and abi1 and abi2 mutants. The Plant Cell 9: 409–423.

Pei ZM, Ghassemian M, Kwak CM, McCourt P, Schroeder JI. 1998. Role of farnesyltransferase in ABA regulation of guard cell anion channels and plant water loss. Science 282: 287–290.

Pei ZM, Ward JM, Schroeder JI. 1999. Magnesium sensitizes slow vacuolar channels to physiological cytosolic calcium and inhibits fast vacuolar channels in fava bean guard cell vacuoles. Plant Physiology 121: 977–986.

Pei ZM, Murata Y, Benning G, et al. 2000. Calcium channels activated by hydrogen peroxide mediate abscisic acid signalling in guard cells. Nature 406: 731–734.

Peiter E, Maathuis FJM, Mills LN, et al. 2005. The vacuolar Ca^{2+}-activated channel TPC1 regulates germination and stomatal movement. Nature 434: 404–408.

Raghavendra AS, Gonugunta VK, Christmann A, Grill E. 2010. ABA per-ception and signalling. Trends in Plant Science 15: 395–401.

Raschke K, Hedrich R, Reckmann U, Schroder JI. 1988. Exploring bio-physical and biochemical components of the osmotic motor that drives stomatal movement. Botanica Acta 101: 283–294.

Roelfsema MRG, Prins HBA. 1997. Ion channels in guard cells of Arabidopsis thaliana. Planta 202: 18–27.

Sanchez J-P, Duque P, Chua N-H. 2004. ABA activates ADPR cyclase and cADPR induces a subset of ABA-responsive genes in Arabidopsis. The Plant Journal 38: 381–395.

Schmidt C, Schroeder JI. 1994. Anion selectivity of slow anion channels in the plasma membrane of guard cells (large nitrate permeability). Plant Physiol 106: 383–391.

Schroeder JI. 1995. Anion channels as central mechanisms for signal trans-duction in guard cells and putative functions in roots for plant–soil inter-actions. Plant Molecular Biology 28: 353–361.

Schroeder JI, Hagiwara S. 1989. Cytosolic calcium regulates ion channels in the plasma membrane of Vicia faba guard cells. Nature 338: 427–430.

Schroeder JI, Hagiwara S. 1990. Repetitive increases in cytosolic Ca^{2+} of guard cells by abscisic acid activation of nonselective Ca^{2+} permeable channels. Proceedings of the National Academy of Sciences of the USA 87: 9305–9309.

Schroeder JI, Kwak JM, Allen GJ. 2001. Guard cell abscisic acid signalling and engineering drought hardiness in plants. Nature 410: 327–330.

Schwartz A. 1985. Role of Ca and EGTA on stomatal movements in Commelina communis L. Plant Physiology 79: 1003–1005.

Siegel RS, Xue S, Murata Y, et al. 2009. Calcium elevation-dependent and attenuated resting calcium-dependent abscisic acid induction of stomatal closure and abscisic acid-induced enhancement of calcium sensitivities of S-type anion and inward-rectifying K channels in Arabidopsis guard cells. The Plant Journal 59: 207–220.

Sirichandra C, Wasilewska A, Vlad F, Valon C, Leung J. 2009. The guard cell as a single-cell model towards understanding drought tolerance and abscisic acid action. Journal of Experimental Botany 60: 1439–1463.

Staxen I, Pical C, Montgomery LT, Gray JE, Hetherington AM, McAinsh MR. 1999. Abscisic acid induces oscillations in guard-cell cytosolic free calcium that involve phosphoinositide-specific phospholipase C. Proceedings of the National Academy of Sciences of the USA 96: 1779–1784.

Suh SJ, Wang Y-F, Frelet A, et al. 2007. The ATP binding cassette transpor-ter AtMRP5 modulates anion and calcium channel activities in arabidop-sis guard cells. Journal of Biological Chemistry 282: 1916–1924.

Vahisalu T, Kollist H, Wang YF, et al. 2008. SLAC1 is required for plant guard cell S-type anion channel function in stomatal signalling. Nature 452: 487–491.

Valerio GS. 2007. The roles of Ca^{2+} in the guard cell ABA signaling pathway and exploration of a possible ion channel gene in Arabidopsis thaliana. MSc Thesis, University of California, San Diego.

Waadt R, Schmidt LK, Lohse M, Hashimoto K, Bock R, Kudla J. 2008. Multicolor bimolecular fluorescence complementation reveals simul-taneous formation of alternative CBL/CIPK complexes in planta. The Plant Journal 56: 505–516.

Ward JM, Schroeder JI. 1994. Calcium-activated K^+ channels and calcium-induced calcium release by slow vacuolar ion channels in guard cell vacuoles implicated in the control of stomatal closure. The Plant Cell 6: 669–683.

Webb AAR, McAinsh MR, Mansfield TA, Hetherington AM. 1996. Carbon dioxide induces increases in guard cell cytosolic free calcium. The Plant Journal 9: 297–304.

Webb AAR, Larman MG, Montgomery LT, Taylor JE, Hetherington AM. 2001. The role of calcium in ABA-induced gene expression and stomatal movements. The Plant Journal 26: 351–362.

Wood NT, Allan AC, Haley A, Viry-Moussaı¨d M, Trewavas AJ. 2000. The characterization of differential calcium signalling in tobacco guard cells. The Plant Journal 24: 335–344.

Xue S, Hu H, Ries A, Merilo E, Kollist H, Schroeder JI. 2011. Central func-tions of bicarbonate in S-type anion channel activation and OST1 protein kinase in CO_2 signal transduction in guard cell. EMBO Journal 30: 1645–1658.

Yang HM, Zhang XY, Wang GX, Li Y, Wei XP. 2003. Cytosolic calcium oscillations induce stomatal closure in Vicia faba. Plant Science 165: 1117–1122.

Yang Y, Costa A, Leonhardt N, Siegel R, Schroeder J. 2008. Isolation of a strong Arabidopsis guard cell promoter and its potential as a research tool. Plant Methods 4: 6.

Young JJ, Mehta S, Israelsson M, Godoski J, Grill E, Schroeder JI. 2006. CO_2 signaling in guard cells: calcium sensitivity response modulation, a Ca^{2+}-independent phase, and CO_2 insensitivity of the gca2 mutant. Proceedings of the NationalAcademyof Sciences of the USA 103: 7506–7511.

Zeller G, Henz SR, Widmer CK, et al. 2009. Stress-induced changes in the Arabidopsis thaliana transcriptome analyzed using whole-genome tiling arrays. The Plant Journal 58: 1068–1082.

Zhu S-Y, Yu X-C, Wang X-J, et al. 2007. Two calcium-dependent protein kinases, CPK4 and CPK11, regulate abscisic acid signal transduction in arabidopsis. The Plant Cell 19: 3019–3036.

Zou J-J, Wei F-J, Wang C, et al. 2010. Arabidopsis calcium-dependent protein kinase CPK10 functions in abscisic acid- and Ca^{2+}-mediated stomatal regu-lation in response to drought stress. Plant Physiology 154: 1232–1243.

Reconstitution of abscisic acid activation of SLAC1 anion channel by CPK6 and OST1 kinases and branched ABI1 PP2C phosphatase action

Benjamin Brandt[a,1], Dennis E. Brodsky[a,1], Shaowu Xue[a,2], Juntaro Negi[b], Koh Iba[b], Jaakko Kangasjärvi[c], Majid Ghassemian[d], Aaron B. Stephan[a], Honghong Hu[a], and Julian I. Schroeder[a,3]

[a]Cell and Developmental Biology Section, Division of Biological Sciences, University of California at San Diego, La Jolla, CA 92093; [b]Department of Biology, Faculty of Sciences, Kyushu University, Fukuoka 812-8581, Japan; [c]Division of Plant Biology, Department of Biosciences, University of Helsinki, FI-00014 Helsinki, Finland; and [d]Biomolecular/Proteomics Mass Spectrometry Facility, Department of Chemistry and Biochemistry, University of California at San Diego, La Jolla, CA 92093-0378

Edited by Jian-Kang Zhu, Purdue University, West Lafayette, IN, and approved May 16, 2012 (received for review October 10, 2011)

The plant hormone abscisic acid (ABA) is produced in response to abiotic stresses and mediates stomatal closure in response to drought via recently identified ABA receptors (pyrabactin resistance/regulatory component of ABA receptor; PYR/RCAR). *SLAC1* encodes a central guard cell S-type anion channel that mediates ABA-induced stomatal closure. Coexpression of the calcium-dependent protein kinase 21 (CPK21), CPK23, or the Open Stomata 1 kinase (OST1) activates SLAC1 anion currents. However, reconstitution of ABA activation of any plant ion channel has not yet been attained. Whether the known core ABA signaling components are sufficient for ABA activation of SLAC1 anion channels or whether additional components are required remains unknown. The Ca^{2+}-dependent protein kinase CPK6 is known to function in vivo in ABA-induced stomatal closure. Here we show that CPK6 robustly activates SLAC1-mediated currents and phosphorylates the SLAC1 N terminus. A phosphorylation site (S59) in SLAC1, crucial for CPK6 activation, was identified. The group A PP2Cs ABI1, ABI2, and PP2CA down-regulated CPK6-mediated SLAC1 activity in oocytes. Unexpectedly, ABI1 directly dephosphorylated the N terminus of SLAC1, indicating an alternate branched early ABA signaling core in which ABI1 targets SLAC1 directly (down-regulation). Furthermore, here we have successfully reconstituted ABA-induced activation of SLAC1 channels in oocytes using the ABA receptor pyrabactin resistant 1 (PYR1) and PP2C phosphatases with two alternate signaling cores including either CPK6 or OST1. Point mutations in ABI1 disrupting PYR1–ABI1 interaction abolished ABA signal transduction. Moreover, by addition of CPK6, a functional ABA signal transduction core from ABA receptors to ion channel activation was reconstituted without a SnRK2 kinase.

Arabidopsis | chloride channel

The perception of the phytohormone abscisic acid (ABA) is achieved by the recently discovered 14-member START protein family of ABA receptors named pyrabactin resistance (PYR), or regulatory component of ABA receptor (RCAR) (1, 2). PYR/RCARs have been shown to bind to clade A PP2Cs and inhibit the activity of these PP2Cs in the presence of ABA (1–5). Structural studies show that PYR1, PYL1, and PYL2 function as ABA receptors, with ABA binding in a protein cavity that locks down the ABA molecule (6–10).

ABA reduces transpirational water loss of plants by inducing stomatal closure (11). ABA can cause an increase in guard cell intracellular Ca^{2+} concentration (12–17), which leads to the down-regulation of inward-rectifying K^+ channels and activation of both slow-sustained (S-type) and rapid-transient (R-type) anion channels (18–20). Previous findings have led to the model that S-type anion channels play a key role in controlling stomatal closure (18, 21, 22). *slac1* mutant plants have greatly reduced S-type anion channel activity (23) and display impaired stomatal closure in response to ABA, elevated CO_2, ozone, reactive oxygen species, calcium, and reduced humidity, underlining that SLAC1 represents a key component functioning downstream of these signals and is crucial for stomatal closure (23, 24).

The subclass III SnRK2 kinase OST1 (Open Stomata 1), also known as SnRK2.6, is required for ABA- and CO_2-induced stomatal closure (25–27). Several members of the PP2C family have been shown to directly interact with (3, 28, 29) and deactivate subclass III SnRK2 protein kinases (SnRK2.2, SnRK2.3, and SnRK2.6/OST1) through dephosphorylation in vitro (28–30).

S-type anion channels in guard cells are activated by phosphorylation events (31, 32). *Xenopus* oocyte electrophysiology experiments demonstrated that SLAC1 in the presence of the protein kinases OST1, calcium-dependent protein kinase 23 (CPK23), and, to a lesser extent, CPK21 can generate S-type anion channel activity (33–35). An S120A mutation in SLAC1 prevents channel activation by OST1, but CPK23 is still able to induce SLAC1 S120A-mediated currents in *Xenopus* oocytes (33, 34). SLAC1-mediated anion currents are down-regulated by the PP2C-type phosphatases ABI1, ABI2 (33, 34), and PP2CA (35). However, whether ABA activation of anion channels can be reconstituted in *Xenopus* oocytes with these core signaling components remains unknown (33–36).

The role and function of CPKs in the regulation of SLAC1 are still ambiguous. In vivo, CPK6 functions as a positive regulator of ABA control of S-type anion channels in guard cells (37). In *cpk3cpk6* double knockout mutant *Arabidopsis* plants, ABA- and Ca^{2+}-induced stomatal closure, as well as activation of S-type anion channel activity, was impaired in vivo, with CPK6 playing a more prominent role than CPK3 (37). CPK21 and CPK23 activate SLAC1 in *Xenopus laevis* oocytes (34), but *cpk21* and *cpk23* mutants show enhanced drought and salt tolerance (38, 39) rather than drought sensitivity. Furthermore, CPK6 was reported to weakly interact with SLAC1 in *Xenopus* oocytes (34). Here we functionally reconstitute activation of SLAC1 channels by ABA with either CPK6 or OST1 in the ABA signaling core and identify mechanisms of this signaling pathway. Interestingly, these findings further show that an alternate early ABA signaling core can be functionally reconstituted for ABA activation of

Author contributions: J.I.S., B.B., and D.E.B. designed research; B.B., D.E.B., S.X., M.G., and A.B.S. performed research; J.N., K.I., J.K., and H.H. contributed new reagents/analytic tools; B.B., D.E.B., M.G., and J.I.S. analyzed data; and B.B., D.E.B., and J.I.S. wrote the paper.

The authors declare no conflict of interest.

This article is a PNAS Direct Submission.

[1]B.B. and D.E.B. contributed equally to this work.

[2]Present address: Institute of Molecular Science, Shanxi University, Taiyuan 030006, China.

[3]To whom correspondence should be addressed. E-mail: julian@biomail.ucsd.edu.

This article contains supporting information online at www.pnas.org/lookup/suppl/doi:10.1073/pnas.1116590109/-/DCSupplemental.

a plant ion channel without inclusion of a SnRK2 kinase. Furthermore, in addition to the known dephosphorylation of OST1 by the ABI1 PP2C, we demonstrate that ABI1 directly dephosphorylates the N terminus of SLAC1, enabling tight control of anion channel activity.

Results

CPK6 Activates SLAC1 in *Xenopus* Oocytes and Phosphorylates the N Terminus of SLAC1. Two-electrode voltage-clamp experiments in *X. laevis* oocytes were performed to analyze SLAC1 regulation. When *SLAC1* cRNA was injected into oocytes alone, average inward currents were similar to those of water-injected control oocytes (Fig. 1 *A* and *B*). We investigated whether CPK6, which functions in S-type anion channel activation in vivo (37), can activate SLAC1 channels. Coexpression of SLAC1 and individual protein kinases, including CPK6 and CPK23, significantly activated SLAC1-dependent ion currents compared with those of SLAC1 alone (Fig. 1 *A* and *B* and Fig. S1*A*; $P = 0.001$ and $P = 0.04$ for CPK6 and CPK23, respectively; Mann–Whitney *U* test at −180 mV). It was also confirmed that CPK6 was able to activate SLAC1 consistently throughout six of the tested batches of oocytes ($P < 0.001$; two-way ANOVA). Reversal potentials of SLAC1 and kinase-activated ion currents were close to the equilibrium potential for Cl^-, consistent with the anion selectivity of S-type anion channels. Robust CPK6 activation of SLAC1 channels (Fig. 1 *A* and *B* and Fig. S1*A*) did not require experimentally imposed linkage of SLAC1 to the protein kinase using split yellow fluorescent protein (YFP-BiFC) fusions, as shown for OST1 (33). The calcium dependent protein kinases closely related to CPK6 and CPK23 [CPK12 and CPK31, respectively (40)] were not able to stimulate SLAC1 activity (Fig. 1 *A* and *B* and Fig. S1*A*; CPK12, $P = 0.305$; Student's *t* test; CPK31, $P = 0.234$; Mann–Whitney *U* test at −180 mV). Coexpressing the kinase-inactive variant of CPK6 (D209A) together with SLAC1 did not activate SLAC1 (Fig. S1*B*), indicating a kinase activity-dependent event. Comparison of SLAC1 activity in the presence of the tested kinases suggests that SLAC1 activations by CPK6 and CPK23 are statistically comparable (Fig. S1*A*; $P = 0.561$; Mann–Whitney *U* test at −180 mV), whereas CPK3 and CPK31 showed no significant activation of SLAC1 (Fig. S1*A*; $P = 0.363$ and $P = 0.321$ for CPK3 and CPK31, respectively; Mann–Whitney *U* test at −180 mV).

Localizations and abundances of CPK6 and CPK23 were analyzed in *Xenopus* oocytes. Confocal laser microscopy of cryomicrodissected CPK fusion protein (mTurquoise; mTq)-expressing *Xenopus* oocytes revealed that a significant proportion of the CPK6 and CPK23 proteins are located at the cell surface, with an additional weak fluorescence distributed throughout the cytoplasm (Fig. 2 *A* and *B*). Quantification of the fluorescence intensities showed that CPK6-mTq and CPK23-mTq abundance

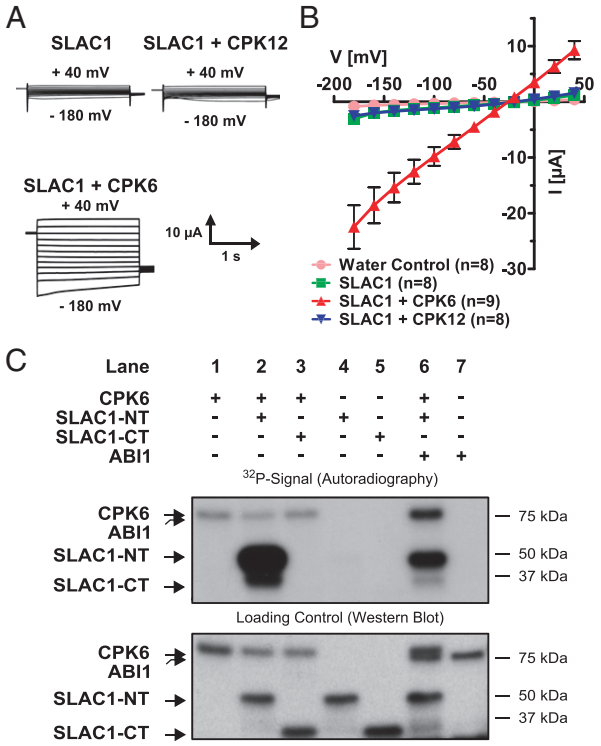

Fig. 1. Strong activation of SLAC1 channels by the CPK6 protein kinase in *Xenopus* oocytes and in vitro. (*A*) Whole-cell voltage-clamp recordings for oocytes expressing SLAC1, in the presence or absence of CPKs, show that coexpression of SLAC1 with CPK6 results in large Cl^- currents, as opposed to SLAC1 with CPK12. (*B*) The average steady-state current–voltage relationships are shown in water-injected (pink circles), SLAC1-injected (green squares), and SLAC1 + CPK-injected oocytes. The protein kinase CPK6 (red triangles) stimulates SLAC1 activity, whereas CPK12 (blue triangles), a homolog of CPK6, did not increase SLAC1 activity in oocytes. Representative data from one batch of oocytes are shown (of >3 batches tested). Error bars represent SEM. (*C*) Autoradiograph of in vitro kinase assays using recombinant proteins (*Upper*) and Western blot analysis detecting GST as loading control for the individual proteins (*Lower*). The kinase CPK6 (lane 1) is able to transphosphorylate the N terminus of SLAC1 (lane 2; SLAC1-NT) but not the C terminus (lane 3; SLAC1-CT). No signal could be detected upon incubation of SLAC1-NT (lane 4) or SLAC1-CT alone (lane 5). Coincubation of CPK6 with ABI1 decreased SLAC1-NT transphosphorylation (lane 6). Assaying ABI1 alone did not result in a ^{32}P signal (lane 7).

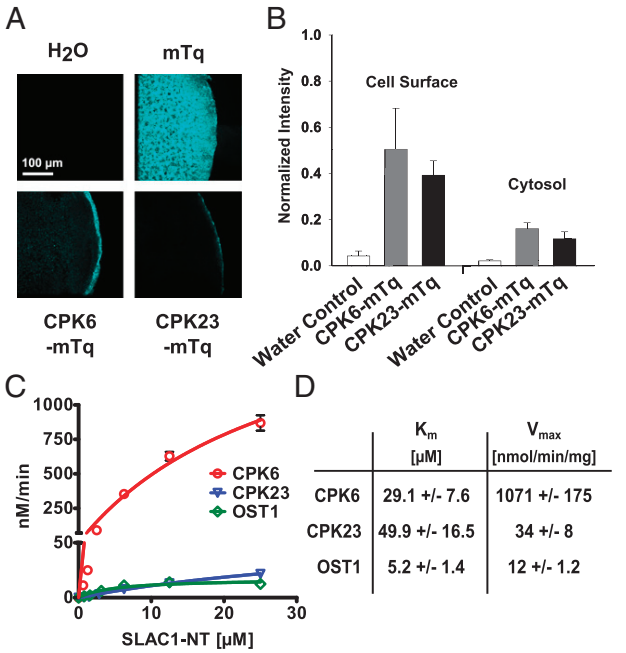

Fig. 2. CPK6 is expressed at the cell surface and high in vitro CPK6 activity toward SLAC1-NT phosphorylation. (*A*) Kinases CPK6 and CPK23 are localized at the cell surface, whereas mTurquoise (mTq) alone is uniformly spread throughout oocytes. (*B*) Analysis of fluorescence intensity (normalized to mTq) highlights the strong cell-surface localization of both CPK6 and CPK23 (data points represent mean ± SE; $n > 3$). (*C*) P81 filter-based protein kinase assays show kinetics of SLAC1-NT phosphorylation by CPK6 (red circles), CPK23 (blue triangles), and OST1 (green diamonds). Data points represent mean values ± SE ($n = 3$). (*D*) K_m values are given in µM SLAC1-NT, and maximum specific activities are in nmol PO_4 incorporated·min^{-1}·mg^{-1} kinase.

did not significantly differ (Fig. 2*B*; cell surface, $P = 0.474$; cytosol, $P = 0.344$; Student's *t* test). To estimate a saturation point of CPK6 and CPK23-dependent SLAC1 activation, defined amounts of cRNA encoding the protein kinases CPK6 and CPK23 were injected into oocytes: a standard [*CPK6/23*] cRNA amount (~25 ng; [1.0]), an intermediate cRNA amount (~12.5 ng *CPK6/23*; [0.5]), or one-tenth cRNA amount (~2.5 ng *CPK6/23*; [0.1]). For these experiments, oocytes were coinjected with 25 ng *SLAC1* cRNA. Halving the injected cRNA amount resulted in no significant change in SLAC1 channel activity (Fig. S2; $P > 0.685$ at −180 mV; Student's *t* test). However, injecting one-tenth of the amount of cRNA resulted in a strong reduction of SLAC1-mediated anion currents (Fig. S2; $P < 0.01$ at −180 mV; Mann–Whitney *U* test), suggesting that the injected *CPK6/23* cRNA amount at 25 ng was near the saturation point when 25 ng *SLAC1* cRNA was coinjected.

In vitro protein kinase assays were performed to assess whether CPK6 can phosphorylate cytosolic domains of the SLAC1 channel. Wild-type recombinant CPK6 protein showed weak autophosphorylation (Fig. 1*C*, *Upper*, lane 1). The N terminus of SLAC1 (SLAC1-NT; amino acids 1–186), but not the C terminus (SLAC1-CT; amino acids 497–556), was strongly phosphorylated by CPK6 (Fig. 1*C*, *Upper*, lanes 2 and 3). The SLAC1 termini incubated alone did not show any signal (Fig. 1*C*, *Upper*, lanes 4 and 5). The strong CPK6-mediated SLAC1-NT phosphorylation was dependent on the presence of free Ca^{2+} in the reaction buffer (Fig. S3).

To quantify the degree of CPK6-mediated SLAC1 phosphorylation activity, P81-grade filter-based kinetic in vitro phosphorylation assays were performed (Fig. 2 *C* and *D*). The K_m and V_{max} values of the kinase substrate pairs reveal that CPK6 very efficiently and, to a lower extent, CPK23 and OST1, phosphorylates the SLAC1-NT in vitro (Fig. 2 *C* and *D*).

Identification and Characterization of Sites Phosphorylated by CPK6. Due to activation of SLAC1-mediated ion currents by CPK6 (Figs. 1 and 3) and the in vivo function of CPK6 in guard cells (37), we focused on deciphering the properties of this regulation. To date, the only known amino acid that is crucial for SLAC1 activation by a protein kinase is serine 120 (33, 34, 41). To determine which residues may be relevant, trypsin-digested SLAC1-NT, phosphorylated by CPK6 in the presence of nonradioactive ATP, was analyzed by high-pressure liquid chromatography (HPLC) coupled to tandem mass spectroscopy (LC-MS/MS) using nanospray ionization. A SLAC1-NT phosphorylation site was identified at the amino acid serine 59 (Fig. 3*A*). Consequently, this amino acid was replaced by either alanine (which cannot be phosphorylated; SLAC1 S59A) or aspartate (putative phosphomimetic; SLAC1 S59D), and CPK6 activation of SLAC1 was analyzed in oocytes. Voltage-clamp recordings showed that SLAC1 S59A was not activated by CPK6 (Fig. 3*B*). SLAC1 S59D did not exhibit constitutive activation of anion current activity compared with wild-type SLAC1 (Fig. S4*B*), indicating that either this mutant is not a functional phosphomimetic or that additional phosphorylation sites are required. These findings indicate that serine 59 represents a crucial amino acid for CPK6-mediated activation of SLAC1.

Down-Regulation of CPK6-Activated SLAC1 Channels by Group A PP2Cs. We tested several PP2Cs that function in ABA signaling for their ability to inhibit CPK6-mediated SLAC1 activation. Experiments showed that the PP2C protein phosphatases ABI1 (42, 43), ABI2, and PP2CA (44–46) were able to almost completely down-regulate CPK6-activated anion currents in oocytes (Fig. 4 *A* and *B*).

In in vitro kinase assays, the phosphorylation of the SLAC1-NT by CPK6 (Fig. 1*C*, *Upper*, lane 2) was decreased when recombinant ABI1 protein was included in the reaction (Fig. 1*C*, *Upper*, lane 6 and Fig. 4*C*, *Upper*, lane 5). Data further indicate that ABI1 might also be phosphorylated by CPK6 (Fig. 1*C*, *Upper*, lane 6). ABI1 alone did not produce any signal on the autoradiogram (Fig. 1*C*, lane 7).

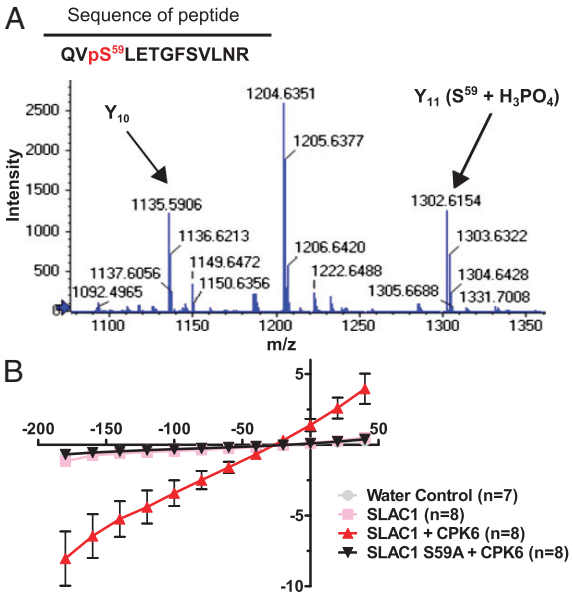

Fig. 3. Serine 59 of SLAC1 is crucial for CPK6-mediated activation of the anion channel. (*A*) Zoomed-in spectrum section of product ion scan for the peptide QVpSLETGFSVLNR [$(M + 2H)^+ = 765.4$]. The fragment ion (Y_{11}) corresponding to phosphorylated serine (S59) is labeled in the figure (Y_{11} (S^{59} + H_3PO_4)). The Y_{10} fragment is labeled to demonstrate that T62 and S65 are not phosphorylated for this ion. The complete spectrum and statistical parameters are presented in Fig. S4*A* and Table S1. (*B*) Average steady-state current–voltage relationships show that the point mutation of serine 59 to alanine (black triangles) abolishes anion channel activity due to CPK6 (red triangles). Representative data from one batch of oocytes are shown (of two batches tested).

Experiments were pursued to address whether ABI1 is able to dephosphorylate amino acid residues in the N terminus of SLAC1 after phosphorylation by CPK6. The kinase inhibitor staurosporine strongly inhibited CPK6 transphosphorylation activity (Fig. 4*C*, *Upper*, lane 4). To probe the ability of the PP2C ABI1 to dephosphorylate SLAC1 directly, the SLAC1-NT was first phosphorylated by CPK6 (Fig. 4*C*, *Upper*, lane 1). Ten minutes later, either staurosporine alone (Fig. 4*C*, lane 3, 10 min) or staurosporine and recombinant ABI1 protein (Fig. 4*C*, lane 2, 10 min) were added, and the reaction was incubated for an additional 35 min. Ten-minute delayed addition of staurosporine alone did not change the phosphorylation state of the SLAC1-NT (Fig. 4*C*, *Upper*, lane 3), but coincubation with ABI1 strongly decreased the prior CPK6-mediated phosphorylation (Fig. 4*C*, *Upper*, lane 2). Thus, CPK6 phosphorylates the N terminus of SLAC1. Unexpectedly, ABI1 reduces this phosphorylation by directly dephosphorylating the SLAC1-NT, which differs from previously reported OST1–ABI1 interactions in which ABI1 did not directly dephosphorylate SLAC1 after OST1-mediated phosphorylation (33). This points to a mechanism for ABA-induced SLAC1 regulation (*Discussion*).

Can ABA Regulate CPK6- or OST1-Dependent SLAC1 Anion Channel Activity in Oocytes? In previous studies, reconstitution of ABA activation of SLAC1 channels has not been studied (33–36). To assess whether ABA activation of SLAC1 can be reconstituted, we coinjected cRNAs of *SLAC1*, *ABI1*/*ABI2*, the *PYR1* ABA receptor, and either *CPK6* or *OST1* into oocytes. In the absence

PLANT BIOLOGY

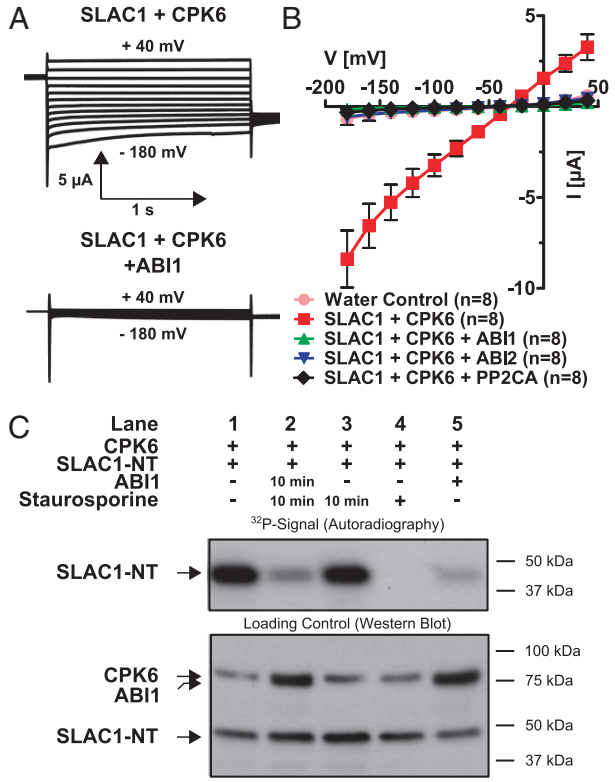

Fig. 4. Strong inhibition of CPK6-mediated SLAC1 activation by PP2C protein phosphatases and direct SLAC1 N terminus dephosphorylation by ABI1. (*A*) Whole-cell current recordings for oocytes show that protein phosphatase ABI1 strongly inactivated CPK6-induced SLAC1 ion channel current. (*B*) Current–voltage relationships in oocytes containing SLAC1 and CPK6 demonstrate that the PP2Cs ABI1 (green triangles), ABI2 (blue triangles), and PP2CA (black diamonds) are capable of strongly inhibiting CPK6-mediated SLAC1 activity (red squares). Data from one representative batch of oocytes (of >3 batches) are shown. (*C*) (*Upper*) ^{32}P phosphorylation of the N terminus of SLAC1. (*Lower*) Loading controls of the individual proteins CPK6, ABI1, and SLAC1. After initial CPK6 exposure, the strong phosphorylation state of SLAC1-NT phosphorylated by CPK6 (*Upper*, lane 1) decreases if subsequently coincubated with ABI1 and staurosporine 10 min after CPK6 exposure (lane 2). However, phosphorylation of SLAC1-NT by preexposure to CPK6 is not reduced if the protein kinase inhibitor staurosporine alone is added 10 min after CPK6 exposure (lane 3). If staurosporine is added simultaneously with CPK6, SLAC1-NT transphosphorylation is strongly inhibited (lane 4). The ABI1 protein phosphatase added simultaneously with CPK6 inhibits phosphorylation of SLAC1-NT (lane 5).

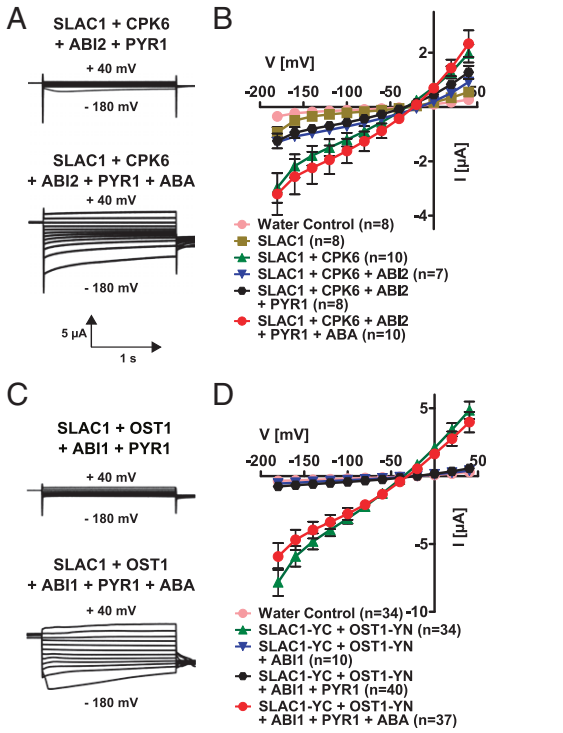

Fig. 5. Functional reconstitution of ABA activation of SLAC1 channels in (*A* and *B*) CPK6- and (*C* and *D*) OST1-containing signaling pathways. Current traces (*A* and *C*) show examples of the ABA activation of SLAC1 channel currents in oocytes. An ABA-dependent signaling pathway was reconstituted in oocytes using the protein kinases CPK6 (*A* and *B*) and OST1 (*C* and *D*). Split YFP (BiFC) was used in the case of SLAC1 and OST1 coexpression (*C* and *D*). The PP2C phosphatase ABI2 (*A* and *B*) or ABI1 (*C* and *D*) is able to inhibit SLAC1 currents (blue triangles in *B* and *D*). In the absence of ABA, the ABA receptor PYR1 does not activate SLAC1 currents (black hexagons in *B* and *D*). However, in the presence of injected ABA, SLAC1 currents are strongly activated (red circles in *B* and *D*). Data from one representative batch of oocytes (of >3 batches) are shown in *D*. Data from two to five independent batches were averaged in *B*.

of ABA, PYR1 did not affect the small magnitude of anion currents in oocytes expressing the PP2Cs ABI2 or ABI1 with SLAC1 and CPK6 (Fig. 5*B*) or OST1 (Fig. 5*D*). Extracellular ABA application did not result in SLAC1 activation ($n > 6$). When ABA was injected into the cytoplasm of oocytes 15 min before the recording of oocyte currents, anion channel activity was dramatically enhanced in oocytes containing SLAC1, ABI1/ABI2, PYR1, and either CPK6 or OST1 (Fig. 5). Note that to enhance the activation of SLAC1 via OST1 (Fig. 5*D*), split YFP (BiFC) constructs were attached to the anion channel and kinase (33) to irreversibly link these proteins. In contrast, ABA activation of SLAC1 channels via CPK6 did not require imposed linkage of the expressed signaling proteins (Fig. 5 *A* and *B*). Therefore, the analyzed ABA signaling pathway components were sufficient to reconstitute ABA activation of SLAC1 currents with either the CPK6 or OST1-Yn protein kinases. Thus, a functional ABA signaling core was reconstituted with CPK6, enabling ABA activation of SLAC1 without a SnRK2 kinase (Fig. 5 *A* and *B*).

We attempted to reconstitute the ABA signaling core including PYR1, ABI1, CPK6, and SLAC1-NT in vitro. Inhibition of CPK6-mediated SLAC1-NT phosphorylation by ABI1 (Fig. 6*A*, *Upper*, lanes 5, 6, and 8) is decreased if the ABA receptor PYR1 and ABA are present (Fig. 6*A*, *Upper*, lane 7). Addition of PYR1 or ABA alone did not alter CPK6- and ABI1-dependent SLAC1-NT phosphorylation (Fig. 6*A*, *Upper*, lanes 1, 4, 5, and 8).

The tryptophan 300 residue of ABI1 was identified as being crucial for stabilizing the PYL1–ABA–ABI1 complex due to interaction of this residue with the narrow hydrophobic ABA-binding pocket (7, 10). When the ABA-dependent signaling pathway containing the ABI1 W300L mutant was expressed in oocytes, ABI1 W300L was able to inhibit SLAC1 ion currents similarly to wild-type ABI1 (Fig. S5). However, SLAC1 anion currents could not be activated upon injection of ABA when coexpressing PYR1, OST1, and ABI1 W300L (Fig. S5).

Discussion

In the present study, we show that the calcium-dependent protein kinase CPK6 activates SLAC1-dependent anion currents in *Xenopus* oocytes (Figs. 1, 3, and 4). In vitro kinase assays demonstrate that CPK6 phosphorylates the SLAC1 N terminus (Fig. 1*C*), as previously observed for CPK21, CPK23, and OST1 (33–

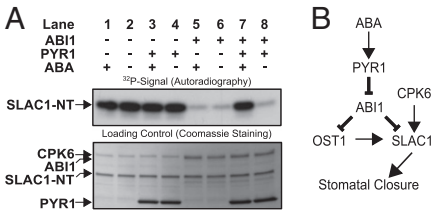

Fig. 6. (*A*) In vitro reconstitution of an ABA-dependent signal transduction pathway including PYR1, ABI1, CPK6, and SLAC1-NT protein. Independent of ABA, CPK6 phosphorylates SLAC1-NT (lanes 1 and 2). The presence of ABI1, but not PYR1, inhibits SLAC1-NT phosphorylation, with or without ABA (lanes 3–6). If CPK6, ABI1, and PYR1 are present, addition of ABA leads to the release of ABI1-mediated inhibition of SLAC1 phosphorylation (lane 7). (*B*) Model for ABA activation of the SLAC1 channel via the OST1 and CPK6 protein kinases and down-regulation by the ABI1 protein phosphatase. ABA binds to PYR1, which causes inhibition of PP2C protein phosphatases, including ABI1. This leads to ABA-induced activation of SLAC1 channels in *Xenopus* oocytes by CPK6, which functions in native guard cells in ABA activation of S-type anion channels (37). Note that the ABI1 protein phosphatase can directly dephosphorylate the SLAC1 N terminus, which represents a previously unknown target for ABI1 and a mechanism for tight negative SLAC1 regulation, in addition to the known down-regulation of OST1.

35, 41). Here, LC-MS/MS experiments revealed a phosphorylation site in SLAC1 (S59) that is crucial for SLAC1 channel activation by CPK6 in *Xenopus* oocytes (Fig. 3). This SLAC1 phosphorylation may lead to conformational changes in the channel, resulting in rearrangement of the phenylalanine residue 450, which is crucial for the gating of SLAC1 (47). Kinetic protein kinase quantification analyses reveal a high catalytic efficiency of CPK6 toward SLAC1-NT phosphorylation (Fig. 2 *C* and *D*), which is comparable to other plant kinases (48, 49).

A 1:10 cRNA ratio of channel versus activating kinase injection led to only very weak SLAC1 activation (Fig. S2 *A* and *B*), which appears to be puzzling, as protein kinases are potentially able to phosphorylate and thereby activate multiple channels. Potential reasons could include (*i*) direct CPK6-protein linkage to SLAC1, (*ii*) a lower expression level of the kinase compared with SLAC1, or (*iii*) that endogenous oocyte phosphatases might be able to remove the phosphate groups added by the kinases and thereby inhibit kinase-mediated SLAC1 activation until a certain threshold is reached. The effect of CPK3 expression on SLAC1 activity in the oocytes was statistically insignificant (Fig. S1*A*). Recent studies have shown differential effects of CPK3 and CPK6 on stomatal closing (50, 51). Consistent with these findings, CPK3 and CPK6 are not in the same CPK subfamily (37, 40). The CPK6 activation of SLAC1 in oocytes reported in this work and reduced ABA- and Ca^{2+}-induced S-type anion channel activation in guard cell protoplasts (37) are in line with the recently reported drought-resistant phenotype of CPK6-overexpressing *Arabidopsis* plants (52).

We have further observed strong inhibition of CPK6-activated SLAC1 channel activity in the presence of the three group A PP2Cs ABI1, ABI2, and PP2CA (Fig. 4 *A* and *B*). SnRK2 kinases have been shown to be directly regulated by PP2C phosphatases through dephosphorylation of the kinase-activation loop (28–30). Phosphorylation experiments at the N terminus of a SLAC1 homolog (SLAH3) by CPK21 suggested that ABI1 inhibits kinase activity, but does not dephosphorylate the N terminus of SLAH3 (36). Interestingly, the present findings provide biochemical evidence suggesting that the ABI1 protein phosphatase can directly dephosphorylate SLAC1 (Figs. 4*C* and 6*B*). Consequently, our results with CPK6 indicate an alternate ABA signaling pathway that is distinct from the linear PYR/RCAR–PP2C–SnRK2 (OST1)–SLAC1 such that, in addition to SnRK2 down-regulation, the PP2C ABI1 directly competes with CPK6 for (de)phosphorylation of the SLAC1 N terminus, which can add a mechanism for the tight regulation of S-type anion channels found in guard cells (20, 21) (Figs. 4*C* and 6*B*). The question of whether ABI1 additionally inhibits CPK6 activity will require further investigation.

We further demonstrate functional reconstitution of ABA activation of SLAC1 ion channel activity using either the CPK6 or OST1 protein kinase coexpressed with ABI1, ABI2, and PYR1 in *Xenopus* oocytes (Fig. 5). We show that ABA activation requires intracellular injection of ABA. Also, CPK6 mediates SLAC1-NT phosphorylation in vitro in response to ABA in the presence of PYR1 and ABI1 (Fig. 6*A*). An earlier study reported reconstitution of an ABA-dependent signaling pathway consisting of PYR/RCARs, group A PP2Cs, SnRK2 kinases, and the transcription factor ABF2 using a protoplast system with a luciferase reporter (53). Interestingly, the reconstituted ABA signal transduction pathway found here expands the present model for ABA signaling cores, by showing that the calcium-dependent protein kinase CPK6 can mediate an ABA-activated ion channel response in the absence of a SnRK2 protein kinase.

Conclusions

Our findings demonstrate the complete reconstitution of ABA activation of a plant ion channel, SLAC1, in a heterologous system including CPK6. Whereas strong activation of SLAC1 via the OST1 protein kinase required induced interaction of the OST1–SLAC1 pair via split YFP fusion, CPK6 strongly activates SLAC1 channels without using additional components that enhance protein–protein interactions. A regulatory phosphorylation site in CPK6 activation of SLAC1, S59, is identified (Fig. 3). The present study expands the current model for early ABA signaling mechanisms in which ABA binds to ABA receptors, including PYR1, leading to inhibition of PP2Cs and subsequent SnRK2 kinase activation. We show here that CPKs can replace SnRK2 kinases in ABA regulation of SLAC1 channels, suggesting that both of these protein kinase families function in parallel in vivo (Fig. 6*B*). These data further correlate with findings showing calcium dependence of ABA-induced stomatal closure (12–15, 17, 20) and parallel Ca^{2+}-independent mechanisms (20, 54). Moreover, data show that ABI1 directly dephosphorylates the N terminus of SLAC1, indicating a branched configuration: ABI1 deactivates SLAC1 by directly interacting with and down-regulating SnRK2s (28–30) and dephosphorylating the SLAC1 N terminus (Figs. 4*C* and 6*B*).

Materials and Methods

Construct Preparation, Electrophysiology, and Histology in *X. laevis* Oocytes. All constructs were cloned into the pNB1 oocyte expression vector using the USER method (55). cRNA was prepared using the mMessage mMachine Transcription Kit (Ambion). Approximately 25 ng of each tested cRNA, in a total volume of 50 nL, was injected into each oocyte for voltage-clamp recordings, if not otherwise stated. mTq fusion proteins were visualized in fixed sections using confocal laser microscopy. For information on instrument setup, solutions used, and analyses, see *SI Materials and Methods*.

Site-Directed Mutagenesis, Protein Expression, Isolation, in Vitro Kinase Assays, and Western Blot Analyses. CPK6, OST1, ABI1, PYR1, and SLAC1 N and C terminus coding sequences were cloned into modified pGEX-6P1 (GE Healthcare) vectors using the USER method (55), and the proteins were overexpressed in *Escherichia coli* Rosetta (DE3) pLysS (Novagen) and isolated using Strep-Tactin MacroPrep (IBA) (Fig. S6). In vitro kinase assays were performed as previously described (34). To assess phosphorylation kinetics, P81-grade filter paper (Whatman) and a scintillation counter were used. More detailed information for all methods is given in *SI Materials and Methods*.

ACKNOWLEDGMENTS. We thank Drs. Rainer Waadt and Cawas Engineer for critical reading of the manuscript and Dr. Malik Keshwani for instruction on kinase kinetics assays. This research was supported by National Institutes of Health R01GM060396 and National Science Foundation MCB0918220; in part by grants from the Chemical Sciences, Geosciences, and Biosciences Division

of the Office of Basic Energy Sciences at the US Department of Energy (DOE; DE-FG02-03ER15449, to J.I.S.), a German Academic Exchange Service doctoral fellowship (to B.B.), and in part by Grant-in-Aid for Scientific Research on Innovative Areas 21114002 from the Ministry of Education, Science and Culture of Japan and by the Program for Promotion of Basic and Applied Research for Innovations in Bio-Oriented Industry (K.I.). A.B.S. is a Department of Energy-Biosciences Fellow of the Life Sciences Research Foundation.

1. Ma Y, et al. (2009) Regulators of PP2C phosphatase activity function as abscisic acid sensors. *Science* 324:1064–1068.
2. Park S-Y, et al. (2009) Abscisic acid inhibits type 2C protein phosphatases via the PYR/PYL family of START proteins. *Science* 324:1068–1071.
3. Nishimura N, et al. (2010) PYR/PYL/RCAR family members are major in-vivo ABI1 protein phosphatase 2C-interacting proteins in *Arabidopsis*. *Plant J* 61:290–299.
4. Santiago J, et al. (2009) Modulation of drought resistance by the abscisic acid receptor PYL5 through inhibition of clade A PP2Cs. *Plant J* 60:575–588.
5. Szostkiewicz I, et al. (2010) Closely related receptor complexes differ in their ABA selectivity and sensitivity. *Plant J* 61(1):25–35.
6. Melcher K, et al. (2009) A gate-latch-lock mechanism for hormone signalling by abscisic acid receptors. *Nature* 462:602–608.
7. Miyazono K-i, et al. (2009) Structural basis of abscisic acid signalling. *Nature* 462: 609–614.
8. Nishimura N, et al. (2009) Structural mechanism of abscisic acid binding and signaling by dimeric PYR1. *Science* 326:1373–1379.
9. Santiago J, et al. (2009) The abscisic acid receptor PYR1 in complex with abscisic acid. *Nature* 462:665–668.
10. Yin P, et al. (2009) Structural insights into the mechanism of abscisic acid signaling by PYL proteins. *Nat Struct Mol Biol* 16:1230–1236.
11. Cutler SR, Rodriguez PL, Finkelstein RR, Abrams SR (2010) Abscisic acid: Emergence of a core signaling network. *Annu Rev Plant Biol* 61:651–679.
12. Allen GJ, Kuchitsu K, Chu SP, Murata Y, Schroeder JI (1999) *Arabidopsis* abi1-1 and abi2-1 phosphatase mutations reduce abscisic acid-induced cytoplasmic calcium rises in guard cells. *Plant Cell* 11:1785–1798.
13. DeSilva DLR, Cox RC, Hetherington AM, Mansfield TA (1985) Suggested involvement of calcium and calmodulin in the responses of stomata to abscisic acid. *New Phytol* 101:555–563.
14. Grabov A, Blatt MR (1998) Membrane voltage initiates Ca^{2+} waves and potentiates Ca^{2+} increases with abscisic acid in stomatal guard cells. *Proc Natl Acad Sci USA* 95: 4778–4783.
15. MacRobbie EAC (2000) ABA activates multiple Ca^{2+} fluxes in stomatal guard cells, triggering vacuolar $K^+(Rb^+)$ release. *Proc Natl Acad Sci USA* 97:12361–12368.
16. McAinsh MR, Brownlee C, Hetherington AM (1990) Abscisic acid-induced elevation of guard cell cytosolic Ca^{2+} precedes stomatal closure. *Nature* 343(6254):186–188.
17. Schwartz A (1985) Role of Ca^{2+} and EGTA on stomatal movements in *Commelina communis* L. *Plant Physiol* 79:1003–1005.
18. Schroeder JI, Hagiwara S (1989) Cytosolic calcium regulates ion channels in the plasma membrane of *Vicia faba* guard cells. *Nature* 338:427–430.
19. Hedrich R, Busch H, Raschke K (1990) Ca^{2+} and nucleotide dependent regulation of voltage dependent anion channels in the plasma membrane of guard cells. *EMBO J* 9: 3889–3892.
20. Siegel RS, et al. (2009) Calcium elevation-dependent and attenuated resting calcium-dependent abscisic acid induction of stomatal closure and abscisic acid-induced enhancement of calcium sensitivities of S-type anion and inward-rectifying K^+ channels in *Arabidopsis* guard cells. *Plant J* 59:207–220.
21. Pei ZM, Kuchitsu K, Ward JM, Schwarz M, Schroeder JI (1997) Differential abscisic acid regulation of guard cell slow anion channels in *Arabidopsis* wild-type and abi1 and abi2 mutants. *Plant Cell* 9:409–423.
22. Schroeder JI, Schmidt C, Sheaffer J (1993) Identification of high-affinity slow anion channel blockers and evidence for stomatal regulation by slow anion channels in guard cells. *Plant Cell* 5:1831–1841.
23. Vahisalu T, et al. (2008) SLAC1 is required for plant guard cell S-type anion channel function in stomatal signalling. *Nature* 452:487–491.
24. Negi J, et al. (2008) CO_2 regulator SLAC1 and its homologues are essential for anion homeostasis in plant cells. *Nature* 452:483–486.
25. Mustilli A-C, Merlot S, Vavasseur A, Fenzi F, Giraudat J (2002) *Arabidopsis* OST1 protein kinase mediates the regulation of stomatal aperture by abscisic acid and acts upstream of reactive oxygen species production. *Plant Cell* 14:3089–3099.
26. Xue S, et al. (2011) Central functions of bicarbonate in S-type anion channel activation and OST1 protein kinase in CO_2 signal transduction in guard cell. *EMBO J* 30: 1645–1658.
27. Yoshida R, et al. (2002) ABA-activated SnRK2 protein kinase is required for dehydration stress signaling in *Arabidopsis*. *Plant Cell Physiol* 43:1473–1483.
28. Umezawa T, et al. (2009) Type 2C protein phosphatases directly regulate abscisic acid-activated protein kinases in *Arabidopsis*. *Proc Natl Acad Sci USA* 106:17588–17593.
29. Vlad F, et al. (2009) Protein phosphatases 2C regulate the activation of the Snf1-related kinase OST1 by abscisic acid in *Arabidopsis*. *Plant Cell* 21:3170–3184.
30. Belin C, et al. (2006) Identification of features regulating OST1 kinase activity and OST1 function in guard cells. *Plant Physiol* 141:1316–1327.
31. Li JX, Wang XQ, Watson MB, Assmann SM (2000) Regulation of abscisic acid-induced stomatal closure and anion channels by guard cell AAPK kinase. *Science* 287:300–303.
32. Schmidt C, Schelle I, Liao YJ, Schroeder JI (1995) Strong regulation of slow anion channels and abscisic acid signaling in guard cells by phosphorylation and dephosphorylation events. *Proc Natl Acad Sci USA* 92:9535–9539.
33. Geiger D, et al. (2009) Activity of guard cell anion channel SLAC1 is controlled by drought-stress signaling kinase-phosphatase pair. *Proc Natl Acad Sci USA* 106: 21425–21430.
34. Geiger D, et al. (2010) Guard cell anion channel SLAC1 is regulated by CDPK protein kinases with distinct Ca^{2+} affinities. *Proc Natl Acad Sci USA* 107:8023–8028.
35. Lee SC, Lan W, Buchanan BB, Luan S (2009) A protein kinase-phosphatase pair interacts with an ion channel to regulate ABA signaling in plant guard cells. *Proc Natl Acad Sci USA* 106:21419–21424.
36. Geiger D, et al. (2011) Stomatal closure by fast abscisic acid signaling is mediated by the guard cell anion channel SLAH3 and the receptor RCAR1. *Sci Signal* 4:ra32.
37. Mori IC, et al. (2006) CDPKs CPK6 and CPK3 function in ABA regulation of guard cell S-type anion- and Ca^{2+}-permeable channels and stomatal closure. *PLoS Biol* 4:e327.
38. Franz S, et al. (2011) Calcium-dependent protein kinase CPK21 functions in abiotic stress response in *Arabidopsis thaliana*. *Mol Plant* 4(1):83–96.
39. Ma S-Y, Wu W-H (2007) AtCPK23 functions in *Arabidopsis* responses to drought and salt stresses. *Plant Mol Biol* 65:511–518.
40. Hrabak EM, et al. (2003) The *Arabidopsis* CDPK-SnRK superfamily of protein kinases. *Plant Physiol* 132:666–680.
41. Vahisalu T, et al. (2010) Ozone-triggered rapid stomatal response involves the production of reactive oxygen species, and is controlled by SLAC1 and OST1. *Plant J* 62: 442–453.
42. Leung J, et al. (1994) *Arabidopsis* ABA response gene ABI1: Features of a calcium-modulated protein phosphatase. *Science* 264:1448–1452.
43. Meyer K, Leube MP, Grill E (1994) A protein phosphatase 2C involved in ABA signal transduction in *Arabidopsis thaliana*. *Science* 264:1452–1455.
44. Kuhn JM, Boisson-Dernier A, Dizon MB, Maktabi MH, Schroeder JI (2006) The protein phosphatase AtPP2CA negatively regulates abscisic acid signal transduction in *Arabidopsis*, and effects of abh1 on AtPP2CA mRNA. *Plant Physiol* 140(1):127–139.
45. Sheen J (1998) Mutational analysis of protein phosphatase 2C involved in abscisic acid signal transduction in higher plants. *Proc Natl Acad Sci USA* 95:975–980.
46. Yoshida T, et al. (2006) ABA-hypersensitive germination3 encodes a protein phosphatase 2C (AtPP2CA) that strongly regulates abscisic acid signaling during germination among *Arabidopsis* protein phosphatase 2Cs. *Plant Physiol* 140(1):115–126.
47. Chen YH, et al. (2010) Homologue structure of the SLAC1 anion channel for closing stomata in leaves. *Nature* 467:1074–1080.
48. Curran A, et al. (2011) Calcium-dependent protein kinases from *Arabidopsis* show substrate specificity differences in an analysis of 103 substrates. *Front Plant Sci* 2:36.
49. Hashimoto K, et al. (2012) Phosphorylation of calcineurin B-like (CBL) calcium sensor proteins by their CBL-interacting protein kinases (CIPKs) is required for full activity of CBL-CIPK complexes toward their target proteins. *J Biol Chem* 287:7956–7968.
50. Cousson A (2011) *Arabidopsis* Ca^{2+}-dependent protein kinase CPK3 mediates relationship of putative inositol triphosphate receptor with slow-type anion channel. *Biol Plant* 55:507–521.
51. Munemasa S, Hossain MA, Nakamura Y, Mori IC, Murata Y (2011) The *Arabidopsis* calcium-dependent protein kinase, CPK6, functions as a positive regulator of methyl jasmonate signaling in guard cells. *Plant Physiol* 155:553–561.
52. Xu J, et al. (2010) AtCPK6, a functionally redundant and positive regulator involved in salt/drought stress tolerance in *Arabidopsis*. *Planta* 231:1251–1260.
53. Fujii H, et al. (2009) In vitro reconstitution of an abscisic acid signalling pathway. *Nature* 462:660–664.
54. Allan AC, Fricker MD, Ward JL, Beale MH, Trewavas AJ (1994) Two transduction pathways mediate rapid effects of abscisic acid in *Commelina* guard cells. *Plant Cell* 6: 1319–1328.
55. Nour-Eldin HH, Hansen BG, Nørholm MHH, Jensen JK, Halkier BA (2006) Advancing uracil-excision based cloning towards an ideal technique for cloning PCR fragments. *Nucleic Acids Res* 34:e122.

Supporting Information

Brandt et al. 10.1073/pnas.1116590109

SI Materials and Methods

Construct Preparation and Electrophysiology in *Xenopus laevis* Oocytes. All constructs were cloned into the pNB1 oocyte expression vector using the USER method (1). cRNA was prepared using the mMessage mMachine Transcription Kit (Ambion). Approximately 25 ng of each tested cRNA, in a total volume of 50 nL, was injected into each oocyte for voltage-clamp recordings, if not otherwise stated. The recordings were performed 2–3 d after injection, with a Cornerstone (Dagan) TEV-200 two-electrode voltage-clamp amplifier. Data analyses were performed using an Axon Instruments Digidata 1440A Low-Noise Data Acquisition System (Molecular Devices). The last 0.5 s of each voltage pulse were averaged using Clampfit 10.2 software for all current–voltage graphs. Oocytes were subjected to voltage pulses, with a holding potential of 0 mV, using a voltage protocol with a range of −180 mV to +40 mV in +20-mV increments, followed by a −120-mV voltage "tail" pulse. Data were low-pass-filtered at 20 Hz throughout all recordings. Oocytes were recorded in 75 mM NaCl, 20 mM $CaCl_2$, 1 mM $MgCl_2$, 10 mM Hepes (pH 7.4; titrated with Tris base), and osmolarity was balanced to 220–260 mmol osmotically active substances/kg with D-mannitol for the recordings. The oocytes were impaled with electrodes filled with 3 M KCl. For the oocyte groups with injected abscisic acid (ABA), 500 μM ABA was injected into each oocyte (to a final concentration of ∼50 μM ABA, assuming an approximate 500-nL total volume of oocytes). ABA microinjections were performed 15 min before voltage-clamp experiments. Error bars indicate SEM. Statistical analyses were performed using the Student's *t* test and two-way ANOVA (for datasets with a determined normal distribution) or the Mann–Whitney *U* test (for datasets with a nonnormal distribution). All experiments were performed at room temperature. The numbers (*n*) of individual oocytes analyzed in *n* batches are given in the figure legends. If not otherwise mentioned, data represent measurements of one representative batch of oocytes, as current magnitudes vary from batch to batch.

Oocyte Histology. Four days after fusion-protein [calcium-dependent protein kinase (CPK)6 and CPK23 coding sequences were fused to mTurquoise (2) in the pNB1 vector, and cRNA was prepared using the mMessage mMachine Transcription Kit (Ambion)] mRNA injection, three to five oocytes per freezing mold were submerged in 3 mL O.C.T. compound (Tissue-Tek). The samples were flash-frozen in liquid nitrogen and sliced into 100-μm sections using a cryostat microtome. The sections were collected on microscope slides, taking care to keep the sections from drying out by application of cool water vapor to the slide face containing the sections. Coverslips were immediately mounted on the slides with an airtight barrier formed by a thin ring of silicone vacuum grease (Beckman) sandwiched between the coverslip and the slide along the perimeter.

The prepared slides were temporarily stored in a dark, humidified chamber to be imaged within 1 h of sectioning. Each section was imaged on a Nikon Eclipse TE2000-U spinning disk confocal microscope with a 10× objective.

Site-Directed Mutagenesis, in Vitro Kinase Assays, Protein Expression, Isolation, and Western Blot Analyses. CPK6, Open Stomata 1 (OST1), ABI1, and SLAC1 N and C terminus coding sequences were cloned into a modified pGEX-6P1 (GE Healthcare) vector using the USER method (1). In the pGEX-6P1 vector, a USER cassette followed by a StrepII-tag was introduced. The PYR1 coding sequence was cloned into a modified pGEX-6P1 vector, resulting in an N-terminal StrepII-tag fusion. Plasmids were transformed into *Escherichia coli* Rosetta (DE3) pLysS (Novagen) and grown to $OD_{(A600)}$ ∼0.6. Protein expression was induced by adding isopropyl-β-D-thiogalactopyranoside to a final concentration of 0.5 mM and carried out for 3 h at room temperature. For PYR1 protein isolation, the culture was incubated at 15 °C for 18 h. Harvesting the bacteria was achieved by centrifugation (4,000 × *g*; 15 min) and bacterial pellets were resuspended in buffer W (100 mM Tris, 150 mM NaCl, pH 8.0) supplemented with 1 mg/mL lysozyme and protease inhibitor mixture (Complete EDTA-free; Roche). After lysis of the cells by three 30-s sonication pulses (Heat Systems; Ultrasonics), insoluble cell debris was removed by centrifugation (25,000 × *g* for 30 min at 4 °C). CPK6, ABI1, PYR1, and SLAC1 N and C terminus were purified using Strep-Tactin MacroPrep (IBA) by gravity flow in Micro Bio-Spin chromatography columns (Bio-Rad) following instructions listed in the manufacturer's manual. Eluted recombinant proteins were supplemented with 10% (vol/vol) glycerol and stored at −20 °C. In vitro kinase assays were performed as previously described (3). The kinase buffer consisted of 50 mM Hepes (pH 7.5), 10 mM $MgCl_2$, 1× protease inhibitor (Complete EDTA-free; Roche), 2 mM DTT, 5 mM EGTA, 5 μCi [γ-^{32}P]ATP, and 4.87 mM $CaCl_2$ to gain a final free Ca^{2+} concentration of ∼3 μM (calculated with http://www.stanford.edu/∼cpatton/webmaxc/webmaxcE.htm) in most of the 20-μL reaction volumes. To remove free Ca^{2+} from the reaction buffer, no $CaCl_2$ was added and the reaction buffer was supplemented with 12.9 mM $MgCl_2$ to gain a final free Mg^{2+} concentration of 10 mM (calculated with http://www.stanford.edu/∼cpatton/webmaxc/webmaxcE.htm). For the in vitro reconstitution, either 5 μM ABA (dissolved in ethanol; lanes indicated with + ABA) or an equivalent amount of ethanol (lanes indicated with − ABA) was used. Using [γ-^{32}P]ATP, the reactions were started, carried out at room temperature for 10 min for most of the experiments, and subsequently stopped by adding 6× SDS-loading dye. To the reaction mixtures shown in lanes 2 and 3, components indicated by "10 min" were added after the initial 10-min incubation time and incubated for an additional 35 min before being stopped using 6× SDS-loading dye. After incubation at 98 °C for 5 min, proteins were separated by SDS/PAGE in 4–15% gradient gels (Mini Protean TGX; Bio-Rad) and subsequently stained using Page Blue (Fermentas). Radioactivity of ^{32}P was monitored using HyBlot CL autoradiography films (Denville Scientific).

Loading of proteins was controlled by performing Western blot analysis (Figs. 1*C* and 4*C*) as well as Coomassie staining. The reactions used for subsequent Western blot analysis were treated exactly the same way as those used for in vitro kinase assays with the only difference that no [γ-^{32}P]ATP was added. Proteins were separated by SDS/PAGE in 4–15% gradient gels (Mini Protean TGX; Bio-Rad) and subsequently blotted on Immobilon-P^{SQ} membranes (Millipore). GST-fusion proteins were detected using an anti–GST-HRP conjugate antibody (GE Healthcare), SuperSignal West Pico (Pierce), and BioMax MR film (Kodak). For Coomassie-stained loading controls, photographs of the gels were taken before detection of radioactivity by autoradiography.

P81 Filter Paper-Based Kinase Kinetics Assay. Recombinant SLAC1-NT (N terminus of SLAC1) used for kinase kinetics assays was concentrated using Amicon Ultra devices (Ultracell 30k; Millipore) and thereby the buffer was changed to 50 mM Tris·HCl (pH 7.5), 150 mM NaCl, 2 mM DTT. For determining concentrations of recombinant CPK6, CPK23, OST1, and SLAC1-NT, proteins were subjected to SDS/PAGE, Coomassie-stained, and dried

between two cellophane sheets to assess purity (Fig. S6). Subsequently, protein concentrations were measured using the BCA Protein Assay Kit (Pierce). To determine kinetic parameters, 20 nmol kinase was incubated in a buffer containing 75 mM Tris·HCl (pH 7.5), 10 mM $MgCl_2$, 3 mM DTT, 75 mM NaCl, and variable concentrations of SLAC1-NT (0.625–25 μM) in a 10-μL reaction for 2.5 min, 5.5 min, or 10 min at room temperature for CPK6, CPK23, or OST1, respectively. Note that for CPK6 and CPK23, the reaction buffer was supplemented with 4.87 mM $CaCl_2$ and 5 mM EGTA, resulting in ~3 μM free Ca^{2+} (calculated with http://www.stanford.edu/~cpatton/webmaxc/webmaxcE.htm). After quenching the reactions by adding 90 μL 30% (vol/vol) acetic acid, 50 μL was spotted on P81-grade filter paper discs (Whatman) and subsequently washed in 0.5% (vol/vol) phosphoric acid five times for 5 min. After washing the filter discs in acetone for 2 min followed by air drying, ^{32}P incorporation was determined using scintillation fluid (Ecoscint; National Diagnostics) and a counter (Beckman). Using GraphPad Prism 5, kinetic constants were calculated.

***In Gel* Digest and LC-MS/MS.** Isolated recombinant SLAC1-NT protein was incubated with and without CPK6 protein for 10 min at room temperature using the same buffer conditions as used for in vitro kinase assays, with the only difference that instead of 5 μCi [γ-^{32}P]ATP, 100 μM ATP was present. After separation by SDS/PAGE and subsequent Coomassie staining, SLAC1-NT–corresponding bands were cut out. The gel slices were cut to 1-mm cubes and destained three times by first washing with 100 μL of 100 mM ammonium bicarbonate for 15 min, followed by addition of the same volume of acetonitrile (ACN) for 15 min. Samples were dried in a SpeedVac. Samples were then reduced by mixing with 200 μL of 100 mM ammonium bicarbonate, 10 mM DTT and incubated at 56 °C for 30 min. The liquid was removed and 200 μL of 100 mM ammonium bicarbonate, 55 mM iodoacetamide was added to the gel pieces and incubated at room temperature in the dark for 20 min. After the removal of the supernatant and one wash with 100 mM ammonium bicarbonate for 15 min, the same volume of ACN was added to dehydrate the gel pieces. The solution was then removed and samples were dried in a SpeedVac. For digestion, enough solution of ice-cold trypsin (0.01 μg/μL) in 50 mM ammonium bicarbonate was added to cover the gel pieces and set on ice for 30 min. After complete rehydration, the excess trypsin solution was removed, replaced with fresh 50 mM ammonium bicarbonate, and left overnight at 37 °C. The peptides were extracted twice by the addition of 50 μL of 0.2% (vol/vol) formic acid and 5% (vol/vol) ACN and vortex mixing at room temperature for 30 min. The supernatant was removed and saved. A total of 50 μL of 50% ACN/0.2% (vol/vol) formic acid was added to the sample, which was vortexed again at room temperature for 30 min. The supernatant was removed and combined with the supernatant from the first extraction. The combined extractions were analyzed directly by liquid chromatography (LC) in combination with tandem mass spectroscopy (MS/MS) using electrospray ionization. Trypsin-digested peptides were analyzed by HPLC coupled with tandem mass spectroscopy (LC-MS/MS) using nanospray ionization. The nanospray ionization experiments were performed using a TripleTof 5600 hybrid mass spectrometer (ABSCIEX) interfaced with nano-scale reversed-phase HPLC (Tempo; Eksigent, ABSCIEX) using a 10 cm × 100 μm i.d. glass capillary packed with 5-μm C18 Zorbax beads (Agilent Technologies). Peptides were eluted from the C18 column into the mass spectrometer using a linear gradient [5–60% (vol/vol)] of ACN at a flow rate of 250 μL/min for 1 h. The buffers used to create the ACN gradient were buffer A [98% H_2O, 2% ACN, 0.2% formic acid, 0.005% TFA (vol/vol)] and buffer B [100% ACN, 0.2% formic acid, 0.005% TFA (vol/vol)]. MS/MS data were acquired in a data-dependent manner in which the MS1 data were acquired for 250 ms at an *m/z* of 400–1,250 Da and the MS/MS data were acquired from an *m/z* of 50–2,000 Da. For independent data acquisition (IDA) method parameters were as follows: a 250 ms time of flight survey scan (MS1-TOF) was followed by 50 product ion scans (MS2) of 25 ms each. For MS2 IDA criteria, ions that had reached the threshold of 200-counts and had the charge state +2, +3, or +4 where selected. Four-second exclusion criteria was chosen to limit the number of repetitive MS2 events on the same ion. Finally, the collected data were analyzed using Mascot (Matrix Science) and ProteinPilot 4.0 (AB SCIEX) for peptide identification. To further analyze phosphorylation of serine 59, product ion scan methods were constructed and carried out for the product of *m/z* = 765.4 [QVpSLETGFSVLNR (M + 2H)]. All LC conditions were identical to the above settings. For the product ion scans, the Q1 resolution was set to unit and the collision energy was set to 39 at an accumulation time of 200-ms scans.

1. Nour-Eldin HH, Hansen BG, Nørholm MHH, Jensen JK, Halkier BA (2006) Advancing uracil-excision based cloning towards an ideal technique for cloning PCR fragments. *Nucleic Acids Res* 34:e122.
2. Goedhart J, et al. (2010) Bright cyan fluorescent protein variants identified by fluorescence lifetime screening. *Nat Methods* 7(2):137–139.
3. Geiger D, et al. (2010) Guard cell anion channel SLAC1 is regulated by CDPK protein kinases with distinct Ca^{2+} affinities. *Proc Natl Acad Sci USA* 107:8023–8028.

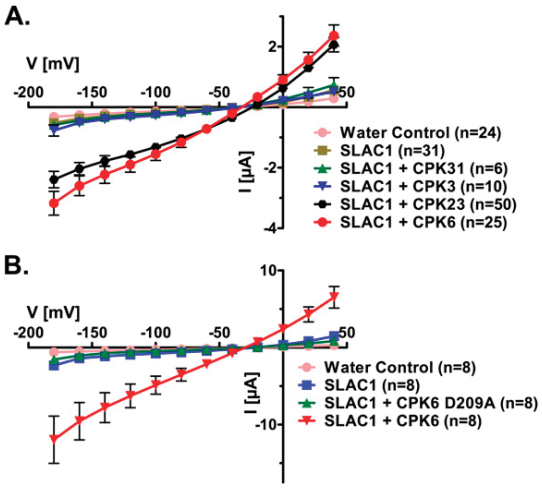

Fig. S1. Strong kinase activity-dependent activation of SLAC1 channel currents by the CPK6 protein kinase in *Xenopus* oocytes. (*A*) The average steady-state current–voltage relationships are shown in water-injected (pink circles), SLAC1-injected (brown squares), and SLAC1 + CPK-injected oocytes. The protein kinases CPK6 (red circles) and CPK23 (black hexagons) are able to increase SLAC1 activity, whereas CPK31 (green triangles), a homolog of CPK23, and CPK3 (blue triangles) did not significantly increase SLAC1 activity in oocytes. Representative data from one batch of oocytes are shown (CPK3, CPK31; of >3 batches), except for SLAC1 + CPK6 and SLAC1 + CPK23, which show average data from two to five independent oocyte batches. (*B*) SLAC1 was not activated by a kinase-inactive CPK6 mutant (D209A; green triangles), whereas coexpression of wild-type CPK6 (red triangles) together with SLAC1 resulted in a large anion current (n = 3 batches). Note that the degree of SLAC1 activation in *A* and *B* differed, as experiments were conducted in independent batches of oocytes, resulting in typical differences among oocyte batches. Therefore, the illustrated internal controls were always coinjected in the same batch of oocytes.

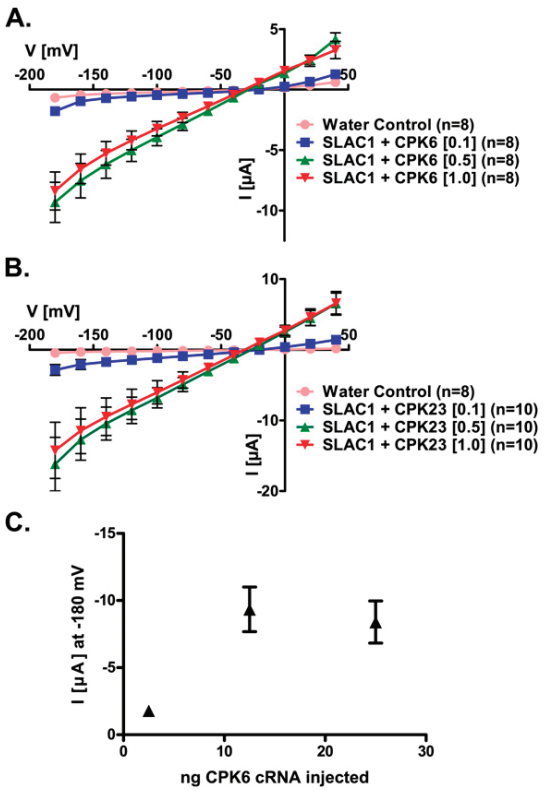

Fig. S2. CPK6 and CPK23 cRNA concentration-dependent activation of SLAC1 anion currents. (*A* and *B*) SLAC1 activity in response to injection of full cRNA content of CPK6 and CPK23 kinases (~25 ng per oocyte; red triangles) was compared with SLAC1 and 1/2 (~12.5 ng; green triangles) or 1/10 (~2.5 ng; blue squares) cRNA content of *CPK6*, to investigate the saturation point of SLAC1-mediated currents. Representative data from one batch of oocytes (of >2 batches) are shown in *A*. (*C*) Maximum SLAC1-mediated current activation as a function of injected CPK6 cRNA amount.

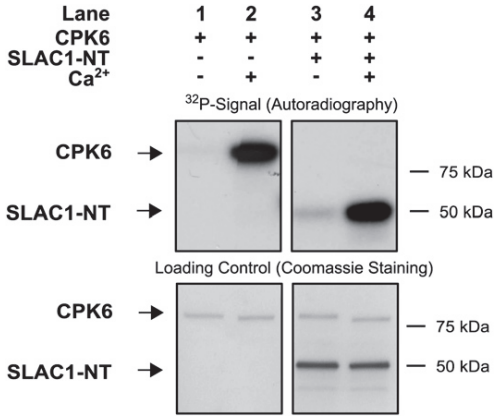

Fig. S3. SLAC1-NT phosphorylation is Ca^{2+}-dependent in vitro. In the absence of free Ca^{2+}, both CPK6 auto- (lane 1; *Upper*) and SLAC1-NT cross-phosphorylation (lane 3; *Upper*) are strongly decreased compared with the ^{32}P signal in the presence of Ca^{2+} (lanes 2 and 4; *Upper*). Note that the CPK6 migrating speed in the SDS/PAGE is Ca^{2+}-dependent (lanes 1–4; *Lower*), as previously reported for several CPKs (1–3).

1. Harmon AC, Putnam-Evans C, Cormier MJ (1987) A calcium-dependent but calmodulin-independent protein kinase from soybean. *Plant Physiol* 83:830–837.
2. Romeis T, Piedras P, Jones JDG (2000) Resistance gene-dependent activation of a calcium-dependent protein kinase in the plant defense response. *Plant Cell* 12:803–816.
3. Yoon GM, Cho HS, Ha HJ, Liu JR, Lee HS (1999) Characterization of NtCDPK1, a calcium-dependent protein kinase gene in *Nicotiana tabacum*, and the activity of its encoded protein. *Plant Mol Biol* 39:991–1001.

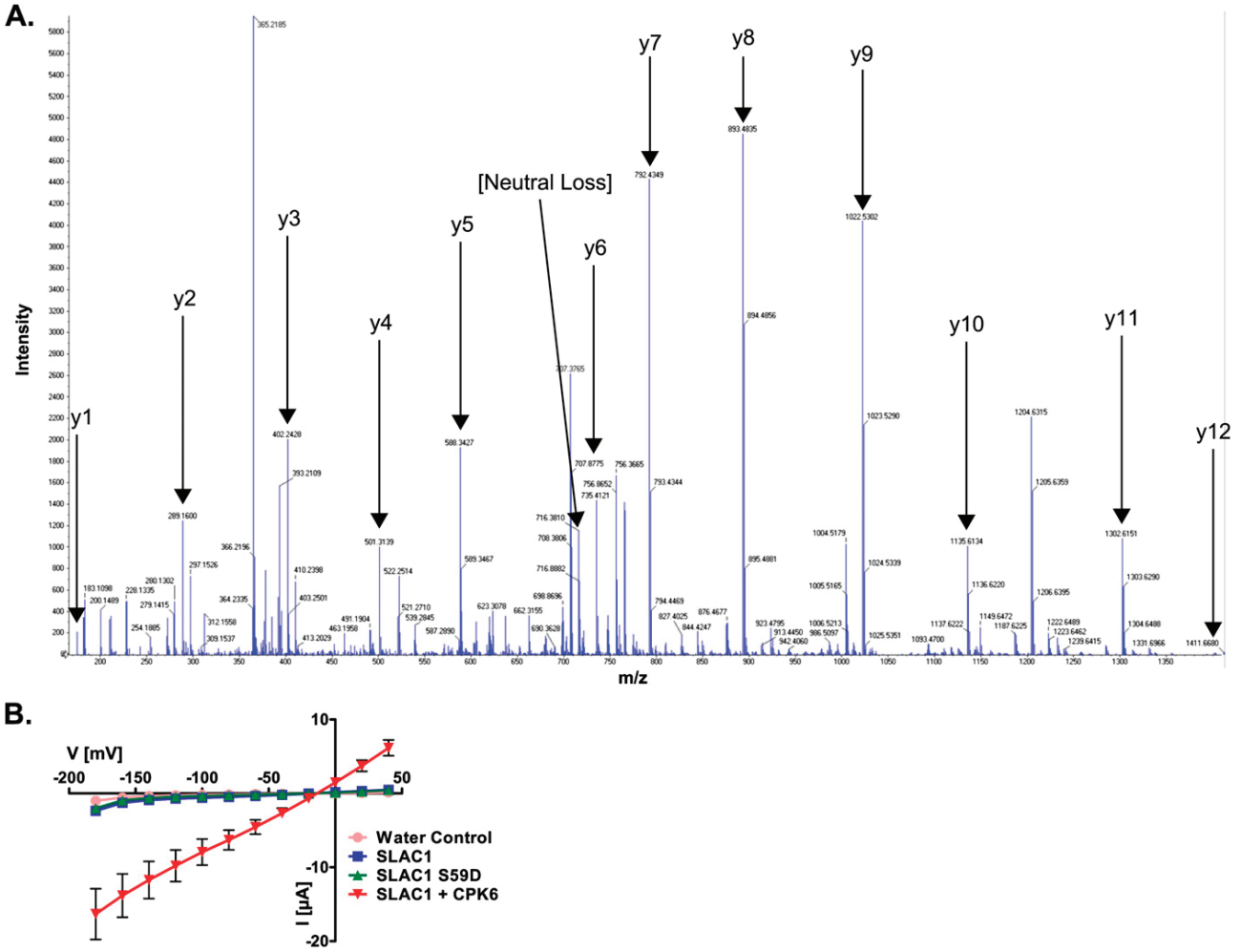

Fig. S4. LC-MS/MS identification of SLAC1-NT serine 59 phosphorylation by CPK6 and constitutive activation of SLAC1 by point mutation to aspartate (S59D). (*A*) Product ion scan spectrum for the peptide QVpSLETGFSVLNR [$(M + 2H)^+ = 765.4$]. Besides y ions, the peak for the neutral ion loss of 765.4, which is 716.4, is also labeled. (*B*) Additional control data from the same batch of oocytes as shown in Fig. 3*B*: Point mutation of serine 59 to aspartate (S59D) did not result in constitutive activation of SLAC1 in oocytes (SLAC1 S59D; green triangles). Blue squares represent wild-type SLAC1 without CPK6. CPK6 was able to activate SLAC1 (red triangles) ($n > 6$ oocytes per condition).

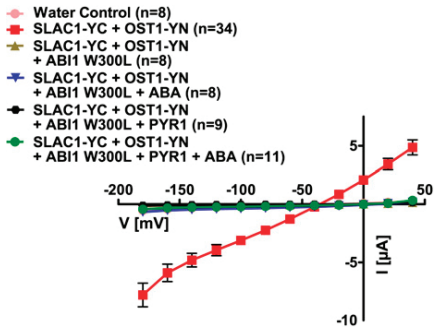

Fig. S5. The W300L point mutation in the PP2C phosphatase ABI1 disrupts ABA activation of SLAC1 ion currents mediated by OST1 in *Xenopus* oocytes. ABI1 W300L was able to inhibit SLAC1 activity similar to wild-type ABI1 (gold triangles), but exhibited an inability of PYR1 to enhance SLAC1-mediated inward currents in the presence of ABA (green circles). Data from one representative batch (of two batches) of oocytes are shown except for OST1 data without ABI1 (red squares; >3 batches averaged).

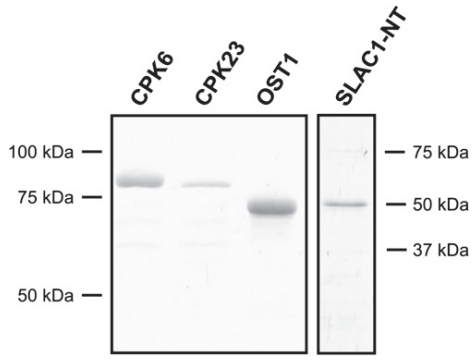

Fig. S6. Coomassie-stained SDS/PAGE of isolated recombinant proteins used for kinase kinetics assays.

Table S1. Statistical analysis of the identified peptide using Paragon algorithm/ProteinPilot

N	Unused	Total	% cov	% cov (50)	% cov (95)	Accessions	Confidence score (%)	Sequence	Modifications	dMass
1	56.4	56.4	83.18	65.9	58.76	GST-SLAC1-NT-StrepII	99.00000095	QVSLETGFSVLNR	Gln→pyro-Glu@N-term	−0.00014535
1	56.4	56.4	83.18	65.9	58.76	GST-SLAC1-NT-StrepII	99.00000095	QVSLETGFSVLNR	Gln→pyro-Glu@N-term; Phospho(S)@3	0.00593622
1	56.4	56.4	83.18	65.9	58.76	GST-SLAC1-NT-StrepII	99.00000095	QVSLETGFSVLNR	Gln→pyro-Glu@N-term	−0.00014535
1	56.4	56.4	83.18	65.9	58.76	GST-SLAC1-NT-StrepII	99.00000095	QVSLETGFSVLNR	Gln→pyro-Glu@N-term; Phospho(S)@3	0.00044304
1	56.4	56.4	83.18	65.9	58.76	GST-SLAC1-NT-StrepII	99.00000095	QVSLETGFSVLNR		0.00043076
1	56.4	56.4	83.18	65.9	58.76	GST-SLAC1-NT-StrepII	99.00000095	QVSLETGFSVLNR	Gln→pyro-Glu@N-term; Phospho(S)@3	0.00178582
1	56.4	56.4	83.18	65.9	58.76	GST-SLAC1-NT-StrepII	99.00000095	QVSLETGFSVLNR	Phospho(S)@3	0.00126418
1	56.4	56.4	83.18	65.9	58.76	GST-SLAC1-NT-StrepII	99.00000095	QVSLETGFSVLNR	Gln→pyro-Glu@N-term; Phospho(S)@3	−0.00126594
1	56.4	56.4	83.18	65.9	58.76	GST-SLAC1-NT-StrepII	99.00000095	QVSLETGFSVLNR		−0.0005458
1	56.4	56.4	83.18	65.9	58.76	GST-SLAC1-NT-StrepII	99.00000095	QVSLETGFSVLNR		0.00030869
1	56.4	56.4	83.18	65.9	58.76	GST-SLAC1-NT-StrepII	99.00000095	QVSLETGFSVLNR		−0.00457413
1	56.4	56.4	83.18	65.9	58.76	GST-SLAC1-NT-StrepII	99.00000095	QVSLETGFSVLNR	Gln→pyro-Glu@N-term; Phospho(S)@3	0.00178582
1	56.4	56.4	83.18	65.9	58.76	GST-SLAC1-NT-StrepII	99.00000095	QVSLETGFSVLNR	Gln→pyro-Glu@N-term; Phospho(S)@3	−0.00419564
1	56.4	56.4	83.18	65.9	58.76	GST-SLAC1-NT-StrepII	99.00000095	QVSLETGFSVLNR		−0.0005458
1	56.4	56.4	83.18	65.9	58.76	GST-SLAC1-NT-StrepII	99.00000095	QVSLETGFSVLNR		0.00043076
1	56.4	56.4	83.18	65.9	58.76	GST-SLAC1-NT-StrepII	99.00000095	QVSLETGFSVLNR	Gln→pyro-Glu@N-term; Phospho(S)@3	−0.00126594
1	56.4	56.4	83.18	65.9	58.76	GST-SLAC1-NT-StrepII	99.00000095	QVSLETGFSVLNR		−0.00457413
1	56.4	56.4	83.18	65.9	58.76	GST-SLAC1-NT-StrepII	98.01999927	QVSLETGFSVLNR	Gln→pyro-Glu@N-term; Phospho(S)@3	−0.00285286
1	56.4	56.4	83.18	65.9	58.76	GST-SLAC1-NT-StrepII	96.96000218	QVSLETGFSVLNR	Phospho(S)@3	0.00626907
1	56.4	56.4	83.18	65.9	58.76	GST-SLAC1-NT-StrepII	95.01000047	QVSLETGFSVLNR		−0.00274307
1	56.4	56.4	83.18	65.9	58.76	GST-SLAC1-NT-StrepII	91.40999913	QVSLETGFSVLNR	Phospho(S)@3	0.00126418
1	56.4	56.4	83.18	65.9	58.76	GST-SLAC1-NT-StrepII	90.8100009	QVSLETGFSVLNR		−0.0005458
1	56.4	56.4	83.18	65.9	58.76	GST-SLAC1-NT-StrepII	89.37000036	QVSLETGFSVLNR	Gln→pyro-Glu@N-term; Phospho(S)@3	0.00044304
1	56.4	56.4	83.18	65.9	58.76	GST-SLAC1-NT-StrepII	76.56999826	QVSLETGFSVLNR		−0.00457413
1	56.4	56.4	83.18	65.9	58.76	GST-SLAC1-NT-StrepII	42.6699996	QVSLETGFSVLNR		0.00030869

N: The rank of the specified protein relative to all other proteins in the list of detected proteins. Unused (ProtScore): A measure of the protein confidence for a detected protein, calculated from the peptide confidence for peptides from spectra that are not already completely "used" by higher-scoring winning proteins. Total (ProtScore): A measure of the total amount of evidence for a detected protein. The Total ProtScore is calculated using all of the peptides detected for the protein. The Total ProtScore does not indicate the percent confidence for the identification of a protein. % cov (Coverage): The percentage of matching amino acids from identified peptides having confidence greater than 0 divided by the total number of amino acids in the sequence. % cov (50): The percentage of matching amino acids from identified peptides having confidence greater than or equal to 50% divided by the total number of amino acids in the sequence. % cov (95): The percentage of matching amino acids from identified peptides having confidence greater than or equal to 95% divided by the total number of amino acids in the sequence. Accessions: The accession number for the protein. A custom FASTA sequence entry was created for SLAC1 proteins with the name: "GST-SLAC1-NT-StrepII" and pasted into swissprot database for the protein pilot searches. Confidence score (%): The confidence for the peptide identification, expressed as a percentage. Sequence: Sequence of the identified peptide. Modifications: Modifications found by the search dMass (Delta Mass). dMass: The difference in mass between the precursor molecular weight (MW) and the theoretical MW of the matching peptide sequence (including modifications).

Calcium-Dependent and -Independent Stomatal Signaling Network and Compensatory Feedback Control of Stomatal Opening via Ca^{2+} Sensitivity Priming[W]

Kristiina Laanemets[2], Benjamin Brandt[2], Junlin Li[2], Ebe Merilo[2], Yong-Fei Wang, Malik M. Keshwani, Susan S. Taylor, Hannes Kollist[3], and Julian I. Schroeder[3]*

Institute of Technology, University of Tartu, Tartu 50411, Estonia (K.L., E.M., H.K.); Division of Biological Sciences, Cell and Developmental Biology Section, University of California, San Diego, La Jolla, California 92093–0116 (B.B., J.L., J.I.S.); College of Forest Resources and Environment, Nanjing Forestry University, Nanjing 210037, China (J.L.); Institute of Plant Physiology and Ecology, Shanghai Institute for Biological Sciences, The Chinese Academy of Sciences, Shanghai 200032, China (Y.-F.W.); and Department of Pharmacology, School of Medicine, Howard Hughes Medical Institute, University of California, San Diego, La Jolla, California 92093–0654 (M.M.K., S.S.T.)

In the past 15 years or more, many mutants that are impaired in stimulus-induced stomatal closing and opening have been identified and functionally characterized in Arabidopsis (*Arabidopsis thaliana*), leading to a mechanistic understanding of the guard cell signal transduction network. However, evidence has only recently emerged that mutations impairing stomatal closure, in particular those in slow anion channel SLOW ANION CHANNEL-ASSOCIATED1 (SLAC1), unexpectedly also exhibit slowed stomatal opening responses. Results suggest that this compensatory slowing of stomatal opening can be attributed to a calcium-dependent posttranslational down-regulation of stomatal opening mechanisms, including down-regulation of inward K^+ channel activity. Here, we discuss this newly emerging stomatal compensatory feedback control model mediated via constitutive enhancement (priming) of intracellular Ca^{2+} sensitivity of ion channel activity. The CALCIUM-DEPENDENT PROTEIN KINASE6 (CPK6) is strongly activated by physiological Ca^{2+} elevations and a model is discussed and open questions are raised for cross talk among Ca^{2+}-dependent and Ca^{2+}-independent guard cell signal transduction pathways and Ca^{2+} sensitivity priming mechanisms.

Stomatal pores formed by two guard cells enable CO_2 uptake from the atmosphere, but also ensure leaf cooling and provide a pulling force for nutrient uptake from the soil via transpiration. These vitally important processes are inevitably accompanied by water loss through stomata. Stomatal opening and closure is caused by the uptake and release of osmotically active substances and is tightly regulated by signaling pathways that lead to the activation or inactivation of guard cell ion channels and pumps. Potassium ions enter guard cells through the inward-rectifying K^+ channels (K^+_{in}) during stomatal opening and are released via outward-rectifying K^+ channels during stomatal closure (Schroeder et al., 1987; Hosy et al., 2003; Roelfsema and Hedrich 2005). Cytosolic Ca^{2+}, an important second messenger in plants, mediates ion channel regulation, particularly down-regulation of inward-conducting K^+_{in} channels and activation of S-type anion channels, thus mediating stomatal closure and inhibiting stomatal opening (Schroeder and Hagiwara, 1989; Dodd et al., 2010; Kim et al., 2010). Stomatal closure is initiated by anion efflux via the slow S-type anion channel SLAC1 (Negi et al., 2008; Vahisalu et al., 2008; Kollist et al., 2011) and the voltage-dependent rapid R-type anion channel QUICK-ACTIVATING ANION CHANNEL1 (Meyer et al. 2010; Sasaki et al., 2010).

In recent years, advances have been made toward understanding mechanisms mediating abscisic acid (ABA)-induced stomatal closure (Cutler et al., 2010; Kim et al., 2010; Raghavendra et al., 2010). The core ABA signaling module, consisting of PYR/RCAR (for pyrabactin resistance 1/regulatory components of ABA receptors) receptors, clade A protein phosphatases (PP2Cs), SNF-related protein kinase OPEN STOMATA1 (OST1), and downstream targets, is Ca^{2+}-independent (Ma et al., 2009; Park et al., 2009; Hubbard et al., 2010). However, ABA-induced stomatal closure was reduced to only 30% of the normal stomatal closure response under conditions that

[1] This work was supported by the National Science Foundation (grant no. MCB0918220) and National Institutes of Health (grant no. R01GM060396) to J.I.S. K^+ channel analyses were supported in part by the Division of Chemical Sciences, Geosciences, and Biosciences, Office of Basic Energy Sciences of the U.S. Department of Energy (grant no. DE–FG02–03ER15449). H.K. was supported by an Institutional Research Funding Grant (grant no. IUT2–21) and by the European Regional Fund (Center of Excellence in Environmental Adaptation).

[2] These authors contributed equally to the article.

[3] These authors contributed equally to the article.

* Address correspondence to jischroeder@ucsd.edu.

[W] The online version of this article contains Web-only data.
www.plantphysiol.org/cgi/doi/10.1104/pp.113.220343

inhibited intracellular cytosolic free calcium ($[Ca^{2+}]_{cyt}$) elevations in Arabidopsis (Siegel et al., 2009), consistent with previous findings in other plants (De Silva et al., 1985; Schwartz, 1985; McAinsh et al., 1991; MacRobbie, 2000). Together these and other studies show the importance of $[Ca^{2+}]_{cyt}$ for a robust ABA-induced stomatal closure. Here, we discuss Ca^{2+}-dependent and Ca^{2+}-independent signaling pathways in guard cells and open questions on how these may work together.

Plants carrying mutations in the SLAC1 anion channel have innately more open stomata, and exhibit clear impairments in ABA-, elevated CO_2-, Ca^{2+}-, ozone-, air humidity-, darkness-, and hydrogen peroxide-induced stomatal closure (Negi et al., 2008; Vahisalu et al., 2008; Merilo et al., 2013). Recent research, however, unexpectedly revealed that mutations in SLAC1 also down-regulate stomatal opening mechanisms and slow down stomatal opening (Laanemets et al., 2013).

UNEXPECTED SLOWING OF STOMATAL OPENING IN *SLAC1* MUTANT ALLELES

Stomatal opening in plants is mediated by increased light intensity or enhanced air humidity and by decreased CO_2 concentrations inside the leaf (C_i) that occur as a result of photosynthesis. During light-induced stomatal opening, phototropin-related blue-light signaling leads to the activation of H^+-ATPases, resulting in H^+ efflux and plasma membrane hyperpolarization (for review, see Shimazaki et al., 2007), which in turn leads to the uptake of K^+ via K^+ channels (Schroeder et al., 1984). Simultaneously, due to active photosynthesis, C_i is reduced and S-type anion channels are inactivated, which further favors stomatal opening (Roelfsema et al., 2002). Mutations in the *SLAC1* gene result in impaired anion efflux, and would therefore be expected to accelerate stomatal opening in response to opening stimuli. Unexpectedly, the opposite was detected: Stomatal opening of intact whole rosettes induced by three independent biological stimuli (light, low C_i, and high humidity) was slower in *slac1* mutants (Laanemets et al., 2013). Independent research showed that *slac1* mutant guard cells show a greatly reduced activity of K^+_{in} channels (Laanemets et al., 2013), which contribute to stomatal opening (Kwak et al., 2001; Figs. 1 and 2). These independent findings suggest that plants possess a system that counteracts the impaired stomatal closing of S-type anion channels in *slac1* mutants by down-regulating stomatal opening mechanisms to prevent excessive water loss.

IMPAIRED ANION EFFLUX LEADS TO A CHANGED IONOMIC PROFILE IN *SLAC1* GUARD CELLS

Severely reduced S-type anion channel activity and reduced anion efflux in *slac1* guard cells change the entire ionomic profile of guard cells. Elevated accumulation of anions such as chloride, malate, and fumarate, but also potassium was observed (Negi et al., 2008). Hyperaccumulation of chloride and malate can suppress H^+-coupled anion transport (Sanders et al., 1989). Accordingly, the cytosolic pH (pH_{cyt}) of *slac1* guard cells was slightly more alkaline (Wang et al., 2012). Furthermore, the removal of S-type anion channel activity in *slac1* mutant guard cells (Vahisalu et al., 2008) is expected to cause a more negative ("hyperpolarized") membrane potential due to the reduced anion efflux from guard cells. This is predicted to enhance the activity of hyperpolarization-activated Ca^{2+} influx channels resulting in a slightly

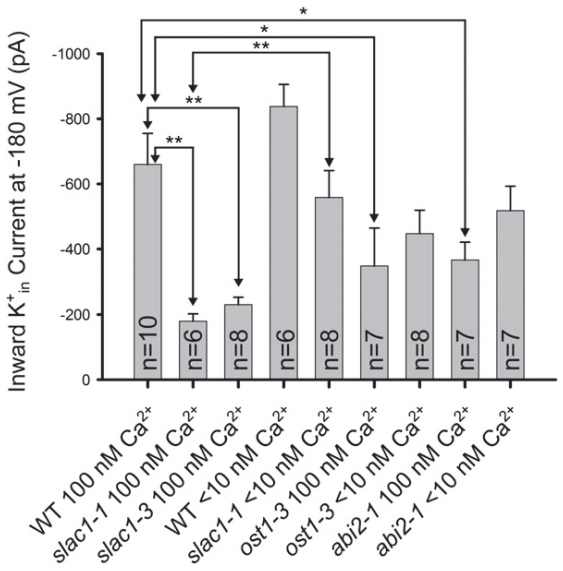

Figure 1. K^+_{in} channel current activity is reduced in the stomatal closing impaired mutants *slac1*, *ost1*, and *abi2-1* and this K^+ channel down-regulation is rapidly reversed in *slac1* guard cells by lowering $[Ca^{2+}]_{cyt}$ to less than 10 nM. Average K^+_{in} channel current magnitudes at −180 mV are shown for wild-type Columbia-0 (WT) and the *slac1*, *ost1*, and *abi2-1* alleles. The concentrations of buffered $[Ca^{2+}]_{cyt}$ concentrations are indicated. Whole-cell patch clamp recordings were performed on guard cell protoplasts at the indicated cytosolic free Ca^{2+} concentrations. Note that an *abi2-1* allele in the Columbia-0 accession was analyzed (Nishimura et al., 2004). Error bars (SEM) for the indicated number of guard cells analyzed are depicted. K^+_{in} channel current magnitudes in *slac1* recovered at less than 10 nM $[Ca^{2+}]_{cyt}$ compared with 100 nM $[Ca^{2+}]_{cyt}$ ($P < 0.005$). Statistical analyses showed significant down-regulation of K^+_{in} channel current magnitudes in the *slac1-1*, *slac1-3* ($P < 0.001$), *ost1* ($P < 0.04$), and *abi2-1* (Columbia-0; $P < 0.02$) mutants compared with wild-type guard cells at 100 nM free $[Ca^{2+}]$ in the cytosol. Small but statistically nonsignificant differences for comparisons of K^+_{in} channel current magnitudes in response to lowering $[Ca^{2+}]$ from 100 nM to less than 10 nM for *ost1-3* (P value = 0.525) and *abi2-1* (P value = 0.109) were found. *$P <$ 0.05; **$P < 0.01$. Unpaired Student's t tests were applied to assess significance. Data from WT < 10 nM and *slac1-1* < 10 nM are from Laanemets et al., 2013. Methods were as described in Laanemets et al., 2013 (see Supplemental Text S1).

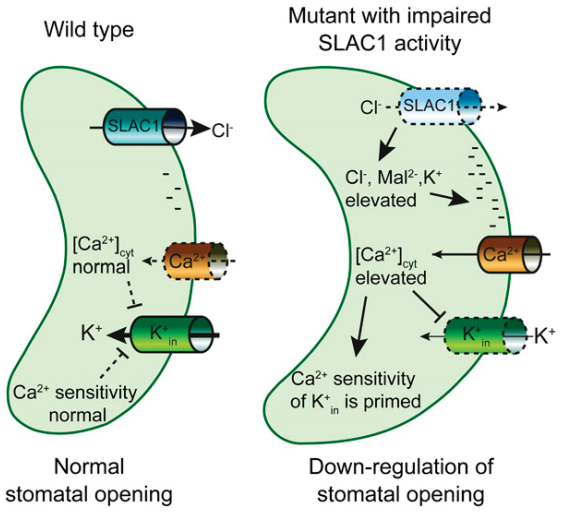

Figure 2. Schematic model for K^+_{in} down-regulation in mutants with impaired SLAC1 activity. Without SLAC1, ions accumulate in guard cells, and the plasma membrane is charged more negatively (hyperpolarization) due to reduced anion efflux, which leads to activation of hyperpolarization-dependent Ca^{2+}-permeable influx channels and elevated levels of $[Ca^{2+}]_{cyt}$. The increased $[Ca^{2+}]_{cyt}$ concentration down-regulates K^+_{in} channel activity. Furthermore, K^+_{in} channels exhibit an enhanced (primed) Ca^{2+} sensitivity, thus enhancing K^+_{in} channel down-regulation. The negative charges shown at the inner side of the plasma membrane (right model) indicate the more negative (hyperpolarized) membrane potential expected for *slac1* mutant alleles.

elevated $[Ca^{2+}]_{cyt}$ in *slac1* guard cells (Grabov and Blatt, 1998; Hamilton et al., 2000; Pei et al., 2000). Slightly elevated $[Ca^{2+}]_{cyt}$ in *slac1* guard cells was experimentally observed in two studies (Wang et al., 2012; Laanemets et al., 2013) and causes down-regulation of K^+_{in} activity (Schroeder and Hagiwara, 1989; Siegel et al., 2009), thereby slowing stomatal opening in *slac1*.

DOWN-REGULATION OF GUARD CELL K^+ UPTAKE CHANNEL ACTIVITY BY ENHANCED $[Ca^{2+}]_{CYT}$ SENSITIVITY IN *SLAC1*

Analyses of guard cell ion channel transcript levels showed only partially reduced expression of K^+_{in} and H^+-ATPase gene transcripts in *slac1* guard cells, suggesting that posttranslational mechanisms may down-regulate K^+_{in} (Laanemets et al., 2013). The patch clamp method enables clamping of defined $[Ca^{2+}]_{cyt}$ and pH_{cyt} conditions by rapidly equilibrating the cytosol with the patch pipette solution. The first experiments showing dramatic down-regulation of K^+_{in} channel activity in plants lacking SLAC1 (*slac1-1* and *slac1-3*) were performed at 250 nM free $[Ca^{2+}]_{cyt}$. Interestingly, the reduction of K^+_{in} activity was rapidly reversed by lowering $[Ca^{2+}]_{cyt}$ to a subphysiological $[Ca^{2+}]_{cyt}$ concentration of less than 10 nM (Laanemets et al., 2013), indicating that Ca^{2+}-induced inhibition of K^+_{in} is more sensitive to $[Ca^{2+}]_{cyt}$ in *slac1* than in wild-type plants (Fig. 1). However, whether K^+_{in} channel activity in *slac1* guard cells is also affected at resting $[Ca^{2+}]_{cyt}$ levels had not yet been investigated. Additional patch clamp experiments show that K^+_{in} activity of *slac1-1* and *slac1-3* is also greatly reduced at physiological resting $[Ca^{2+}]_{cyt}$ of 100 nM (Fig. 1; Supplemental Fig. S1), indicating a down-regulation of K^+_{in} activity in *slac1* plants even at resting $[Ca^{2+}]_{cyt}$. These results demonstrate that the sensitivity of K^+_{in} channels to physiological $[Ca^{2+}]_{cyt}$ is constitutively enhanced (primed) in *slac1* guard cells. These findings support the hypothesis that the sensitivity of Ca^{2+} signaling mechanisms in guard cells can be enhanced such that guard cells respond to resting $[Ca^{2+}]_{cyt}$ levels, thus resulting in possible residual $[Ca^{2+}]_{cyt}$ signaling (Siegel et al., 2009).

The priming of K^+_{in} channel sensitivity to $[Ca^{2+}]_{cyt}$ leads to reduced K^+ influx representing a mechanism to counteract the potential adverse effect of more open stomata in *slac1* plants (Laanemets et al., 2013). Guard cell $[Ca^{2+}]_{cyt}$ elevation alone is not sufficient to explain the slowed stomatal opening of *slac1* mutants. As mentioned above, anion accumulation in the *slac1* mutant resulted in elevated pH_{cyt} (Wang et al., 2012), which might also slow stomatal opening. In sum, the primed Ca^{2+} sensitivity of K^+_{in} channels, together with higher $[Ca^{2+}]_{cyt}$ and more alkaline pH_{cyt}, provide a feedback mechanism helping to prevent excessive water loss in *slac1* mutant plants that are defective in stomatal closure (Fig. 2).

The next question was whether *slac1* plants always show higher Ca^{2+} sensitivity of K^+_{in} channels or whether this is reversible. Patch clamp experiments showed that the reduction of K^+_{in} activity was reversed by lowering $[Ca^{2+}]_{cyt}$ to a subphysiological Ca^{2+} concentration (Laanemets et al., 2013). If stomata of *slac1* plants are in a more closed state, does this provide feedback to $[Ca^{2+}]_{cyt}$, pH_{cyt}, and most importantly to Ca^{2+}-priming of K^+_{in} channels, resulting in a wild-type-like stomatal opening rate? The answer to this question requires further research, but results so far indicate that the Ca^{2+}-priming of K^+_{in} channels is indeed reversible and depends on initial stomatal "openness". When *slac1* and wild-type plants showed nearly similar steady-state starting stomatal conductances (Laanemets et al., 2013), the differences in half-times for stomatal opening between *slac1* and wild-type plants were only moderate (Table I). However, when the starting stomatal apertures of *slac1* plants were considerably larger than those of the wild type, the differences in half-times for stomatal opening were also larger, about 2-fold (Wang et al., 2012), indicating that in the latter experiments the compensatory feedback control of stomatal opening functioned to counteract further stomatal opening in this already open state.

Table I. *Increase in stomatal conductance is slower in slac1-1, slac1-3, and ost1-3 mutants (background Columbia-0) and in abi2-1 mutant (background Ler)*

*$P < 0.1$; **$P < 0.05$ (statistical difference from the wild type, one-way ANOVA, $n = 5–18$).

Genotype	Half-Times for Stomatal Opening[a]	
	Low CO_2	Light
	min	
Wild type (Columbia-0)	18.8 ± 0.9	15.4 ± 0.6
slac1-1	22.8 ± 2.0*	21.1 ± 1.1**
slac1-3	26.3 ± 2.3**	19.7 ± 1.4**
ost1-3	24.3 ± 1.2**	22.1 ± 1.3**
Wild type (Ler)	19.8 ± 0.8	10.1 ± 0.8
abi2-1	24.9 ± 3.3	16.6 ± 3.9**

[a]In light experiments, plants were kept in the measurement cuvettes (Kollist et al., 2007) overnight and stomatal opening was measured during the onset of the light period in the morning. In CO_2 experiments, plants were kept at ambient CO_2 (400 mmol mol^{-1}) for 2 h, then the CO_2 was decreased to 40 mmol mol^{-1}The stomatal opening response, within first 45 min, was scaled to the range from 0% to 100%, directly yielding the half-times for stomatal opening. Plant growth conditions were as described in Laanemets et al., 2013. See Supplemental Text S1 for further experimental details.

SLOWED STOMATAL OPENING AND DOWN-REGULATION OF GUARD CELL K^+ UPTAKE CHANNEL ACTIVITY IS ALSO OBSERVED IN OTHER MUTANTS WITH MORE OPEN STOMATA

If down-regulation of K^+_{in} channel activity via Ca^{2+} priming is caused by the open stomata phenotype of *slac1* mutants, the question arises whether the same phenotype is also present in other mutants with constitutively more open stomata. To address this point, experiments were performed with *ost1-3* (Mustilli et al., 2002; Yoshida et al., 2002) and the dominant mutant *aba insensitive2* (*abi2-1;* Koornneef et al., 1984). OST1 is a protein kinase that activates SLAC1 anion channels via phosphorylation (Geiger et al., 2009; Lee et al., 2009; Vahisalu et al., 2010) and functional ABA activation of SLAC1 channels via OST1 was reconstituted in oocytes (Brandt et al., 2012). An unexpected reduced K^+_{in} channel activity in *abi2-1* mutant guard cells was shown in an earlier study (Pei et al., 1997). The dominant *abi2-1* mutation generates a mutant ABI2 protein phosphatase that is refractory to ABA-induced inhibition by PYR/RCAR receptors and suppresses OST1 activation (Ma et al., 2009; Park et al., 2009; Umezawa et al., 2009). Guard cells lacking functional OST1 or having a dominant active ABI2, are likely to hyperaccumulate ions and exhibit more negative plasma membrane potential, which would lead to an increase in $[Ca^{2+}]_{cyt}$ (Grabov and Blatt, 1998; Hamilton et al., 2000; Pei et al., 2000). Our gas-exchange experiments showed that both light- and low-CO_2-induced stomatal opening responses were slower in *ost1-3* and *abi2-1* plants compared with corresponding wild types (Table I). Additional patch clamp experiments with *abi2-1* and *ost1-3* guard cells were performed and K^+_{in} channel activity was found to be reduced in *ost1-3* guard cells and confirmed to be reduced in *abi2-1* guard cells (Pei et al., 1997; Fig. 1; Supplemental Figs. S2 and S3). However, reducing $[Ca^{2+}]_{cyt}$ to a subphysiological Ca^{2+} concentration (less than 10 nM) only slightly improved K^+_{in} activity in *ost1-3* and in *abi2-1* guard cells compared with *slac1* (Fig. 1; Supplemental Figs. S2 and S3; Laanemets et al., 2013). These recent studies also highlight that K^+_{in} channel activities in guard cells do not always correlate with the predominant phenotype of a given mutant, as illustrated for the *slac1*, *abi2-1*, and *ost1* mutants (Pei et al., 1997; Laanemets et al., 2013; Fig. 1; Supplemental Figs. S1–S3).

Taken together, elevated $[Ca^{2+}]_{cyt}$, combined with an increased sensitivity of Ca^{2+}-mediated K^+_{in} inhibition in *slac1* plants (Wang et al., 2012; Laanemets et al., 2013), leads to the down-regulation of K^+_{in} channel activity, even at physiological resting $[Ca^{2+}]_{cyt}$ concentrations (Fig. 1; Supplemental Fig. S1). This results in slowed stomatal opening of intact *slac1* plants in response to several stimuli such as air humidity, CO_2, and light. Reduced K^+_{in} activity and slowed stomatal opening of *ost1-3* and *abi2-1* mutants further suggests that this may be a general characteristic of plants with more open stomata or of plants with impaired S-type anion channel activation. Further research of mutants with an enhanced open stomata phenotype independent of S-type anion channels is needed to address this point. Importantly, in *slac1* mutants the down-regulation of K^+_{in} channel activity was reversible at low $[Ca^{2+}]_{cyt}$, whereas it was not clearly reversible in *ost1-3* and only partly reversible in *abi2-1* mutants, indicating that either active OST1 is involved in the increase of K^+_{in} at low $[Ca^{2+}]_{cyt}$ or this type of reversible compensatory regulation of ion channel activity is a unique characteristic related to the impaired SLAC1 anion channel.

PHYSIOLOGICAL STIMULI RAPIDLY ENHANCE $[Ca^{2+}]_{CYT}$ SENSITIVITY

Considering that the Arabidopsis genome encodes over 200 calcium binding (EF-hand containing) proteins (Day et al., 2002), understanding the mechanisms that mediate specific responses to Ca^{2+} is a subject of current research interest in plants and in eukaryotes in general (Berridge, 2012). Several mechanisms have been proposed to mediate specificity in Ca^{2+} signaling in plants, all of which may contribute to this phenomenon (Dodd et al., 2010; Kudla et al., 2010). However, strong cellular and biochemical evidence for any given model is missing and needed in plants, as well as in other systems (Berridge, 2012). Research on guard cell signal transduction has led to a new model that can contribute a mechanism for specificity in Ca^{2+} signaling. Studies in different plant species have shown that calcium is required for both ABA- and

CO_2-induced stomatal closing (De Silva et al., 1985; Schwartz, 1985; Webb et al., 1996; Grabov and Blatt, 1998; Staxén et al., 1999; MacRobbie, 2000; Mori et al., 2006; Young et al., 2006; Siegel et al., 2009). Several independent findings support the model that the stomatal closing signals, ABA and elevated CO_2, "prime" specific early Ca^{2+} sensing mechanisms, switching them from a relatively inactivated state to a Ca^{2+}-responsive "primed" state, and therefore tightly controlling Ca^{2+} responsiveness. Here, we briefly review evidence supporting this Ca^{2+} sensitivity priming model (Table II).

Ca^{2+} imaging in guard cells resolved "spontaneous" repetitive $[Ca^{2+}]_{cyt}$ transients that are more likely to occur at increasingly negative membrane potentials (Grabov and Blatt, 1998; Allen et al., 1999; Klüsener et al., 2002; Young et al., 2006; Siegel et al., 2009; Table II). Surprisingly, repetitive $[Ca^{2+}]_{cyt}$ elevations even occurred when the stomatal opening stimulus low CO_2 was applied (Young et al., 2006). The following question arose: How can $[Ca^{2+}]_{cyt}$ be required for stomatal closing if $[Ca^{2+}]_{cyt}$ elevations are also observed while applying stomatal opening stimuli (Young et al., 2006)? Previous research showed that any imposed $[Ca^{2+}]_{cyt}$ elevation above a threshold value can cause a rapid Ca^{2+}-reactive stomatal closure (Allen et al., 2001; Table II). Moreover, the $[Ca^{2+}]_{cyt}$ oscillation frequency and pattern did not affect this rapid "Ca^{2+}-reactive" stomatal closure response (Allen et al., 2001). (Note that the Ca^{2+} elevation pattern does affect the ability of closed stomata to reopen later, a response called "Ca^{2+}-programmed" stomatal response [Allen et al., 2001; Cho et al., 2009; Eisenach et al., 2012].) The above findings together led to the hypothesis that stomatal closing stimuli may modulate and thus enhance the Ca^{2+} sensitivity of specific Ca^{2+}-activated stomatal closing mechanisms (Young et al., 2006).

Further studies are consistent with the stimulus-induced Ca^{2+} sensitivity priming hypothesis (Table II). In brief, an early study showed that raising $[Ca^{2+}]_{cyt}$ alone does not trigger S-type anion channel activation in Arabidopsis guard cells (Allen et al., 2002). However, if the guard cell protoplasts were preexposed to high external Ca^{2+} during isolations prior to recordings, then elevated $[Ca^{2+}]_{cyt}$ rapidly activated S-type anion currents (figure 3 in Allen et al., 2002). A similar and physiologically more relevant effect was found for ABA: when guard cells were preexposed to ABA, elevated $[Ca^{2+}]_{cyt}$ strongly activated S-type anion currents by shifting the $[Ca^{2+}]_{cyt}$ sensitivity to lower $[Ca^{2+}]_{cyt}$ levels (Siegel et al., 2009; Chen et al., 2010). Interestingly, ABA preincubation also primed K^+_{in} down-regulation by $[Ca^{2+}]_{cyt}$ (Siegel et al., 2009). An increase in the Ca^{2+} sensitivity of S-type anion channel activation was also triggered by elevated CO_2 (Xue et al., 2011). Intracellular bicarbonate and CO_2 levels lead to strong S-type anion channel activation in the presence of 2 μM $[Ca^{2+}]_{cyt}$, but not at 0.1 μM $[Ca^{2+}]_{cyt}$, already 3 to 5 min after achieving the patch clamp whole-cell configuration, which allows equilibration of the pipette solution with the cytosol (Xue et al., 2011). This rapid Ca^{2+} sensitivity priming indicates that the underlying processes are less likely mediated by transcriptional changes. Early ABA signaling mechanisms were determined to indirectly or partially affect CO_2 control of stomatal closing (Merilo et al., 2013), which could be explained by the finding that both pathways require S-type anion channels and the OST1 protein kinase (Roelfsema et al., 2004; Hu et al., 2010; Xue et al., 2011; Merilo et al., 2013). Furthermore, basal ABA signaling in guard cells may partially prime guard cells to respond stronger to other stimuli such as CO_2 elevation (Merilo et al., 2013).

In preliminary experiments we have observed that simply continuously increasing the extracellular Ca^{2+} concentration appears to show a weaker Ca^{2+} reactive stomatal closure response than when oscillations in extracellular Ca^{2+} are imposed. As hyperpolarization of guard cells causes Ca^{2+} oscillations (Grabov and Blatt, 1998; Staxén et al., 1999; Klüsener et al., 2002; Siegel et al., 2009), *slac1* mutants may enhance (prime)

Table II. *Evidence for stimulus-induced Ca^{2+} sensitivity enhancement (priming) in guard cells*

Experimental Observations	Reference
Spontaneous calcium transients found in guard cells	Grabov and Blatt, 1998; Allen et al., 1999; Staxén et al., 1999; Klüsener et al., 2002; Young et al., 2006
Spontaneous calcium transients found in guard cells even when stomatal opening stimulus is applied	Young et al., 2006
Rapid Ca^{2+} reactive stomatal closing occurs for any Ca^{2+} elevation pattern above a threshold level	Allen et al., 2001; Supplemental Fig. S4: http://www.nature.com/nature/journal/v411/n6841/extref/4111053a0_S1.htm
Calcium is required for both ABA and CO_2 induced stomatal closing	e.g De Silva et al., 1985; Schwartz, 1985; Webb et al., 1996; Staxén et al., 1999; MacRobbie, 2000; Mori et al., 2006; Young et al., 2006; Zhu et al., 2007; Siegel et al., 2009
Priming (enhancement) of $[Ca^{2+}]_{cyt}$ sensitivity of S-type anion and K^+_{in} channel regulation by ABA, elevated CO_2 and high external Ca^{2+}	Allen et al., 2002; Siegel et al., 2009; Chen et al., 2010; Xue et al., 2011
Constitutive priming of Ca^{2+} sensitivity of K^+_{in} channel down-regulation in *slac1* guard cells	Laanemets et al., 2013

the cytosolic Ca^{2+} sensitivity via this pathway. Thus, prior Ca^{2+} exposure itself can play a role in Ca^{2+} sensitivity priming (see figure 3 in Allen et al., 2002). More work is needed, however, to identify the underlying mechanisms.

The result showing that the compensatory down-regulation of K^+_{in} channels in *slac1* guard cells can be rapidly reversed by lowering $[Ca^{2+}]_{cyt}$ provides additional strong evidence that the $[Ca^{2+}]_{cyt}$ sensitivity of mechanisms leading to stomatal movements can be primed (Laanemets et al., 2013). Interestingly, in *slac1* mutants, $[Ca^{2+}]_{cyt}$ down-regulation of K^+_{in} channels is constitutively primed under these conditions (Laanemets et al., 2013; Fig. 1). Moreover, it was reported that ABA-induced stomatal closure does not require preceding $[Ca^{2+}]_{cyt}$ signaling (Levchenko et al., 2005; but see De Silva et al., 1985; Schwartz, 1985; Grabov and Blatt, 1998; Staxén et al., 1999; MacRobbie, 2000; Mori et al., 2006; Young et al., 2006; Siegel et al., 2009; Chen et al., 2010). Ca^{2+} sensitivity priming, such that physiological resting $[Ca^{2+}]_{cyt}$ levels enable Ca^{2+} signaling, may explain this (Levchenko et al., 2005).

Modulation of the sensitivity of calcium sensors provides a mechanism which could contribute to the specificity in Ca^{2+} signaling in other plant responses and might help to resolve the crucial question of how Ca^{2+} elevations are "translated" into specific responses with numerous Ca^{2+} binding proteins expressed in individual cells. Further research is needed to determine whether this mechanism might also occur in other cell types and represent a more broadly used option to achieve specificity in responses to $[Ca^{2+}]_{cyt}$ in plants.

PUTATIVE BIOCHEMICAL MECHANISMS THAT MAY MEDIATE Ca^{2+} SENSITIVITY PRIMING

In vivo research has shown that CPKs are important mediators of Ca^{2+}-dependent stomatal closing and S-type anion channel activation (Mori et al., 2006; Zhu et al., 2007; Zou et al., 2010). The CPKs that are presently known to function in Ca^{2+}-induced stomatal closing in vivo are CPK6, CPK3, CPK4, CPK10, and CPK11 (Mori et al., 2006; Zhu et al., 2007; Zou et al., 2010; Hubbard et al., 2012). In addition, CPK23 and CPK21 mutants were reported to show enhanced drought resistance (Ma and Wu, 2007; Franz et al., 2011), whereas recent data showed slightly impaired stomatal closing phenotypes in response to environmental stimuli for a CPK23 mutant (Merilo et al., 2013). However, the cellular and molecular signaling mechanisms mediating Ca^{2+} sensitivity priming remain unknown. Research in *Xenopus laevis* oocytes and in vitro biochemistry are providing insights into how CPKs may mediate stomatal closing. Expression of the Ca^{2+}-dependent protein kinases CPK23, CPK21, and CPK6 showed that these CPKs activate SLAC1 anion channels in oocytes (Geiger et al., 2010; Brandt et al., 2012). Furthermore, expression of a truncated and constitutively active CPK3 also resulted in SLAC1 activation (Scherzer et al., 2012).

Although CPK6 functions in Ca^{2+}-, ABA-, and methyl jasmonate-induced activation of S-type anion channels in vivo (Mori et al., 2006; Munemasa et al., 2011), CPK6 was reported to interact with SLAC1 only weakly (Geiger et al., 2010) and not to show physiologically relevant Ca^{2+}-activated protein kinase activity in vitro (Scherzer et al., 2012). However, quantitative phosphorylation analyses showed a strong preference for CPK6 to phosphorylate the N terminus of SLAC1 in a Ca^{2+}-dependent manner (Brandt et al., 2012). A stringent biochemical analysis (modified after Hastie et al., 2006) of CPK6 protein kinase activity reveals that CPK6 is strongly activated by elevation in $[Ca^{2+}]$ in the physiological range of $[Ca^{2+}]_{cyt}$ increases from baseline levels of approximately 100 to 150 nM to concentrations greater than or equal to 300 nM (Fig. 3). Taken together, CPK6 is activated by physiological $[Ca^{2+}]$ increases and interacts with SLAC1 to phosphorylate SLAC1 Ca^{2+} dependently (Fig. 3; Brandt et al., 2012). One hypothesis for a mechanism mediating Ca^{2+} sensitivity priming is that the clade A PP2Cs directly down-regulate CPK activity (see Fig. 4), similar to PP2C-mediated down-regulation of OST1 activity (Belin et al., 2006; Yoshida et al., 2006; Umezawa et al., 2009; Vlad et al., 2009). However, to date no study has shown the down-regulation of CPK activity by PP2Cs,

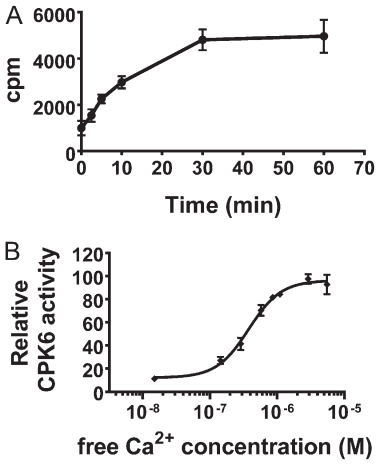

Figure 3. Quantitative phosphorylation assays show a strong Ca^{2+} activation of CPK6 activity for physiological $[Ca^{2+}]$ elevations. A, To determine proper conditions, the time-dependent phosphorylation of Syntide-2 (400 μM) by CPK6 (75 nM) was analyzed by measuring the incorporation of ^{32}P into the substrate (in counts per minute [cpm]). B, A time point in the linear range of product phosphorylation in A (4.5 min) was chosen to determine CPK6 activities at defined free Ca^{2+} concentrations. CPK6 activity is strongly dependent on the free Ca^{2+} concentration (fit parameters: K_A = 508 nM; Hill coefficient = 1.8 ± 0.2 SE; R^2 = 0.98). Error bars represent SD (n = 3 experiments). See Supplemental Text S1 for a detailed description of the method used.

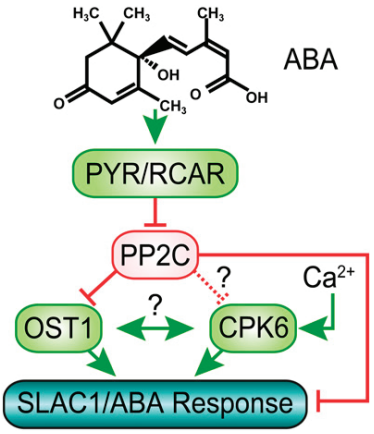

Figure 4. Simplified model of abscisic acid signaling in guard cells. In the presence of ABA, PYR/RCAR proteins inhibit PP2C phosphatases. This enables activation of the protein kinase OST1, which in turn phosphorylates and activates SLAC1, representing the Ca^{2+}-independent branch of SLAC1 activation. Furthermore, the ABI1 PP2C directly dephosphorylates SLAC1 leading to deactivation of SLAC1. Decreased PP2C activity induced by ABA also leads to decreased negative regulation of SLAC1 activation by calcium dependent protein kinases. Whether this regulation solely occurs by dephosphorylation of SLAC1 or whether in addition PP2Cs directly regulate CPKs remains to be determined (see text). A potential mechanism of cross talk between Ca^{2+}-dependent and -independent SLAC1 activation may occur by cross regulation of OST1 and CPKs, which is indicated by ?, but is hypothetical and remains to be investigated.

neither in vivo nor in vitro, and thus more research is needed to address this or other hypotheses.

Studies showed that the Ca^{2+}-independent protein kinase OST1 can activate SLAC1 in *X. laevis* oocytes and that this is inhibited by the presence of clade A PP2C phosphatases (Geiger et al., 2009; Lee et al., 2009). Moreover, a recent study demonstrated that functional ABA-activation of SLAC1 channels can be reconstituted in *X. laevis* oocytes by coexpression of ABA receptors, PP2Cs, protein kinase, and SLAC1 (Brandt et al., 2012). Either the Ca^{2+}-dependent protein kinase CPK6 (Fig. 3) or the Ca^{2+}-independent protein kinase OST1 was sufficient for functional reconstitution of ABA activation of SLAC1 (Brandt et al., 2012). Further research is needed to determine the genetic and cell signaling mechanisms that mediate stimulus-induced enhancement (priming) of $[Ca^{2+}]_{cyt}$ -dependent signal transduction.

COMMUNICATION AMONG Ca^{2+}-DEPENDENT AND Ca^{2+}-INDEPENDENT MECHANISMS

It remains unknown how the above-described Ca^{2+}-dependent and Ca^{2+}-independent pathways communicate with one another in guard cells in vivo. Several nonexclusive models can be envisioned as discussed below, although other mechanisms may also mediate this communication. A hypothesis in which PP2Cs may down-regulate CPKs (Fig. 4) remains to be investigated, as discussed above. Given that Ca^{2+}-dependent and Ca^{2+}-independent stomatal closing appear to depend on one another quantitatively (Mustilli et al., 2002; Siegel et al., 2009), an additional hypothesis is that CPKs and OST1 (cross) regulate each other (Fig. 4). However, no biochemical evidence for such cross regulation or protein-protein interaction has presently been reported, in vivo or in vitro, and this hypothesis would need to be investigated. In addition to these models, recent research demonstrated that the ABI1 PP2C phosphatase directly dephosphorylates the N terminus of SLAC1 (Fig. 4; Brandt et al., 2012). (Note that PP2Cs are Mg^{2+}-requiring protein phosphatases and millimolar Mg^{2+} concentrations are best included at all times, including during all PP2C protein purification steps, to assess their roles in target dephosphorylation.) The dephosphorylation of SLAC1 by ABI1 provides a mechanism for the required tight regulation of S-type anion channel activity in guard cells (Fig. 4; Pei et al., 1997). Direct regulation of ion channels by protein phosphatases has been reported for other plant and animal ion channels (Westphal et al., 1999; Chérel et al., 2002; Lee et al., 2007; Zhou et al., 2010). Furthermore, OST1 may regulate $[Ca^{2+}]_{cyt}$ levels via the NADPH oxidases respiratory burst oxidase homolog D and F and subsequent reactive oxygen species bursts (Sirichandra et al., 2009). Through this pathway, OST1 could control $[Ca^{2+}]_{cyt}$ (Kwak et al., 2003) and regulate CPK activities. A fourth hypothesis, which does not exclude the above models, is that SLAC1 serves as a coincidence detector for phosphorylation and activation by OST1 and CPKs (Fig. 4). OST1 has been shown to phosphorylate residues including Ser 120 (S120) in the N terminus of SLAC1 and S120 phosphorylation is essential for the SLAC1 activation by OST1 in oocytes (Geiger et al., 2009) and for stomatal closing (Vahisalu et al., 2010). However, recent experiments showed that stomatal closure induced by environmental factors were clearly less impaired in *slac1-7* plants that carry S120F mutation than those observed for SLAC1 knockout plants, further suggesting that SLAC1 activation is a process that involves phosphorylation of multiple amino acids by multiple protein kinases (Merilo et al., 2013). In line with this assumption, S120A mutation did not disrupt activation of SLAC1 by CPK23 (Geiger et al., 2010). Moreover, CPK6 phosphorylated Ser 59 (S59) in the SLAC1 N terminus and S59 phosphorylation is essential for SLAC1 activation by CPK6 (Brandt et al., 2012). Data show that S59 can also be phosphorylated by OST1 in vitro (Vahisalu et al., 2010). However, whether this is required for OST1 activation of SLAC1 remains unknown. Thus, a combination of the above options and/or additional mechanisms may mediate Ca^{2+} specificity and sensitivity priming and synergistic effects of Ca^{2+}-dependent and Ca^{2+}-independent signal transduction. These models await investigation and could lead to a detailed mechanistic understanding of

a network that mediates specificity in plant calcium signal transduction.

SUMMARY

In conclusion, recent findings show that stomata compensate for excessively open apertures by mechanisms that include constitutive priming (enhancement) of Ca^{2+} sensitivity, as found in *slac1* guard cells (Laanemets et al., 2013; Figs. 1 and 2; Supplemental Fig. S1). The finding that stomatal regulation can adapt to and compensate for impaired stomatal responses (Laanemets et al., 2013) could be of broader relevance for plant-environment interactions. A precise biochemical and cellular understanding of the mechanisms that ensure compensatory regulation of stomatal movements and detailed mechanisms mediating specificity in Ca^{2+} signaling remain to be elucidated in plants. ABA- and CO_2-induced Ca^{2+} sensitivity priming in guard cells (Young et al., 2006; Siegel et al., 2009; Chen et al., 2010; Xue et al., 2011) provides a system that can explain calcium signaling specificity in guard cells and adds to other (nonexclusive) models for Ca^{2+} signaling specificity in plants (Kudla et al., 2010). An in depth biochemical and cellular understanding of mechanisms mediating specificity in Ca^{2+} signaling is also a present goal in animal cell signaling research (Berridge, 2012). The hypotheses and models proposed here (Fig. 4) could enable the underlying specificity mechanisms to be characterized at an in depth mechanistic level in a plant cell system.

Sequence data from this article can be found in the GenBank/EMBL data libraries under accession numbers supplied in Supplemental Text S1.

Supplemental Data

The following materials are available in the online version of this article.

Supplemental Figure S1. *slac1* shows enhanced Ca^{2+} sensitivity at resting $[Ca^{2+}]_{cyt}$.

Supplemental Figure S2. K^+_{in} channels are down-regulated in *ost1-3* mutant plants.

Supplemental Figure S3. K^+_{in} channels are down-regulated in *abi2-1* mutant plants.

Supplemental Text S1. Supplemental Materials and Methods.

Received April 23, 2013; accepted June 10, 2013; published June 13, 2013.

LITERATURE CITED

Allen GJ, Chu SP, Harrington CL, Schumacher K, Hoffmann T, Tang YY, Grill E, Schroeder JI (2001) A defined range of guard cell calcium oscillation parameters encodes stomatal movements. Nature **411:** 1053–1057

Allen GJ, Kwak JM, Chu SP, Llopis J, Tsien RY, Harper JF, Schroeder JI (1999) Cameleon calcium indicator reports cytoplasmic calcium dynamics in Arabidopsis guard cells. Plant J **19:** 735–747

Allen GJ, Murata Y, Chu SP, Nafisi M, Schroeder JI (2002) Hypersensitivity of abscisic acid-induced cytosolic calcium increases in the *Arabidopsis* farnesyltransferase mutant *era1-2*. Plant Cell **14:** 1649–1662

Belin C, de Franco P-O, Bourbousse C, Chaignepain S, Schmitter J-M, Vavasseur A, Giraudat J, Barbier-Brygoo H, Thomine S (2006) Identification of features regulating OST1 kinase activity and OST1 function in guard cells. Plant Physiol **141:** 1316–1327

Berridge MJ (2012) Calcium signalling remodelling and disease. Biochem Soc Trans **40:** 297–309

Brandt B, Brodsky DE, Xue S, Negi J, Iba K, Kangasjärvi J, Ghassemian M, Stephan AB, Hu H, Schroeder JI (2012) Reconstitution of abscisic acid activation of SLAC1 anion channel by CPK6 and OST1 kinases and branched ABI1 PP2C phosphatase action. Proc Natl Acad Sci USA **109:** 10593–10598

Chen ZH, Hills A, Lim CK, Blatt MR (2010) Dynamic regulation of guard cell anion channels by cytosolic free Ca^{2+} concentration and protein phosphorylation. Plant J **61:** 816–825

Chérel I, Michard E, Platet N, Mouline K, Alcon C, Sentenac H, Thibaud J-B (2002) Physical and functional interaction of the *Arabidopsis* K^+ channel AKT2 and phosphatase AtPP2CA. Plant Cell **14:** 1133–1146

Cho D, Kim SA, Murata Y, Lee S, Jae SK, Nam HG, Kwak JM (2009) Deregulated expression of the plant glutamate receptor homolog *AtGLR3.1* impairs long-term Ca^{2+}-programmed stomatal closure. Plant J **58:** 437–449

Cutler SR, Rodriguez PL, Finkelstein RR, Abrams SR (2010) Abscisic acid: emergence of a core signaling network. Annu Rev Plant Biol **61:** 651–679

Day IS, Reddy VS, Shad Ali G, Reddy AS (2002) Analysis of EF-hand-containing proteins in Arabidopsis. Genome Biol **3:** H0056

De Silva DLR, Cox RC, Hetherington AM, Mansfield TA (1985) Suggested involvement of calcium and calmodulin in the responses of stomata to abscisic acid. New Phytol **101:** 555–563

Dodd AN, Kudla J, Sanders D (2010) The language of calcium signaling. Annu Rev Plant Biol **61:** 593–620

Eisenach C, Chen ZH, Grefen C, Blatt MR (2012) The trafficking protein SYP121 of Arabidopsis connects programmed stomatal closure and K^+ channel activity with vegetative growth. Plant J **69:** 241–251

Franz S, Ehlert B, Liese A, Kurth J, Cazalé A-C, Romeis T (2011) Calcium-dependent protein kinase CPK21 functions in abiotic stress response in Arabidopsis thaliana. Mol Plant **4:** 83–96

Geiger D, Scherzer S, Mumm P, Stange A, Marten I, Bauer H, Ache P, Matschi S, Liese A, Al-Rasheid KAS, et al (2009) Activity of guard cell anion channel SLAC1 is controlled by drought-stress signaling kinase-phosphatase pair. Proc Natl Acad Sci USA **106:** 21425–21430

Geiger D, Scherzer S, Mumm P, Marten I, Ache P, Matschi S, Liese A, Wellmann C, Al-Rasheid KAS, Grill E, et al (2010) Guard cell anion channel SLAC1 is regulated by CDPK protein kinases with distinct Ca^{2+} affinities. Proc Natl Acad Sci USA **107:** 8023–8028

Grabov A, Blatt MR (1998) Membrane voltage initiates Ca^{2+} waves and potentiates Ca^{2+} increases with abscisic acid in stomatal guard cells. Proc Natl Acad Sci USA **95:** 4778–4783

Hamilton DWA, Hills A, Kohler B, Blatt MR (2000) Ca^{2+} channels at the plasma membrane of stomatal guard cells are activated by hyperpolarization and abscisic acid. Proc Natl Acad Sci USA **97:** 4967–4972

Hastie CJ, McLauchlan HJ, Cohen P (2006) Assay of protein kinases using radiolabeled ATP: a protocol. Nat Protoc **1:** 968–971

Hosy E, Vavasseur A, Mouline K, Dreyer I, Gaymard F, Porée F, Boucherez J, Lebaudy A, Bouchez D, Very AA, et al (2003) The Arabidopsis outward K^+ channel GORK is involved in regulation of stomatal movements and plant transpiration. Proc Natl Acad Sci USA **100:** 5549–5554

Hu H, Boisson-Dernier A, Israelsson-Nordstroem M, Boehmer M, Xue S, Ries A, Godoski J, Kuhn JM, Schroeder JI (2010) Carbonic anhydrases are upstream regulators of CO2-controlled stomatal movements in guard cells. Nat Cell Biol **12:** 87–93

Hubbard KE, Nishimura N, Hitomi K, Getzoff ED, Schroeder JI (2010) Early abscisic acid signal transduction mechanisms: newly discovered components and newly emerging questions. Genes Dev **24:** 1695–1708

Hubbard KE, Siegel RS, Valerio G, Brandt B, Schroeder JI (2012) Abscisic acid and CO_2 signalling via calcium sensitivity priming in guard cells, new CDPK mutant phenotypes and a method for improved resolution of stomatal stimulus-response analyses. Ann Bot (Lond) **109:** 5–17

Kim TH, Böhmer M, Hu H, Nishimura N, Schroeder JI (2010) Guard cell signal transduction network: advances in understanding abscisic acid, CO_2, and Ca^{2+} signaling. Annu Rev Plant Biol **61:** 561–591

Klüsener B, Young JJ, Murata Y, Allen GJ, Mori IC, Hugouvieux V, Schroeder JI (2002) Convergence of calcium signaling pathways of

pathogenic elicitors and abscisic acid in Arabidopsis guard cells. Plant Physiol **130:** 2152–2163

Kollist H, Jossier M, Laanemets K, Thomine S (2011) Anion channels in plant cells. FEBS J **278:** 4277–4292

Kollist T, Moldau H, Rasulov B, Oja V, Rämma H, Hüve K, Jaspers P, Kangasjärvi J, Kollist H (2007) A novel device detects a rapid ozone-induced transient stomatal closure in intact Arabidopsis and its absence in abi2 mutant. Physiol Plant **129:** 796–803

Koornneef M, Reuling G, Karssen CM (1984) The isolation and characterization of abscisic acid-insensitive mutants of *Arabidopsis thaliana*. Physiol Plant **61:** 377–383

Kudla J, Batistič O, Hashimoto K (2010) Calcium signals: the lead currency of plant information processing. Plant Cell **22:** 541–563

Kwak JM, Murata Y, Baizabal-Aguirre VM, Merrill J, Wang M, Kemper A, Hawke SD, Tallman G, Schroeder JI (2001) Dominant negative guard cell K^+ channel mutants reduce inward-rectifying K^+ currents and light-induced stomatal opening in Arabidopsis. Plant Physiol **127:** 473–485

Kwak JM, Mori IC, Pei ZM, Leonhardt N, Torres MA, Dangl JL, Bloom RE, Bodde S, Jones JDG, Schroeder JI (2003) NADPH oxidase AtrbohD and AtrbohF genes function in ROS-dependent ABA signaling in Arabidopsis. EMBO J **22:** 2623–2633

Laanemets K, Wang YF, Lindgren O, Wu J, Nishimura N, Lee S, Caddell D, Merilo E, Brosche M, Kilk K, et al (2013) Mutations in the SLAC1 anion channel slow stomatal opening and severely reduce K^+ uptake channel activity via enhanced cytosolic [Ca^{2+}] and increased Ca^{2+} sensitivity of K^+ uptake channels. New Phytol **197:** 88–98

Lee SC, Lan WZ, Kim BG, Li LG, Cheong YH, Pandey GK, Lu GH, Buchanan BB, Luan S (2007) A protein phosphorylation/dephosphorylation network regulates a plant potassium channel. Proc Natl Acad Sci USA **104:** 15959–15964

Lee SC, Lan W, Buchanan BB, Luan S (2009) A protein kinase-phosphatase pair interacts with an ion channel to regulate ABA signaling in plant guard cells. Proc Natl Acad Sci USA **106:** 21419–21424

Levchenko V, Konrad KR, Dietrich P, Roelfsema MR, Hedrich R (2005) Cytosolic abscisic acid activates guard cell anion channels without preceding Ca^{2+} signals. Proc Natl Acad Sci USA **102:** 4203–4208

Ma S-Y, Wu W-H (2007) AtCPK23 functions in Arabidopsis responses to drought and salt stresses. Plant Mol Biol **65:** 511–518

Ma Y, Szostkiewicz I, Korte A, Moes D, Yang Y, Christmann A, Grill E (2009) Regulators of PP2C phosphatase activity function as abscisic acid sensors. Science **324:** 1064–1068

MacRobbie EAC (2000) ABA activates multiple Ca^{2+} fluxes in stomatal guard cells, triggering vacuolar K^+ (Rb^+) release. Proc Natl Acad Sci USA **97:** 12361–12368

McAinsh MR, Brownlee C, Hetherington AM (1991) Partial inhibition of ABA-induced stomatal closure by calcium-channel blockers. Proc R Soc Lond, Ser B Biol Sci **243:** 195–201

Merilo E, Laanemets K, Hu H, Xue S, Jakobson L, Tulva I, Gonzalez-Guzman M, Rodriguez PL, Schroeder JI, Broschè M, et al (May 28, 2013) PYR/RCAR receptors contribute to ozone-, reduced air humidity-, darkness- and CO_2-induced stomatal regulation. Plant Physiol http://dx.doi.org/10.1104/pp.113.220608

Meyer S, Mumm P, Imes D, Endler A, Weder B, Al-Rasheid KA, Geiger D, Marten I, Martinoia E, Hedrich R (2010) AtALMT12 represents an R-type anion channel required for stomatal movement in Arabidopsis guard cells. Plant J **63:** 1054–1062

Mori IC, Murata Y, Yang Y, Munemasa S, Wang Y-F, Andreoli S, Tiriac H, Alonso JM, Harper JF, Ecker JR, et al (2006) CDPKs CPK6 and CPK3 function in ABA regulation of guard cell S-type anion- and Ca^{2+}-permeable channels and stomatal closure. PLoS Biol **4:** e327

Munemasa S, Hossain MA, Nakamura Y, Mori IC, Murata Y (2011) The Arabidopsis calcium-dependent protein kinase, CPK6, functions as a positive regulator of methyl jasmonate signaling in guard cells. Plant Physiol **155:** 553–561

Mustilli A-C, Merlot S, Vavasseur A, Fenzi F, Giraudat J (2002) *Arabidopsis* OST1 protein kinase mediates the regulation of stomatal aperture by abscisic acid and acts upstream of reactive oxygen species production. Plant Cell **14:** 3089–3099

Negi J, Matsuda O, Nagasawa T, Oba Y, Takahashi H, Kawai-Yamada M, Uchimiya H, Hashimoto M, Iba K (2008) CO_2 regulator SLAC1 and its homologues are essential for anion homeostasis in plant cells. Nature **452:** 483–486

Nishimura N, Yoshida T, Murayama M, Asami T, Shinozaki K, Hirayama T (2004) Isolation and characterization of novel mutants affecting the abscisic acid sensitivity of Arabidopsis germination and seedling growth. Plant Cell Physiol **45:** 1485–1499

Park SY, Fung P, Nishimura N, Jensen DR, Fujii H, Zhao Y, Lumba S, Santiago J, Rodrigues A, Chow TF, et al (2009) Abscisic acid inhibits type 2C protein phosphatases via the PYR/PYL family of START proteins. Science **324:** 1068–1071

Pei ZM, Kuchitsu K, Ward JM, Schwarz M, Schroeder JI (1997) Differential abscisic acid regulation of guard cell slow anion channels in *Arabidopsis* wild-type and *abi1* and *abi2* mutants. Plant Cell **9:** 409–423

Pei Z-M, Murata Y, Benning G, Thomine S, Klüsener B, Allen GJ, Grill E, Schroeder JI (2000) Calcium channels activated by hydrogen peroxide mediate abscisic acid signalling in guard cells. Nature **406:** 731–734

Raghavendra AS, Gonugunta VK, Christmann A, Grill E (2010) ABA perception and signalling. Trends Plant Sci **15:** 395–401

Roelfsema MRG, Hanstein S, Felle HH, Hedrich R (2002) CO_2 provides an intermediate link in the red light response of guard cells. Plant J **32:** 65–75

Roelfsema MRG, Hedrich R (2005) In the light of stomatal opening: new insights into 'the Watergate'. New Phytol **167:** 665–691

Roelfsema MRG, Levchenko V, Hedrich R (2004) ABA depolarizes guard cells in intact plants, through a transient activation of R- and S-type anion channels. Plant J **37:** 578–588

Sanders D, Hopgood M, Jennings IR (1989) Kinetic response of H^+-coupled transport to extracellular pH: critical role of cytosolic pH as a regulator. J Membr Biol **108:** 253–261

Sasaki T, Mori IC, Furuichi T, Munemasa S, Toyooka K, Matsuoka K, Murata Y, Yamamoto Y (2010) Closing plant stomata requires a homolog of an aluminum-activated malate transporter. Plant Cell Physiol **51:** 354–365

Scherzer S, Maierhofer T, Al-Rasheid KA, Geiger D, Hedrich R (2012) Multiple calcium-dependent kinases modulate ABA-activated guard cell anion channels. Mol Plant **5:** 1409–1412

Schroeder JI, Raschke K, Neher E (1987) Voltage dependence of K^+ channels in guard-cell protoplasts. Proc Natl Acad Sci USA **84:** 4108–4112

Schroeder JI, Hedrich R, Fernandez JM (1984) Potassium-selective single channels in guard cell protoplasts of *Vicia faba*. Nature **312:** 361–362

Schroeder JI, Hagiwara S (1989) Cytosolic calcium regulates ion channels in the plasma membrane of *Vicia faba* guard cells. Nature **338:** 427–430

Schwartz A (1985) Role of Ca^{2+} and EGTA on stomatal movements in *Commelina communis* L. Plant Physiol **79:** 1003–1005

Shimazaki KI, Doi M, Assmann SM, Kinoshita T (2007) Light regulation of stomatal movement. Annu Rev Plant Biol **58:** 219–247

Siegel RS, Xue S, Murata Y, Yang Y, Nishimura N, Wang A, Schroeder JI (2009) Calcium elevation-dependent and attenuated resting calcium-dependent abscisic acid induction of stomatal closure and abscisic acid-induced enhancement of calcium sensitivities of S-type anion and inward-rectifying K^+ channels in Arabidopsis guard cells. Plant J **59:** 207–220

Sirichandra C, Gu D, Hu HC, Davanture M, Lee S, Djaoui M, Valot B, Zivy M, Leung J, Merlot S, et al (2009) Phosphorylation of the Arabidopsis AtrbohF NADPH oxidase by OST1 protein kinase. FEBS Lett **583:** 2982–2986

Staxén I, Pical C, Montgomery LT, Gray JE, Hetherington AM, McAinsh MR (1999) Abscisic acid induces oscillations in guard-cell cytosolic free calcium that involve phosphoinositide-specific phospholipase C. Proc Natl Acad Sci USA **96:** 1779–1784

Umezawa T, Sugiyama N, Mizoguchi M, Hayashi S, Myouga F, Yamaguchi-Shinozaki K, Ishihama Y, Hirayama T, Shinozaki K (2009) Type 2C protein phosphatases directly regulate abscisic acid-activated protein kinases in Arabidopsis. Proc Natl Acad Sci USA **106:** 17588–17593

Vahisalu T, Kollist H, Wang YF, Nishimura N, Chan WY, Valerio G, Lamminmäki A, Brosché M, Moldau H, Desikan R, et al (2008) SLAC1 is required for plant guard cell S-type anion channel function in stomatal signalling. Nature **452:** 487–491

Vahisalu T, Puzõrjova I, Brosché M, Valk E, Lepiku M, Moldau H, Pechter P, Wang Y-S, Lindgren O, Salojärvi J, et al (2010) Ozone-triggered rapid stomatal response involves the production of reactive oxygen species, and is controlled by SLAC1 and OST1. Plant J **62:** 442–453

Vlad F, Rubio S, Rodrigues A, Sirichandra C, Belin C, Robert N, Leung J, Rodriguez PL, Laurière C, Merlot S (2009) Protein phosphatases 2C

regulate the activation of the Snf1-related kinase OST1 by abscisic acid in *Arabidopsis*. Plant Cell **21:** 3170–3184

Wang Y, Papanatsiou M, Eisenach C, Karnik R, Williams M, Hills A, Lew VL, Blatt MR (2012) Systems dynamic modeling of a guard cell Cl^- channel mutant uncovers an emergent homeostatic network regulating stomatal transpiration. Plant Physiol **160:** 1956–1967

Webb AAR, McAinsh MR, Mansfield TA, Hetherington AM (1996) Carbon dioxide induces increases in guard cell cytosolic free calcium. Plant J **9:** 297–304

Westphal RS, Tavalin SJ, Lin JW, Alto NM, Fraser IDC, Langeberg LK, Sheng M, Scott JD (1999) Regulation of NMDA receptors by an associated phosphatase-kinase signaling complex. Science **285:** 93–96

Xue S, Hu H, Ries A, Merilo E, Kollist H, Schroeder JI (2011) Central functions of bicarbonate in S-type anion channel activation and OST1 protein kinase in CO_2 signal transduction in guard cell. EMBO J **30:** 1645–1658

Yoshida R, Hobo T, Ichimura K, Mizoguchi T, Takahashi F, Aronso J, Ecker JR, Shinozaki K (2002) ABA-activated SnRK2 protein kinase is required for dehydration stress signaling in Arabidopsis. Plant Cell Physiol **43:** 1473–1483

Yoshida R, Umezawa T, Mizoguchi T, Takahashi S, Takahashi F, Shinozaki K (2006) The regulatory domain of SRK2E/OST1/SnRK2.6 interacts with ABI1 and integrates abscisic acid (ABA) and osmotic stress signals controlling stomatal closure in Arabidopsis. J Biol Chem **281:** 5310–5318

Young JJ, Mehta S, Israelsson M, Godoski J, Grill E, Schroeder JI (2006) CO_2 signaling in guard cells: calcium sensitivity response modulation, a Ca^{2+}-independent phase, and CO_2 insensitivity of the *gca2* mutant. Proc Natl Acad Sci USA **103:** 7506–7511

Zhou X-B, Wulfsen I, Utku E, Sausbier U, Sausbier M, Wieland T, Ruth P, Korth M (2010) Dual role of protein kinase C on BK channel regulation. Proc Natl Acad Sci USA **107:** 8005–8010

Zhu S-Y, Yu X-C, Wang X-J, Zhao R, Li Y, Fan R-C, Shang Y, Du S-Y, Wang X-F, Wu F-Q, et al (2007) Two calcium-dependent protein kinases, CPK4 and CPK11, regulate abscisic acid signal transduction in *Arabidopsis*. Plant Cell **19:** 3019–3036

Zou JJ, Wei FJ, Wang C, Wu JJ, Ratnasekera D, Liu WX, Wu WH (2010) Arabidopsis calcium-dependent protein kinase CPK10 functions in abscisic acid- and Ca^{2+}-mediated stomatal regulation in response to drought stress. Plant Physiol **154:** 1232–1243

Supplemental Figures

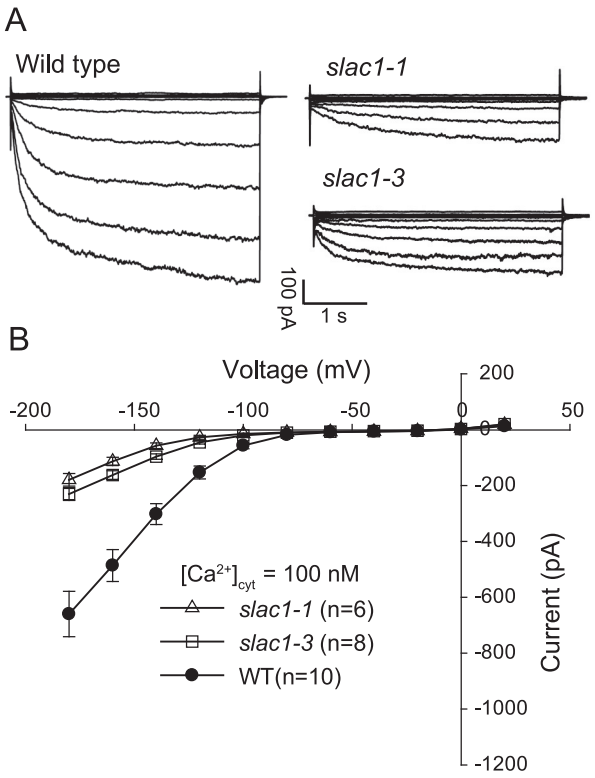

Supplemental Figure S1. *slac1* mutants dramatically reduce inward K^+ channel currents in Arabidopsis guard cells at resting free $[Ca^{2+}]_{cyt}$ of 0.1 μM. (A) Whole-cell recordings of inward K^+ channel currents in the presence of 30 mM KCl in the bath solution were made in wild-type, *slac1-1*, and *slac1-3* guard cells with 0.1 μM free Ca^{2+} in the pipette solution. (B) Average current–voltage relationships. K^+_{in} channel currents were activated by voltage pulses with +20 mV increments from -180 mV to +20 mV. WT control data are from the same experimental set and are the same as in Figures S2 and S3. Error bars indicate ± SEM. Methods in figures S1, S2 and S3 were as in Laanemets et al., 2013 (see supplemental methods section).

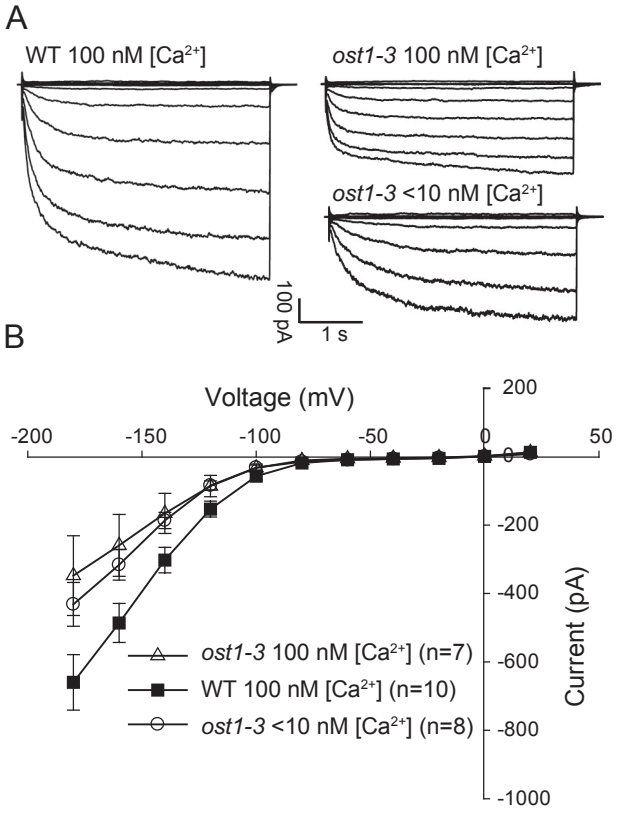

Supplemental Figure S2. *ost1-3* mutant guard cells exhibit reduced inward K^+ channel currents at resting free cytosolic $[Ca^{2+}]_{cyt}$ of 0.1 µM but lowering the free cytosolic Ca^{2+} concentration to <10 nM did not significantly affect K^+_{in} activity in *ost1-3* guard cells. (A) Whole-cell recordings of inward K^+ currents in the presence of 30 mM KCl in the bath solution were conducted in wild-type and *ost1-3* guard cells with 0.1 µM free Ca^{2+} in the pipette solution. (B) Average current–voltage relationships. K^+_{in} channel currents were activated by voltage pulses of +20 mV increments from -180 mV to +20 mV. Error bars indicate ± SEM. WT data control data are the same as in figures S1 and S3.

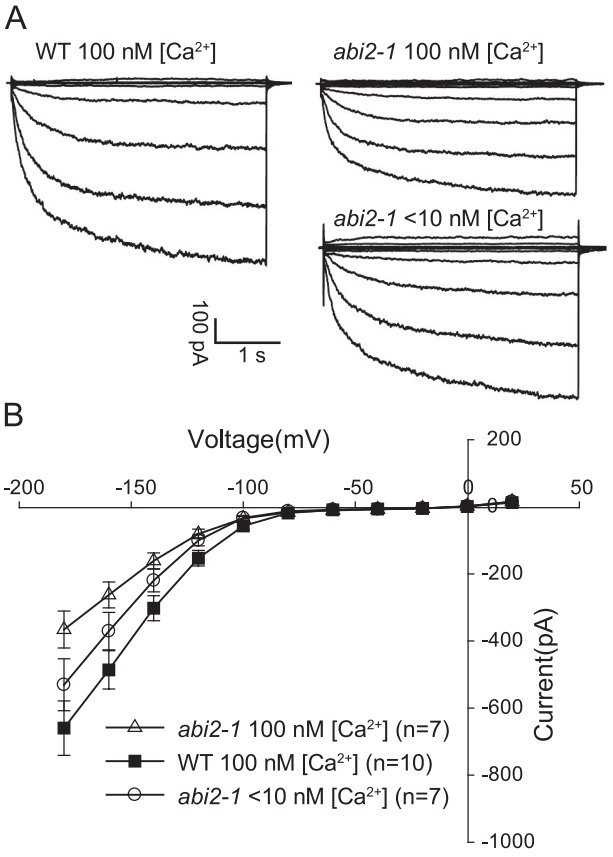

Supplemental Figure S3. Guard cells of the *abi2-1* (Col-0) mutant have reduced inward K^+ channel activity at resting free $[Ca^{2+}]_{cyt}$ of 0.1 µM. Only a slight but non-significant reversal of K^+_{in} activity in *abi2-1* (Col-0) guard cells could be observed by reducing $[Ca^{2+}]_{cyt}$ to <10 nM. (A) Whole-cell recordings of inward K^+ currents in the presence of 30 mM KCl in the bath solution were conducted in wild-type and *abi2-1* guard cells with 100 nM free Ca^{2+} or <10 nM free Ca^{2+} (*abi2-1*) in the pipette solution. (B) Effect of lowering the Ca^{2+}_{cyt} concentration on K^+_{in} channel currents in *abi2-1* guard cells. Average current–voltage relationships are shown. K^+_{in} channel currents were activated by voltage pulses with +20 mV increment from -180 mV to +20 mV. WT data control data are the same as in Figures S1 and S2. Error bars indicate ± SEM.

Supplemental Text S1:

Material and Methods:

Patch clamp in guard cell protoplasts

Plant growth conditions and patch clamp measurements were carried out as described previously (Laanements et al., 2013). *Arabidopsis thaliana* ecotype Columbia (wild type), *slac1-1* (C456T), *slac1-3* (SALK_099139) , *ost1-3* (SALK_008068) and *abi2-1* (G168D) (all mutants are in the Columbia background) were grown in a growth chamber controlling the environment (20–22°C, 70% humidity, 75 µmol m^{-2} s^{-1} white light, 16-h-light/8-h-dark). Arabidopsis guard cell protoplasts (GCPs) were prepared enzymatically from rosette leaves of 4- to 6-week-old plants as described previously (Pei et al., 1997). The GCPs were incubated for 5-7 min after achieving the whole cell configuration to allow equilibration of the cytosol with the pipette solution. Inward-rectifying potassium (K^+_{in}) channel currents were recorded using an Axopatch 200 amplifier (Axon Instruments, Foster City, CA) by voltage pulses with a +20 mV increment from -180 mV to +20 mV. The pipette solution was composed of 30 mM KCl, 70 mM K-Glu, 2 mM $MgCl_2$, 6.7 mM EGTA, 5 mM ATP and 10 mM HEPES (Tris, pH 7.1). To adjust guard cell cytoplasmic free Ca^{2+} concentrations ($[Ca^{2+}]_{cyt}$) to 100 nM the pipette solution was supplemented with 2 mM $CaCl_2$. For measurements at a $[Ca^{2+}]_{cyt}$ of <10 nM, no $CaCl_2$ was added to the pipette solution. The bath solution contained 30 mM KCl, 1 mM $CaCl_2$, 2 mM $MgCl_2$ and 10 mM MES (Tris, pH 5.6). Osmolarity was adjusted by D-sorbitol to 500 mmol kg^{-1} for the pipette solution and 485 mmol·kg^{-1} for the bath solution.

Quantitative protein kinase activity measurements

Protein expression and isolation was performed as described in Brandt et al., 2012. The CPK6 coding sequence was cloned into a modified pGEX-6P1 *E.coli* expression vector (GE Healthcare) employing the USER cloning method (Nour-Eldin et al., 2006) resulting in CPK6 protein fused to glutathione S-transferase (GST) and StrepII at the N- and C-terminus, respectively. *E.coli* Rosetta (DE3) pLysS (Novagen) carrying the above described vector were grown in LB-medium to an $OD_{(A600)}$ of approximately 0.5 and protein expression was induced by adding isopropyl-β-D-thiogalactopyranoside (0.5 mM final concentration). After 4 h incubation at room temperature the bacteria were pelleted (centrifugation at 5,000 × g for 15 min) and stored at -80 °C. Isolation of CPK6 was achieved by a combined gravity flow and batch affinity purification approach with Strep-Tactin Sepharose (IBA) as resin using the buffers recommended by the manufacturer. Please note that the elution buffer was supplemented with 20 % (v/v) Glycerol and after flash freezing in liquid nitrogen aliquots of the purified protein were stored at -80 °C. To assess protein purity and concentration different volumes of the isolated protein together with defined amounts of bovine serum albumine (BSA) were subjected to SDS-PAGE. After coomassie staining of the proteins the gel was dried between 2 cellophane sheets.

The dried gel was scanned and band intensities were measured using Fiji (http://fiji.sc/Fiji). CPK6 protein concentrations were calculated based on the equation of the linear regression of the BSA standards (similar to Hashimoto et al., 2012).

Time dependent Syntide-2 phosphorylation by CPK6 was assessed as described in the following: 75 nM CPK6 and 400 µM Syntide-2 (Sigma) were incubated in 100 mM HEPES pH 7.5, 2 mM DTT, 10 mM $MgCl_2$, 1 mM EGTA, 100 µM ATP, ~0.15 µCi/µl [γ-^{32}P] ATP and 3.8 µM free Ca^{2+} (calculated with http://www.stanford.edu/~cpatton/webmaxc/webmaxcE.htm) at room temperature. After 0, 2.5, 5, 10, 30, 60 min the reactions were quenched by at adding glacial acetic acid (27% v/v final concentration). Subsequently, a part of the quenched reactions was spotted on P81 grade filter paper discs (Whatman). The filter discs were washed 5 times for 5 min with 0.5% (v/v) phosphoric acid, incubated with acetone for 2 min, and air dried. To quantify incorporated ^{32}P the discs were immersed in scintillation fluid (EcoScint) followed by measuring the radioactivity (in counts per minute; cpm) in a scintillation counter (Beckman). To measure Ca^{2+}-dependent CPK6 activities the same conditions were used (4.5 min incubation time) with the only difference that free Ca^{2+} concentrations in the reaction buffer were adjusted to a range from 15 nM to 7 µM. Data points are normalized relative to the maximum CPK6 activity in each experiment. Error bars represent SD of the mean (n=3).

Whole plant gas exchange measurements

Seeds of Arabidopsis thaliana (L.) Heynh Columbia (Col-0) and Landsberg erecta (Ler) and their respective mutants *slac1-1*, *slac1-3*, *ost1-3* and *abi2-1* were planted in soil containing 4 : 3 (v : v) peat:vermiculite and were grown through a hole in a glass plate covering pot (Kollist et al., 2007) in growth chambers (AR-66LX and AR-22L, Percival Scientific, IA, USA) with 70-75% air humidity and 12 h light (23°C, 150 µmol m^{-2} s^{-1})/12 h dark period (18°C). Stomatal conductance of 23-26 days old intact plants was measured using a custom-made rapid-response gas exchange measurement device (described in Kollist et al., 2007).

In light experiments, plants were inserted into the device (ambient CO_2, light=150 µmol m^{-2} s^{-1}, RH=60-75%) in the evening prior to measurements, kept in the measurement cuvettes overnight while maintaining the same photoperiod of 12hr light/12hr dark as in growth chambers and stomatal opening was measured during the onset of the light period in the morning. In CO_2 experiments, plants were inserted into the device and kept at ambient CO_2 concentration (400 mmol mol^{-1}), until stomatal conductance had stabilized (for ~2 h). Then the CO_2 concentration was decreased to 40 mmol mol^{-1} by filtering air through a granular potassium hydroxide. In both experiments, increases in stomatal conductance were followed during ~45 min. Photographs of plants were taken after the experiments and rosette leaf area was calculated using ImageJ 1.37v (National Institutes of Health, USA). Stomatal conductance for water vapour was calculated with a custom written program (Kollist et al., 2007).

Accession numbers of the genes

OST1: AT4G33950; ABI2: AT5G57050; SLAC1: AT1G12480; CPK6: AT2G17290

Literature cited:

Brandt B, Brodsky DE, Xue S, Negi J, Iba K, Kangasjärvi J, Ghassemian M, Stephan AB, Hu H, Schroeder JI (2012) Reconstitution of abscisic acid activation of SLAC1 anion channel by CPK6 and OST1 kinases and branched ABI1 PP2C phosphatase action. Proc Natl Acad Sci USA **109**: 10593-10598

Hashimoto K, Eckert C, Anschuetz U, Scholz M, Held K, Waadt R, Reyer A, Hippler M, Becker D, Kudla J (2012) Phosphorylation of Calcineurin B-like (CBL) calcium sensor proteins by their CBL-interacting protein kinases (CIPKs) is required for full activity of CBL-CIPK complexes towards their target proteins. J Biol Chem **287**: 7956-7968

Laanemets K, Wang YF, Lindgren O, Wu J, Nishimura N, Lee S, Caddell D, Merilo E, Brosche M, Kilk K, Soomets U, Kangasjärvi J, Schroeder JI, Kollist H (2013) Mutations in the SLAC1 anion channel slow stomatal opening and severely reduce K^+ uptake channel activity via enhanced cytosolic [Ca^{2+}] and increased Ca^{2+} sensitivity of K^+ uptake channels. New Phytol **197**: 88-98

Kollist T, Moldau H, Rasulov B, Oja V, Rämma H, Hüve K, Jaspers P, Kangasjärvi J, Kollist H (2007) A novel device detects a rapid ozone-induced transient stomatal closure in intact Arabidopsis and its absence in abi2 mutant. Physiol Plant **129**: 796-803

Pei ZM, Kuchitsu K, Ward JM, Schwarz M, Schroeder JI (1997) Differential abscisic acid regulation of guard cell slow anion channels in Arabidopsis wild-type and *abi1* and *abi2* mutants. Plant Cell **9**: 409-423

Calcium Specificity Mechanism in Abscisic Acid Signal Transduction in *Arabidopsis* Guard Cells

Benjamin Brandt[1,a], Shintaro Munemasa[1,2,a], Cun Wang[1], Desiree Nguyen[1], Thomas Belknap[1], Fernando Aleman[1], Julian I. Schroeder[1,b]

[1] Division of Biological Sciences, Cell and Developmental Biology Section, University of California, San Diego, 9500 Gilman Drive, La Jolla, CA 92093-0116, USA

[2] present address: Graduate School of Environmental and Life Science, Okayama University, 1-1-1 Tsushima-naka, Kita-ku, Okayama, 7008530 JAPAN

[a] These authors contributed equally to this work.

[b] Corresponding author:

University of California San Diego,

La Jolla, San Diego, CA- 92093-0116

USA

Telephone: 858-534-7759

Fax: 858-534-7108

Email: jischroeder@ucsd.edu

Abstract

A key question is how specificity in cellular responses to the eukaryotic second messenger Ca^{2+} is achieved. Plant guard cells, that form stomatal pores for plant gas exchange, provide a powerful system for in depth investigation of Ca^{2+}-signaling specificity. Abscisic acid (ABA) primes the Ca^{2+}-sensitivity of downstream signaling events that result in stomatal closure, providing a mechanism for specificity in Ca^{2+}-signaling. However, the underlying mechanisms remain unknown. Here we show that protein phosphatase 2Cs prevent non-specific Ca^{2+}-signaling by direct regulation of key targets in the downstream ABA-signaling network. Moreover, we show an interdependence of Ca^{2+}-dependent and Ca^{2+}-independent signaling pathways and that the anion channel SLAC1 can function as coincidence detector of these pathways, thus ensuring a specific Ca^{2+}-response and robust regulation of ABA signaling. We identify novel mechanisms explaining how specificity and robustness within Ca^{2+}-signaling is achieved on a cellular, genetic, and biochemical level.

Introduction

Cytosolic calcium ($[Ca^{2+}]_{cyt}$) functions as key cellular second messenger in a plethora of crucial processes in eukaryotes (1-6). Elucidation of the mechanisms mediating specificity in Ca^{2+}-signaling is fundamental to understanding signal transduction (1-4). In a few cases, the biochemical and cellular mechanisms mediating Ca^{2+}-signaling specificity have been revealed (e.g. 7-13). More than one (non-exclusive) mechanism could contribute to specificity in Ca^{2+}-signal transduction (1, 14). However, the characterization of the combined cellular, biochemical, and genetic mechanism underlying Ca^{2+}-specificity in a single cell type has not been achieved to our knowledge.

Plant genomes encode over 200 EF-hand Ca^{2+}-binding proteins (15), with many of these genes co-expressed in the same cell types (16), illustrating the need for Ca^{2+} specificity mechanisms. Two plant guard cells form a stomatal pore representing the gateway for CO_2 influx, which is inevitably accompanied by plant water loss. The aperture of stomatal pores is consequently tightly regulated by the guard cells. Intracellular Ca^{2+} represents a major second messenger in stomatal closing (2, 17-20), but intracellular Ca^{2+} also functions in stomatal opening (21-26). The underlying mechanisms mediating specificity in guard cell Ca^{2+}-signaling are not well understood. The development of genetic, electrophysiological, and cell signaling tools for the dissection of Ca^{2+}-signaling within this model cell type renders guard cells a powerful system for the investigation of specificity mechanisms within Ca^{2+}-signal transduction. Recent studies have shown that stomatal closing stimuli including abscisic acid (ABA) and CO_2 enhance the intracellular Ca^{2+} ($[Ca^{2+}]_{cyt}$)-sensitivity of downstream signaling mechanisms, switching them from an inactivated state to a Ca^{2+}-responsive "primed" state, thus tightly controlling specificity in Ca^{2+} responsiveness (26-30). However, the biochemical and genetic mechanisms mediating Ca^{2+}-sensitivity priming remain unknown.

SLAC1 represents the major anion channel mediating S-type anion currents in guard cells (31, 32) and Ca^{2+}-activation of S-type anion current activation is an early and crucial step in stomatal closure (28, 29, 33). Ca^{2+}-independent SnRK2 protein kinases, most importantly OST1 (34, 35), have been shown to activate SLAC1 in *Xenopus leavis* oocytes (36-38). The full length Ca^{2+}-dependent protein kinases 6, 21, and 23 (CPK6,

CPK21, and CPK23) also activate SLAC1 in oocytes (38, 39). Moreover, functional ABA-activation of SLAC1 via signal transduction pathway reconstitution has been demonstrated including either the Ca^{2+}-independent OST1 or the Ca^{2+}-dependent CPK6 protein kinases (38). However, whether the Ca^{2+}-dependent and –independent branches in these signal transduction pathways are functionally linked and depend on one-another *in vivo* remains unknown. Here we present biochemical, genetic and cellular signaling findings that describe mechanisms underlying specificity and robustness in Ca^{2+}-signaling within a single cell type.

Results

Previous studies have shown that *Arabidopsis thaliana* single or double mutants in Ca^{2+}-dependent protein kinases (CPKs) cause partial ABA-insensitivities in guard cell signaling (18, 40, 41). We addressed the question whether higher order *CPK* gene disruption mutant plants display more strongly impaired ABA responses. CPK23 and CPK6 were shown to activate SLAC1 in *Xenopus* oocytes and disruption of the corresponding genes in plants leads to a partial reduction of S-type anion current activation in guard cells (38-40). The closest homolog to CPK6, CPK5, is associated with reactive oxygen species signaling (42, 43). CPK5 also activates SLAC1 in oocytes (Figure 1-figure supplement 1A-B). We investigated S-type anion channel current activation in *cpk5/6/11/23* quadruple T-DNA insertion mutant guard cells. Either ABA application or high external Ca^{2+} shock renders wild type guard cells sensitive to physiological cytosolic free Ca^{2+} concentration ($[Ca^{2+}]_{cyt}$) increases (27-29, 44). Notably, even when previously exposed to ABA or high external Ca^{2+}, 2 µM $[Ca^{2+}]_{cyt}$ did not result in S-type anion current activation in *cpk5/6/11/23* quadruple mutant guard cells in contrast to WT (Col0) plants (Figure 1A-D) underlining the important role of these calcium sensing protein kinases in S-type anion channel activation.

The clade A protein phosphatase 2Cs (PP2Cs) play important roles as negative regulators of ABA signaling (45) and were shown to inhibit CPK-activation of SLAC1 in oocytes (38, 39). To determine whether these PP2Cs are involved in the ABA-triggered enhancement of the $[Ca^{2+}]_{cyt}$-sensitivity in guard cells, we performed whole-cell patch-

clamp analysis using a plant line carrying T-DNA insertion mutations in the key ABA signaling PP2Cs *ABI1*, *ABI2*, *HAB1*, and *PP2CA* (*abi1-2/abi2-2/hab1-1/pp2ca-1*). Remarkably, in *abi1-2/abi2-2/hab1-1/pp2ca-1* guard cells, strong Ca^{2+}-activated S-type anion currents were observed even without pre-exposure to ABA (Figure 2A-D; for 0.1 µM $[Ca^{2+}]_{cyt}$ see Figure 2-figure supplement 1A-B), providing genetic evidence that these PP2Cs are essential for the ABA-triggered Ca^{2+}-sensitivity priming in guard cells.

Based on these results we sought to determine the biochemical mechanisms mediating the role of these PP2Cs within the Ca^{2+}-sensitivity priming. The main SLAC1-activating protein kinase in the Ca^{2+}-independent pathway, OST1 (34), is directly inactivated by PP2Cs through de-phosphorylation of the activation loop (46, 47). We tested whether CPKs might be down-regulated by PP2Cs in a similar manner and whether *pp2c* quadruple mutant plants may also exhibit a constitutive OST1 activity. Our first approach to test whether CPK activity is regulated by ABA through PP2Cs was an in-gel kinase assay using protein extracts of *Arabidopsis* seedlings, which is routinely used to test ABA activation of OST1 (Figure 3A-B; for 0.4 µM Ca^{2+} see Figure 3-figure supplement 1A-B) (34) and also CPK activation by flg22 (42). A reaction buffer with 3 µM free Ca^{2+} led to strong Ca^{2+}-activated phosphorylation signals compared to resting Ca^{2+} at 150 nM (Figure 3A-B). To determine whether these Ca^{2+}-activated signals are CPK-derived we included two distinct quadruple mutants, *cpk5/6/11/23* and *cpk1/2/5/6*, in the in-gel kinase assays. Several Ca^{2+}-activated bands disappeared when extracts were tested from *cpk5/6/11/23* and *cpk1/2/5/6* plants, consistent with CPK kinase activities found at these molecular weights (42, 43) (Figure 3B, lanes 13-16). Exposing *Arabidopsis* seedlings to ABA led to OST1 activation (Figure 3A-B, lanes 1-2 and 9-10; "OST1" inset). However, CPK-derived band intensities did not change in the presence of ABA, indicating that CPK activities are not ABA-regulated (Figure 3B). These findings were also obtained at 0.4 µM free Ca^{2+} (Figure 3-figure supplement 1A-B). Moreover, in-gel CPK kinase activities were not altered with or without ABA using protein extracts of *abi1-2/abi2-2/hab1-1/pp2ca-1* quadruple mutant plants (Figure 3A-B, lanes 3-4 and 11-12; Figure 3-figure supplement 1A-B). Interestingly, the *pp2c* quadruple mutants did not enable constitutive OST1 activation *in vivo* (Figure 3A-B, lanes 3-4 and 11-12 and Figure 3-figure supplement 1A-B; see "OST1" inset). Furthermore, OST1-derived band intensities were

not changed in the *cpk5/6/11/23* and *cpk1/2/5/6* mutant plants showing that these *cpk* quadruple mutants retain ABA-activation of OST1 (Figure 3A-B, lanes 5-8 and 13-16; see "OST1" inset).

To test whether PP2Cs can directly down-regulate CPKs we next investigated whether the SLAC1-activating calcium-dependent protein kinase CPK6 (38), is negatively regulated by the PP2Cs ABI1 and PP2CA. In-gel kinase assays using recombinant proteins were pursued in which kinases and phosphatases are separated by size prior to substrate phosphorylation. CPK6, and as positive control OST1, were pre-incubated either alone or with ABI1 or PP2CA with and without ATP before being subjected to in-gel kinase assays. CPK6 trans-phosphorylation activities were not inhibited by pre-incubation with either ABI1 or PP2CA (Figure 3C, Lanes 2-3 and 5-6). In contrast, control OST1-derived substrate phosphorylation band intensities strongly decreased when ABI1 or PP2CA protein were present during the pre-incubation period (Figure 3D, Lanes 2-3 and 5-6). These results indicate that OST1 but not CPK6 activity is directly down-regulated by ABI1 and PP2CA. CPKs have been previously shown to interact with ABI1 (39). An electro-mobility shift can be observed for OST1 as well as for CPK6 (Figure 3C-D), which could be due to de-phosphorylation of CPK6 and OST1 by PP2Cs (Figure 3-figure supplement 2). However, de-phosphorylation by PP2Cs did not inhibit CPK6 activity (Figure 3C). An additional independent biochemical assay measuring ATP consumption also did not show down-regulation of CPK6 activity in the presence of ABI1 and PP2CA (Figure 3-figure supplement 3).

Our results suggest that PP2Cs neither down-regulate CPK activity directly *in vitro* (Figure 3C-D and Figure 3-figure supplement 3) nor in native plant protein extracts (Figure 3A-B). We next investigated the kinetics and specificity of PP2C down-regulation of SLAC1 activation by CPKs through de-phosphorylation of the SLAC1 channel, a mechanism reported for CPK-dependent transcription factor regulation (48) and consistent with previous findings (38). First, we determined whether SLAC1 interacts with the PP2C ABI1 *in planta* using bi-molecular fluorescence complementation (BiFC). We observed clear BIFC signals for full length SLAC1 co-expressed with CPK6 and ABI1 with comparable intensities (Figure 4A-C). Protein-protein interaction of SLAC1 with PP2CA

in BiFC experiments was reported earlier (36). As shown in Figure 4D-E, the ABI1 mediated de-phosphorylation of the N-terminus of SLAC1 (SLAC1-NT) previously phosphorylated by CPK6 (38) is very rapid as already 1 min after the addition of ABI1 a strong decrease of the phosphorylation signal was observed. This was also found when the phosphatase PP2CA was added instead of ABI1 (Figure 4D and F). To test whether this is a general phenomenon, we phosphorylated the SLAC1-NT with the SLAC1-activating and -phosphorylating kinases CPK21, CPK23, and OST1 (36, 37, 39) (Figure 4G-I and Figure 4-figure supplement 1, Lane 1) and analyzed whether ABI1 and PP2CA are able to remove phospho-groups added by these kinases. After inhibiting the kinase with Staurosporine, band intensities decreased only after addition of the PP2C protein phosphatases for all combinations (Figure 4G-I and Figure 4-figure supplement 1, lanes 5-6), showing that this rapid SLAC1 de-phosphorylation by PP2Cs is a general mechanism.

It has remained unclear whether the Ca^{2+}-independent and Ca^{2+}-dependent branches of ABA signaling are interdependent. In the *cpk5/6/11/23* quadruple mutant, ABA-activation of S-type anion currents in guard cells was strongly impaired (Figure 1A-D) providing evidence for interdependence. *ost1-2* knock out plants (Col0 ecotype) show intermediate S-type anion current activation by ABA (37). We disrupted the genes of 2 additional Ca^{2+}-independent SnRK kinases, SnRK2.2 and SnRK2.3, which can activate SLAC1 in oocytes (37). *snrk2.2/snrk2.3/ost1* triple mutants were strongly impaired in ABA- and notably also external Ca^{2+}-activation at 2 µM $[Ca^{2+}]_{cyt}$ (Figure 5A-D). These findings suggest an interdependence of the Ca^{2+}-dependent and -independent branches of the ABA signaling network. A putative mechanism for interdependence between Ca^{2+}-dependent and -independent ABA signaling could be direct cross-regulation of OST1 and CPKs. However, in yeast 2 hybrid assays no protein-protein interaction between CPK6 and OST1 could be detected and *in vitro* assays show no evidence for a direct cross-phosphorylation of OST1 and CPK6 (Figure 5-figure supplement 1-2). Also, in-gel protein kinase assays from *in vivo* protein extracts showed no change in ABA-activated OST1-derived band intensities in two separate CPK quadruple mutants under several ABA and Ca^{2+} conditions (Figure 3A-B and Figure 3-figure supplement 1). These independent

approaches provide no evidence for a direct cross-regulation of the Ca^{2+}-dependent and –independent protein kinases in the ABA signaling core.

Another non-mutually exclusive possible mechanism for the requirement of both SnRK and CPK kinases for ABA activation of SLAC1 could be that SLAC1 serves as coincidence detector through differential phosphorylation by protein kinases of the Ca^{2+}-dependent and -independent branches. SLAC1 S120A has been shown to be required for OST1, but not for CPK23 activation of SLAC1 (37, 39). A different site, serine 59, has been shown to be required for SLAC1 activation by CPK6 (38). Thus we investigated whether several CPKs can activate the SLAC1 S120A mutant in oocyte and whether the SLAC1 S59A mutant is activated by OST1 and other CPKs in oocytes. CPK5, CPK6, and CPK23 activation of SLAC1 S120A was similar to WT SLAC1 activation (Figure 6A-F and Figure 6-figure supplement 1A-B). In contrast, SLAC1 S59A activation by these CPKs was strongly impaired (Figure 6A-F and Figure 6-figure supplement 1A-B). Interestingly however, OST1-mediated activation of SLAC1 S59A was comparable to WT SLAC1 (Figure 6D-F). These results suggest that S59 is required for activation by protein kinases of the Ca^{2+}-dependent CPK branch, while S120 represents a crucial amino acid for the Ca^{2+}-independent branch of the ABA signaling core. Co-expression of low CPK6 and OST1 levels with SLAC1 show a clear synergistic SLAC1 activation in oocytes Figure 6G-J). Together, these findings indicate a synergistic relationship of the Ca^{2+}-dependent and –independent branches in the guard cell signaling core.

Discussion

Dissection of Ca^{2+}-signaling specificity mechanisms can be advanced through characterization of the combined cellular, genetic, and biochemical mechanisms in a single cell type. Biochemical and cellular mechanisms that function in Ca^{2+} specificity have been characterized, e.g. (7-13). Ca^{2+} is a major hub within the signaling network of plant guard cells (2, 17-20) but the mechanisms mediating specificity have remained unknown. In guard cells, the stomatal closing stimuli ABA and CO_2 enhance (prime) $[Ca^{2+}]_{cyt}$-sensitivity (26-30).

194 Here we report genetic, cellular and biochemical mechanisms that underpin ABA-
195 induced Ca^{2+}-sensitivity priming. In the absence of the specific signal, ABA, Ca^{2+}-
196 responsiveness is inhibited by PP2Cs, thereby preventing responses to unrelated Ca^{2+}
197 elevations (Figure 7) (21-26, 49, 50). As PP2Cs inhibit OST1 and also down-regulate
198 SLAC1 directly, this network not only enables stimulus specific activation of SLAC1 via
199 phosphorylation, but also provides a tight off switch via PP2C-catalyzed de-
200 phosphorylation of SLAC1 (Figure 7). This mechanism could also prevent SLAC1
201 activation by CPK23 which exhibits a moderate Ca^{2+} sensitivity (39). Moreover, as PP2Cs
202 control Ca^{2+} signaling specificity downstream of the Ca^{2+} sensor (Figure 7), CPKs could
203 still be capable of fulfilling other signaling roles (42, 43, 51, 52).

204 The presented data provide evidence for interdependence of the Ca^{2+}-dependent
205 and –independent branches to trigger the downstream response within in this signaling
206 network further tightening the regulation of stomatal closure (Figure 7). Oocytes may
207 permit more promiscuous SLAC1 phosphorylation due to kinase abundance. For
208 example, to strongly activate SLAC1 with OST1, the interaction has to be forced by fusing
209 the proteins to split YFP moieties (39). For the SLAC1 channel to serve as a coincidence
210 detector *in planta*, phosphorylation of both S59 (38) and S120 (37, 53) would produce a
211 synergistic activation of the channel (Figure 6G-I). Further research is needed to elucidate
212 details of the mechanisms of this synergistic regulation. Increased SLAC1 activation by
213 co-expression of (non-split YFP moieties) OST1 and CPK6 provides evidence for the
214 hypothesis of a synergistic SLAC1 activation by the Ca^{2+}-dependent and Ca^{2+}-
215 independent pathways (Figure 6G-I).

216 The control of ABA-triggered stomatal closure by parallel interdependent Ca^{2+}-
217 dependent and –independent mechanisms can contribute to the robustness of this
218 essential signaling network (17). Genome analyses have revealed the existence of more
219 than 200 genes encoding for proteins containing Ca^{2+}-binding EF-hands (15) with
220 overlapping expression of many genes in the same cell type, including guard cells (16).
221 The mechanism described here could represent a more general principle present in plants
222 and possibly other eukaryotes contributing to Ca^{2+}-specificity within cellular signaling

while also maintaining the availability of Ca^{2+}-sensors for distinct Ca^{2+}-dependent signaling outputs.

Material and Methods

Mutant plant lines

All *Arabidopsis* thaliana plants used in this study are in the Col0 ecotype. *cpk5/6/11/23* quadruple T-DNA insertion mutant plants were established by crossing *cpk5/6/11* (sail_657C06/salk_025460/salk_054495) kindly provided by Jen Sheen (Harvard Medical School) (42) with *cpk23-1* (salk_007958) obtained from ABRC (39, 54). Dr. Ping He (Texas A&M University) shared *cpk1/2/5/6* (salk_096452/salk_059237/sail_657C06/salk_025460) mutant seeds (51). The PP2C quadruple knock-out plants (*abi1-2/abi2-2/hab1-1/pp2ca-1*; salk_72009/salk_15166/salk_2104/salk_028132) and *snrk2.2/2.3/ost1* (GABI-Kat_807G04/salk_107315/salk_008068) were kindly provided by Dr. Pedro L. Rodriguez (University of Valencia) (55). A second independent *snrk2.2/2.3/ost1* (GABI-Kat_807G04/salk_107315/salk_008068) line was established by crossing *snrk2.2/2.3* with *ost1-3* supplied by Drs. Jian-Kang Zhu (Shanghai Center for Plant Stress Biology) and Rainer Waadt (University of California, San Diego), respectively.

Patch Clamp analyses

Arabidopsis plants were grown on soil in the growth chamber at 21°C under a 16-h-light/8-h-dark photoperiod with a photon flux density of 80 µmol/(m^2*s). The plants were watered from bottom trays with deionized water once or twice per week and sprayed with deionized water every day. The growth chamber humidity was 50 to 70%.

Arabidopsis guard cell protoplasts were isolated enzymatically as previously described (56). One or two rosette leaves of 4- to 5-week-old plants were blended in a blender with deionized water at room temperature for approximately 30 sec. For isolation of guard cell protoplasts from *snrk2.2/snrk2.3/ost1* triple mutants, four or five rosette leaves were used. Epidermal tissues were collected using a 100-µm nylon mesh and rinsed well with deionized water. The epidermal tissues were then incubated in 10 ml of enzyme solution containing 1% (w/v) Cellulase R-10 (Yakult, Japan), 0.5% (w/v) Macerozyme R-10 (Yakult, Japan), 0.1 mM KCl, 0.1 mM $CaCl_2$, 500 mM D-mannitol, 0.5% (w/v) BSA, 0.1% (w/v) kanamycin sulfate, and 10 mM ascorbic acid for 16 h at 25°C on a circular shaker at 40 rpm. Guard cell protoplasts were then collected by filtering through a 20-µm nylon mesh. Subsequently, the protoplasts were washed twice with washing solution containing 0.1 mM KCl, 0.1 mM $CaCl_2$, and 500 mM D-sorbitol (pH 5.6 with KOH)

by centrifugation for 10 min at 200 x g. The guard cell protoplast suspension was kept on ice before use.

To investigate ABA activation of S-type anion channels, the guard cell protoplast suspension was pre-incubated with 10 µM (Figure 1A-C) or 50 µM (Figures 2A-D and 5C-D as well as Figure 2-figure supplement 1A-B) +/- ABA (Sigma) for 30 min. S-type anion channel currents in guard cell protoplasts were recorded by the whole-cell patch-clamp technique as previously described (28, 32, 56). The pipette solution contained 150 mM CsCl, 2 mM $MgCl_2$, 5 mM Mg-ATP, 6.7 mM EGTA, and 10 mM Hepes-Tris (pH 7.1). To obtain a $[Ca^{2+}]_{cyt}$ of 2 µM and 110 nM, 5.86 mM and 1.79 mM of $CaCl_2$ were added to the pipette solution, respectively. Osmolality of the pipette solution was adjusted to 500 mmol/l using D-sorbitol. The bath solution contained 30 mM CsCl, 2 mM $MgCl_2$, 1 mM $CaCl_2$, and 10 mM MES-Tris (pH5.6). Osmolality of the bath solution was adjusted to 485 mmol/l using D-sorbitol. To investigate external Ca^{2+}-activation of S-type anion channels, guard cell protoplasts were pre-incubated with the bath solution containing 40 mM $CaCl_2$, instead of 1 mM $CaCl_2$ for 30 min. Whole-cell currents were recorded 3 to 5 min after achieving the whole-cell configuration. The seal resistance was no less than 10 GΩ. The voltage was decreased from +35 mV to –145 mV with 30 mV decrements and the holding potential was +30 mV.

Recombinant protein isolation

Over-expression and purification of recombinant proteins were performed as described in (38) with minor adjustments: For the isolation of the PP2C proteins ABI1, ABI2, and PP2C additionally 5 mM $MgCl_2$ and 5 % Glycerol were added to the buffer in which the bacterial pellet was resuspended (buffer W in IBA manual). Also, all proteins except SLAC1-NT were eluted in elution buffer supplemented with 20% Glycerol instead of 10% and stored at -80 °C instead of -20 °C. To assess protein concentrations, several volumes of the eluates were loaded on a gel together with several defined bovine serum albumin (BSA) protein amounts. After separating the proteins by SDS-PAGE (57), the proteins were stained with coomassie brilliant blue R-250, dried between two sheets of cellophane, and then scanned. BSA and recombinant protein band intensities were measured using Fiji (58). After subtracting the background signal, BSA band signal intensities were used to plot a standard curve. Concentrations of isolated recombinant proteins were then calculated based on the equation resulting from the linear regression of the BSA standard curve.

Whole plant protein extraction

Seeds were sterilized by incubation in sterilization medium (70% Ethanol and 0.04% (w/v) SDS) for 15 min followed by 3 washes in 100% Ethanol. After drying, the seeds for all genotypes were plated on one plate with ½ Murashige and Skoog Basal Medium (MS; Sigma-Aldrich) and 0.8% phyto-agar. The plate was then stored at 4°C for

>3 days and subsequently transferred to a growth cabinet (16/8 light/dark and 22°C). After a growth phase of 10-14 days >10 seedlings per genotype were floated on liquid ½ MS and equilibrated for 60-90 min in the growth cabinet. Either +/- ABA (Sigma) to a final concentration of 50 µM (indicated by + in the figure) or the same volume of solvent control (Ethanol; indicated by – in the figure) was added to the floating seedlings. After 30 min the seedlings were removed from the ½ MS and flash frozen in liquid nitrogen. Plant tissue was disrupted by shaking the frozen seedlings together with steel balls in a shaker (Retsch) for 3 times 30 seconds at 30 Hz in pre-cooled mountings. Subsequently, extraction buffer (100 mM HEPES-NaOH pH 7.5, 5 mM EDTA, 5 mM EGTA, 0.5% (v/v) Triton X-100, 150 mM NaCl, 0.5 mM DTT, 10mM NaF, 0.5% (v/v) protease inhibitor (Sigma-Aldrich), 0.5% (v/v) phosphatase inhibitor 2 (Sigma-Aldrich), 0.5% (v/v) phosphatase inhibitor 3 (Sigma-Aldrich), 5 mM Na_3VO_4, and 5 mM β-Glycerophosphate disodium salt hydrate) was added. The samples were then treated in a sonication water bath (Fisher Scientific) with ice added to the water for 30 seconds. Cell debris was removed via centrifugation at 20.000 x g and 4°C for 40 min. Protein concentrations of the supernatants were measured using the BCA Protein Assay Kit (Pierce). 20 µg of total protein for each genotype and treatment were subjected to SDS-PAGE (57) under denaturing conditions (see in gel kinase assay).

***In vitro* kinase assays:**

The reaction buffer consisted of 100 mM HEPES-NaOH pH 7.5, 10 mM $MgCl_2$, 2 mM DTT, 1 mM EGTA, and $CaCl_2$ was added to get a final concentration of 2.5 µM free Ca^{2+} (calculated with http://www.stanford.edu/~cpatton/webmaxc/webmaxcE.htm). Note that the pH of the reaction buffer dropped to pH 7.3 after adding all components and free Ca^{2+} calculations were performed accordingly. The flow charts in the respective figures indicate the components which were added subsequently in sequence (from top to bottom) and the respective incubation times. For the experiments shown in Figure 4D-I and Figure 4-figure supplement 1, SLAC1-NT (1.5 ug) was mixed together with 200 nM of the protein kinases CPK6, CPK23, OST1, and CPK21 in reaction buffer. Staurosporine was added to a final concentration of 100 µM and the final concentration of the PP2Cs ABI1 and PP2CA was 600 nM. For the reactions shown in Figure 3-figure supplement 2 0.5 µg of CPK6 and 1 µg of the PP2Cs ABI1, ABI2, and PP2CA were used. The addition of EGTA for reactions shown in Extended Data Fig. 2c lanes 2-4 resulted in a free Ca^{2+} concentration < 10 nM (calculated with http://www.stanford.edu/~cpatton/webmaxc/webmaxcE.htm). In the reactions depictured in Figure 4-figure supplement 1 250 nM of CPK6 and 750 nM of OST1 were mixed together with 1.2 µg of CPK6 D209A, OST1 D140A, and SLAC1-NT in reaction buffer. To start all *in vitro* kinase reactions, 5 µCi of [γ-^{32}P]-ATP (Perkin-Elmer) was added and the reactions were incubated at room temperature (RT) for 10 min. The final volumes were 20 µl and the reactions were stopped by the addition of 4 µl of 6x loading dye with

subsequent incubation at 95°C for 5 min. The proteins were then separated by SDS polyacrylamide gel electrophoresis (SDS-PAGE, (57)) in 4-20% acryl amide gradient gels (Biorad). After, the proteins were stained with coomassie brilliant blue R-250 (Sigma). To visualize the ^{32}P-derived radioactive signals, gels were exposed to a storage phosphor screen (Molecular Dynamics; Figure 4D-I, Figure 4-figure supplement 1, and Figure 5-figure supplement 1) or HyBlot CL autoradiography films (Denville Scientific; Figure 3-figure supplement 2). The phosphor storage screen was read out using a Typhoon scanner (Amersham Bioscience).

To compare CPK6 activities by measuring ATP consumption (Figure 3-figure supplement 3) with or without the PP2Cs ABI1 and PP2CA, 0.5 µM of the kinase was incubated at room temperature for 7.5 min either alone or with 1 µM of PP2C protein in the above mentioned reaction buffer supplemented with 10 µM ATP and ~ 150 µM Histone III-S (Sigma). The reactions were stopped by the addition of Staurosporine. Residual ATP levels were quantified using the KinaseGlo kit (Promega) according to the manufacturer's instructions resulting in luminescence signals measured in a plate reader (Berthold Mithras LB 940) (59). ATP consumption was calculated by first assessing the maximum range (ΔR_{max}) of luminescence by subtracting the signal intensity of the background (no ATP added; R_B) from the maximum signal (no kinase added; R_{max}). To calculate the ATP consumption, signal intensities derived from the residual ATP in the reactions (R_x) were subtracted from the maximum signal (R_{max}) and then related to the maximum range (ΔR_{max}) and plotted in per cent ($[(R_{max}-R_x)/\Delta R_{max}]*100$).

In gel kinase assays

For in gel kinase assays using recombinant proteins shown in Figure 3C-D, 500 ng of OST1 and CPK6 kinase and the PP2Cs ABI1 and PP2CA in a 1:3 molar ration were mixed in reaction buffer with 2.5 µM free Ca^{2+} (for buffer composition see *in vitro* kinase assay section). The reactions labelled with "(ATP)" were additionally supplemented with 100 µM ATP. All samples were incubated at RT for 20 min and stopped by adding SDS loading dye and heating at 95°C for 5 min.

These samples as well as the samples described in the "whole plant protein extraction" section were subjected to SDS-PAGE (57). The 10% SDS acryl amide resolving gels were supplemented with 0.25-0.5 mg/ml Histone III-S (Sigma-Aldrich). After electrophoresis, the gel was washed three times with washing buffer (25 mM Tris–HCl pH 8.0, 0.5 mM DTT, 0.1 mM Na_3VO_4, 5 mM NaF, 0.5 mg/ml BSA, and 0.1% (v/v) Triton X-100) for 30 min each at room temperature, followed by two washes with renaturation buffer (25 mM Tris–HCl pH 8.0, 1 mM DTT, 0.1 mM Na_3VO_4, and 5 mM NaF) for 30 min each at room temperature and one wash at 4°C overnight. Then, the gels were equilibrated with reaction buffer (see *in vitro* kinase assay) for 30-45 min at room temperature and incubated in 20 ml of reaction buffer supplemented with 50 µCi [γ-^{32}P]-

ATP (Perkin-Elmer). The reaction times were: Figure 3A-B: 90 minutes; Figure 3C: 60 min; Figure 3D: 120 min. To stop the reactions and to remove background signals the gels were subsequently extensively washed with a solution containing 5% (v/v) trichloroacetic acid and 1% (v/v) phosphoric acid for at least 6 times for 15 min each. The gels were then stained with coomassie brilliant blue R-250, dried on Whatman 3MM paper, and exposed to a storage phosphor screen (Molecular Dynamics). The storage phosphor screen was scanned with a Typhoon reader (Amersham Bioscience). For the in gel kinase assays shown in Figure 3A-B and Figure 3-figure supplement 1 all steps except the equilibration in reaction buffer and the reactions were carried out together and exactly the same way which allows the autoradiographs to be compared. The image files given by the Typhoon reader software are automatically adjusted to best display the bands with the highest intensity. Ca^{2+}-activated kinase signals are stronger than OST1-derived bands which renders OST1 bands hardly visible by the Typhoon reader software. To better visualize OST1 activity, the signal intensity of the ~41 kDa regions (blue box) in Figure 3A-B and Figure 3-figure supplement 1 were adjusted as described in the following: The output files (.gel) of the Typhoon scanner software was opened using Fiji (58) and in order to enhance the visibility of OST1-derived bands the maximum signal was adjusted for the entire image including controls in accordance with journal policies (http://jcb.rupress.org/content/166/1/11.full). Subsequently, the regions around 41 kDa were saved as .jpg file which was used for the preparation of the figures. The parallel adjustment of the whole image showing both gels which are depicted in either Figure 3A-B or Figure 3-figure supplement 1 allows the comparisons of band intensities within each figure. Additionally, in Figure 3-figure supplement 1 several lanes of the same gel have been cut out indicated by the black line as explained in http://jcb.rupress.org/content/166/1/11.full.

Quantitative bimolecular fluorescence complementation

Quantitative bimolecular fluorescence complementation (BiFC) experiments were carried out as described in (60) with changes explained in the following: BIFC vectors were altered to be USER cloning (61) compatible (indicated by the “u” addition to the vector name) as described in (62). Subsequently, SLAC1, CPK6, and ABI1 cDNAs were amplified using the PfuX7 polymerase (63) and subsequently USER-cloned into pSPYCE(MR)u, pSPYNE173u, and pSPYNE(R)173u, respectively. Microscopy was performed using the following setup: Nikon Eclipse TE2000-U microscope with Nikon Plan 20x/0.40 ∞/0.17 WD; 1.3 and Plan Apo 60x/1.20 WI ∞/0.15-0.18 WD; 0.22 objectives. Attached were a CL-2000 diode pumped crystal laser (LaserPhysics Inc.), and a LS 300 Kr/Ar laser (Dynamic Laser), a Photometrics CascadeII 512 camera, a QLC-100 spinning disc (VisiTech international), and a MFC2000 z-motor (Applied Scientific Instruments). The software used to acquire the pictures was Metamorph (version 7.7.7.0; Molecular Devices). Figure 4B images depict maximum projections of z-stacks.

Electrophysiological measurements in *Xenopus* laevis oocytes

Two electrode voltage clamp measurements in *Xenopus leavis* oocytes were carried out as described previously (38) with adjustments listed in the following. The recording solution contained 10 mM MES/Tris (pH 5.6), 1 mM $CaCl_2$, 1 mM $MgCl_2$, 2 mM KCl, 24 mM NaCl, and 70 mM Na-gluconate. Osmolality was adjusted to 220 mM using D-sorbitol. Oocytes were held at a holding potential of 0mV, and subjected to voltage pulse from +40 mV to -140 mV or -120 mV in -20 mV decrements. For the experiments shown in Figure 6G-J the amounts of injected cRNA were 5 ng of SLAC1, 0.5 ng of CPK6, and 7.5 ng of OST1.

Yest-2-Hybrid protein-protein interaction assay

The vectors pGBT9.BS (for fusion to the Gal4-binding domain; BD) and pGAD.GH (results in activation domain fusions; AD) (64) were altered (62) to be compatible to the USER cloning method (61). All cDNA were amplified using the PfuX7 polymerase (63) and cloned into the prepared vectors. For ABI1 a truncated version (amino acids 125 to 434) was used to avoid an auto-activation similar to HAB1 (65). To disrupt the myrostilation site in CPK6 (66), glycine 2 was mutated to alanine. The prepared vectors were transformed into the PJ69-4A yeast strain (67) employing the polyethylene glycol/lithium acetate method (68) and subsequently selected for successful transformation by incubating transformations for 1-2 days at 28°C on CSM-agar (BD Biosciences) not containing tryptophane and leucine (CSM-Leu-Trp). Single growing colonies of yeast containing both plasmids were re-streaked on new CSM-Leu-Trp plates and grown for additional 1-2 days. Subsequently, serial dilutions from OD_{A600} 1 to 0.0001 (as indicated by the arrow in the figure) in 2% Glucose were spotted on CSM-Leu-Trp and on CSM medium lacking leucine, tryptophane and histidine (CSM-Leu-Trp-His) supplemented with 1 mM 3-amino-1,2,4-triazole (3-AT) and grown for 3 days at 28°C. Growth indicates a physical protein-protein interaction between the two proteins tested.

Acknowledgements

We would like to thank Drs. Jen Sheen, Pedro L. Rodriguez, and Ping He for supplying mutant seeds, Dr. Stephan Clemens for vector construction, and members of the Schroeder laboratory, in particular Rainer Waadt and Felix Hauser, for comments and discussions. This work has been supported by the National Institute of Health (GM060396-P42ES010337), National Science Foundation (MCB0918220), and protein-protein interaction studies were supported by the Division of Chemical, Geo, and Biosciences, Office of Basic Energy Sciences, US Department of Energy (DE-FG02-03ER15449) to J.I.S, a German academic exchange service PhD fellowship to B.B., and a Japanese Society for the Promotion of Science (JSPS) Postdoctoral Fellowship for Research Abroad to S.M.

Figure Legends

Figure 1: CPK quadruple loss of function mutants are ABA and Ca^{2+} insensitive.

Intracellular Ca^{2+}-activation of S-type anion channels enabled by pre-exposure to ABA (A-C) or high external Ca^{2+} (A,B, and D) is strongly impaired in *cpk5/6/11/23* guard cells at 2 µM $[Ca^{2+}]_{cyt}$. Representative whole cell currents (A-B), average steady-state current-voltage relationships +/- SEM, and guard cell numbers are shown (C-D).

Figure 1–figure supplement 1: CPK5 activates SLAC1 in Xenopus oocytes.

(A-B) Whole cell currents were measured in *Xenopus* oocytes expressing SLAC1 together with CPK5 and, as a control, CPK6. Large Cl^- currents demonstrate that CPK5 is capable of activating SLAC1. Representative current traces (A), average steady-state current-voltage relationships (+/- SEM), and numbers of individual cells are shown (B).

Figure 2: In PP2C quadruple mutant plants, Ca^{2+} activation of S-type anion currents is constitutively primed.

2 µM $[Ca^{2+}]_{cyt}$ activates S-type anion currents in WT if the guard cells were pre-exposed to ABA (A, C). In PP2C quadruple mutant guard cells ABA pre-exposure is not required for 2 µM $[Ca^{2+}]_{cyt}$-activation of S-type anion currents (B, D). Average steady-state current-voltage relationships +/- SEM, guard cell numbers (C-D), and representative whole cell currents (A-B) are presented.

Figure 2–figure supplement 1: ABA activation of S-type anion current in PP2C quadruple mutant guard cells requires elevated $[Ca^{2+}]_{cyt}$.

(A-B) ABA application in WT and *abi1-2/abi2-2/hab1-1/pp2ca-1* guard cells with $[Ca^{2+}]_{cyt}$ buffered to a resting level of 0.1 µM does not result in large S-type anion current

activation. Typical current traces (A), averaged steady-state currents in response to applied voltages (+/- SEM), and numbers of individual measured cells are shown (B).

Figure 3: CPK activity is not changed by ABA or constitutively or hyper-activated in *pp2c* quadruple mutants.

(A-B) In gel kinase assays with Histone as substrate for whole plant protein extracts show (B) 3 µM Ca^{2+}-activated trans-phosphorylation kinase activities independent of application of 50 µM ABA (lanes 9 and 10). In contrast, ABA activation of OST1 is clearly visible (lanes 1-2 and 9-10 at ~ 41 kDa lower; "OST1" inset shows the same signal optimized autoradiography at the ~ 41 kDa region; See Methods). Disrupting 4 PP2C genes (*ABI1*, *ABI2*, *HAB1*, and *PP2CA*) does not result in constitutive Ca^{2+}-activated and OST1 kinase activities (lanes 3-4 and 11-12). In gel kinase activities of two independent CPK quadruple mutant lines indicate that the Ca^{2+}-activated kinase signals are CPK-derived (compare lanes 9-10 with 13-16 in B; predicted MWs for CPK1, CPK2, CPK5, CPK6, CPK11, and CPK23 are 68.3 kDa, 72.3 kDa, 62.1 kDa, 61.1 kDa, 55.9 kDa, 58.7 kDa, respectively). (C-D) In gel kinase assays with recombinant proteins show that incubation of the protein kinases with the PP2Cs ABI1 and PP2CA does (C) not change CPK6 activity while (D) OST1 activity is strongly down-regulated by PP2Cs. Each experiment has been repeated at least 3 times with similar results.

Figure 3–figure supplement 1: Kinase activities are not altered by ABA-application at 150 nM and 400 nM free Ca^{2+}.

(A-B) Whole plant protein extracts were analyzed in in gel kinase assays with the free Ca^{2+} concentration buffered to either 150 nM or 400 nM. No differences in the band pattern could be found between these different free Ca^{2+} concentrations (A-B). The presence of 400 nM free Ca^{2+} does not change ABA activation of OST1 (lower inset "OST1" in A and B) in WT, *abi1-2/abi2-2/hab1-1/pp2ca-1* or *cpk5/6/11/23* plants. PP2Cs have been shown to be involved in $[Ca^{2+}]_{cyt}$ regulation (69).

Figure 3–figure supplement 2: CPK6 is de-phosphorylated by the PP2Cs ABI1, ABI2, and PP2CA.

In *in vitro* kinase assays, recombinant CPK6 was incubated in the presence of 5 µM free Ca^{2+} which results in auto-phosphorylation signals (Lanes 1 and 5). After the initial auto-phosphorylation period the kinase inhibitor Staurosporine (Stau.) and the PP2Cs ABI1, ABI2, and PP2CA were added to the reactions (Lanes 2-4 and 6-8). For the samples displayed in Lanes 2-4, the Ca^{2+}-chelator EGTA, which buffers free Ca^{2+} concentrations to <10 nM, was added together with Staurosporine and the indicated PP2Cs. Addition of Staurosporine and the PP2Cs ABI1, ABI2, and PP2CA resulted in decreased auto-phosphorylation signals showing that PP2Cs de-phosphorylate CPK6 (Lanes 2-4 and 6-8).

Figure 3–figure supplement 3: CPK6 kinase activity is not inhibited in the presence of ABI1 or PP2CA.

In vitro kinase assays measuring the kinase activity via ATP consumption show that Staurosporine but not ABI1 or PP2CA inhibited CPK6 kinase activity. The increased ATP-consumption signal in the presence of ABI1 and PP2CA can be explained by higher ATP consumption triggered by kinase auto-phosphorylation of residues removed by the PP2C protein phosphatases. Data shown represent the mean of 3 experiments +/- SD.

Figure 4: PP2Cs interact and directly and rapidly de-phosphorylate the N-terminus of SLAC1 when previously phosphorylated by several SLAC1-activating CPK and OST1 protein kinases.

(A-C) Bi-molecular fluorescence complementation (BiFC) experiments in *N. benthamiana* leaves show YFP-derived fluorescence signals of SLAC1-YC co-expressed with CPK6-YN and YN-ABI1 of comparable intensity. Data shown in (C) represent the average fluorescence intensity of randomly picked leaf areas (n=9; +/- SEM). (D-F) CPK6 phosphorylated SLAC1-NT is rapidly de-phosphorylated by ABI1 and PP2CA. SLAC1-NT phosphorylation by CPK6 (E-F, lane 1) is strongly inhibited if the PP2C protein phosphatase was added before starting the reaction (E-F, lane 2), but remains stable after addition of elution buffer (Elu.) and kinase inhibitor Staurosporine (Stau.) with subsequent 10 min incubation (E-F, lane 3). If (E) ABI1 or (F) PP2CA together with Staurosporine are added after the initial 10 min CPK6 mediated phosphorylation period, the SLAC1-NT phosphorylation signal rapidly decreases within 1 min (E-F, lanes 4-7). Staurosporine pre-exposure control inhibits SLAC1-NT phosphorylation by CPK6 (E-F, lane 8). (G-I) PP2Cs de-phosphorylate the SLAC1-NT which was phosphorylated by major SLAC1-activating kinases CPK23 and OST1. The N-terminus of SLAC1 is phosphorylated by CPK23 (H, lane 1) and OST1 (I, lane 1) which is inhibited when the PP2Cs ABI1 and PP2CA are added before starting the reactions (H-I, lanes 2-3). When adding Staurosporine and elution buffer after the initial phosphorylation period and incubating for 10 min the signal does not change (H-I, lane 4). Addition of ABI1 or PP2CA after supplementing the reaction with Staurosporine leads to rapid (10 min) de-phosphorylation of the SLAC1-NT previously phosphorylated by the above mentioned kinases (H-I, lanes 5-6).

Figure 4–figure supplement 1: When previously phosphorylated by CPK21, the SLAC1-NT is de-phosphorylated by the PP2Cs ABI1 and PP2CA.

Recombinant SLAC1-NT phosphorylation by CPK21 (Lane 1) is inhibited if the protein phosphatases ABI1 and PP2CA are added before starting the reaction (Lanes 2-3). The phosphorylated SLAC1-NT derived signal is rapidly and strongly decreased if the PP2Cs ABI1 and PP2CA (Lanes 4-7) are added after the addition of Staurosporine.

Figure 5: Both, ABA- and high external Ca2+-activation of S-type anion currents at elevated $[Ca^{2+}]_{cyt}$ are abrogated in *snrk2.2/2.3/ost1* triple mutant guard cells.

In whole cell patch clamp experiments, *snrk2.2/2.3/ost1* triple mutant guard cells disrupt Ca^{2+}-activation of S-type anion currents even if pre-incubated with (A-B) high external Ca^{2+} shock (44) or (C-D) ABA. Typical current responses (A and C), average steady-state current-voltage relationships +/- SEM, and the number of measured cells are presented (B and D). In (B) data for *snrk2.2/2.3/ost1* triple mutants with and without ABA overlap with WT controls.

Figure 5–figure supplement 1: CPK6 and OST1 do not trans-phosphorylate one another *in vitro*.

We analyzed whether CPK6 and OST1 trans-phosphorylated one another by using the respective active and inactive mutant kinase versions (OST1 D140A and CPK6 D209A). This approach allowed us to distinguish between auto- and trans-phosphorylation derived ^{32}P-signals. Kinase inactive versions of OST1 (D140A (37)) and CPK6 (D209A (38)) are not phosphorylated by active CPK6 and OST1, respectively (lanes 1 and 3). When OST1 D140A and CPK6 D209A were incubated alone no signal can be seen (lanes 2 and 4). Both, OST1 and CPK6 phosphorylated the SLAC1-NT which shows that the kinase proteins used exhibit trans-phosphorylation activities (lanes 5-6). The auto-phosphorylation activities of CPK6 (lanes 1 and 5) and OST1 (lanes 3 and 6) can be seen.

Figure 5–figure supplement 2: In yeast-2hybrid assays, OST1 interacts with ABI1 but not with CPK6

In yeast-2-hybrid assays, OST1 interacts with ABI1 as indicated by yeast growth on CSM-Leu-Trp-His (right panel). No growth can be observed when OST1 was co-transformed with CPK6 under identical conditions, indicating no physical protein-protein interaction of OST1 and CPK6 in yeast. Empty: Control experiments with empty vectors.

Figure 6: Ca^{2+}-dependent protein kinase and OST1 protein kinase activation of SLAC1 requires serine 59 or serine 120, respectively. SLAC1 is synergistically activated by CPKs and OST1.

SLAC1 activation by CPK6 in *Xenopus* oocytes (A and C) is abolished when serine 59 is mutated to alanine (S59A) but (B-C) is comparable to wild type SLAC1 activation for the SLAC1 S120A mutated version. (D-F) OST1 activation of SLAC1 (E-F) is abolished in the SLAC1 S120A mutant, while (D and F) the SLAC1 S59A activation by OST1 is similar to the wild type. (G-J) If SLAC1 (5 ng cRNA) is expressed alone or with non-BIFC OST1 (7.5 ng), no anion currents can be detected (I-J). If CPK6 (0.5 ng) is co-expressed, SLAC1-mediated currents can be seen (G, I and J) which are synergistically enhanced when OST1 (7.5 ng) is added (H-J). Due to overlapping data of “SLAC1” and “SLAC1 + OST1” alternating data points are shown in (I). Typical current responses (A-B, D-E and

G-H), average steady-state current-voltage relationships +/- SEM, and the number of measured cells are presented (C, F, and I). Steady-state current responses at -140 mV are plotted in g (*** indicates p=0.005; unpaired t-test with Welch's correction).

Figure 6–figure supplement 1: SLAC1 serine 59 but not serine 120 is required for CPK5 or CPK23 activation.

SLAC1 activation by CPK5 (A) and CPK23 (B) is comparable to WT when serine 120 is substituted by alanine (S120A) while the CPK5 and CPK23 activation of SLAC1 S59A is completely impaired. Representative current traces (A), average steady-state current-voltage relationships (+/- SEM), and numbers of individual measured cells are depictured (B).

Figure 7: Schematic model for Ca^{2+}-specificity mechanism within ABA-dependent SLAC1 activation in guard cells.

Without ABA, spontaneous or un-specifically induced Ca^{2+} transients (26, 28) do not lead to SLAC1 activation as PP2C phosphatases directly negatively regulate SLAC1 activation (left panel). In the presence of ABA this SLAC1 inhibition is released, OST1 and CPKs phosphorylate, and thereby activate the channel (right panel). ABA also causes $[Ca^{2+}]_{cyt}$ elevation via PP2C inhibition (70, 71). Data indicate a cross-talk between Ca^{2+}-dependent and -independent ABA-activation of SLAC1 which could be mediated through synergistic target coincidence detection activity via differential SLAC1 phosphorylation by OST1 and CPKs (right panel).

References

1. Berridge MJ, Bootman MD, Roderick HL. 2003. Calcium signalling: Dynamics, homeostasis and remodelling. *Nat Rev Mol Cell Biol* **4**:517-529. doi:10.1038/nrm1155.
2. Hetherington AM, Woodward FI. 2003. The role of stomata in sensing and driving environmental change. *Nature* **424**:901-908. doi:10.1038/nature01843.
3. Webb AAR. 2013. Calcium Signaling. *Plant Physiol* **163**:457-458. doi:10.1104/pp.113.900472.
4. Clapham DE. 2007. Calcium Signaling. *Cell* **131**:1047-1058. doi:10.1016/j.cell.2007.11.028.
5. Charpentier M, Oldroyd GED. 2013. Nuclear Calcium Signaling in Plants. *Plant Physiol* **163**:496-503. doi:10.1104/pp.113.220863.
6. McAinsh MR, Pittman JK. 2009. Shaping the calcium signature. *New Phytol* **181**:275-294. doi:10.1111/j.1469-8137.2008.02682.x.
7. Dolmetsch RE, Pajvani U, Fife K, Spotts JM, Greenberg ME. 2001. Signaling to the Nucleus by an L-type Calcium Channel-Calmodulin Complex Through the MAP Kinase Pathway. *Science* **294**:333-339. doi:10.1126/science.1063395.
8. Dolmetsch RE, Xu KL, Lewis RS. 1998. Calcium oscillations increase the efficiency and specificity of gene expression. *Nature* **392**:933-936. doi:10.1038/31960.
9. Oancea E, Meyer T. 1998. Protein Kinase C as a Molecular Machine for Decoding Calcium and Diacylglycerol Signals. *Cell* **95**:307-318. doi:10.1016/S0092-8674(00)81763-8.
10. De Koninck P, Schulman H. 1998. Sensitivity of CaM Kinase II to the Frequency of Ca^{2+} Oscillations. *Science* **279**:227-230. doi:10.1126/science.279.5348.227.
11. Chao Luke H, Stratton M, Lee I-H, Rosenberg Oren S, Levitz J, Mandell Daniel J, Kortemme T, Groves Jay T, Schulman H, Kuriyan J. 2011. A Mechanism for Tunable Autoinhibition in the Structure of a Human Ca^{2+}/Calmodulin- Dependent Kinase II Holoenzyme. *Cell* **146**:732-745. doi:10.1016/j.cell.2011.07.038.
12. Bradshaw JM, Kubota Y, Meyer T, Schulman H. 2003. An ultrasensitive Ca^{2+}/calmodulin-dependent protein kinase II-protein phosphatase 1 switch facilitates specificity in postsynaptic calcium signaling. *Proc Natl Acad Sci USA* **100**:10512-10517. doi:10.1073/pnas.1932759100.
13. Rellos P, Pike ACW, Niesen FH, Salah E, Lee WH, von Delft F, Knapp S. 2010. Structure of the CaMKIIδ/Calmodulin Complex Reveals the Molecular Mechanism of CaMKII Kinase Activation. *PLoS Biol* **8**:e1000426. doi:10.1371/journal.pbio.1000426.
14. Dodd AN, Kudla J, Sanders D. 2010. The Language of Calcium Signaling. *Annu Rev Plant Biol* **61**:593-620. doi:10.1146/annurev-arplant-070109-104628.
15. Day IS, Reddy VS, Ali GS, Reddy ASN. 2002. Analysis of EF-hand-containing proteins in Arabidopsis. *Genome Biol* **3**:research0056.1–research0056.24. doi:10.1186/gb-2002-3-10-research0056.

16. Winter D, Vinegar B, Nahal H, Ammar R, Wilson GV, Provart NJ. 2007. An "Electronic Fluorescent Pictograph" Browser for Exploring and Analyzing Large-Scale Biological Data Sets. *PloS one* **2**:e718. doi:10.1371/journal.pone.0000718.
17. Hetherington AM. 2001. Guard Cell Signaling. *Cell* **107**:711-714. doi:10.1016/S0092-8674(01)00606-7.
18. Hubbard KE, Siegel RS, Valerio G, Brandt B, Schroeder JI. 2012. Abscisic acid and CO_2 signalling via calcium sensitivity priming in guard cells, new CDPK mutant phenotypes and a method for improved resolution of stomatal stimulus–response analyses. *Ann Bot* **109**:5-17. doi:10.1093/aob/mcr252.
19. MacRobbie EAC. 2000. ABA activates multiple Ca^{2+} fluxes in stomatal guard cells, triggering vacuolar K^+(Rb^+) release. *Proc Natl Acad Sci USA* **97**:12361-12368. doi:10.1073/pnas.220417197.
20. McAinsh MR, Brownlee C, Hetherington AM. 1990. Abscisic acid-induced elevation of guard cell cytosolic Ca^{2+} precedes stomatal closure. *Nature* **343**:186-188. doi:10.1038/343186a0.
21. Shimazaki K-i, Kinoshita T, Nishimura M. 1992. Involvement of Calmodulin and Calmodulin-Dependent Myosin Light Chain Kinase in Blue Light-Dependent H+ Pumping by Guard Cell Protoplasts from Vicia faba L. *Plant Physiol* **99**:1416-1421. doi:10.1104/pp.99.4.1416.
22. Shimazaki K-i, Tominaga M, Shigenaga A. 1997. Inhibition of the Stomatal Blue Light Response by Verapamil at High Concentration. *Plant Cell Physiol* **38**:747-750. doi:10.1093/oxfordjournals.pcp.a029230.
23. Irving HR, Gehring CA, Parish RW. 1992. Changes in cytosolic pH and calcium of guard cells precede stomatal movements. *Proc Natl Acad Sci USA* **89**:1790-1794. doi:10.1073/pnas.89.5.1790.
24. Curvetto N, Darjania L, Delmastro S. 1994. Effect of 2 cAMP analogs on stomatal opening in Vicia Faba. Possible relationship with cytosolic calcium-concentration. *Plant Physiol Bioch* **32**:365-372.
25. Cousson A, Vavasseur A. 1998. Putative involvement of cytosolic Ca2+ and GTP-binding proteins in cyclic-GMP-mediated induction of stomatal opening by auxin in Commelina communis L. *Planta* **206**:308-314. doi:10.1007/s004250050405.
26. Young JJ, Mehta S, Israelsson M, Godoski J, Grill E, Schroeder JI. 2006. CO_2 signaling in guard cells: Calcium sensitivity response modulation, a Ca^{2+}-independent phase, and CO_2 insensitivity of the *gca2* mutant. *Proc Natl Acad Sci USA* **103**:7506-7511. doi:10.1073/pnas.0602225103.
27. Munemasa S, Oda K, Watanabe-Sugimoto M, Nakamura Y, Shimoishi Y, Murata Y. 2007. The *coronatine-insensitive 1* Mutation Reveals the Hormonal Signaling Interaction between Abscisic Acid and Methyl Jasmonate in Arabidopsis Guard Cells. Specific Impairment of Ion Channel Activation and Second Messenger Production. *Plant Physiol* **143**:1398-1407. doi:10.1104/pp.106.091298.

28. Siegel RS, Xue S, Murata Y, Yang Y, Nishimura N, Wang A, Schroeder JI. 2009. Calcium elevation-dependent and attenuated resting calcium-dependent abscisic acid induction of stomatal closure and abscisic acid-induced enhancement of calcium sensitivities of S-type anion and inward-rectifying K^+ channels in Arabidopsis guard cells. *Plant J* **59**:207-220. doi:10.1111/j.1365-313X.2009.03872.x.
29. Chen ZH, Hills A, Lim CK, Blatt MR. 2010. Dynamic regulation of guard cell anion channels by cytosolic free Ca^{2+} concentration and protein phosphorylation. *Plant J* **61**:816-825. doi:10.1111/j.1365-313X.2009.04108.x.
30. Xue S, Hu H, Ries A, Merilo E, Kollist H, Schroeder JI. 2011. Central functions of bicarbonate in S-type anion channel activation and OST1 protein kinase in CO_2 signal transduction in guard cell. *EMBO J* **30**:1645-1658. doi:10.1038/emboj.2011.68.
31. Negi J, Matsuda O, Nagasawa T, Oba Y, Takahashi H, Kawai-Yamada M, Uchimiya H, Hashimoto M, Iba K. 2008. CO_2 regulator SLAC1 and its homologues are essential for anion homeostasis in plant cells. *Nature* **452**:483-486. doi:doi:10.1038/nature06720.
32. Vahisalu T, Kollist H, Wang Y-F, Nishimura N, Chan W-Y, Valerio G, Lamminmaki A, Brosche M, Moldau H, Desikan R, Schroeder JI, Kangasjarvi J. 2008. SLAC1 is required for plant guard cell S-type anion channel function in stomatal signalling. *Nature* **452**:487-491. doi:doi:10.1038/nature06608.
33. Schroeder JI, Hagiwara S. 1989. Cytosolic calcium regulates ion channels in the plasma membrane of Vicia faba guard cells. *Nature* **338**:427-430. doi:10.1038/338427a0.
34. Mustilli A-C, Merlot S, Vavasseur A, Fenzi F, Giraudat J. 2002. Arabidopsis OST1 Protein Kinase Mediates the Regulation of Stomatal Aperture by Abscisic Acid and Acts Upstream of Reactive Oxygen Species Production. *Plant Cell* **14**:3089-3099. doi:10.1105/tpc.007906.
35. Yoshida R, Hobo T, Ichimura K, Mizoguchi T, Takahashi F, Aronso J, Ecker JR, Shinozaki K. 2002. ABA-Activated SnRK2 Protein Kinase is Required for Dehydration Stress Signaling in Arabidopsis. *Plant Cell Physiol* **43**:1473-1483. doi:10.1093/pcp/pcf188.
36. Lee SC, Lan W, Buchanan BB, Luan S. 2009. A protein kinase-phosphatase pair interacts with an ion channel to regulate ABA signaling in plant guard cells. *Proc Natl Acad Sci USA* **106**:21419-21424. doi:10.1073/pnas.0910601106.
37. Geiger D, Scherzer S, Mumm P, Stange A, Marten I, Bauer H, Ache P, Matschi S, Liese A, Al-Rasheid KAS, Romeis T, Hedrich R. 2009. Activity of guard cell anion channel SLAC1 is controlled by drought-stress signaling kinase-phosphatase pair. *Proc Natl Acad Sci USA* **106**:21425-21430. doi:10.1073/pnas.0912021106.
38. Brandt B, Brodsky DE, Xue S, Negi J, Iba K, Kangasjärvi J, Ghassemian M, Stephan AB, Hu H, Schroeder JI. 2012. Reconstitution of abscisic acid activation of SLAC1 anion channel by CPK6 and OST1 kinases and branched ABI1 PP2C phosphatase action. *Proc Natl Acad Sci USA* **109**:10593-10598. doi:10.1073/pnas.1116590109.

39. Geiger D, Scherzer S, Mumm P, Marten I, Ache P, Matschi S, Liese A, Wellmann C, Al-Rasheid KAS, Grill E, Romeis T, Hedrich R. 2010. Guard cell anion channel SLAC1 is regulated by CDPK protein kinases with distinct Ca^{2+} affinities. *Proc Natl Acad Sci USA* **107**:8023–8028. doi:10.1073/pnas.0912030107.
40. Mori IC, Murata Y, Yang Y, Munemasa S, Wang Y-F, Andreoli S, Tiriac H, Alonso JM, Harper JF, Ecker JR, Kwak JM, Schroeder JI. 2006. CDPKs CPK6 and CPK3 Function in ABA Regulation of Guard Cell S-Type Anion- and Ca^{2+}-Permeable Channels and Stomatal Closure. *PLoS Biol* **4**:e327. doi:10.1371/journal.pbio.0040327.
41. Zhu S-Y, Yu X-C, Wang X-J, Zhao R, Li Y, Fan R-C, Shang Y, Du S-Y, Wang X-F, Wu F-Q, Xu Y-H, Zhang X-Y, Zhang D-P. 2007. Two Calcium-Dependent Protein Kinases, CPK4 and CPK11, Regulate Abscisic Acid Signal Transduction in Arabidopsis. *Plant Cell* **19**:3019-3036. doi:10.1105/tpc.107.050666.
42. Boudsocq M, Willmann MR, McCormack M, Lee H, Shan L, He P, Bush J, Cheng S-H, Sheen J. 2010. Differential innate immune signalling via Ca^{2+} sensor protein kinases. *Nature* **464**:418-422. doi:10.1038/nature08794.
43. Dubiella U, Seybold H, Durian G, Komander E, Lassig R, Witte C-P, Schulze WX, Romeis T. 2013. Calcium-dependent protein kinase/NADPH oxidase activation circuit is required for rapid defense signal propagation. *Proc Natl Acad Sci USA* **110**:8744-8749. doi:10.1073/pnas.1221294110.
44. Allen GJ, Murata Y, Chu SP, Nafisi M, Schroeder JI. 2002. Hypersensitivity of Abscisic Acid–Induced Cytosolic Calcium Increases in the Arabidopsis Farnesyltransferase Mutant *era1-2*. *Plant Cell* **14**:1649-1662. doi:10.1105/tpc.010448.
45. Cutler SR, Rodriguez PL, Finkelstein RR, Abrams SR. 2010. Abscisic Acid: Emergence of a Core Signaling Network. *Annu Rev Plant Biol* **61**:651-679. doi:10.1146/annurev-arplant-042809-112122.
46. Umezawa T, Sugiyama N, Mizoguchi M, Hayashi S, Myouga F, Yamaguchi-Shinozaki K, Ishihama Y, Hirayama T, Shinozaki K. 2009. Type 2C protein phosphatases directly regulate abscisic acid-activated protein kinases in *Arabidopsis*. *Proc Natl Acad Sci USA* **106**:17588-17593. doi:10.1073/pnas.0907095106.
47. Vlad F, Rubio S, Rodrigues A, Sirichandra C, Belin C, Robert N, Leung J, Rodriguez PL, Lauriere C, Merlot S. 2009. Protein Phosphatases 2C Regulate the Activation of the Snf1-Related Kinase OST1 by Abscisic Acid in *Arabidopsis*. *Plant Cell* **21**:3170-3184. doi:10.1105/tpc.109.069179.
48. Lynch T, Erickson BJ, Finkelstein R. 2012. Direct interactions of ABA-insensitive(ABI)-clade protein phosphatase(PP)2Cs with calcium-dependent protein kinases and ABA response element-binding bZIPs may contribute to turning off ABA response. *Plant Mol Biol* **80**:647-658. doi:10.1007/s11103-012-9973-3.
49. Roelfsema MRG, Hanstein S, Felle HH, Hedrich R. 2002. CO_2 provides an intermediate link in the red light response of guard cells. *Plant J* **32**:65-75. doi:10.1046/j.1365-313X.2002.01403.x.

50. Klüsener B, Young JJ, Murata Y, Allen GJ, Mori IC, Hugouvieux V, Schroeder JI. 2002. Convergence of Calcium Signaling Pathways of Pathogenic Elicitors and Abscisic Acid in Arabidopsis Guard Cells. *Plant Physiol* **130**:2152-2163. doi:10.1104/pp.012187.

51. Gao X, Chen X, Lin W, Chen S, Lu D, Niu Y, Li L, Cheng C, McCormack M, Sheen J, Shan L, He P. 2013. Bifurcation of *Arabidopsis* NLR Immune Signaling via Ca^{2+}-Dependent Protein Kinases. *PLoS Pathog* **9**:e1003127. doi:10.1371/journal.ppat.1003127.
52. Munemasa S, Hossain MA, Nakamura Y, Mori IC, Murata Y. 2011. The Arabidopsis Calcium-Dependent Protein Kinase, CPK6, Functions as a Positive Regulator of Methyl Jasmonate Signaling in Guard Cells. *Plant Physiol* **155**:553-561. doi:10.1104/pp.110.162750.
53. Vahisalu T, Puzõrjova I, Brosché M, Valk E, Lepiku M, Moldau H, Pechter P, Wang Y-S, Lindgren O, Salojärvi J, Loog M, Kangasjärvi J, Kollist H. 2010. Ozone-triggered rapid stomatal response involves the production of reactive oxygen species, and is controlled by SLAC1 and OST1. *Plant J* **62**:442-453. doi:10.1111/j.1365-313X.2010.04159.x.
54. Ma S-Y, Wu W-H. 2007. AtCPK23 functions in Arabidopsis responses to drought and salt stresses. *Plant Mol Biol* **65**:511-518. doi:10.1007/s11103-007-9187-2.
55. Antoni R, Gonzalez-Guzman M, Rodriguez L, Peirats-Llobet M, Pizzio GA, Fernandez MA, De Winne N, De Jaeger G, Dietrich D, Bennett MJ, Rodriguez PL. 2013. PYRABACTIN RESISTANCE1-LIKE8 Plays an Important Role for the Regulation of Abscisic Acid Signaling in Root. *Plant Physiol* **161**:931-941. doi:10.1104/pp.112.208678.
56. Pei ZM, Kuchitsu K, Ward JM, Schwarz M, Schroeder JI. 1997. Differential Abscisic Acid Regulation of Guard Cell Slow Anion Channels in Arabidopsis Wild-Type and *abi1* and *abi2* Mutants. *Plant Cell* **9**:409-423. doi:10.1105/tpc.9.3.409.
57. Laemmli UK. 1970. Cleavage of Structural Proteins During Assembly of Head of Bacteriophage-T4. *Nature* **227**:680-&. doi:10.1038/227680a0.
58. Schindelin J, Arganda-Carreras I, Frise E, Kaynig V, Longair M, Pietzsch T, Preibisch S, Rueden C, Saalfeld S, Schmid B, Tinevez J-Y, White DJ, Hartenstein V, Eliceiri K, Tomancak P, Cardona A. 2012. Fiji: an open-source platform for biological-image analysis. *Nature* **9**:676-682. doi:10.1038/nmeth.2019.
59. Latz A, Mehlmer N, Zapf S, Mueller TD, Wurzinger B, Pfister B, Csaszar E, Hedrich R, Teige M, Becker D. 2012. Salt stress triggers phosphorylation of the Arabidopsis vacuolar K^+ channel TPK1 by calcium dependent protein kinases (CDPKs). *Mol Plant* **6**:1274-1289. doi:10.1093/mp/sss158.
60. Waadt R, Schmidt LK, Lohse M, Hashimoto K, Bock R, Kudla J. 2008. Multicolor bimolecular fluorescence complementation reveals simultaneous formation of alternative CBL/CIPK complexes in planta. *Plant J* **56**:505-516. doi:10.1111/j.1365-313X.2008.03612.x.

61. Nour-Eldin HH, Hansen BG, Norholm MHH, Jensen JK, Halkier BA. 2006. Advancing uracil-excision based cloning towards an ideal technique for cloning PCR fragments. *Nucl Acids Res* **34**:e122-. doi:10.1093/nar/gkl635.
62. Nour-Eldin HH, Geu-Flores F, Halkier BA. 2010. USER Cloning and USER Fusion: The Ideal Cloning Techniques for Small and Big Laboratories. In: FettNeto AG, editor. *Plant Secondary Metabolism Engineering: Methods and Applications*. Methods in Molecular Biology. 6432010. p. 185-200.
63. Norholm M. 2010. A mutant Pfu DNA polymerase designed for advanced uracil-excision DNA engineering. *BMC Biotechnol* **10**:21. doi:10.1186/1472-6750-10-21.
64. Elledge SJ, Mulligan JT, Ramer SW, Spottswood M, Davis RW. 1991. Lambda YES: a multifunctional cDNA expression vector for the isolation of genes by complementation of yeast and Escherichia coli mutations. *Proc Natl Acad Sci USA* **88**:1731-1735.
65. Saez A, Rodrigues A, Santiago J, Rubio S, Rodriguez PL. 2008. HAB1–SWI3B Interaction Reveals a Link between Abscisic Acid Signaling and Putative SWI/SNF Chromatin-Remodeling Complexes in Arabidopsis. *Plant Cell* **20**:2972-2988. doi:10.1105/tpc.107.056705.
66. Benetka W, Mehlmer N, Maurer-Stroh S, Sammer M, Koranda M, Neumüller R, Betschinger J, Knoblich JA, Teige M, Eisenhaber F. 2008. Experimental testing of predicted myristoylation targets involved in asymmetric cell division and calcium-dependent signalling. *Cell Cycle* **7**:3709-3719.
67. James P, Halladay J, Craig EA. 1996. Genomic Libraries and a Host Strain Designed for Highly Efficient Two-Hybrid Selection in Yeast. *Genetics* **144**:1425-1436.
68. Gietz D, Stjean A, Woods RA, Schiestl RH. 1992. Improved method for high-efficiency transformation of intact yeast-cells. *Nucleic Acids Res* **20**:1425-1425. doi:10.1093/nar/20.6.1425.
69. Allen GJ, Kuchitsu K, Chu SP, Murata Y, Schroeder JI. 1999. Arabidopsis *abi1-1* and *abi2-1* Phosphatase Mutations Reduce Abscisic Acid–Induced Cytoplasmic Calcium Rises in Guard Cells. *Plant Cell* **11**:1785-1798. doi:10.1105/tpc.11.9.1785.
70. Murata Y, Pei Z-M, Mori IC, Schroeder J. 2001. Abscisic Acid Activation of Plasma Membrane Ca^{2+} Channels in Guard Cells Requires Cytosolic NAD(P)H and Is Differentially Disrupted Upstream and Downstream of Reactive Oxygen Species Production in *abi1-1* and *abi2-1* Protein Phosphatase 2C Mutants. *Plant Cell* **13**:2513-2523. doi:10.1105/tpc.010210.
71. Wang Y, Chen Z-H, Zhang B, Hills A, Blatt MR. 2013. PYR/PYL/RCAR Abscisic Acid Receptors Regulate K^+ and Cl^- Channels through Reactive Oxygen Species-Mediated Activation of Ca^{2+} Channels at the Plasma Membrane of Intact Arabidopsis Guard Cells. *Plant Physiol* **163**:566-577. doi:10.1104/pp.113.219758.

Brandt et al., Figure 1

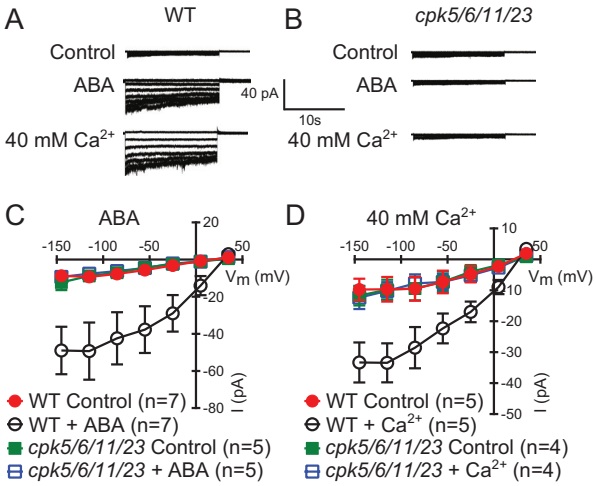

Figure 1: CPK quadruple loss of function mutants are ABA and Ca^{2+} insensitive.

Intracellular Ca^{2+}-activation of S-type anion channels enabled by pre-exposure to ABA (A-C) or high external Ca^{2+} (A,B, and D) is strongly impaired in *cpk5/6/11/23* guard cells at 2 µM $[Ca^{2+}]_{cyt}$. Representative whole cell currents (A-B), average steady-state current-voltage relationships +/- SEM, and guard cell numbers are shown (C-D).

Brandt et al., Figure 1-figure supplement 1

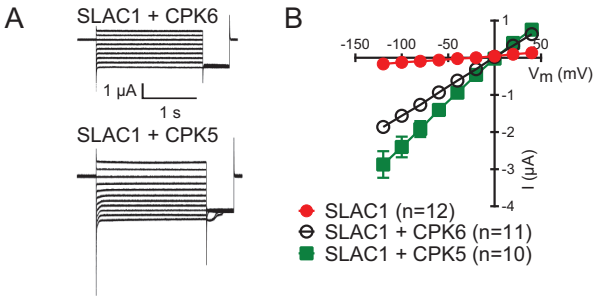

Figure 1–figure supplement 1: CPK5 activates SLAC1 in *Xenopus* oocytes.

(A-B) Whole cell currents were measured in *Xenopus* oocytes expressing SLAC1 together with CPK5 and, as a control, CPK6. Large Cl^- currents demonstrate that CPK5 is capable of activating SLAC1. Representative current traces (A), average steady-state current-voltage relationships (+/- SEM), and numbers of individual cells are shown (B).

Brandt et al., Figure 2

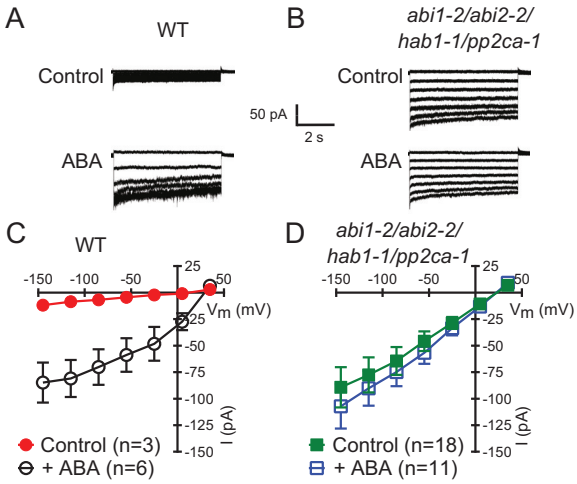

Figure 2: In PP2C quadruple mutant plants, Ca^{2+} activation of S-type anion currents is constitutively primed.

2 µM $[Ca^{2+}]_{cyt}$ activates S-type anion currents in WT if the guard cells were pre-exposed to ABA (A, C). In PP2C quadruple mutant guard cells ABA pre-exposure is not required for 2 µM $[Ca^{2+}]_{cyt}$-activation of S-type anion currents (B, D). Average steady-state current-voltage relationships +/- SEM, guard cell numbers (C-D), and representative whole cell currents (A-B) are presented.

Brandt et al., Figure 2-figure supplement 1

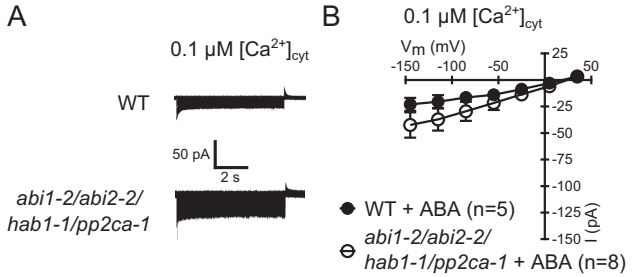

Figure 2–figure supplement 1: ABA activation of S-type anion current in PP2C quadruple mutant guard cells requires elevated $[Ca^{2+}]_{cyt}$.

(A-D) ABA application in WT and *abi1-2/abi2-2/hab1-1/pp2ca-1* guard cells with $[Ca^{2+}]_{cyt}$ buffered to a resting level of 0.1 µM does not result in large S-type anion current activation. Typical current traces (A), averaged steady-state currents in response to applied voltages (+/- SEM), and numbers of individual measured cells are shown (B).

Brandt et al., Figure 3

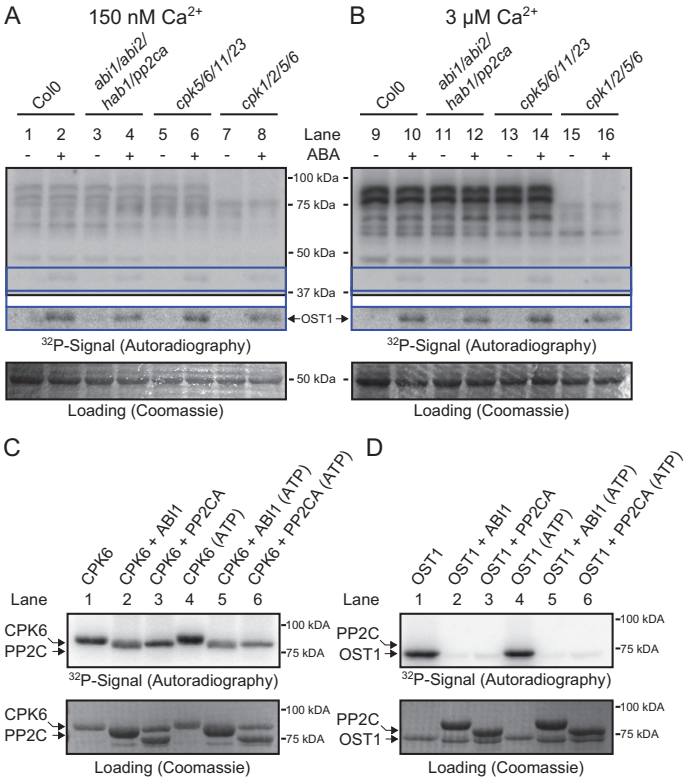

Figure 3: CPK activity is not changed by ABA or constitutively or hyper-activated in *pp2c* quadruple mutants.

(A-B) In gel kinase assays with Histone as substrate for whole plant protein extracts show (B) 3 µM Ca^{2+}-activated trans-phosphorylation kinase activities independent of application of 50 µM ABA (lanes 9 and 10). In contrast, ABA activation of OST1 is clearly visible (lanes 1-2 and 9-10 at ~ 41 kDa lower; "OST1" inset shows the same signal optimized autoradiography at the ~ 41 kDa region; See Methods). Disrupting 4 PP2C genes (ABI1, ABI2, HAB1, and PP2CA) does not result in constitutive Ca^{2+}-activated and OST1 kinase activities (lanes 3-4 and 11-12). In gel kinase activities of two independent CPK quadruple mutant lines indicate that the Ca^{2+}-activated kinase signals are CPK-derived (compare lanes 9-10 with 13-16 in B; predicted MWs for CPK1, CPK2, CPK5, CPK6, CPK11, and CPK23 are 68.3 kDa, 72.3 kDa, 62.1 kDa, 61.1 kDa, 55.9 kDa, 58.7 kDa, respectively). (C-D) In gel kinase assays with recombinant proteins show that incubation of the protein kinases with the PP2Cs ABI1 and PP2CA does (C) not change CPK6 activity while (D) OST1 activity is strongly down-regulated by PP2Cs. Each experiment has been repeated at least 3 times with similar results.

.

Brandt et al., Figure 3-figure supplement 1

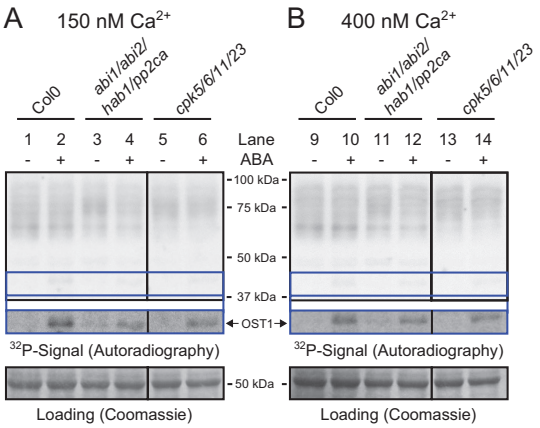

Figure 3–figure supplement 1: Kinase activities are not altered by ABA-application at 150 nM and 400 nM free Ca^{2+}.

(A-B) Whole plant protein extracts were analyzed in in gel kinase assays with the free Ca^{2+} concentration buffered to either 150 nM or 400 nM. No differences in the band pattern could be found between these different free Ca^{2+} concentrations (A-B). The presence of 400 nM free Ca^{2+} does not change ABA activation of OST1 (lower inset "OST1" in A and B) in WT, *abi1-2/abi2-2/hab1-1/pp2ca-1* or *cpk5/6/11/23* plants. PP2Cs have been shown to be involved in $[Ca^{2+}]_{cyt}$ regulation (54).

Brandt et al., Figure 3-figure supplement 2

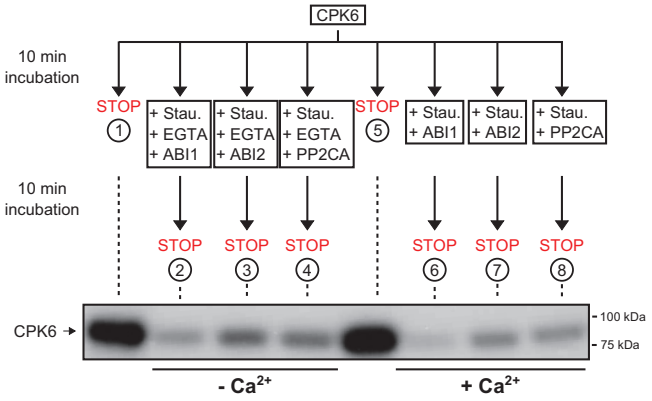

Figure 3–figure supplement 2: CPK6 is de-phosphorylated by the PP2Cs ABI1, ABI2, and PP2CA.

In *in vitro* kinase assays, recombinant CPK6 was incubated in the presence of 5 µM free Ca^{2+} which results in auto-phosphorylation signals (Lanes 1 and 5). After the initial auto-phosphorylation period the kinase inhibitor Staurosporine (Stau.) and the PP2Cs ABI1, ABI2, and PP2CA were added to the reactions (Lanes 2-4 and 6-8). For the samples displayed in Lanes 2-4, the Ca^{2+}-chelator EGTA, which buffers free Ca^{2+} concentrations to <10 nM, was added together with Staurosporine and the indicated PP2Cs. Addition of Staurosporine and the PP2Cs ABI1, ABI2, and PP2CA resulted in decreased auto-phosphorylation signals showing that PP2Cs de-phosphorylate CPK6 (Lanes 2-4 and 6-8).

Brandt et al., Figure 3-figure supplement 3

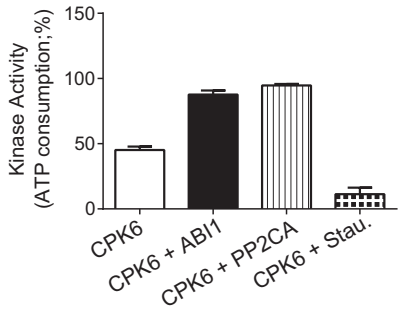

Figure 3–figure supplement 3: CPK6 kinase activity is not inhibited in the presence of ABI1 or PP2CA.

In vitro kinase assays measuring the kinase activity via ATP consumption show that Staurosporine but not ABI1 or PP2CA inhibited CPK6 kinase activity. The increased ATP-consumption signal in the presence of ABI1 and PP2CA can be explained by higher ATP consumption triggered by kinase auto-phosphorylation of residues removed by the PP2C protein phosphatases. Data shown represent the mean of 3 experiments +/- SD.

Brandt et al., Figure 4

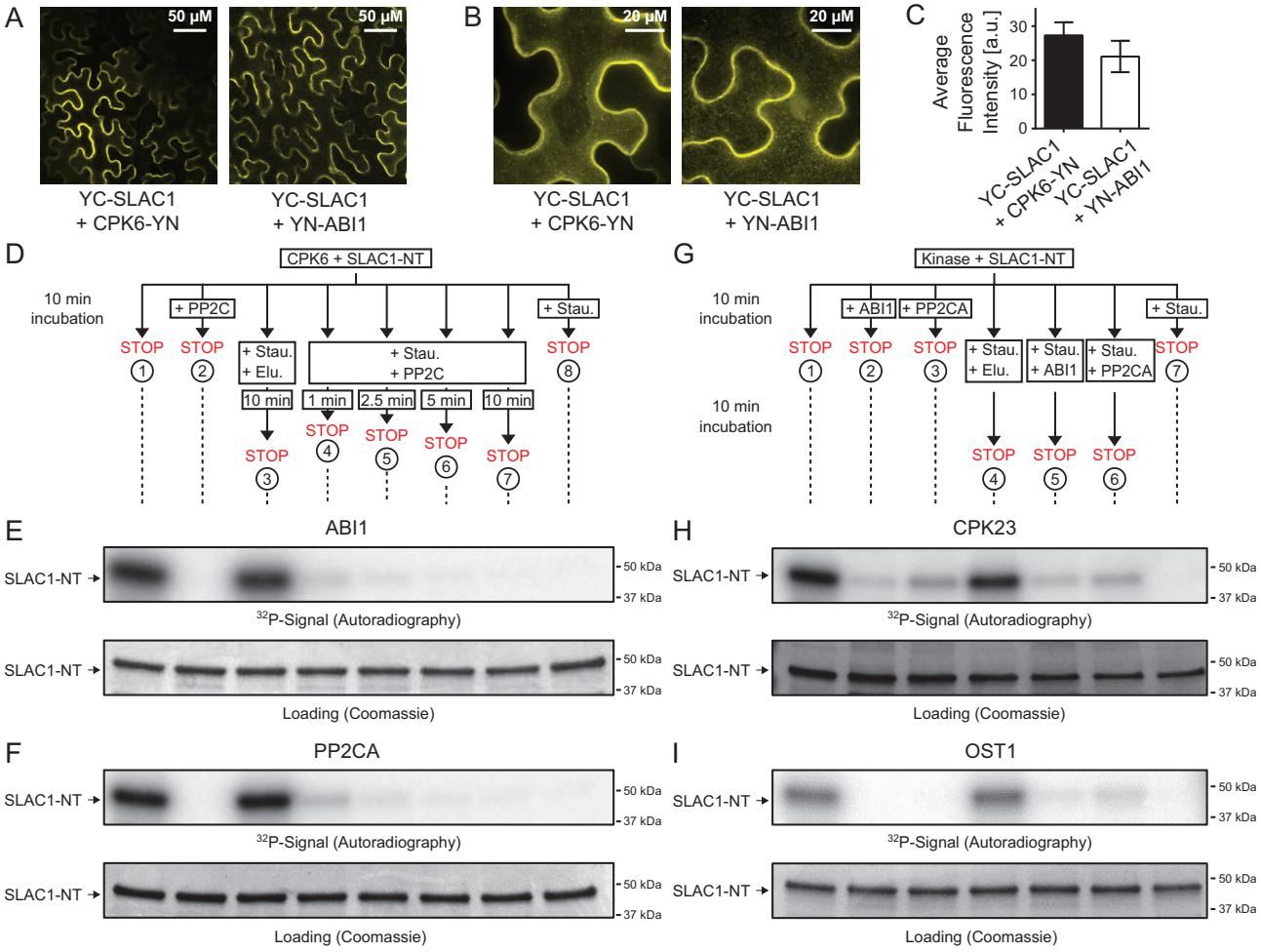

Figure 4: PP2Cs interact and directly and rapidly de-phosphorylate the N-terminus of SLAC1 when previously phosphorylated by several SLAC1-activating CPK and OST1 protein kinases.

(A-C) Bi-molecular fluorescence complementation (BiFC) experiments in N. benthamiana leaves show YFP-derived fluorescence signals of SLAC1-YC co-expressed with CPK6-YN and YN-ABI1 of comparable intensity. Data shown in (C) represent the average fluorescence intensity of randomly picked leaf areas (n=9; +/- SEM). (D-F) CPK6 phosphorylated SLAC1-NT is rapidly de-phosphorylated by ABI1 and PP2CA. SLAC1-NT phosphorylation by CPK6 (E-F, lane 1) is strongly inhibited if the PP2C protein phosphatase was added before starting the reaction (E-F, lane 2), but remains stable after addition of elution buffer (Elu.) and kinase inhibitor Staurosporine (Stau.) with subsequent 10 min incubation (E-F, lane 3). If (E) ABI1 or (F) PP2CA together with Staurosporine are added after the initial 10 min CPK6 mediated phosphorylation period, the SLAC1-NT phosphorylation signal rapidly decreases within 1 min (E-F, lanes 4-7). Staurosporine pre-exposure control inhibits SLAC1-NT phosphorylation by CPK6 (E-F, lane 8). (G-I) PP2Cs de-phosphorylate the SLAC1-NT which was phosphorylated by major SLAC1-activating kinases CPK23 and OST1. The N-terminus of SLAC1 is phosphorylated by CPK23 (H, lane 1) and OST1 (I, lane 1) which is inhibited when the PP2Cs ABI1 and PP2CA are added before starting the reactions (H-I, lanes 2-3). When adding Staurosporine and elution buffer after the initial phosphorylation period and incubating for 10 min the signal does not change (H-I, lane 4). Addition of ABI1 or PP2CA after supplementing the reaction with Staurosporine leads to rapid (10 min) de-phosphorylation of the SLAC1-NT previously phosphorylated by the above mentioned kinases (H-I, lanes 5-6).

Brandt et al., Figure 4-figure supplement 1

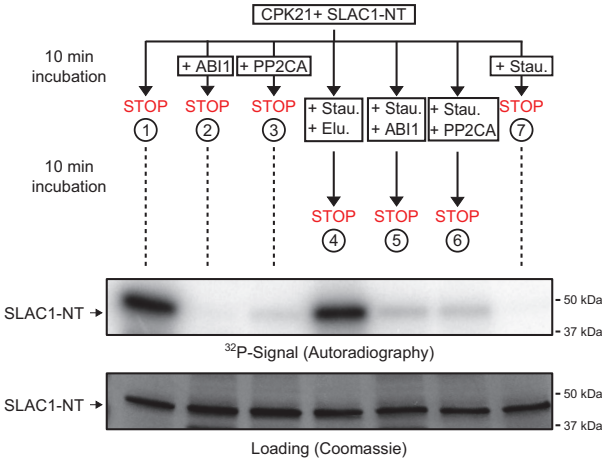

Figure 4–figure supplement 1: When previously phosphorylated by CPK21, the SLAC1-NT is de-phosphorylated by the PP2Cs ABI1 and PP2CA.

Recombinant SLAC1-NT phosphorylation by CPK21 (Lane 1) is inhibited if the protein phosphatases ABI1 and PP2CA are added before starting the reaction (Lanes 2-3). The phosphorylated SLAC1-NT derived signal is rapidly and strongly decreased if the PP2Cs ABI1 and PP2CA (Lanes 4-7) are added after the addition of Staurosporine.

Brandt et al., Figure 5

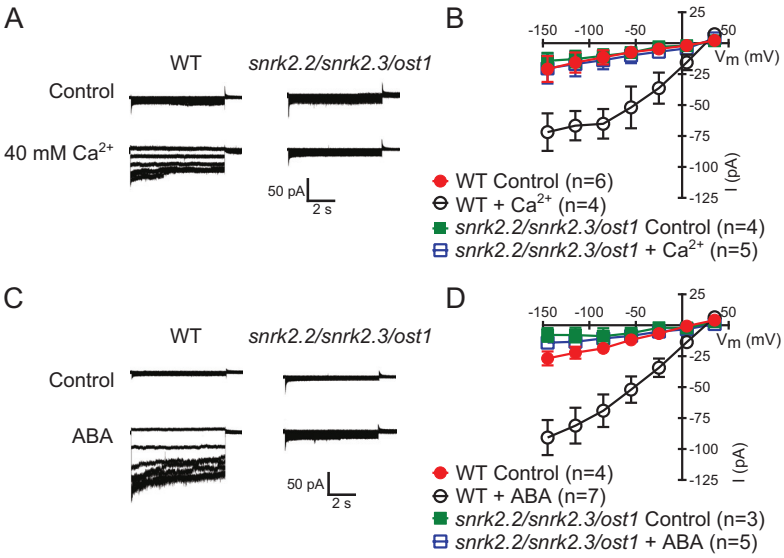

Figure 5: Both, ABA- and high external Ca^{2+}-activation of S-type anion currents at elevated $[Ca^{2+}]_{cyt}$ are abrogated in *snrk2.2/2.3/ost1* triple mutant guard cells.

In whole cell patch clamp experiments, *snrk2.2/2.3/ost1* triple mutant guard cells disrupt Ca^{2+}-activation of S-type anion currents even if pre-incubated with (A-B) high external Ca^{2+} shock (35) or (C-D) ABA. Typical current responses (A and C), average steady-state current-voltage relationships +/- SEM, and the number of measured cells are presented (B and D). In (B) data for *snrk2.2/2.3/ost1* triple mutants with and without ABA overlap with WT controls.

Brandt et al., Figure 5-figure supplement 1

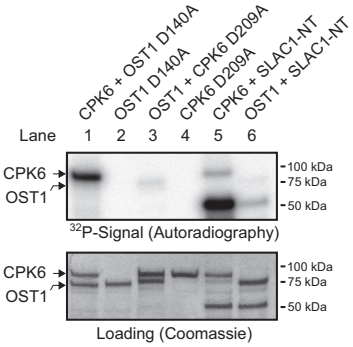

Figure 5–figure supplement 1: CPK6 and OST1 do not trans-phosphorylate one another *in vitro*.

We analyzed whether CPK6 and OST1 trans-phosphorylated one another by using the respective active and inactive mutant kinase versions (OST1 D140A and CPK6 D209A). This approach allowed us to distinguish between auto- and trans-phosphorylation derived ^{32}P-signals. Kinase inactive versions of OST1 (D140A (28)) and CPK6 (D209A (29)) are not phosphorylated by active CPK6 and OST1, respectively (lanes 1 and 3). When OST1 D140A and CPK6 D209A were incubated alone no signal can be seen (lanes 2 and 4). Both, OST1 and CPK6 phosphorylated the SLAC1-NT which shows that the kinase proteins used exhibit trans-phosphorylation activities (lanes 5-6). The auto-phosphorylation activities of CPK6 (lanes 1 and 5) and OST1 (lanes 3 and 6) can be seen.

Brandt et al., Figure 5-figure supplement 2

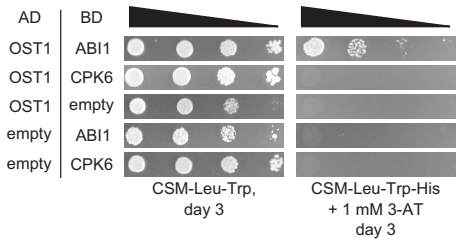

Figure 5–figure supplement 2: In yeast-2hybrid assays, OST1 interacts with ABI1 but not with CPK6

IIn yeast-2-hybrid assays, OST1 interacts with ABI1 as indicated by yeast growth on CSM-Leu-Trp-His (right panel). No growth can be observed when OST1 was co-transformed with CPK6 under identical conditions, indicating no physical protein-protein interaction of OST1 and CPK6 in yeast. Empty: Control experiments with empty vectors.

Brandt et al., Figure 6

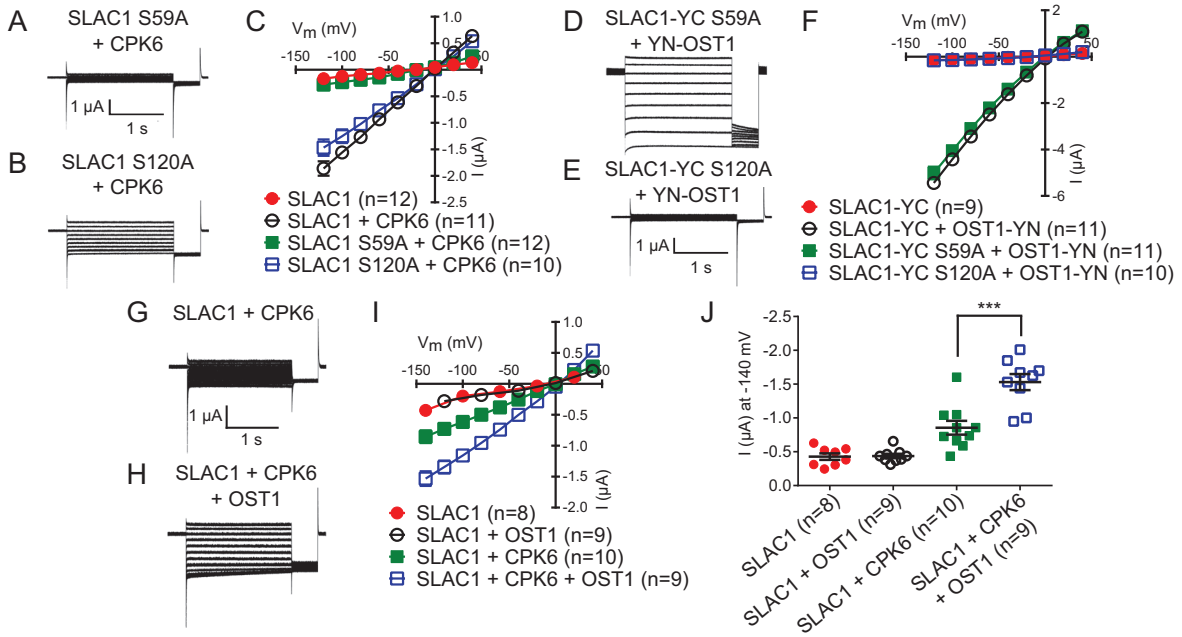

Figure 6: Ca^{2+}-dependent protein kinase and OST1 protein kinase activation of SLAC1 requires serine 59 or serine 120, respectively. SLAC1 is synergistically activated by CPKs and OST1.

SLAC1 activation by CPK6 in Xenopus oocytes (A and C) is abolished when serine 59 is mutated to alanine (S59A) but (B-C) is comparable to wild type SLAC1 activation for the SLAC1 S120A mutated version. (D-F) OST1 activation of SLAC1 (E-F) is abolished in the SLAC1 S120A mutant, while (D and F) the SLAC1 S59A activation by OST1 is similar to the wild type. (G-J) If SLAC1 (5 ng cRNA) is expressed alone or with non-BIFC OST1 (7.5 ng), no anion currents can be detected (I-J). If CPK6 (0.5 ng) is co-expressed, SLAC1-mediated currents can be seen (G, I and J) which are synergistically enhanced when OST1 (7.5 ng) is added (H-J). Due to overlapping data of “SLAC1” and “SLAC1 + OST1” alternating data points are shown in (I). Typical current responses (A-B, D-E and G-H), average steady-state current-voltage relationships +/- SEM, and the number of measured cells are presented (C, F, and I). Steady-state current responses at -140 mV are plotted in g (*** indicates p=0.005; unpaired t-test with Welch’s correction).

Brandt et al., Figure 6-figure supplement 1

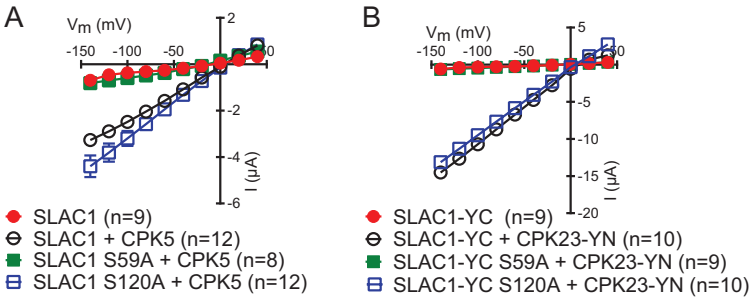

Figure 6–figure supplement 1: SLAC1 serine 59 but not serine 120 is required for CPK5 or CPK23 activation.

SLAC1 activation by CPK5 (A) and CPK23 (B) is comparable to WT when serine 120 is substituted by alanine (S120A) while the CPK5 and CPK23 activation of SLAC1 S59A is completely impaired. Representative current traces (A), average steady-state current-voltage relationships (+/- SEM), and numbers of individual measured cells are depictured (B).

Brandt et al., Figure 7

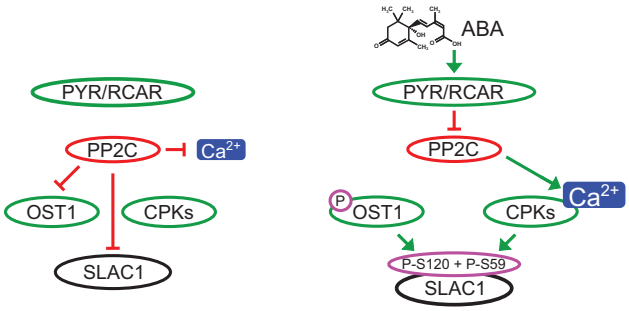

Figure 7: Schematic model for Ca^{2+}-specificity mechanism within ABA-dependent SLAC1 activation in guard cells.

Without ABA, spontaneous or un-specifically induced Ca^{2+} transients (21, 29) do not lead to SLAC1 activation as PP2C phosphatases directly negatively regulate SLAC1 activation (left panel). In the presence of ABA this SLAC1 inhibition is released, OST1 and CPKs phosphorylate, and thereby activate the channel (right panel). ABA also causes $[Ca^{2+}]_{cyt}$ elevation via PP2C inhibition (64, 65). Data indicate a cross-talk between Ca^{2+}-dependent and -independent ABA-activation of SLAC1 which could be mediated through synergistic target coincidence detection activity via differential SLAC1 phosphorylation by OST1 and CPKs (right panel).

RUNNING HEAD

Identification of OST1-interacting proteins

SnRK2 and PP2A interaction with OST1

(50 characters)

CORRESPONDING AUTHOR

Julian I. Schroeder

University of California San Diego, Division of Biological Sciences, Cell and Developmental Biology Section and Center for Food and Fuel for the 21st Century, 9500 Gilman Drive #0116, La Jolla, CA 92093-0116, USA.

Phone: (858) 534-7759, Fax: (858) 534-7108, Email: jischroeder@ucsd.edu

RESEARCH AREA

Signaling and Response

Identification of OST1-interacting proteins reveals SnRK2-type protein kinase homo- and heterodimerization and interactions with PP2A-type phosphatases

Rainer Waadt[1*], Bianca Manalansan[1*], Navin Rauniyar[2], Christian Waadt, Dmitri A. Nusinow[3], Shintaro Munemasa[1,4], Benjamin Brandt[1], Steve A. Kay[5], Hans Henning Kunz[1], Alison DeLong[6], John R. Yates[2], and Julian I. Schroeder[1#]

[1] University of California San Diego, Division of Biological Sciences, Cell and Developmental Biology Section and Center for Food and Fuel for the 21st Century, 9500 Gilman Drive #0116, La Jolla, CA 92093-0116, USA.

[2]The Scripps Research Institue, 10550 North Torrey Pines Road, Department of Chemical Physiology, SR11, La Jolla, CA-92037, USA.

[3]Danforth Plant Science Center, 975 N. Warson Rd., St. Louis, MO 63132, USA.

[4]Present Address: Okayama University, Division of Agricultural and Life Science, Graduate School of Environmental and Life Science, 1-1-1 Tsushima-Naka, Okayama 7008530, Japan.

[5]University of Southern California, Molecular and Computational Biology Section, Los Angeles, CA 90089, USA.

[6]Brown University, Department of Molecular Biology, Cell Biology, and Biochemistry, Providence RI, 02912, USA.

[*] these authors contributed equally

[#] corresponding author

SUMMARY

Plant stress hormone abscisic acid-activated protein kinases interact among each other and with regulatory subunits of type 2A protein phosphatases, which function in abscisic acid responses.

This work was supported by a Feodor Lynen-fellowship of the Alexander von Humboldt-Foundation to RW and by grants from the National Institute of Health (GM060396 to JIS) and the National Science Foundation (MCB0918220 to JIS). Root growth analyses were supported by a grant from the Division of Chemical Sciences, Geosciences, and Biosciences, Office of Basic Energy Sciences of the U.S. Department of Energy (DE-FG02-03ER15449 to JIS). The development of the HF-tag was supported by grants from the National Institute of General Medical Sciences and the National Institute of Health (R01GM056006 and R01GM067837 to SAK).

Address correspondence to jischroeder@ucsd.edu.

ABSTRACT

The plant hormone abscisic acid (ABA) controls growth and development and regulates plant water status through a well-established signaling pathway. In the presence of ABA, pyrabactin resistance/regulatory component of ABA receptor (PYR/RCAR) ABA receptor proteins inhibit type 2C protein phosphatases (PP2C) to enable the activation of SNF1-related kinases 2 (SnRK2). OST1/SnRK2.6/SRK2E is the major protein kinase responsible for mediating ABA responses in guard cells. Recessive *ost1-3* mutant plants transformed with OST1-6xHis-3xFLAG were used for the co-purification and identification of OST1-interacting proteins after osmotic stress or ABA treatments. These analyses revealed the homo- and heterodimerization of OST1 with other SnRK2-type protein kinases and identified proteins involved in lipid and galactolipid metabolism and type 2A protein phosphatases (PP2A) as OST1-interacting proteins. Further analyses revealed protein-protein interactions of regulatory PP2AA- and PP2AB-subunits with various SnRK2-type protein kinases. *pp2a* double mutants exhibited a reduced sensitivity to ABA during seed germination and stomatal closure but an enhanced sensitivity during seedling growth.

INTRODUCTION

Land plants adapted the molecule ABA as a hormone to control plant water status and to regulate developmental processes in response to limited water conditions (Cutler et al., 2010; Raghavendra et al., 2010; Hauser et al., 2011). In particular, ABA regulates seed dormancy (Finkelstein et al., 2008), root growth and development (De Smet et al., 2006; Duan et al., 2013) and stomatal movements (Kim et al., 2010) in response to environmental cues including drought and salinity.

ABA is perceived by a family of PYR/RCAR ABA receptors (Ma et al., 2009; Park et al., 2009), which in complex with ABA interact with and negatively regulate PP2C-type phosphatases (Ma et al., 2009; Park et al., 2009; Santiago et al., 2009; Szostkiewicz et al., 2009; Nishimura et al., 2010). Inhibition of PP2C-type phosphatases enables the activation of SnRK2-type protein kinases (Fujii et al., 2009; Melcher et al., 2009) through a release of dephosphorylation and sterical inhibition (Umezawa et al., 2009; Vlad et al., 2009; Soon et al., 2012; Xie et al., 2012).

SnRK2-type protein kinases consist of a ten member family in Arabidopsis (Hrabak et al., 2003). While salt- and osmotic-stress activate nine family members (Boudsocq et al., 2004, 2007; Umezawa et al., 2004; Yoshida et al., 2006), the major kinases activated by ABA are SnRK2.2/SRK2D (SnRK2.2), SnRK2.3/SRK2I (SnRK2.3) and OST1/SnRK2.6/SRK2E (OST1) (Mustilli et al., 2002; Yoshida et al., 2002, 2006; Boudsocq et al., 2004, 2007; Fujii et al., 2007; Fujii and Zhu, 2009; Nakashima et al., 2009; Umezawa et al., 2009). In addition, OST1 is also activated by low humidity (Yoshida et al., 2002, 2006). SnRK2 activation requires the phosphorylation of the activation loop within the kinase domain and its stabilization by the DI-domain/SnRK2-box, located C-terminal to the activation loop (Belin et al., 2006; Boudsocq, et al., 2007; Umezawa et al., 2009; Vlad et al., 2010; Yunta et al., 2011). Phosphorylation of the activation loop can occur through intra(*cis*)- or intermolecular(*trans*)-autophosphorylation (Belin et al., 2006; Ng et al., 2011) or potentially also through not yet identified kinases. Detailed analyses of OST1 showed that the C-terminal DII-domain/ABA-box is required for PP2C-type phosphatase interaction and ABA activation (Belin et al., 2006; Yoshida et al., 2006). However, the deletion of this domain did not affect the activation of OST1 in response to osmotic stress and low humidity, suggesting ABA-dependent and independent activation mechanisms of OST1 (Yoshida et al., 2006).

Substrates or interacting proteins of SnRK2-type protein kinases include AREB/ABF/ABI5-type transcription factors (Kobayashi et al., 2005; Furihata et al., 2006; Sirichandra et al., 2010), the ion channels SLAC1, QUAC1 and KAT1 (Geiger et al., 2009; Lee et al., 2009; Sato et al., 2009; Sasaki et al., 2010; Brandt et al., 2012; Imes et al., 2013), the NADPH oxidase RbohF (Sirichandra et al., 2009), 14-3-3 proteins (Shin et al., 2007), the calcium sensor SCS (Bucholc et al., 2011) and the functionally unknown protein SNS1 (Umezawa et al., 2013). In addition putative substrates were identified through mapping peptide phosphorylation preferences (Vlad et al., 2008; Sirichandra et al., 2010) and through phosphoproteomics approaches (Shin et al., 2007; Umezawa et al., 2013; Wang et al., 2013). However, validation and functional analyses of such putative SnRK2 substrates or interacting proteins are incomplete.

Consistent with the environmental conditions in which SnRK2-type protein kinases are activated, mutations in SnRK2-type protein kinases rendered Arabidopsis plants hypersensitive to drought, osmotic stress and low humidity, and insensitive to elevated CO_2 (Mustilli et al., 2002; Yoshida et al., 2002, 2006; Umezawa et al., 2004; Xie et al., 2006; Fujii et al., 2007, 2011; Fujii and Zhu, 2009; Fujita et al., 2009; Xue et al., 2011; Merilo et al., 2013). These defects were linked to altered gene expression of stress responsive genes (Umezawa et al., 2004; Fujii et al., 2007, 2011; Fujii and Zhu, 2009; Fujita et al., 2009; Nakashima et al., 2009) and impaired stomatal responses (Merlot et al., 2002; Mustilli et al, 2002; Yoshida et al., 2002; Xie et al., 2006; Vahisalu et al., 2010; Xue et al., 2011; Merilo et al., 2013). Of the ABA-activated SnRK2-type protein kinases SnRK2.2 and SnRK2.3 function together predominantly during seed germination, seedling development and root growth (Fujii et al., 2007; Fujii and Zhu, 2009; Fujita et al., 2009; Nakashima et al., 2009), while OST1 plays a major role in guard cells (Merlot et al., 2002; Mustilli et al, 2002; Yoshida et al., 2002; Xie et al., 2006; Xue et al., 2011). However, disruption of all three ABA-activated SnRK2-type protein kinases resulted in an even more reduced ABA sensitivity, which affected seed dormancy and leaf water loss (Fujii and Zhu, 2009; Fujita et al., 2009; Nakashima et al., 2009).

PP2A-type phosphatases are heterotrimeric holoenzyme complexes consisting of regulatory PP2AA- and PP2AB- and catalytic PP2AC-subunits (Xu et al., 2006; Shi, 2009). The Arabidopsis genome encodes for three PP2AA-, seventeen PP2AB- (two PP2AB-, nine PP2AB'-, six PP2AB''-) and five PP2AC-subunits (DeLong, 2006; Farkas et al., 2007). Forward and

reverse genetics approaches revealed functional roles of PP2A-type phosphatases in ABA signaling (Kwak et al., 2002; Pernas et al., 2007) in regulation of auxin fluxes (Fischer et al., 1996; Garbers et al., 1996; Rashotte et al., 2001; Michniewicz et al., 2007; Ballesteros et al., 2012; Dai et al., 2012), brassinosteroid signaling (Tang et al., 2010; Wu et al., 2011), ethylene signaling and biosynthesis (Larsen and Cancel, 2003; Skottke et al., 2011), methyl jasmonate signaling (Saito et al., 2008; Trotta et al., 2011) blue light signaling (Tseng and Briggs, 2010) and microtubule organization (McClinton and Sung, 1997; Camilleri et al., 2002; Kirik et al., 2012).

PP2AA-subunits consist of 15 tandem HEAT-repeats, forming a hook-like structure for binding to the PP2AB- and PP2AC-subunits (Farkas et al., 2007; Xu et al., 2006). Severe developmental defects were observed in PP2AA-subunit double mutants, however only when *pp2aa1* (*rcn1*) was combined with either *pp2aa2* or *pp2aa3,* indicating that RCN1 plays a major role in the regulation of PP2A activity (Zhou et al., 2004; Michniewicz et al., 2007). In the Arabidopsis Wassilewskija (Ws) accession, *RCN1* mutation resulted in an ABA hyposensitivity in seed germination and stomatal closure (Kwak et al., 2002; Saito et al., 2008). In contrast the catalytic subunit mutant *pp2ac2* exhibited an ABA hypersensitivity in seed germination, root growth and seedling development (Pernas et al., 2007), leading to the question about the role of other catalytic PP2AC-subunits in ABA responses.

The goal of this study was the identification and characterization of novel OST1-interacting proteins. Using *in planta* OST1 protein complex isolations we identified family members of the SnRK2-type protein kinases, PP2A-type phosphatases and proteins involved in lipid and galactolipid metabolism as OST1-interacting proteins. Further analyses revealed that regulatory PP2AA- and PP2AB-subunits form an interaction network with ABA-activated SnRK2-type protein kinases. Phenotypically *pp2a* double mutant combinations were ABA hyposensitive during seed germination and stomatal closure but hypersensitive to ABA in root growth assays. Together, our data add PP2A-type phosphatases as another family of protein phosphatases into the interaction network of SnRK2-type protein kinases.

RESULTS

Generation and functional characterization of OST1-HF lines

The SnRK2-type protein kinase OST1 was fused at its C-terminus to a 6xHis-3xFLAG (HF)-tag, resulting in the OST1-HF construct. As a control a green fluorescent protein GFP-HF fusion was generated. Further, the kinase inactive $OST1_{DA}$-HF, harboring the D140A mutation in the proton acceptor site (http://www.uniprot.org/uniprot/Q940H6), the $OST1_{SA}$-HF, harboring the S175A mutation of the major phosphorylaton site in the activation loop (Umezawa et al., 2009; Vlad et al., 2009) and the $OST1_{\Delta C}$-HF construct, with deletion of the DII-domain/ABA-box (amino acids P319-M362; Belin et al., 2006; Yoshida et al., 2006), were generated. All constructs, driven by the pUBQ10 promoter, were transformed into the *ost1-3* mutant in the Col-0 background (SALK_008068; Yoshida et al., 2002) and proper expression was verified by western blot and anti-FLAG immunodetection (Supplemental Fig. S1A).

To confirm the functionality of the OST1-HF constructs, initial co-immunoprecipitation (co-IP) experiments were performed using the PP2C-type phosphatase ABI1 as positive control (Yoshida et al., 2006; Umezawa et al., 2009; Nishimura et al., 2010) and the fluorescent protein mVenus (Nagai et al., 2002) as negative control (Supplemental Fig. S1B). In these experiments, OST1-HF was probed for interaction with mVenus-ABI1 or mVenus, and HF-ABI1 was probed for interaction with mVenus-OST1 or mVenus (Supplemental Fig. S1B). After transient expression in *N. benthamiana* leaves purification of OST1-HF and HF-ABI1 did not result in co-purification of mVenus. In purified OST1-HF fractions mVenus-ABI1 was hardly detected, while HF-ABI1 co-purified mVenus-OST1 very efficiently (Supplemental Fig. S1B). These results suggest, that the HF-tag fused adjacent to the DII-domain/ABA-box of OST1 might interfere with PP2C-type phosphatase interaction (see Discussion).

OST1 loss of function mutants are characterized by a reduced leaf temperature, an impairment of stomatal closure in response to ABA and CO_2 and an enhanced water loss under low humidity and drought conditions (Merlot et al., 2002; Mustilli et al., 2002; Yoshida et al., 2002; Xie et al., 2006; Xue et al., 2011). ABA inhibition of seed germination and root growth was not drastically affected in *ost1-3* mutants (Yoshida et al., 2002; Fujii and Zhu 2009; Fujita et al., 2009).

ABA response analyses were performed to investigate whether the different OST1-HF constructs could complement the *ost1-3* mutant phenotype (Fig. 1). Seed germination analyses

revealed that *ost1-3*, *ost1-3*/GFP-HF and *ost1-3*/OST1$_{SA}$-HF (inactive activation loop mutant) exhibited a slight but significant ABA hyposensitivity when compared to Col-0 wild type at 0.5 µM ABA (Fig. 1A-C). *ost1-3*/OST1-HF and *ost1-3*/OST1$_{\Delta C}$-HF seed germination was comparable to Col-0 wild type (Fig. 1A-C). However, *ost1-3*/OST1$_{DA}$-HF seeds, over-expressing the inactive proton acceptor site mutation version, exhibited a much stronger pronounced ABA hyposensitivity when compared to the other investigated lines (Fig. 1A,B yellow line and Fig. 1C). Also in cotyledon expansion/greening assays the kinase inactive *ost1-3*/OST1$_{DA}$-HF and *ost1-3*/OST1$_{SA}$-HF lines exhibited a significantly reduced ABA sensitivity (Fig. 1D), indicating a dominant negative effect of over-expressed inactive OST1 versions. When 4-day-old seedlings were transferred to 0.5 MS media supplemented with 10 µM ABA root growth of *ost1-3*/OST1-HF was strongly inhibited in comparison to the other investigated lines and to *ost1-3*/OST1-HF grown on control media (Fig. 1E,F). Also *ost1-3*/OST1$_{\Delta C}$-HF exhibited a slight but significant ABA hypersensitivity in the root growth assay (Fig. 1E,F). Investigations of ABA-induced stomatal closure revealed that only the OST1-HF wild type construct could complement the *ost1-3* mutant phenotype (Fig. 1G), consistent with Col-0 wild type-like wilting kinetics after rosette leaves were detached from the roots (Supplemental Movie S1). Note, that also stomata of *ost1-3*/GFP-HF plants responded slightly to ABA (Fig. 1G).

Taken together, while over-expression of inactive OST1 versions induces a dominant negative effect in seed germination and cotyledon expansion/greening (Fig. 1A-D), OST1-HF and OST1$_{\Delta C}$-HF over-expression renders plant roots hypersensitive to ABA (Fig. 1E,F), but only OST1-HF rescues the stomatal ABA response (Fig. 1G) and the accelerated wilting phenotype of *ost1-3* (Supplemental Movie S1). These data provide evidence for the *in planta* functionality of OST1-HF. Together with the reduced interaction of OST1-HF with mVenus-ABI1 (Supplemental Fig. S1B), the OST1-HF construct could enable the identification of novel OST1-interacting proteins.

OST1-HF protein complex isolations and validations of interactions

Protein complex isolations of transgenic Arabidopsis lines were conducted on 15-day-old seedlings as described in Materials and Methods. LC-MS/MS acquired peptide data were collected from seven experiments treated with 200 mM sorbitol for 5, 30 or 60 min and from seven experiments treated with 50 µM ABA for 30 or 60 min. For each treatment three

experiments were performed on *ost1-3*/OST1-HF and three on *ost1-3*/GFP-HF as background control. In addition one experiment was conducted on *ost1-3*/OST1$_{\Delta C}$-HF treated with 200 mM sorbitol and one experiment on *ost1-3*/OST1$_{DA}$-HF treated with 50 μM ABA. A list of all experiments is provided in Supplemental Table S1. From all experiments a total of 120299 peptides were identified and probed against the TAIR10 protein database. OST1-interacting proteins were either identified through only unique peptides (Supplemental Table S2) or through any peptide, which matches the respective protein sequence (Supplemental Table S3). Note that Supplemental Table S2 and Supplemental Table S3 list only proteins which were not detected in the respective *ost1-3*/GFP-HF background control experiments. Only proteins identified in at least three experiments or with ten peptides were considered as potential OST1-interacting proteins.

Based on these data potential OST1-interacting proteins were selected for further analyses. These proteins are labeled in red in Supplemental Table S2 and Supplemental Table S3 and listed in Table I. PP2C-type phosphatases were not detected in our analyses, most likely due to the HF-tag fusion C-terminal of the OST1 DII-domain/ABA-box. Also other known OST1-interacting proteins or substrates (see Introduction) were not detected. Our analyses detected 3-5 SnRK2-type protein kinases and 5-7 type 2A protein phosphatase subunits by unique or non-unique peptides (Table I; Supplemental Table S2; Supplemental Table S3). Top candidate OST1-interacting protein was the UDP-D-glucose 4 epimerase 2 (UGE2), which was identified in all OST1-HF purifications (Table I).

Subcellular localization analyses (Supplemental Fig. S2A), protein-protein interaction analyses using bimolecular fluorescence complementation (BiFC) (Supplemental Fig. S2B,C) and co-IP analyses (Supplemental Fig. S2D) were performed on proteins listed in Table I. OST1-interacting proteins were localized in various subcellular compartments, including the plasma membrane and tonoplast (NPC4), the nucleus and nuclear bodies (OIP1 and RS31a), the chloroplast envelope membrane (SFR2) or punctuate structures (OIP6 and OIP26) (Supplemental Fig. S2A). In general the subcellular localization of the OST1-interacting protein determined the subcellular localization of its complex with OST1, which was investigated using BiFC (Supplemental Fig. S2B,C). In BiFC analyses UDP-D-glucose 4 epimerase 2 (UGE2) and the non specific phospholipase C4 (NPC4) exhibited the strongest BiFC emission, which was comparable to the interaction of OST1 with the PP2C-type phosphatase ABI1 (Supplemental

Fig. S2C top graph). Only OIP26, which located in punctuate structures (Supplemental Fig. S2A bottom right image), did not form complexes with OST1 in BiFC analyses (Supplemental Fig. S2B bottom right image and Supplemental Fig. S2C bottom graph). In co-IP analyses all investigated HF-tagged OST1-interacting proteins could efficiently co-purify mVenus-OST1 or (mT)urquoise-OST1 (Supplemental Fig. S2D). Note, that OIP1-, OIP4- and the galactolipid-remodeling enzyme sensitive to freezing 2 (SFR2)-HF proteins were not detected by anti-FLAG detection after immunoprecipitation (Supplemental Fig. S2D right panel), indicating a low expression level or an inefficient purification of these proteins. However, in these co-IP analyses mT-OST1 was still co-purified (Supplemental Fig. S2D right panel).

OST1 interacts with SnRK2-type protein kinases in BiFC and co-IP analyses

One major finding from the *in vivo* SnRK2 kinase OST1 protein complex isolations was that 3-5 other SnRK2-type protein kinases co-purified with OST1-HF (Table I; Supplemental Table S2; Supplemental Table S3). Subcellular localization analyses using (mT)urquoise fusion proteins revealed that SnRK2.2, SnRK2.3, OST1 and SnRK2.8 localized in the cytoplasm and the nucleus, similar to the PP2C-type phosphatase ABI1 (Fig. 2A). BiFC analyses indicated OST1 interactions with the respective SnRK2-type protein kinases in the cytoplasm and the nucleus, and also with ABI1, used as a positive control (Fig. 2B). Quantification of the BiFC emissions indicated a stronger OST1-OST1 homodimer vs. OST1-SnRK2 heterodimer formation (Fig. 2C). OST1 and SnRK2 interactions were weaker compared to the OST1 and ABI1 interaction (Fig. 2C). In co-IP analyses SnRK2-HF and mT-OST1 (Fig. 2D) or OST1-HF and (mT)urquoise-SnRK2 interactions were investigated (Fig. 2E). In these analyses, OST1-OST1 homodimerization and OST1-SnRK2 heterodimerizations were confirmed (Fig. 2D,E). Note, that in western blot analyses of the raw protein extracts, indicated as ‘Input’ in Fig. 2D,E, OST1-HF was not always detected. However after HF-purification (IP), OST1-HF was likely enriched and clearly detected (Fig. 2D top panel and Fig. 2E left panel). Taken together, protein complex isolations, BiFC and co-IP analyses provide evidence for OST1-OST1 and OST1-SnRK2-type protein kinase interactions.

SnRK2-type protein kinases form an interaction network with regulatory PP2AA- and PP2AB'-subunits

Interaction of the SnRK2-type protein kinase OST1 with the PP2A-type phosphatase regulatory subunit PP2AB'beta (Supplemental Fig. S2) and the identification of 5-7 PP2A-subunits in the OST1-HF protein complex isolations (Table I) raised the question whether OST1 generally interacts with PP2A-type phosphatases. Therefore initial BiFC analyses were conducted to investigate interactions of OST1 with all three regulatory PP2AA-, three regulatory PP2AB'-(PP2AB'alpha, PP2AB'beta and PP2AB'delta) and all five catalytic PP2AC-subunits (Supplemental Fig. S3A,D). In these analyses BiFC emissions were observed for all OST1 and PP2A-type phosphatase subunit combinations, however with very low BiFC emissions of OST1 and the catalytic PP2AC-subunit complexes (Supplemental Fig. S3D inset). In general OST1 and PP2A-subunit complexes were localized in the cytoplasm and the nucleus, with the exception of OST1 and the regulatory subunit PP2AB'delta interaction, which was not detected in the nucleus (Supplemental Fig. S3A top right panel). In addition, OST1 interaction with the regulatory PP2AB'beta- and PP2AB'delta-subunits and with the catalytic PP2AC-subunits was also observed in punctuate structures (Supplemental Fig. S3A arrows). Additional analyses were conducted to investigate whether PP2A-type phosphatase subunits form an interaction network with SnRK2-type protein kinases. Therefore the regulatory PP2A-subunits PP2AA1 (RCN1) and PP2AB'beta were probed for interactions with the ABA-activated SnRK2.2, SnRK2.3 and OST1 protein kinases in BiFC analyses (Supplemental Fig. S3B,C,E,F). Results indicated interactions of RCN1 (Supplemental Fig. S3B) and of PP2AB'beta (Supplemental Fig. S3C) with all three investigated SnRK2-type protein kinases in the cytoplasm and the nucleus. Compared to the OST1 and ABI1 BiFC emission, the RCN1 and SnRK2 BiFC emission was 41-67 % (Supplemental Fig. S3E) and the PP2AB'beta and SnRK2 BiFC emission was 9-11 % (Supplemental Fig. S3F).

The SnRK2-type protein kinase and PP2A-type phosphatase subunit interaction network was further investigated using co-IP analyses. In these analyses the regulatory PP2A-subunits PP2AA1 (RCN1) and PP2AB'beta were fused to the HF-tag and co-expressed with (mT)urquoise-tagged SnRK2-type protein kinases or (mT)urquoise alone, which was used as a negative control (Fig. 3A,B). The results clearly demonstrate, that purification of RCN1-HF (Fig. 3A) and HF-PP2AB'beta (Fig. 3B) could efficiently co-purify the SnRK2-type protein kinases

SnRK2.2, SnRK2.3 and OST1, but not mTurquoise alone (Fig. 3A,B anti-GFP blots). In additional experiments the SnRK2-type protein kinase OST1 fused to the HF-tag was co-expressed with (mT)urquoise- (Goedhart et al., 2010) or mVenus-tagged PP2A-subunits or with (mT)urquoise alone (Fig. 3C,D). Purification of OST1-HF efficiently co-purified the regulatory PP2AA-subunits RCN1 and PP2AA3, but not PP2AA2 and (mT)urquoise (Fig. 3C). Also the regulatory PP2AB'alpha, -B'beta and -B'delta-subunits were efficiently co-purified with OST1-HF (Fig. 3D), consistent with data of our protein complex isolations (Table I). Co-purification of the catalytic PP2AC3-subunit with OST1-HF was barely detected (Fig. 3D). These results were consistent with the very low BiFC fluorescence emission of OST1 and PP2AC-subunits in BiFC analyses (Supplemental Fig. S3D inset).

In summary, BiFC and co-IP analyses revealed strong evidence for the formation of a protein-protein interaction network between SnRK2-type protein kinases with PP2A-type phosphatase regulatory PP2AA- and PP2AB'-subunits.

PP2A-type phosphatase subunit mutants exhibit altered ABA responses

PP2A-subunits are known to be involved in ABA responses. In the Arabidopsis Ws accession the regulatory subunit mutant *rcn1-1* exhibited ABA hyposensitive phenotypes, while the single catalytic subunit mutant *pp2ac2* was ABA hypersensitive (Kwak et al., 2002; Pernas et al., 2007). For our analyses, we used T-DNA insertion lines in the Columbia-0 (Col-0) accession as described in Materials and Methods. Currently it is unknown, which regulatory PP2AB-subunits function in ABA responses. Because the Arabidopsis genome encodes for seventeen PP2AB-subunits including nine PP2AB'-subunits (Farkas et al., 2007), we focused on functional characterizations of regulatory PP2AA-subunits and on catalytic PP2AC-subunits.

Seed germination analyses in response to 1 μM ABA revealed a reduced ABA sensitivity of the regulatory PP2AA-subunit mutant *rcn1-6* and of the catalytic PP2AC-subunit mutants *pp2ac3*, *pp2ac4* and *pp2ac5* (Fig. 4A,B). Seed germination of these lines was significantly inceased when grown on 0.5 MS media supplemented with 1 μM ABA and compared to Col-0 wild type on day four after stratification (Fig. 4C). Also a significantly higher amount of *rcn1-6* mutant seedlings were green with expanded cotyledons on day seven after stratification (Fig. 4C). ABA sensitivities of *pp2aa3* and *pp2ac2* mutant lines were similar to Col-0 wild type (Fig. 4).

Analysis of seedling growth on 0.5 MS media supplemented with or without 5 μM ABA was compared to the ABA insensitive *abi1-1* mutant in the Col-0 background (Supplemental Fig. S4). In contrast to *abi1-1*, which was insensitive to ABA, the *pp2a* mutants exhibited a root growth reduction similar to Col-0 wild type in response to ABA (Supplemental Fig. S4B). Note that *rcn1-6* exhibited an agravitropic root growth on control media, which was further enhanced in the presence of 5 μM ABA (Supplemental Fig. S4A).

In Arabidopsis PP2A ternary complexes could potentially consist of 255 different PP2A-subunit combinations. We further investigated ABA responses of regulatory PP2AA- and catalytic PP2AC-subunit double mutant combinations, in which only a limited number of potential PP2A-type phosphatase ternary complexes can be formed. The regulatory PP2AA1-subunit RCN1 plays a major role in PP2A-type phosphatase regulation in the Ws accession (Zhou et al., 2004; Michniewicz et al., 2007). Therefore also *rcn1-6* and *pp2ac* double mutant combinations were generated and functionally analyzed.

In seed germination and cotyledon expansion/greening assays on 0.5 MS control media, the investigated double mutant combinations exhibited germination rates and seedling growth similar to Col-0 wild type (Fig. 5A,C,D). However, in response to 0.8 μM ABA all investigated *rcn1-6/pp2ac* and *pp2ac* double mutant combinations exhibited an ABA hyposensitive increased seed germination rate when compared to Col-0 wild type (Fig. 5B). In particular, on day four after stratification seed germination of *rcn1-6/pp2ac2*, *rcn1-6/pp2ac5*, *pp2ac3/pp2ac5* and *pp2ac4/pp2ac5* was significantly increased and ≥ 2-fold higher compared to Col-0 wild type (Fig. 5C). The number of seedlings with green and expanded cotyledons on day six after stratification was significantly higher for *rcn1-6/pp2ac2*, *rcn1-6/pp2ac5* and *pp2ac3/pp2ac5* (Fig. 5D). The *rcn1-6/pp2ac3* double mutant had no significant effect on ABA inhibition of seed germination and cotyledon expansion in these experimental conditions (Fig. 5C,D).

In contrast to the reduced ABA sensitivity during seed germination, the *rcn1-6/pp2ac2*, *pp2ac3/pp2ac5* and *pp2ac4/pp2ac5* double mutants exhibited a significantly enhanced sensitivity to 5 μM ABA in root growth assays (Fig. 5E,F). Root growth of these mutants was inhibited to 42-60 % of control conditions compared to 70 % of *rcn1-6/pp2ac5* and 91 % of Col-0 wild type (Fig. 5F). Interestingly, when grown on control media, all investigated *rcn1-6/pp2ac* double mutants exhibited an *rcn1-6*-like agravitropic root growth phenotype (Fig. 5E top row and

Supplemental Fig. S4E). Such agravitropic root growth was also observed for *pp2ac3/pp2ac5* but not for *pp2ac4/pp2ac5* (Fig. 5E top row).

None of the investigated *rcn1-6/pp2ac* and *pp2ac* double mutant combinations in the Col-0 accession exhibited altered responses for ABA-induced stomatal closure (Fig. 5G). Therefore we investigated stomatal responses of regulatory *pp2aa* double mutant combinations (Fig. 6). Stomata of Col-0 wild type and the *pp2aa2-1/pp2aa3-1* double mutant significantly responded to 5 µM ABA and closed to 75 % and 86 % of apertures in control conditions (Fig. 6). In contrast, stomata of the *rcn1-6/pp2aa2-1* and *rcn1-6/pp2aa3-1* double mutants did not respond significantly to 5 µM ABA (Fig. 6). Note that the *rcn1-6/pp2aa2-1* and *rcn1-6/pp2aa3-1* double mutants exhibited a strongly reduced growth when compared to Col-0 wild type and the *pp2aa2-1/pp2aa3-1* double mutant (Supplemental Fig. S5). These data are consistent with a previous report on *rcn1-1/pp2aa2-1* and *rcn1-1/pp2aa3-1* double mutants (Zhou et al., 2004). In summary, disruption of PP2A activity renders Arabidopsis Col-0 plants less sensitive to ABA during seed germination and stomatal closure but hypersensitive to ABA during seedling development.

Regulatory PP2AA- and catalytic PP2AC-subunits interact in BiFC and yeast-two-hybrid analyses

Due to the huge numbers of potential PP2A-type phosphatase ternary complexes, knowledge of PP2A-subunit expression, subcellular localization and interaction patterns is essential for understanding PP2A-type phosphatase function. BiFC- (Fig. 7) subcellular localization- (Supplemental Fig. S6) and yeast-two-hybrid analyses (Supplemental Fig. S7) were performed to investigate whether PP2AA- and PP2AC-subunit interactions and PP2A-subunit localizations correlate with the observed differences in ABA responses of *pp2a* single and double mutants (Fig. 4 and Fig. 5). BiFC emission was observed for all possible regulatory PP2AA- and catalytic PP2AC-subunit combinations (Fig. 7) Protein complexes of PP2AA1 (RCN1) (Fig. 7A), PP2AA2 (Fig. 7B) and PP2AA3 (Fig. 7C) with PP2AC-subunits were located predominantly in the cytoplasm. However, the single PP2AA- and PP2AC-subunit proteins fused to (mT)urquoise or mVenus localized in the cytoplasm and the nucleus (Supplemental Figure S6A,B), while PP2AB-subunits were differentially distributed within the cell (Supplemental Figure S6C-E). Although the PP2AA- and PP2AC-subunit BiFC emissions were relatively weak for all

complexes, differences in emission intensities were detected, indicating a reduced interaction of RCN1 with PP2AC5 (Fig. 7D). PP2AA2 interacted predominantly with PP2AC3 (Fig. 7E) and PP2AA3 with PP2AC3-PP2AC5 (Fig. 7F). Yeast-two-hybrid analyses confirmed the broad interaction spectrum of PP2AA- and PP2AC-subunits (Supplemental Fig. S7). However, in our experimental condition PP2AA3 did not interact with PP2AC4 in yeast-two-hybrid analyses (Supplemental Fig. S7C).

Taken together regulatory PP2AA- and catalytic PP2AC-subunits form a broad interaction spectrum of complexes which are localized mainly in the cytoplasm. The single fluorescent protein-fused PP2AA- and PP2AC-subunits were also observed in the nucleus. Regulatory PP2AB-subunits were more diversely localized, which is consistent with their proposed roles in subcellular targeting of PP2A-type phosphatase complexes (DeLong, 2006; Farkas et al., 2007).

DISCUSSION

Design and ABA responses of OST1-HF lines

The SnRK2-type protein kinase OST1 is one of the major ABA signaling components in guard cells (Merlot et al., 2002; Mustilli et al., 2002; Yoshida et al., 2002; Xie et al., 2006; Acharya et al., 2013). Our goal was the identification of novel OST1-interacting proteins using *in planta* protein complex isolations followed by LC-MS/MS analyses. We ubiquitously expressed OST1-HF constructs, including inactive D140A and S175A mutations, and the C-terminally truncated $OST1_{\Delta C}$-HF construct, lacking the DII-domain/ABA-box, in the *ost1-3* mutant background (Supplemental Fig. S1A). From these constructs only OST1-HF could complement guard cell related phenotypes of *ost1-3* (Fig. 1G and Supplemental Movie S1), indicating that these responses require the active kinase and the DII-domain/ABA-box. These results were consistent with previous reports, which analyzed the ABA activation and phenotypes of similar constructs (Belin et al., 2006; Yoshida et al., 2006; Boudsocq et al., 2007). Interestingly ectopic expression of OST1-HF rendered roots hypersensitive to ABA (Fig. 1E,F). Similarly, over-expression of the ABA receptors PYR1, PYL2 and PYL5, as positive regulators of ABA signaling, enhances ABA sensitivity (Santiago et al., 2009; Mosquna et al., 2011; Waadt et al., 2014b), while over-expression of the PP2C-type phosphatases ABI1 and HAB1, as negative regulators, decreases ABA sensitivity (Santiago et al., 2009; Nishimura et al., 2010). However, the enhanced ABA

sensitivity of the *ost1-3*/OST1-HF line could also be explained by the strongly reduced interaction of OST1-HF with the PP2C-type phosphatases ABI1 (Supplemental Fig. S1B), resulting in an inefficient inhibition of OST1-HF by ABI1 or probably also other Group A PP2C-type phoshpatases. Expression of the inactive $OST1_{DA}$-HF construct resulted in a reduced ABA sensitivity during seed germination and young seedling development (Fig. 1B-D). $OST1_{DA}$-HF might compete with endogenous ABA-activated SnRK2-type protein kinases for substrate binding and thereby inhibiting ABA responses. These data are consistent with the inhibition of ABA responses in *Vicia faba* guard cells through over-expression of an ABA-activated protein kinase AAPK, which was inactivated through a mutation in the ATP-binding site (Li et al., 2000).

Identification of OST1-interacting proteins

LC-MS/MS analyses of proteins co-purified with OST1-HF identified several potential OST1-interacting proteins (Table I and Supplemental Tables S2-S4). However, none of the known OST1 substrates (see introduction) were identified in our analyses. Three possible reasons could explain this result: 1) low protein abundance of known OST1-interacting proteins in total protein extracts due to tissue specific expression (e.g. guard cells), 2) reduced interactions of OST1-HF with PP2C-type phosphatases due to the HF-tag fusion adjacent to the DII-domain/ABA-box (Supplemental Fig. S1B) and 3) OST1 interactions with substrates can be transient and may occur only during signaling. The present analyses demonstrate the interactions of various proteins previously not known to interact with SnRK2-type protein kinases. These interactions have been confirmed using co-IP and, except for OST1 and OIP26 interaction, also in BiFC analyses (Supplemental Fig. S2). Below we discuss some interesting aspects of novel OST1-interacting proteins.

Novel OST1 interactors are implicated in lipid metabolism

Among the top OST1-interacting protein candidates identified in the *in planta* protein complex isolations were the UDP-D-glucose 4 epimerase 2 (UGE2), the non specific phospholipase C4 (NPC4) and the galactolipid-remodeling enzyme sensitive to freezing 2 (SFR2) (Table I). BiFC of OST1 with UGE2 and NPC4 exhibited the strongest fluorescence emission, when compared to

OST1 with ABI1 and other OST1 interactors (Supplemental Fig. S2C). Co-IP analyses confirmed interactions of OST1 with UGE2, NPC4 and SFR2 (Supplemental Fig. S2D).

NPC4 hydrolyzes phosphatidylcholin or phosphatidylethanolamine to produce P_i-containing headgroups and diacylglycerol and has been implicated in phosphate recycling from phospholipids during phosphate deprivation (Nakamura et al., 2005). Diacylglycerol produced by NPC4 can be converted to phosphatidic acid, which acts as a signaling molecule and is also involved in ABA signaling (Jacob et al., 1999; Testerink and Munnik, 2005; Peters et al., 2010). Analyses of *npc4* mutants revealed its role in salt-, osmotic stress and ABA responses (Peters et al., 2010; Kocourcová et al., 2011).

UGE activity has been implicated to provide UDP-Galactose for cell wall and for galactolipid biosynthesis (Dörmann and Benning 1998; Rösti et al., 2007). Galactolipids are synthesized at the chloroplast envelope membranes from UDP-galactose and diacylglycerol to produce monogalactosyldiacylglycerol which can be further processed to digalactosyldiacylglycerol (Moellering and Benning, 2011). Both of these galactolipids are substrates of OST1-interacting protein SFR2 (Table I, Supplemental Fig. S2), which produces oligogalactolipids and diacylglycerol (Benning and Ohta, 2005; Moellering et al., 2010; Moellering and Benning, 2011). SFR2 was originally identified through a screen for mutants sensitive to freezing (Warren et al., 1996; Thorlby et al., 2004). Interestingly, SFR2 activity was also induced by osmotic stress and dehydration (Moellering et al., 2010) and the modulation of lipid compositions is known to occur in response to abiotic stresses (Moellering and Benning, 2011). Thus NPC4, UGE2 and SFR2 might be involved in ABA-mediated responses to abiotic stresses through membrane lipid remodeling, which could be regulated through OST1.

OST1 interacts with other SnRK2-type protein kinases

One major finding of the *in planta* protein complex isolations was, that OST1 formed OST1-OST1 homo- and OST1-SnRK2-type protein kinase heterodimer complexes (Table I), which was confirmed for SnRK2.2, SnRK2.3 and SnRK2.8 in BiFC and co-IP analyses (Fig. 2). Such complexes could contribute to the amplification of the SnRK2 phosphorylation- and activation status through *trans*-(auto)phosphorylation. *In vitro trans*-(auto)phosphorylation of OST1 has been reported (Ng et al., 2011). Analyses of recombinant OST1 protein suggested a monomeric status of OST1 (Yunta et al., 2011). However, the present study provides evidence, that SnRK2-

type protein kinases form oligomers *in planta* (Table I and Fig. 2). This might indicate that other plant components are needed for SnRK2-type protein kinase oligomerization *in planta*.

SnRK2-type protein kinases interact with type 2A protein phosphatase regulatory subunits

Among the potential OST1-interacting proteins identified from the *in planta* protein complex isolations were 5-7 PP2A-type phosphatase subunits (Table I). More detailed analyses revealed, that OST1 interacted with regulatory PP2AA- and PP2AB'-subunits in co-IP and BiFC analyses (Fig. 3, Supplemental Fig. S3). In addition interactions were also confirmed for the regulatory subunits PP2AA1 (RCN1) and PP2AB'beta with three ABA-activated SnRK2-type protein kinases (Fig. 3 and Supplemental Fig. S3). These data suggest a broad interaction network between SnRK2-type protein kinases and PP2A-type phosphatases besides the well-established interactions of SnRK2-type protein kinases with type 2C protein phosphatases (Yoshida et al., 2006; Umezawa et al., 2009; Vlad et al., 2009; Nishimura et al., 2010).

PP2A-type phosphatases function in ABA responses

Earlier studies on PP2A-type phosphatase subunit mutants in the Arabidopsis Ws accession revealed a reduced ABA sensitivity of the regulatory PP2AA-subunit mutant *rcn1-1* in seed germination and stomatal responses (Kwak et al., 2002; Saito et al., 2008) and an ABA hypersensitivity of the catalytic subunit mutant *pp2ac2* in seed germination and root growth (Pernas et al., 2007). Our analyses on PP2A-subunit mutants in the Arabidopsis Col-0 accession revealed a reduced ABA sensitivity in seed germination assays of *pp2a* single mutants, including *rcn1-6*, and of *rcn1-6/pp2ac* and *pp2ac* double mutants (Fig. 4B-D and Fig. 5B-D). We did not observe any altered ABA responses of the catalytic *pp2ac2* single mutant in our experimental conditions (Fig. 4 and Supplemental Fig. S4). For stomatal responses, a reduced ABA sensitivity of the PP2AA-subunit mutant *rcn1-6* was observed in combination with *pp2aa2-1* or *pp2aa3-1* mutants (Fig. 6), but not in combination with catalytic *pp2ac* mutants. The differences between ABA responses in Ws compared to Col-0 may result from altered expression levels between natural accessions of Arabidopsis. Gene dosages of regulatory PP2AA-subunits were discussed to be important for PP2A-type phosphatase function (DeLong, 2006). Consistently, PP2A-type phosphatase activity in Ws was measured to be four-fold higher compared to Col-0 (Hu et al., 2014).

The regulatory PP2AA-subunit mutant *rcn1-6* exhibited an enhanced root curling in presence of ABA (Supplemental Fig. S4A), and ABA sensitivity of root curling and growth was strongly increased in *rcn1-6/pp2ac* and catalytic subunit *pp2ac* double mutants (Fig. 5E,F). Our ABA response analyses indicate that PP2A-type phosphatases function as positive regulators of ABA responses in seeds and guard cells but as negative regulators in roots. Previous studies on stomatal ABA responses using the PP2A-type phosphatase inhibitor okadaic acid provided evidence that PP2A-type phosphatases function as negative regulators of ABA-responses in *Pisum sativum* and *Vicia Faba* (Schmidt et al., 1995; Hey et al., 1997), but as positive regulators in Arabidopsis (Pei et al., 1997; Kwak et al., 2002). PP2A-type phosphatases function not only in ABA responses but also in other plant hormone and light responses (Lillo et al., 2014). Arabidopsis plants with mutations in PP2A-type phosphatase subunits are characterized by enhanced ethylene levels and ethylene responses (Larsen and Cancel, 2003; Muday et al., 2006; Skottke et al., 2011), altered auxin transport (Garbers et al., 1996; Rashotte et al., 2001; Muday et al., 2006; Michniewicz et al., 2007; Ballesteros et al., 2012) and an enhanced blue light-induced stomatal opening (Tseng and Briggs, 2010). These findings suggest that the observed differences in ABA responses of PP2A-type phosphatase mutants might be a result of their direct interactions with ABA-activated SnRK2-type protein kinases and cross talk with auxin, ethylene and blue light responses.

PP2AA- and PP2AC-subunits interact *in vivo* and PP2AB'-subunits are differentially localized

Information about the subcellular distributions and interaction patterns of PP2A-type phosphatase subunits is essential for understanding their cellular functions. There is limited knowledge about interaction patterns among PP2A-subunits (Haynes et al., 1999) and subcellular localizations are known for the regulatory PP2AA- and for six PP2AB'-subunits (Blakeslee et al., 2008; Matre et al., 2009; Tang et al., 2010; Trotta et al., 2011; Tran et al., 2012). We performed comprehensive interaction analyses of all three regulatory PP2AA- and all five catalytic PP2AC-subunits and detected a broad interaction spectrum using BiFC (Fig. 7) and yeast-two-hybrid analyses (Supplemental Fig. S7). Interestingly, while all regulatory PP2AA and catalytic PP2AC complexes localized in the cytoplasm (Fig. 7), single PP2AA- and PP2AC-subunits were detected also in the nucleus (Supplemental Fig. S6A,B). Regulatory PP2AB-

subunits are thought to be necessary for the subcellular targeting of PP2A holoenzyme complexes (DeLong, 2006; Farkas et al., 2007). This hypothesis is supported by diverse localization patterns of PP2AB-subunits (Supplemental Fig. S6C-E).

CONCLUSIONS

The identification of interacting proteins or substrates of ABA-activated SnRK2-type protein kinases is crucial for unraveling the ABA signaling network and its communication with other signaling pathways. We performed *in vivo* protein complex isolations of the SnRK2-type protein kinase OST1 and identified novel OST1-interacting proteins using LC-MS/MS and confirmed selected interactions using co-IP and BiFC analyses. Our major findings were: 1) OST1 forms homodimers and heterodimers with other SnRK2-type protein kinases, 2) OST1 interacts with enzymes involved in lipid metabolism, and 3) SnRK2-type protein kinases form complexes with regulatory subunits of type 2A protein phosphatases. Further analyses of PP2A-type phosphatases added new findings about the role of regulatory PP2AA- and catalytic PP2AC-subunits in ABA responses which might be directly linked to SnRK2-type protein kinase interactions and potentially also to cross talk with other signaling pathways.

MATERIALS AND METHODS

T-DNA lines and genotyping

T-DNA lines were obtained from the Arabidopsis Biological Resource Center and from the Nottingham Arabidopsis Stock Centre. T-DNA insertions were confirmed by PCR on genomic DNA and sequencing of the left- and right-borders. Genomic DNA was isolated using the CTAB method (Stacey and Isaak, 1994). RNA was isolated using the RNeasy Plant Mini Kit (Quiagen) and reverse transcribed using the First-Strand cDNA Synthesis Kit and Not I $d(T)_{18}$ primers (GE Healthcare). Mutant status was confirmed by RT-PCR (38 cycles) including actin2 as expression control.

The following T-DNA lines in Columbia-0 accession were used in this work: *ost1-3* (SALK_008068; Yoshida et al., 2002), *rcn1-6* (SALK_059903; Blakeslee et al., 2008), *pp2aa2-1* (SALK_042724; Zhou et al., 2004), *pp2aa3-1* (SALK_014113; Zhou et al., 2004), *pp2aa3-2* (SALK_099550; Zhou et al., 2004), *pp2ac2* (GK-072G03), *pp2ac3* (SALK_035009), *pp2ac4* (GK-089F04), *pp2ac5* (SALK_139822; Tang et al., 2010).

Plant growth and ABA response assays

Arabidopsis seeds were surface sterilized in 70 % EtOH and 0.04 % SDS followed by three washes in 100 % EtOH and sown on 0.5 MS media (Sigma) (pH 5.8) supplemented with 0.8 % Phyto Agar (RPI). After four days of stratification at 4 °C in the dark, plants were grown in a growth room in long day conditions (16 h light/8 h dark) with 50 - 80 µE m^{-2} s^{-1} light intensity at 25-27 °C and 25-30 % relative humidity. Six-day-old seedlings were transferred to pots and either grown in the growth room or in a Conviron CMP3244 plant growth chamber with 16 h day, 22 °C/8 h night, 18 °C cycle and 50-100 µE $m^{-2}s^{-1}$ and 40-50 % relative humidity.

ABA response assays were performed as described previously (Waadt et al., 2014b). Seed germination assays were performed in the growth room on 0.5 MS agar media supplemented with 0.5 or 0.8 µM (+)-ABA (TCI) or 1 µM (+/-)-ABA (Sigma) or the respective concentration of EtOH as solvent control. Analyses represent mean values ± SEM of four technical replicates normalized to the seed count of each experiment. Root growth assays were performed on four-day old seedlings, which were transferred to 0.5 MS agar media supplemented with 5-10 µM ABA or the respective concentration of EtOH as solvent control and grown vertically in the growth room for additional 5 days. Root length was measured using Fiji (http://fiji.sc/Fiji; Schindelin et al., 2012) or the Root Detection software (http://www.labutils.de/rd.html) and analyzed as means of seven seedlings ± SEM of 4-5 technical replicates and normalized to the 0.5 MS control conditions.

ABA-induced stomatal closure analyses were performed with detached leaves of 3-5-week-old plants, which were floated in stomatal assay buffer [5 mM KCl, 50 µM $CaCl_2$ and 10 mM MES-Tris pH 6.15 (*pp2a* mutants) or pH 5.6 (*ost1-3* and OST1-HF lines)] for 2 hours. Subsequently, 5-10 µM (+)-ABA or the respective concentration of EtOH as solvent control was added to the opening buffer followed by an additional 2 hour incubation. Leaf epidermal tissue was isolated using the blending method and images were acquired using an inverted light microscope. Stomatal apertures were measured using Fiji Schindelin et al., 2012). Data represent mean stomatal apertures ± SEM of three to six experiments normalized to the solvent control.

For the dry down experiment, rosettes of each genotype were cut from plants grown in soil in the growth chamber, placed immediately on dry Whatman paper and imaged every 0.5

min for 30 min. Significance of data were analyzed in R (Team, 2010) using a one-way- or two-way ANOVA.

Subcellular localization and BiFC analyses

For subcellular localization analyses coding sequences were inserted into plant expression vectors harboring a pGPTVII.bar or pGPTVII.hyg backbone (Walter et al., 2004) and an expression cassette consisting of the pUBQ10 promoter (AT4G05310; Norris et al., 1993; Krebs et al., 2012) or the pUBQ10 driven beta-estradiol inducible system (Schlücking et al., 2013) and the HSP18.2 terminator (T) (AT5G59720; Nagaya et al., 2010) and fused to the fluorescent proteins mTurquoise (Goedhart et al., 2010) or (m)Venus (Nagai et al., 2002). Constructs for BiFC analyses were generated by ligation of coding sequences into hygII-SPYNE(R) and kanII-SPYCE(M) or kanII-SPYCE(MR) plasmids (Waadt et al., 2008). Plasmids were transformed into *Agrobacterium tumefaciens* GV3101 (pMP90; Koncz and Schell, 1986) and transiently expressed in leaves of 5-6-week-old *Nicotiana benthamiana* plants together with the p19 silencing suppressor as described (Waadt et al., 2014a). Subcellular localizations and BiFC analyses were performed by confocal microscopy as described previously (Waadt et al., 2014a; Waadt et al., 2014b).

***In vivo* protein complex isolations and co-immunopreciptation analyses**

Coding sequences were inserted into the pGPTVII.bar plant expression vector harboring either a pUBQ10 - NosT expression cassette (see above and Walter et al., 2004) and a 6xHis-3xFLAG (HF)-tag located 3' of the multiple cloning site or a pUBQ10 - HSP18.2T expression cassette and the HF- tag located 5' of the multiple cloning site and transformed into *Agrobacterium tumefaciens* GV3101 (pMP90; Koncz and Schell, 1986).

For *in vivo* protein complex isolations GFP-HF and $OST1_{(DA,\ SA,\ \Delta C)}$-HF constructs were transformed into the *ost1-3* mutant background (Yoshida et al., 2002) by the floral dip method (Clough and Bent, 1998). Transformants were selected on 0.5 MS agar plates supplemented with 10 μg/mL glufosinate and further selected by western-blot and anti-FLAG immuno-detection. Homozygous T_4 lines were sown on 0.5 MS agar plates (12 plates, 24 seedlings/plate) and grown vertically in the growth room for 15 days. For transient expression, *Agrobacteria* harboring HF-constructs, mTurquoise- or mVenus-tagged constructs and the p19 strain were co-transfected into

one *N. benthamiana* leaf and incubated for 3-4 days. Transient expression in *N. benthamiana* was performed as described (Waadt et al., 2014a).

Plant tissue was harvested and incubated for 1 h in 0.5 MS liquid media. Subsequently, media was exchanged by 0.5 MS liquid media + 200 mM sorbitol, or (+)-ABA was added to a final concentration of 50 µM followed by an incubation for 5, 30 or 60 min. Plant tissue was dried briefly using paper towels, frozen in liquid N_2 and extracted in SII-buffer (100 mM Na_2HPO_4/NaH_2PO_4, pH 8.0, 150 mM NaCl, 5 mM EDTA, 5 mM EGTA, 0.1 % Triton-X-100) supplemented with protease inhibitor (Roche), Phosphatase inhibitors 2 and 3 (Sigma) and 1 mM phenylmethylsulfonyl fluoride (PMSF). After 10 min of rotation at 4 °C, raw extracts were sonicated (20x 0.5 s on ice) followed by 20 min centrifugation at 20,000 *g* and filtration through a 0.45 syringe filter. Protein extracts were mixed with (1/100 v/v) Anti-FLAG M2 magnetic beads (Sigma) equilibrated in SII-buffer and rotated 4 h at 4 °C. Proteins bound to the Anti-FLAG M2 magnetic beads were concentrated using the DynaMag-2 magnetic particle concentrator (Invitrogen) and washed 3-4 times in ≥ 20 bead volumes of SII-buffer, followed by two washes in FLAG-to-His-buffer (100 mM Na_2HPO_4/NaH_2PO_4, pH 8.0, 150 mM NaCl, 0.05 % Triton-X-100). Proteins were eluted four times in one bead volume of FLAG-to-His-buffer supplemented with 500 µg/mL 3xFLAG peptide (Sigma) and stored at -80 °C. Western-blot and immuno-detection was performed using a mouse Anti-FLAG M2 antibody (Sigma) or rabbit monoclonal anti-GFP antibody (Invitrogen) followed by a secondary goat anti mouse or anti rabbit IgG (H + L) horseradish peroxidase-conjugate antibody (BioRad) as described (Waadt et al., 2014a).

For LC-MS/MS analyses proteins were precipitated by addition of 1/3 (v/v) of cold 100 % trichloracetic acid, 30 min incubation on ice and 30 min centrifugation at 20,000 *g* and 4 °C. Protein pellets were washed twice with 100 % ice cold acetone and 10 min centrifugation at 20,000 *g* and 4 °C, air dried and stored at -80 °C.

Mass Spectrometry and Data Analysis

Protein pellets were resolubilized by addition of 50 µl 0.2 % ProteaseMAX™ surfactant prepared in 50 mM ammonium bicarbonate and adjusted to 100 µL volume by addition of 8 M urea. Disulfide bonds in the proteins were reduced by addition of tris(2-carboxyethyl)-phosphine hydrochloride (TCEP) to a final concentration of 5 mM and incubated at room temperature for

20 min. Alkylation was performed in the dark by 10 mM Iodoacetamide treatment for 20 min. Samples were diluted to reduce the urea concentration to less than 2 M and proteins were digested overnight at 37 °C and 750 rpm using Sequencing Grade Modified Trypsin (Promega). Subsequently samples were acidified with formic acid at a final concentration of 5 % followed by a centrifugation at 14,000 rpm for 30 min. The peptide supernatant was transferred to a separate reaction tube and pressure-loaded into a biphasic trap column.

Mass spectrometric analysis of the samples was performed using MudPIT technology (Washburn et al., 2001). Capillary columns were prepared in-house from particle slurries in methanol. An analytical column was generated by pulling a 100 µm ID/360 µm OD capillary (Polymicro Technologies) to a 3 µm ID tip. The pulled column was packed with reverse phase particles (Aqua C18, 3 µm dia., 90 Å pores, Phenomenex) until 15 cm long. A biphasic trapping column was prepared by creating a Kasil frit at one end of an deactivated 250 µm ID/360 µm OD capillary (Agilent Technologies), which was then successively packed with 2.5 cm strong cation exchange particles (Partisphere SCX, 5 µm dia., 100 Å pores, Phenomenex) and 2.5 cm reverse phase particles (Aqua C18, 5 µm dia., 90 Å pores, Phenomenex). The trapping column was equilibrated using buffer A (5 % acetonitrile/0.1 % formic acid) prior to sample loading. After sample loading and prior to MS analysis, the resin-bound peptides were desalted with buffer A by flow through the trap column. The trap and analytical columns were assembled using a zero-dead volume union (Upchurch Scientific).

LC-MS/MS analysis was performed on LTQ OrbitrapVelos (Thermo Scientific) interfaced at the front end with a quaternary HP 1100 series HPLC pump (Agilent Technology) using an in-house built electrospray stage. Electrospray was performed directly from the analytical column by applying the ESI voltage at a tee (150 µm ID, Upchurch Scientific) directly downstream of a 1:1000 split flow used to reduce the flow rate (250 nL/min). A fully automated 4-step MudPIT run was performed on each sample using a three mobile phase system consisting of buffer A, buffer B (80 % acetonitrile/0.1 % formic acid), and buffer C (500 mM ammonium acetate/5 % acetonitrile/0.1 % formic acid). The first step was 60 min reverse-phase run, whereas three subsequent steps were of 120 min duration with different concentrations (10 %, 50 % and 100 %) of buffer C run for 4 min at the beginning of each of the gradient. Peptides were analyzed using a Top-20 data-dependent acquisition method. As peptides were eluted from the microcapillary column, they were electrosprayed directly into the mass spectrometer with the

application of a distal 2.4 kV spray voltage. For each cycle, full-scan MS spectra (*m/z* range 300-1600) were acquired in the Orbitrap with the resolution set to a value of 60,000 at *m/z* 400 and an automatic gain control (AGC) target of 1×10^6 ions and the maximal injection time of 250 ms. For MS/MS scans the target value was 5,000 or 10,000 ions with injection time of 25 ms. Once analyzed, the selected peptide ions were dynamically excluded from further analysis for 120 s to allow for the selection of lower-abundance ions for subsequent fragmentation and detection using the setting for repeat count = 1, repeat duration = 30 ms and exclusion list size = 500. Charge state filtering was enabled. The minimum MS signal for triggering MS/MS was set to 500 and an activation time of 10 ms was used. All tandem mass spectra were collected using normalized collision energy of 35 % and an isolation window of 2 h.

For protein identification an Integrated Proteomics Pipeline (IP2) software and a web-based proteomics data analysis platform were used (Integrated Proteomics Applications, Inc.). Tandem mass spectra were extracted from the Xcalibur data system format into MS2 format using RawXtract1.9.9.2. MS/MS spectra were searched with the ProLuCID algorithm against the TAIR10 database (downloaded January 2011) that was concatenated to a decoy database in which the sequence for each entry in the original database was reversed. The search parameters include 50 ppm peptide precursor mass tolerance and 0.6 Da for the fragment mass tolerance acquired in the ion trap. The initial wide precursor mass tolerance in the database search was subjected to post-search filtering and eventually constrained to 10 ppm. Carbamidomethylation on cysteine was defined as fixed modification and phosphorylation on STY was included as variable modification in the search criteria. The search space also included all fully- and semi-tryptic peptide candidates of length of at least six amino acids. Maximum number of internal miscleavages was kept unlimited. ProLuCID outputs were assembled and filtered using the DTASelect2.0 program (Tabb et al., 2002).

Identified peptide sequences were blasted against the TAIR10 protein database (http://www.arabidopsis.org/index.jsp) and peptide data were used to calculate protein- and experiment-scores for each identified protein using an in house designed 'Dismemberer' Java application. Protein-scores were calculated as the sum of protein matching peptides identified in the $OST1_{(DA,\ \Delta C)}$-HF purification experiments minus the sum of the protein matching peptides identified in the GFP-HF purification experiments. Experiment scores were calculated as the count of $OST1_{(DA,\ \Delta C)}$-HF purification experiments, in which the protein was identified minus the

count of GFP-HF purification experiments, in which the protein was identified. Scores were calculated from unique peptides, of which their sequence matches only one single TAIR10 annotated protein, or from any protein matching peptides, of which their sequence matches any TAIR10 annotated protein. Proteins with experiment scores ≥ 3 or protein scores ≥ 10 were considered as potential OST1-interacting proteins.

Yeast-two-hybrid analyses

Coding sequences were inserted into pGBT9.BS and pGAD.GH vectors (Elledge et al., 1991). The PJ69-4A yeast strain (James et al., 1996) grown at 28 ºC in YPD agar media (2 % Bactopeptone [BD Biosciences, http://www.bd.com], 1 % yeast extract, 2 % glucose, and 2 % bactoagar) was transformed using the polyethylene glycol/lithium acetate method (Gietz et al., 1992) and plated on CSM agar media (3.35 % YNB = Yeast Nitrogen Base/$(NH_4)_2SO_4$, 0.32 % CSM-Leu-Trp, 2 % glucose, 2 % bactoagar) lacking leucine and tryptophan and incubated for 2-3 days at 28 ºC. Successfully transformed yeast colonies were re-streaked to new CSM-Leu-Trp agar media and incubated 1-2 days at 28 ºC. 5 µL of ten-fold dilution series ($OD_{600\ nm}$ of 10^0 - 10^{-4} in 2 % glucose) of transformants were spotted on CSM-Leu-Trp agar media as a control and on CSM-Leu-Trp-His agar media lacking leucine, tryptophan, and histidine and supplemented with 2.5 mM 3-amino-1,2,4-triazole (3-AT) for selection of positive interaction. Yeast transformants were incubated for 5-7 days at 28 ºC and images were acquired for documentation.

ACKNOWLEDGEMENTS

We thank Felix Hauser, James Moresco and Cun Wang for initial help with data analyses and Jörg Kudla (University of Münster) for providing plasmids. This work was supported by a Feodor Lynen-fellowship of the Alexander von Humboldt-Foundation to RW and by grants from the National Institute of Health (GM060396 to JIS) and the National Science Foundation (MCB0918220 to JIS). Root growth analyses were supported by a grant from the Division of Chemical Sciences, Geosciences, and Biosciences, Office of Basic Energy Sciences of the U.S. Department of Energy (DE-FG02-03ER15449 to JIS). The development of the HF-tag was supported by grants from the National Institute of General Medical Sciences and the National Institute of Health (R01GM056006 and R01GM067837 to SAK).

SUPPLEMENTAL DATA

Supplemental Figure S1. Western blot of HF-lines and control co-IP experiments.

Supplemental Figure S2. Subcellular localizations and interaction analyses of OST1 with OST1-interacting proteins.

Supplemental Figure S3. SnRK2-type protein kinases interact with PP2A-type phosphatase subunits in BiFC analyses**.**

Supplemental Figure S4. ABA does not inhibit root growth of *pp2a*-subunit single mutants but induces an enhanced root curling of *rcn1-6*.

Supplemental Figure S5. 39-day-old *rcn1-6/pp2aa2-1* and *rcn1-6/pp2aa3-1* plants exhibit a reduced growth when compared to Col-0 wild type and *pp2aa2-1/pp2aa3-1* plants.

Supplemental Figure S6. Subcellular localizations of PP2A-subunit fluorescent protein fusions.

Supplemental Figure S7. Regulatory PP2AA-subunits interact with catalytic PP2AC-subunits in yeast-two-hybrid analyses.

Supplemental Table S1. List of protein complex isolation experiments and treatments.

Supplemental Table S2. List of proteins identified by unique peptides and found only in *ost1-3*/OST1$_{(DA,\ \Delta C)}$-HF purifications.

Supplemental Table S3. List of proteins identified by any matching peptide and found only in *ost1-3*/OST1$_{(DA,\ \Delta C)}$-HF purifications.

Supplemental Table S4. Summarized list of potential OST1-interacting proteins selected for further analyses (related to Table I).

Supplemental Movie S1. 30 min time-laps movie of wilting detached rosettes.

REFERENCES

Acharya BR, Jeon BW, Zhang W, Assmann SM (2013) Open Stomata 1 (OST1) is limiting in abscisic acid responses of Arabidopsis guard cells. New Phytol **200:** 1049-1063

Ballesteros I, Domínguez T, Sauer M, Paredes P, Duprat A, Rojo E, Sanmartín M, Sánchez-Serrano JJ (2012) Specialised functions of the PP2A subfamily II catalytic subunits PP2A-C3 and PP2A-C4 in the distribution of auxin fluxes and development in Arabidopsis. Plant J

Belin C, de Franco PO, Bourbousse C, Chaignepain S, Schmitter JM, Vavasseur A, Giraudat J, Barbier-Brygoo H, Thomine S (2006) Identification of features regulating OST1 kinase activity and OST1 function in guard cells. Plant Physiol **141:** 1316-1327

Benning C, Ohta H (2005) Three enzyme systems for galactoglycerolipid biosynthesis are coordinately regulated in plants. J Biol Chem **280:** 2397-2400

Blakeslee JJ, Zhou HW, Heath JT, Skottke KR, Barrios JA, Liu SY, DeLong A (2008) Specificity of RCN1-mediated protein phosphatase 2A regulation in meristem organization and stress response in roots. Plant Physiol **146:** 539-553

Boudsocq M, Barbier-Brygoo H, Laurière C (2004) Identification of nine sucrose nonfermenting 1-related protein kinases 2 activated by hyperosmotic and saline stresses in *Arabidopsis thaliana*. J Biol Chem **279:** 41758-41766

Boudsocq M, Droillard MJ, Barbier-Brygoo H, Laurière C (2007) Different phosphorylation mechanisms are involved in the activation of sucrose non-fermenting 1 related protein kinases 2 by osmotic stresses and abscisic acid. Plant Mol Biol **63:** 491-503

Brandt B, Brodsky DE, Xue S, Negi J, Iba K, Kangasjärvi J, Ghassemian M, Stephan AB, Hu H, Schroeder JI (2012) Reconstitution of abscisic acid activation of SLAC1 anion channel by CPK6 and OST1 kinases and branched ABI1 PP2C phosphatase action. Proc Natl Acad Sci U S A **109:** 10593-10598

Bucholc M, Ciesielski A, Goch G, Anielska-Mazur A, Kulik A, Krzywińska E, Dobrowolska G (2011) SNF1-related protein kinases 2 are negatively regulated by a plant-specific calcium sensor. J Biol Chem **286:** 3429-3441

Camilleri C, Azimzadeh J, Pastuglia M, Bellini C, Grandjean O, Bouchez D (2002) The Arabidopsis TONNEAU2 gene encodes a putative novel protein phosphatase 2A regulatory subunit essential for the control of the cortical cytoskeleton. Plant Cell **14:** 833-845

Clough SJ, Bent AF (1998) Floral dip: a simplified method for *Agrobacterium*-mediated transformation of *Arabidopsis thaliana*. Plant J **16:** 735-743

Cutler SR, Rodriguez PL, Finkelstein RR, Abrams SR (2010) Abscisic acid: emergence of a core signaling network. Annu Rev Plant Biol **61:** 651-679

Dai M, Terzaghi W, Wang H (2012) Multifaceted roles of Arabidopsis PP6 phosphatase in regulating cellular signaling and plant development. Plant Signal Behav **8**

De Smet I, Zhang H, Inzé D, Beeckman T (2006) A novel role for abscisic acid emerges from underground. Trends Plant Sci **11:** 434-439

DeLong A (2006) Switching the flip: protein phosphatase roles in signaling pathways. Curr Opin Plant Biol **9:** 470-477

Duan L, Dietrich D, Ng CH, Chan PM, Bhalerao R, Bennett MJ, Dinneny JR (2013) Endodermal ABA signaling promotes lateral root quiescence during salt stress in Arabidopsis seedlings. Plant Cell **25:** 324-341

Dörmann P, Benning C (1998) The role of UDP-glucose epimerase in carbohydrate metabolism of Arabidopsis. Plant J **13:** 641-652

Elledge SJ, Mulligan JT, Ramer SW, Spottswood M, Davis RW (1991) Lambda YES: a multifunctional cDNA expression vector for the isolation of genes by complementation of yeast and *Escherichia coli* mutations. Proc Natl Acad Sci U S A **88:** 1731-1735

Farkas I, Dombrádi V, Miskei M, Szabados L, Koncz C (2007) Arabidopsis PPP family of serine/threonine phosphatases. Trends Plant Sci **12:** 169-176

Finkelstein R, Reeves W, Ariizumi T, Steber C (2008) Molecular aspects of seed dormancy. Annu Rev Plant Biol **59:** 387-415

Fisher RH, Barton MK, Cohen JD, Cooke TJ (1996) Hormonal Studies of *fass*, an Arabidopsis Mutant That Is Altered in Organ Elongation. Plant Physiol **110:** 1109-1121

Fujii H, Verslues PE, Zhu JK (2007) Identification of two protein kinases required for abscisic acid regulation of seed germination, root growth, and gene expression in Arabidopsis. Plant Cell **19:** 485-494

Fujii H, Zhu JK (2009) Arabidopsis mutant deficient in 3 abscisic acid-activated protein kinases reveals critical roles in growth, reproduction, and stress. Proc Natl Acad Sci U S A **106:** 8380-8385

Fujii H, Chinnusamy V, Rodrigues A, Rubio S, Antoni R, Park SY, Cutler SR, Sheen J, Rodriguez PL, Zhu JK (2009) *In vitro* reconstitution of an abscisic acid signalling pathway. Nature **462:** 660-664

Fujii H, Verslues PE, Zhu JK (2011) Arabidopsis decuple mutant reveals the importance of SnRK2 kinases in osmotic stress responses *in vivo*. Proc Natl Acad Sci U S A **108:** 1717-1722

Fujita Y, Nakashima K, Yoshida T, Katagiri T, Kidokoro S, Kanamori N, Umezawa T, Fujita M, Maruyama K, Ishiyama K, Kobayashi M, Nakasone S, Yamada K, Ito T, Shinozaki K, Yamaguchi-Shinozaki K (2009) Three SnRK2 protein kinases are the main positive regulators of abscisic acid signaling in response to water stress in Arabidopsis. Plant Cell Physiol **50:** 2123-2132

Furihata T, Maruyama K, Fujita Y, Umezawa T, Yoshida R, Shinozaki K, Yamaguchi-Shinozaki K (2006) Abscisic acid-dependent multisite phosphorylation regulates the activity of a transcription activator AREB1. Proc Natl Acad Sci U S A **103:** 1988-1993

Garbers C, DeLong A, Deruére J, Bernasconi P, Söll D (1996) A mutation in protein phosphatase 2A regulatory subunit A affects auxin transport in Arabidopsis. EMBO J **15:** 2115-2124

Geiger D, Scherzer S, Mumm P, Stange A, Marten I, Bauer H, Ache P, Matschi S, Liese A, Al-Rasheid KA, Romeis T, Hedrich R (2009) Activity of guard cell anion channel SLAC1 is controlled by drought-stress signaling kinase-phosphatase pair. Proc Natl Acad Sci U S A **106:** 21425-21430

Gietz D, St Jean A, Woods RA, Schiestl RH (1992) Improved method for high efficiency transformation of intact yeast cells. Nucleic Acids Res **20:** 1425

Goedhart J, van Weeren L, Hink MA, Vischer NO, Jalink K, Gadella TW (2010) Bright cyan fluorescent protein variants identified by fluorescence lifetime screening. Nat Methods **7:** 137-139

Hauser F, Waadt R, Schroeder JI (2011) Evolution of abscisic acid synthesis and signaling mechanisms. Curr Biol **21:** R346-355

Haynes JG, Hartung AJ, Hendershot JD, Passingham RS, Rundle SJ (1999) Molecular characterization of the B' regulatory subunit gene family of Arabidopsis protein phosphatase 2A. Eur J Biochem **260:** 127-136

Hey SJ, Bacon A, Burnett E, Neill SJ (1997) Abscisic acid signal transduction in epidermal cells of *Pisum sativum L. Argenteum*: both dehydrin mRNA accumulation and stomatal responses require protein phosphorylation and dephosphorylation. Planta **202:** 85-92

Hrabak EM, Chan CW, Gribskov M, Harper JF, Choi JH, Halford N, Kudla J, Luan S, Nimmo HG, Sussman MR, Thomas M, Walker-Simmons K, Zhu JK, Harmon AC (2003) The Arabidopsis CDPK-SnRK superfamily of protein kinases. Plant Physiol **132:** 666-680

Hu R, Zhu Y, Shen G, Zhang H (2014) TAP46 plays a positive role in the ABSCISIC ACID INSENSITIVE5-regulated gene expression in Arabidopsis. Plant Physiol **164:** 721-734

Imes D, Mumm P, Böhm J, Al-Rasheid KA, Marten I, Geiger D, Hedrich R (2013) Open stomata 1 (OST1) kinase controls R-type anion channel QUAC1 in Arabidopsis guard cells. Plant J **74:** 372-382

Jacob T, Ritchie S, Assmann SM, Gilroy S (1999) Abscisic acid signal transduction in guard cells is mediated by phospholipase D activity. Proc Natl Acad Sci U S A **96:** 12192-12197

James P, Halladay J, Craig EA (1996) Genomic libraries and a host strain designed for highly efficient two-hybrid selection in yeast. Genetics **144:** 1425-1436

Kim TH, Böhmer M, Hu H, Nishimura N, Schroeder JI (2010) Guard cell signal transduction network: advances in understanding abscisic acid, CO_2, and Ca^{2+} signaling. Annu Rev Plant Biol **61:** 561-591

Kirik A, Ehrhardt DW, Kirik V (2012) TONNEAU2/FASS regulates the geometry of microtubule nucleation and cortical array organization in interphase Arabidopsis cells. Plant Cell **24:** 1158-1170

Kobayashi Y, Murata M, Minami H, Yamamoto S, Kagaya Y, Hobo T, Yamamoto A, Hattori T (2005) Abscisic acid-activated SNRK2 protein kinases function in the gene-regulation pathway of ABA signal transduction by phosphorylating ABA response element-binding factors. Plant J **44:** 939-949

Kocourková D, Krcková Z, Pejchar P, Veselková S, Valentová O, Wimalasekera R, Scherer GF, Martinec J (2011) The phosphatidylcholine-hydrolysing phospholipase C NPC4 plays a role in response of Arabidopsis roots to salt stress. J Exp Bot **62:** 3753-3763

Koncz C, Schell J (1986) The promoter of T_L-DNA gene *5* controls the tissue-specific expression of chimaeric genes carried by a novel type of *Agrobacterium* binary vector. *In*. Mol Gen Genet, pp 383-396

Krebs M, Held K, Binder A, Hashimoto K, Den Herder G, Parniske M, Kudla J, Schumacher K (2012) FRET-based genetically encoded sensors allow high-resolution live cell imaging of Ca^{2+} dynamics. Plant J **69:** 181-192

Kwak JM, Moon JH, Murata Y, Kuchitsu K, Leonhardt N, DeLong A, Schroeder JI (2002) Disruption of a guard cell-expressed protein phosphatase 2A regulatory subunit, RCN1, confers abscisic acid insensitivity in Arabidopsis. Plant Cell **14:** 2849-2861

Larsen PB, Cancel JD (2003) Enhanced ethylene responsiveness in the Arabidopsis *eer1* mutant results from a loss-of-function mutation in the protein phosphatase 2A A regulatory subunit, RCN1. Plant J **34:** 709-718

Lee SC, Lan W, Buchanan BB, Luan S (2009) A protein kinase-phosphatase pair interacts with an ion channel to regulate ABA signaling in plant guard cells. Proc Natl Acad Sci U S A **106:** 21419-21424

Li J, Wang XQ, Watson MB, Assmann SM (2000) Regulation of abscisic acid-induced stomatal closure and anion channels by guard cell AAPK kinase. Science **287:** 300-303

Lillo C, Kataya AR, Heidari B, Creighton MT, Nemie-Feyissa D, Ginbot Z, Jonassen EM (2014) Protein phosphatases PP2A, PP4 and PP6 - mediators and regulators in development and responses to environmental cues. Plant Cell Environ

Ma Y, Szostkiewicz I, Korte A, Moes D, Yang Y, Christmann A, Grill E (2009) Regulators of PP2C phosphatase activity function as abscisic acid sensors. Science **324:** 1064-1068

Matre P, Meyer C, Lillo C (2009) Diversity in subcellular targeting of the PP2A B'eta subfamily members. Planta **230:** 935-945

McClinton RS, Sung ZR (1997) Organization of cortical microtubules at the plasma membrane in Arabidopsis. Planta **201:** 252-260

Melcher K, Ng LM, Zhou XE, Soon FF, Xu Y, Suino-Powell KM, Park SY, Weiner JJ, Fujii H, Chinnusamy V, Kovach A, Li J, Wang Y, Peterson FC, Jensen DR, Yong EL, Volkman BF, Cutler SR, Zhu JK, Xu HE (2009) A gate-latch-lock mechanism for hormone signalling by abscisic acid receptors. Nature **462:** 602-608

Merilo E, Laanemets K, Hu H, Xue S, Jakobson L, Tulva I, Gonzalez-Guzman M, Rodriguez PL, Schroeder JI, Broschè M, Kollist H (2013) PYR/RCAR receptors contribute to ozone-, reduced air humidity-, darkness-, and CO_2-induced stomatal regulation. Plant Physiol **162:** 1652-1668

Merlot S, Mustilli AC, Genty B, North H, Lefebvre V, Sotta B, Vavasseur A, Giraudat J (2002) Use of infrared thermal imaging to isolate Arabidopsis mutants defective in stomatal regulation. Plant J **30:** 601-609

Michniewicz M, Zago MK, Abas L, Weijers D, Schweighofer A, Meskiene I, Heisler MG, Ohno C, Zhang J, Huang F, Schwab R, Weigel D, Meyerowitz EM, Luschnig C, Offringa R, Friml J (2007) Antagonistic regulation of PIN phosphorylation by PP2A and PINOID directs auxin flux. Cell **130:** 1044-1056

Moellering ER, Muthan B, Benning C (2010) Freezing tolerance in plants requires lipid remodeling at the outer chloroplast membrane. Science **330:** 226-228

Moellering ER, Benning C (2011) Galactoglycerolipid metabolism under stress: a time for remodeling. Trends Plant Sci **16:** 98-107

Mosquna A, Peterson FC, Park SY, Lozano-Juste J, Volkman BF, Cutler SR (2011) Potent and selective activation of abscisic acid receptors *in vivo* by mutational stabilization of their agonist-bound conformation. Proc Natl Acad Sci U S A **108:** 20838-20843

Muday GK, Brady SR, Argueso C, Deruère J, Kieber JJ, DeLong A (2006) RCN1-regulated phosphatase activity and EIN2 modulate hypocotyl gravitropism by a mechanism that does not require ethylene signaling. Plant Physiol **141:** 1617-1629

Mustilli AC, Merlot S, Vavasseur A, Fenzi F, Giraudat J (2002) Arabidopsis OST1 protein kinase mediates the regulation of stomatal aperture by abscisic acid and acts upstream of reactive oxygen species production. Plant Cell **14:** 3089-3099

Nagai T, Ibata K, Park ES, Kubota M, Mikoshiba K, Miyawaki A (2002) A variant of yellow fluorescent protein with fast and efficient maturation for cell-biological applications. Nat Biotechnol **20:** 87-90

Nagaya S, Kawamura K, Shinmyo A, Kato K (2010) The HSP terminator of *Arabidopsis thaliana* increases gene expression in plant cells. Plant Cell Physiol **51:** 328-332

Nakamura Y, Awai K, Masuda T, Yoshioka Y, Takamiya K, Ohta H (2005) A novel phosphatidylcholine-hydrolyzing phospholipase C induced by phosphate starvation in Arabidopsis. J Biol Chem **280:** 7469-7476

Nakashima K, Fujita Y, Kanamori N, Katagiri T, Umezawa T, Kidokoro S, Maruyama K, Yoshida T, Ishiyama K, Kobayashi M, Shinozaki K, Yamaguchi-Shinozaki K (2009) Three Arabidopsis SnRK2 protein kinases, SRK2D/SnRK2.2, SRK2E/SnRK2.6/OST1 and SRK2I/SnRK2.3, involved in ABA signaling are essential for the control of seed development and dormancy. Plant Cell Physiol **50:** 1345-1363

Ng LM, Soon FF, Zhou XE, West GM, Kovach A, Suino-Powell KM, Chalmers MJ, Li J, Yong EL, Zhu JK, Griffin PR, Melcher K, Xu HE (2011) Structural basis for basal activity and autoactivation of abscisic acid (ABA) signaling SnRK2 kinases. Proc Natl Acad Sci U S A **108:** 21259-21264

Nishimura N, Sarkeshik A, Nito K, Park SY, Wang A, Carvalho PC, Lee S, Caddell DF, Cutler SR, Chory J, Yates JR, Schroeder JI (2010) PYR/PYL/RCAR family members are major *in-vivo* ABI1 protein phosphatase 2C-interacting proteins in Arabidopsis. Plant J **61:** 290-299

Norris SR, Meyer SE, Callis J (1993) The intron of *Arabidopsis thaliana* polyubiquitin genes is conserved in location and is a quantitative determinant of chimeric gene expression. Plant Mol Biol **21:** 895-906

Park SY, Fung P, Nishimura N, Jensen DR, Fujii H, Zhao Y, Lumba S, Santiago J, Rodrigues A, Chow TF, Alfred SE, Bonetta D, Finkelstein R, Provart NJ, Desveaux D, Rodriguez PL, McCourt P, Zhu JK, Schroeder JI, Volkman BF, Cutler SR (2009) Abscisic acid inhibits type 2C protein phosphatases via the PYR/PYL family of START proteins. Science **324:** 1068-1071

Pei ZM, Kuchitsu K, Ward JM, Schwarz M, Schroeder JI (1997) Differential abscisic acid regulation of guard cell slow anion channels in Arabidopsis wild-type and abi1 and abi2 mutants. Plant Cell **9:** 409-423

Pernas M, García-Casado G, Rojo E, Solano R, Sánchez-Serrano JJ (2007) A protein phosphatase 2A catalytic subunit is a negative regulator of abscisic acid signalling. Plant J **51:** 763-778

Peters C, Li M, Narasimhan R, Roth M, Welti R, Wang X (2010) Nonspecific phospholipase C NPC4 promotes responses to abscisic acid and tolerance to hyperosmotic stress in Arabidopsis. Plant Cell **22:** 2642-2659

Raghavendra AS, Gonugunta VK, Christmann A, Grill E (2010) ABA perception and signalling. Trends Plant Sci **15:** 395-401

Rashotte AM, DeLong A, Muday GK (2001) Genetic and chemical reductions in protein phosphatase activity alter auxin transport, gravity response, and lateral root growth. Plant Cell **13:** 1683-1697

Rösti J, Barton CJ, Albrecht S, Dupree P, Pauly M, Findlay K, Roberts K, Seifert GJ (2007) UDP-glucose 4-epimerase isoforms UGE2 and UGE4 cooperate in providing UDP-galactose for cell wall biosynthesis and growth of *Arabidopsis thaliana*. Plant Cell **19:** 1565-1579

Saito N, Munemasa S, Nakamura Y, Shimoishi Y, Mori IC, Murata Y (2008) Roles of RCN1, regulatory A subunit of protein phosphatase 2A, in methyl jasmonate signaling and signal crosstalk between methyl jasmonate and abscisic acid. Plant Cell Physiol **49:** 1396-1401

Santiago J, Rodrigues A, Saez A, Rubio S, Antoni R, Dupeux F, Park SY, Márquez JA, Cutler SR, Rodriguez PL (2009) Modulation of drought resistance by the abscisic acid receptor PYL5 through inhibition of clade A PP2Cs. Plant J **60:** 575-588

Sasaki T, Mori IC, Furuichi T, Munemasa S, Toyooka K, Matsuoka K, Murata Y, Yamamoto Y (2010) Closing plant stomata requires a homolog of an aluminum-activated malate transporter. Plant Cell Physiol **51:** 354-365

Sato A, Sato Y, Fukao Y, Fujiwara M, Umezawa T, Shinozaki K, Hibi T, Taniguchi M, Miyake H, Goto DB, Uozumi N (2009) Threonine at position 306 of the KAT1 potassium channel is essential for channel activity and is a target site for ABA-activated SnRK2/OST1/SnRK2.6 protein kinase. Biochem J **424:** 439-448

Schindelin J, Arganda-Carreras I, Frise E, Kaynig V, Longair M, Pietzsch T, Preibisch S, Rueden C, Saalfeld S, Schmid B, Tinevez JY, White DJ, Hartenstein V, Eliceiri K, Tomancak P, Cardona A (2012) Fiji: an open-source platform for biological-image analysis. Nat Methods **9:** 676-682

Schlücking K, Edel KH, Köster P, Drerup MM, Eckert C, Steinhorst L, Waadt R, Batistic O, Kudla J (2013) A new β-estradiol-inducible vector set that facilitates easy construction and efficient expression of transgenes reveals CBL3-dependent cytoplasm to tonoplast translocation of CIPK5. Mol Plant **6:** 1814-1829

Schmidt C, Schelle I, Liao YJ, Schroeder JI (1995) Strong regulation of slow anion channels and abscisic acid signaling in guard cells by phosphorylation and dephosphorylation events. Proc Natl Acad Sci U S A **92:** 9535-9539

Shi Y (2009) Serine/threonine phosphatases: mechanism through structure. Cell **139:** 468-484

Shin R, Alvarez S, Burch AY, Jez JM, Schachtman DP (2007) Phosphoproteomic identification of targets of the Arabidopsis sucrose nonfermenting-like kinase SnRK2.8 reveals a connection to metabolic processes. Proc Natl Acad Sci U S A **104:** 6460-6465

Sirichandra C, Gu D, Hu HC, Davanture M, Lee S, Djaoui M, Valot B, Zivy M, Leung J, Merlot S, Kwak JM (2009) Phosphorylation of the Arabidopsis AtrbohF NADPH oxidase by OST1 protein kinase. FEBS Lett **583:** 2982-2986

Sirichandra C, Davanture M, Turk BE, Zivy M, Valot B, Leung J, Merlot S (2010) The Arabidopsis ABA-activated kinase OST1 phosphorylates the bZIP transcription factor ABF3 and creates a 14-3-3 binding site involved in its turnover. PLoS One **5:** e13935

Skottke KR, Yoon GM, Kieber JJ, DeLong A (2011) Protein phosphatase 2A controls ethylene biosynthesis by differentially regulating the turnover of ACC synthase isoforms. PLoS Genet **7:** e1001370

Soon FF, Ng LM, Zhou XE, West GM, Kovach A, Tan MH, Suino-Powell KM, He Y, Xu Y, Chalmers MJ, Brunzelle JS, Zhang H, Yang H, Jiang H, Li J, Yong EL, Cutler S, Zhu JK, Griffin PR, Melcher K, Xu HE (2012) Molecular mimicry regulates ABA signaling by SnRK2 kinases and PP2C phosphatases. Science **335:** 85-88

Stacey J, Isaac PG (1994) Isolation of DNA from plants. Methods Mol Biol **28:** 9-15

Szostkiewicz I, Richter K, Kepka M, Demmel S, Ma Y, Korte A, Assaad FF, Christmann A, Grill E (2010) Closely related receptor complexes differ in their ABA selectivity and sensitivity. Plant J **61:** 25-35

Tabb DL, McDonald WH, Yates JR (2002) DTASelect and Contrast: tools for assembling and comparing protein identifications from shotgun proteomics. J Proteome Res **1:** 21-26

Tang W, Yuan M, Wang R, Yang Y, Wang C, Oses-Prieto JA, Kim TW, Zhou HW, Deng Z, Gampala SS, Gendron JM, Jonassen EM, Lillo C, DeLong A, Burlingame AL, Sun Y, Wang ZY (2011) PP2A activates brassinosteroid-responsive gene expression and plant growth by dephosphorylating BZR1. Nat Cell Biol **13:** 124-131

Team, RDC (2010) R: A language and environment for statistical computing. Vienna, Austria: R Foundation for Statistical Computing. Retrieved from http://R-project.org

Testerink C, Munnik T (2005) Phosphatidic acid: a multifunctional stress signaling lipid in plants. Trends Plant Sci **10:** 368-375

Thorlby G, Fourrier N, Warren G (2004) The SENSITIVE TO FREEZING2 gene, required for freezing tolerance in *Arabidopsis thaliana*, encodes a beta-glucosidase. Plant Cell **16:** 2192-2203

Tran HT, Nimick M, Uhrig RG, Templeton G, Morrice N, Gourlay R, DeLong A, Moorhead GB (2012) *Arabidopsis thaliana* histone deacetylase 14 (HDA14) is an α-tubulin deacetylase that associates with PP2A and enriches in the microtubule fraction with the putative histone acetyltransferase ELP3. Plant J **71:** 263-272

Trotta A, Wrzaczek M, Scharte J, Tikkanen M, Konert G, Rahikainen M, Holmström M, Hiltunen HM, Rips S, Sipari N, Mulo P, Weis E, von Schaewen A, Aro EM, Kangasjärvi S (2011) Regulatory subunit B'gamma of protein phosphatase 2A prevents unnecessary defense reactions under low light in Arabidopsis. Plant Physiol **156:** 1464-1480

Tseng TS, Briggs WR (2010) The Arabidopsis *rcn1-1* mutation impairs dephosphorylation of Phot2, resulting in enhanced blue light responses. Plant Cell **22:** 392-402

Umezawa T, Yoshida R, Maruyama K, Yamaguchi-Shinozaki K, Shinozaki K (2004) SRK2C, a SNF1-related protein kinase 2, improves drought tolerance by controlling stress-responsive gene expression in *Arabidopsis thaliana*. Proc Natl Acad Sci U S A **101:** 17306-17311

Umezawa T, Sugiyama N, Mizoguchi M, Hayashi S, Myouga F, Yamaguchi-Shinozaki K, Ishihama Y, Hirayama T, Shinozaki K (2009) Type 2C protein phosphatases directly regulate abscisic acid-activated protein kinases in Arabidopsis. Proc Natl Acad Sci U S A **106:** 17588-17593

Umezawa T, Sugiyama N, Takahashi F, Anderson JC, Ishihama Y, Peck SC, Shinozaki K (2013) Genetics and phosphoproteomics reveal a protein phosphorylation network in the abscisic acid signaling pathway in *Arabidopsis thaliana*. Sci Signal **6:** rs8

Vahisalu T, Puzõrjova I, Brosché M, Valk E, Lepiku M, Moldau H, Pechter P, Wang YS, Lindgren O, Salojärvi J, Loog M, Kangasjärvi J, Kollist H (2010) Ozone-triggered rapid stomatal response involves the production of reactive oxygen species, and is controlled by SLAC1 and OST1. Plant J **62:** 442-453

Vlad F, Turk BE, Peynot P, Leung J, Merlot S (2008) A versatile strategy to define the phosphorylation preferences of plant protein kinases and screen for putative substrates. Plant J **55:** 104-117

Vlad F, Rubio S, Rodrigues A, Sirichandra C, Belin C, Robert N, Leung J, Rodriguez PL, Laurière C, Merlot S (2009) Protein phosphatases 2C regulate the activation of the Snf1-related kinase OST1 by abscisic acid in Arabidopsis. Plant Cell **21:** 3170-3184

Vlad F, Droillard MJ, Valot B, Khafif M, Rodrigues A, Brault M, Zivy M, Rodriguez PL, Merlot S, Laurière C (2010) Phospho-site mapping, genetic and *in planta* activation studies reveal key aspects of the different phosphorylation mechanisms involved in activation of SnRK2s. Plant J **63:** 778-790

Waadt R, Schmidt LK, Lohse M, Hashimoto K, Bock R, Kudla J (2008) Multicolor bimolecular fluorescence complementation reveals simultaneous formation of alternative CBL/CIPK complexes *in planta*. Plant J **56:** 505-516

Waadt R, Schlücking K, Schroeder JI, Kudla J (2014a) Protein fragment bimolecular fluorescence complementation analyses for the *in vivo* study of protein-protein interactions and cellular protein complex localizations. Methods Mol Biol **1062:** 629-658

Waadt R, Hitomi K, Nishimura N, Hitomi C, Adams SR, Getzoff ED, Schroeder JI (2014b) FRET-based reporters for the direct visualization of abscisic acid concentration changes and distribution in Arabidopsis. Elife **3:** e01739

Walter M, Chaban C, Schütze K, Batistic O, Weckermann K, Näke C, Blazevic D, Grefen C, Schumacher K, Oecking C, Harter K, Kudla J (2004) Visualization of protein interactions in living plant cells using bimolecular fluorescence complementation. Plant J **40:** 428-438

Wang P, Xue L, Batelli G, Lee S, Hou YJ, Van Oosten MJ, Zhang H, Tao WA, Zhu JK (2013) Quantitative phosphoproteomics identifies SnRK2 protein kinase substrates and reveals the effectors of abscisic acid action. Proc Natl Acad Sci U S A **110:** 11205-11210

Warren G, McKown R, Marin AL, Teutonico R (1996) Isolation of mutations affecting the development of freezing tolerance in *Arabidopsis thaliana* (L.) Heynh. Plant Physiol **111:** 1011-1019

Washburn MP, Wolters D, Yates JR (2001) Large-scale analysis of the yeast proteome by multidimensional protein identification technology. Nat Biotechnol **19:** 242-247

Wu G, Wang X, Li X, Kamiya Y, Otegui MS, Chory J (2011) Methylation of a phosphatase specifies dephosphorylation and degradation of activated brassinosteroid receptors. Sci Signal **4:** ra29

Xie T, Ren R, Zhang YY, Pang Y, Yan C, Gong X, He Y, Li W, Miao D, Hao Q, Deng H, Wang Z, Wu JW, Yan N (2012) Molecular mechanism for inhibition of a critical component in the *Arabidopsis thaliana* abscisic acid signal transduction pathways, SnRK2.6, by protein phosphatase ABI1. J Biol Chem **287:** 794-802

Xie X, Wang Y, Williamson L, Holroyd GH, Tagliavia C, Murchie E, Theobald J, Knight MR, Davies WJ, Leyser HM, Hetherington AM (2006) The identification of genes involved in the stomatal response to reduced atmospheric relative humidity. Curr Biol **16:** 882-887

Xu J, Li HD, Chen LQ, Wang Y, Liu LL, He L, Wu WH (2006) A protein kinase, interacting with two calcineurin B-like proteins, regulates K^+ transporter AKT1 in Arabidopsis. Cell **125:** 1347-1360

Xu Y, Xing Y, Chen Y, Chao Y, Lin Z, Fan E, Yu JW, Strack S, Jeffrey PD, Shi Y (2006) Structure of the protein phosphatase 2A holoenzyme. Cell **127:** 1239-1251

Xue S, Hu H, Ries A, Merilo E, Kollist H, Schroeder JI (2011) Central functions of bicarbonate in S-type anion channel activation and OST1 protein kinase in CO_2 signal transduction in guard cell. EMBO J **30:** 1645-1658

Yoshida R, Hobo T, Ichimura K, Mizoguchi T, Takahashi F, Aronso J, Ecker JR, Shinozaki K (2002) ABA-activated SnRK2 protein kinase is required for dehydration stress signaling in Arabidopsis. Plant Cell Physiol **43:** 1473-1483

Yoshida R, Umezawa T, Mizoguchi T, Takahashi S, Takahashi F, Shinozaki K (2006) The regulatory domain of SRK2E/OST1/SnRK2.6 interacts with ABI1 and integrates abscisic acid (ABA) and osmotic stress signals controlling stomatal closure in Arabidopsis. J Biol Chem **281:** 5310-5318

Yunta C, Martínez-Ripoll M, Zhu JK, Albert A (2011) The structure of *Arabidopsis thaliana* OST1 provides insights into the kinase regulation mechanism in response to osmotic stress. J Mol Biol **414:** 135-144

Zhou HW, Nussbaumer C, Chao Y, DeLong A (2004) Disparate roles for the regulatory A subunit isoforms in Arabidopsis protein phosphatase 2A. Plant Cell **16:** 709-722

FIGURE LEGENDS

Figure 1. OST1$_{(DA, SA, \Delta C)}$-HF constructs affect ABA responses. A and B, Time-dependent seed germination of Col-0, *ost1-3* and indicated OST1 lines in presence of (A) 0 μM ABA and (B) 0.5 μM ABA. C and D, Seed germination on (C) day three after stratification and (D) cotyledon expansion on day six after stratification in the presence of 0 μM ABA (blue bars) and 0.5 μM ABA (red bars). A to D, Means ± SEM, n = 4 with 49 seeds/n and normalized to the seed count. E, Four-day-old seedlings were transferred to 0.5 MS agar plates supplemented with 0 μM ABA (top row) or 10 μM ABA (bottom row) and grown for additional five days. F, Root growth of seedlings shown in (E) in the presence of 0 μM ABA (blue bars) and 10 μM ABA (red bars; means ± SEM, n = 5, with seven seedlings/n) normalized to the 0 μM ABA control conditions. G, Stomatal apertures of 22-26-day-old 0.5 MS agar grown seedlings 2 h after incubation in 0 μM ABA (blue bars) or 10 μM ABA (red bars; means ± SEM, n = 3-4 with ≥ 17 stomata/n) normalized to the 0 μM ABA control conditions. Statistical values for differences between Col-0 wild type and the mutant and transgenic lines were calculated using a two-way ANOVA (P-values: *, < 0.05; **, < 0.01; ***, < 0.001). See also Supplemental Movie S1.

Figure 2. The SnRK2-type protein kinase OST1 forms homo- and heterodimers with other SnRK2-type protein kinases. A, (mT)urquoise-ABI1 and mT-SnRK2s are localized in the cytoplasm and the nucleus. B, BiFC analyses reveal OST1 interaction with ABI1 and SnRK2s in the cytoplasm and the nucleus. A and B, Maximum projections of 32-plane z-stacks. C, BiFC quantification (means ± SEM, n = 10 images). D, mT-OST1 co-purifies with SnRK2-HF fusion proteins. Western blots of HF-tagged SnRK2s (anti-FLAG, top panel) and mT-OST1 (anti-GFP, bottom panel) after co-expression in *N. benthamiana* (Input) and anti-FLAG immuno-precipitation (IP) of HF-tagged SnRK2s. E, mT-SnRK2 fusion proteins co-purify with OST1-HF. Western blot of OST1-HF (anti-FLAG, left panel) and mT-SnRK2s (anti-GFP, right panel) after co-expression in *N. benthamiana* (Input) and anti-FLAG immuno-precipitation (IP) of OST1-HF.

Figure 3. SnRK2-type protein kinases interact with regulatory PP2A-subunits in co-IP analyses. A, Co-IP analyses of RCN1-HF with (mT)urquoise-SnRK2s and mT. B, Co-IP analyses of HF-PP2AB'beta with mT-SnRK2s and mT. C, Co-IP analyses of OST1-HF with mT-PP2AA regulatory subunits and mT. D, Co-IP analyses of OST1-HF with mT-PP2AB' regulatory subunits and with the mVenus-PP2AC3 catalytic subunit. A to D, Western blots of HF-tagged proteins (anti-FLAG) and mT- or mVenus-tagged proteins (anti-GFP) after co-expression in *N. benthamiana* (Input) and anti-FLAG immuno-precipitation (IP) of HF-tagged proteins.

Figure 4. PP2A-subunit single mutants exhibit a reduced ABA sensitivity during seed germination. A and B, Time-dependent seed germination of Col-0 and indicated *pp2a* single mutants in the presence of (A) 0 μM ABA and (B) 1 μM ABA. C and D, Seed germination on (C) day four after stratification and (D) cotyledon expansion on day seven after stratification in the presence of 0 μM ABA (blue bars) and 1 μM ABA (red bars). A to D, Means ± SEM, n = 4 technical replicates with 49 seeds/n and normalized to the seed count. Statistical values for differences between Col-0 wild type and the *pp2a* single mutant lines were calculated using a two-way ANOVA (P-values: *, < 0.05; **, < 0.01).

Figure 5. *rcn1-6*/*pp2ac* and *pp2ac* double mutants exhibit altered ABA responses during seed germination and seedling growth. A and B, Time-dependent seed germination of Col-0 and indicated *pp2a* double mutants in presence of (A) 0 μM ABA and (B) 0.8 μM ABA. C and D, Seed germination on (C) day four after stratification and (D) cotyledon expansion on day six after stratification in the presence of 0 μM ABA (blue bars) and 0.8 μM ABA (red bars). A to D, Means ± SEM, n = 4 with 49 seeds/n and normalized to the seed count. E, Four-day-old seedlings were transferred to 0.5 MS agar plates supplemented with 0 μM ABA (top row) or 5 μM ABA (bottom row) and grown for additional five days. F, Root growth of seedlings shown in (E) in the presence of 0 μM ABA (blue bars) and 5 μM ABA (red bars; means ± SEM, n = 5, with seven seedlings/n) normalized to the 0 μM ABA control conditions. G, Stomatal apertures 2 h after incubation in 0 μM ABA (blue bars) or 5 μM ABA (red bars; means ± SEM, n = 4 with ≥ 19 stomata/n) normalized to the 0 μM ABA control conditions. Statistical values for differences

between Col-0 wild type and the *pp2a* double mutant lines were calculated using a two-way ANOVA (P-values: *, < 0.05; **, < 0.01; ***, < 0.001).

Figure 6. PP2AA-subunit double mutants exhibit a reduced ABA sensitivity in stomatal closure. Stomatal apertures of 29-33-day-old-plants 2 h after incubation in 0 μM ABA (blue bars) or 5 μM ABA (red bars; means ± SEM, n = 3-6 with ≥ 30 stomata/n) normalized to the 0 μM ABA control conditions. Statistical values for differences between the control and 5 μM ABA treatments were calculated using a one-way ANOVA (P-values: *, < 0.05).

Figure 7. Regulatory PP2AA-subunits interact with catalytic PP2AC-subunits in BiFC analyses. A and D, BiFC analyses of YN-RCN1 with YC-PP2AC1-C5. B and E, BiFC analyses of YN-PP2AA2 with YC-PP2AC1-C5. C and F, BiFC analyses of YN-PP2AA3 with YC-PP2AC1-C5. A to C, 32-plane z-stack maximum projections showing PP2AA- and PP2AC-subunit complex formations in the cytoplasm. D to F, BiFC quantifications (means ± SEM, n = 10 images).

Table I. List of potential OST1-interacting proteins selected for further analyses. Displayed are the agi codes of the respective OST1-interacting proteins (OIPs) with information on phosphorylation status and protein and experiment scores (shown in parentheses). Scores were calculated from 'unique' or 'total' protein matching peptides, which were identified in sorbitol or ABA treated experiments. The sum of scores from sorbitol and ABA treated experiments are also displayed. Protein scores were calculated as the sum of protein-matching peptides from $OST1_{(DA,\ \Delta C)}$-HF purification experiments minus the sum of protein-matching peptides from GFP-HF purification experiments. Experiment scores were calculated as count of $OST1_{(DA,\ \Delta C)}$-HF purification experiments in which the protein was identified minus the count of GFP-HF purification experiments in which the protein was identified.

Supplemental Figure S1. Western blot of HF-lines and control co-IP experiments. A, Anti-FLAG western blot confirms expression of indicated constructs (top panel) and PageBlue loading control (bottom panel). B, Western blots of HF-tagged proteins (anti-FLAG, top panel) and mVenus-tagged proteins (anti-GFP, bottom panel) after co-expression in *N. benthamiana* (Input) and anti-FLAG immuno-precipitation (IP) of HF-tagged proteins. Note, that OST1-HF

cannot efficiently co-purify mVenus-ABI1. However, HF-ABI1 can efficiently co-purify mVenus-OST1.

Supplemental Figure S2. Subcellular localizations and interaction analyses of OST1 with OST1-interacting proteins. A, Subcellular localizations of indicated (mT)urquoise- or mVenus-tagged OST1-interacting proteins (OIPs) after transient expression in *N. benthamiana*. B, Subcellular localizations of BiFC complexes of YN-OST1 with YC-tagged OIPs. A and B, Maximum projections of 32-plane z-stacks. C, BiFC quantifications (means ± SEM, n = 10 images). Note, that BiFC data derived from two separate experiments. D, Western blots of HF-tagged OIPs (anti-FLAG, top panel) and mVenus- or mT-OST1 (anti-GFP, bottom panel) after co-expression in *N. benthamiana* (Input) and anti-FLAG immuno-precipitation (IP) of HF-tagged OIPs.

Supplemental Figure S3. SnRK2-type protein kinases interact with PP2A-type phosphatase subunits in BiFC analyses**.** A and D, BiFC analyses of YN-OST1 with YC-PP2A-subunits and YC-ABI1 as control. B and E, BiFC analyses of YN-SnRK2s with YC-RCN1. C and F, BiFC analyses of YN-SnRK2s with YC-PP2AB'beta. A to C, Maximum projections of 32-plane z-stacks. Punctuate structures are indicated by an arrow. D to F, BiFC quantification (means ± SEM, n = 10 images). For better comparison of the emission signals the scale was adjusted in the inset of (D).

Supplemental Figure S4. ABA does not inhibit root growth of *pp2a*-subunit single mutants but induces an enhanced root curling of *rcn1-6*. A, Four-day-old seedlings of Col-0, *abi1-1* in Col-0 background and *pp2a*-subunit single mutants were transferred to 0.5 MS agar plates supplemented with 0 μM ABA (left panel) or 5 μM ABA (right panel) and grown for additional five days. B, Root length of seedlings shown in (A) in the presence of 0 μM ABA (blue bars) and 5 μM ABA (red bars; means ± SEM, n = 4 with seven seedlings/n) normalized to the 0 μM ABA control conditions. Statistical values for differences between Col-0 wild type and the investigated mutant lines were calculated using a two-way ANOVA (P-values: **, < 0.01).

Supplemental Figure S5. 39-day-old *rcn1-6/pp2aa2-1* and *rcn1-6/pp2aa3-1* plants exhibit a reduced growth when compared to Col-0 wild type and *pp2aa2-1/pp2aa3-1* plants.

Supplemental Figure S6. Subcellular localizations of PP2A-subunit fluorescent protein fusions. A to E, Maximum projections of 32-plane z-stacks of (mT)urquoise-PP2A-subunit (cyan), mVenus-PP2AC (yellow) and PP2A-subunit-mVenus fusion proteins (yellow). The fusion proteins analyzed are indicated. A, PP2AA-subunits are localized in the cytoplasm and the nucleus. B, PP2AC-subunits are localized in the cytoplasm, the nucleus and in punctuate structures (indicated by arrows). C, PP2AB-subunits are localized in the cytoplasm, the nucleus and in punctuate structures. D, PP2AB'-subunits are localized in the cytoplasm and the nucleus (PP2AB'alpha and PP2AB'beta), the cytoplasm and in punctuate structures (PP2AB'gamma and PP2AB'delta), the cytoplasm, nucleus and nucleolus (PP2AB'zeta) and the cytoplasm, nucleus, nucleolus, plasma membrane and punctuate structures (indicated by arrows; PP2AB'eta, PP2AB'theta, PP2AB'kappa). E, PP2AB''-subunits are localized in the cytoplasm and the nucleus, except of PP2AB''gamma, which was observed in the nucleus and in punctuate structures.

Supplemental Figure S7. Regulatory PP2AA-subunits interact with catalytic PP2AC-subunits in yeast-two-hybrid analyses. A to C, Yeast-two-hybrid analyses of (A) RCN1 with PP2AC1-C5, (B) PP2AA2 with PP2AC1-C5 and (C) PP2AA3 with PP2AC1-C5. Indicated combinations of pGAD.GH-PP2AA- and pGBT9.BS-PP2AC-subunits, empty plasmids and pGAD.GH-AKT1/pGBT9.BS-CIPK23 (Xu et al., 2006, positive control) were transformed into PJ69-4A. Decreasing ten-fold dilution series ($OD_{600\ nm}$ of 10^{0} - 10^{-4}), indicated by the black arrows, were spotted onto -LW control media and onto -LWH + 2.5 mM 3-AT media to select for positive interactions and incubated for the indicated time period at 28 °C. Note, that, depending on the experiment, PP2AC-subunits exhibited a slight transactivation, as observed by a weak growth on selective media when yeast was transformed with empty pGAD.GH- and pGBT9.BS-PP2AC plasmids. However, in every case the selective growth of yeast transformed with pGAD.GH-PP2AA and pGBT9.BS-PP2AC plasmids was stronger than the respective transactivation controls.

Supplemental Table S1. List of protein complex isolation experiments and treatments. 14 experiments were conducted on the indicated lines after treatments with either 200 mM sorbitol or 50 μM ABA for the indicated time period.

Supplemental Table S2. List of proteins identified by unique peptides and found only in *ost1-3*/OST1$_{(DA,\ \Delta C)}$-HF purifications. Potential OST1-interacting proteins, which were detected by unique peptides are displayed by their agi code, description, phosphorylation status (detected by MS/MS; 1, phosphorylated; 0, not phosphorylated), protein scores and experiment scores (shown in parentheses). Listed are proteins, which were only identified from *ost1-3*/OST1$_{(DA,\ \Delta C)}$-HF purifications and were not detected in the respective *ost1-3*/GFP-HF background controls. Proteins were designated as potential OST1-interacting proteins according to their protein and experiment score using the following cut-off: protein score ≥ 10 or experiment score ≥ 3. Scores were calculated from treatment specific- or from all purifications. Red labeled proteins were selected for further analyses and are listed in Table I and Supplemental Table S4.

Supplemental Table S3. List of proteins identified by any matching peptide and found only in *ost1-3*/OST1$_{(DA,\ \Delta C)}$-HF purifications. Potential OST1-interacting proteins, which were detected by any matching peptides are displayed by their agi code, description, phosphorylation status (detected by MS/MS; 1, phosphorylated; 0, not phosphorylated), protein scores and experiment scores (shown in parentheses). Listed are proteins, which were only identified from *ost1-3*/OST1$_{(DA,\ \Delta C)}$-HF purifications and were not detected in the respective *ost1-3*/GFP-HF background controls. Proteins were designated as potential OST1-interacting proteins according to their protein and experiment score using the following cut-off: protein score ≥ 10 or experiment score ≥ 3. Scores were calculated from treatment specific- or from all purifications. Red labeled proteins were selected for further analyses and are listed in Table I and Supplemental Table S4.

Supplemental Table S4. Summarized list of potential OST1-interacting proteins selected for further analyses (related to Table I). Given are the agi codes of the respective OST1-interacting proteins (OIPs) with information on the known or predicted biochemical functions, the phosphorylation status and protein and experiment scores (shown in parentheses). Scores were

calculated from ‘unique’ or ‘total’ protein matching peptides, which were identified in sorbitol or ABA treated experiments. The sum of scores from sorbitol and ABA treated experiments are also displayed. Protein scores were calculated as the sum of protein-matching peptides from $OST1_{(DA,\ \Delta C)}$-HF purification experiments minus the sum of protein-matching peptides from GFP-HF purification experiments. Experiment scores were calculated as count of $OST1_{(DA,\ \Delta C)}$-HF purification experiments in which the protein was identified minus the count of GFP-HF purification experiments in which the protein was identified. In addition to Table I, this table summarizes the subcellular localizations of fluorescent protein tagged OIPs and the subcellular localizations of the OST1 complexes with OIPs.

Supplemental Movie S1. 30 min time-laps movie of wilting detached rosettes. From left top to right bottom: wilting of detached rosettes of 29-day-old Col-0, *ost1-3*, *ost1-3*/GFP-HF, *ost1-3*/OST1-HF, *ost1-3*/$OST1_{DA}$-HF, *ost1-3*/$OST1_{SA}$-HF and *ost1-3*/$OST1_{\Delta C}$-HF recorded for a time period of 30 min with 0.5 min/picture frame. Note, that only *ost1-3*/OST1-HF wilts at slower rate similar to Col-0 wild type.

Table I. List of potential OST1-interacting proteins selected for further analyses. Displayed are the agi codes of the respective OST1-interacting proteins (OIPs) with information on phosphorylation status and protein and experiment scores (shown in parentheses). Scores were calculated from 'unique' or 'total' protein matching peptides, which were identified in sorbitol or ABA treated experiments. The sum of scores from sorbitol and ABA treated experiments are also displayed. Protein scores were calculated as the sum of protein-matching peptides from $OST1_{(DA,\ \Delta C)}$-HF purification experiments minus the sum of protein-matching peptides from GFP-HF purification experiments. Experiment scores were calculated as count of $OST1_{(DA,\ \Delta C)}$-HF purification experiments in which the protein was identified minus the count of GFP-HF purification experiments in which the protein was identified.

Agi	OIP	Phospho-rylated	Unique Score Sorbitol	Unique Score ABA	Sum Unique Score	Total Score Sorbitol	Total Score ABA	Sum Total Score
AT4G33950.1	OST1	yes	971 (4)	917 (4)	1888 (8)	3671 (1)	2856 (3)	6527 (4)
AT4G23920.1	UGE2	no	16 (4)	11 (4)	27 (8)	23 (4)	19 (4)	42 (8)
AT3G44690.1	OIP1	no	26 (4)	57 (2)	83 (6)	26 (4)	57 (2)	83 (6)
AT3G03530.1	NPC4	no	24 (4)	53 (2)	77 (6)	34 (4)	57 (2)	91 (6)
AT3G09880.1	PP2AB'beta	no	12 (4)	15 (2)	27 (6)	19 (4)	23 (2)	42 (6)
AT5G14720.1	OIP4	no	4 (1)	31 (4)	35 (5)	4 (1)	31 (4)	35 (5)
AT3G09980.1	OIP6	no	3 (1)	16 (4)	19 (5)	3 (1)	17 (4)	20 (5)
AT5G66880.1	SnRK2.3	no (yes)	5 (2)	5 (3)	10 (5)	2609 (1)	1872 (3)	4481 (4)
AT1G78290.2	SnRK2.8	no	3 (2)	7 (3)	10 (5)	126 (4)	81 (4)	207 (8)
AT4G24800.1	ECIP1	yes	4 (2)	7 (3)	11 (5)	4 (2)	7 (3)	11 (5)
AT2G46610.1	RS31a	no	7 (1)	21 (3)	28 (4)	7 (1)	21 (3)	28 (4)
AT3G06510.2	SFR2	no	-	16 (4)	16 (4)	-	16 (4)	16 (4)
AT5G03470.1	PP2AB'alpha	no	5 (2)	8 (2)	13 (4)	5 (2)	8 (2)	13 (4)
AT1G08050.1	OIP20	yes	-	29 (3)	29 (3)	-	29 (3)	29 (3)
AT1G13320.1	PP2AA3	no	2 (1)	9 (2)	11 (3)	4 (3)	10 (1)	14 (4)
AT1G70770.1	OIP26	yes	-	8 (3)	8 (3)	-	8 (3)	8 (3)
AT3G50500.2	SnRK2.2	no (yes)	4 (2)	1 (1)	5 (3)	2508 (1)	1809 (3)	4317 (4)
AT1G59830.1	PP2AC1	no	2 (1)	2 (1)	4 (2)	5 (2)	4 (1)	9 (3)
AT3G25800.1	PP2AA2	no	1 (1)	0 (0)	1 (1)	5 (3)	6 (0)	11 (3)
AT3G26030.1	PP2AB'delta	no	-	-	-	6 (3)	5 (3)	11 (6)
AT1G10430.1	PP2AC2	no	-	-	-	3 (2)	2 (1)	5 (3)

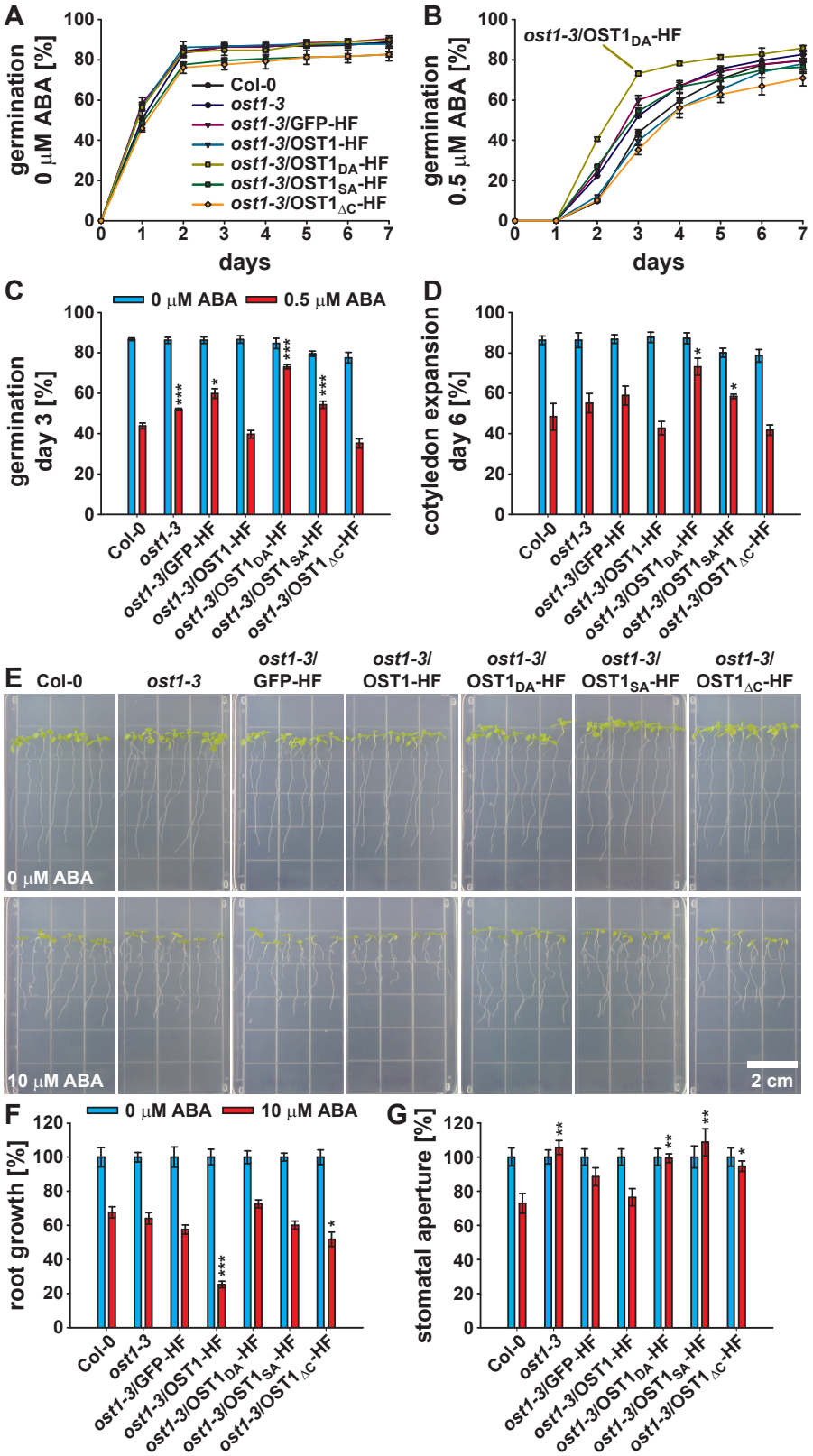
A
germination 0 μM ABA [%]
days
Col-0
ost1-3
ost1-3/GFP-HF
ost1-3/OST1-HF
ost1-3/OST1DA-HF
ost1-3/OST1SA-HF
ost1-3/OST1ΔC-HF
B
germination 0.5 μM ABA [%]
ost1-3/OST1DA-HF
days
C
0 μM ABA
0.5 μM ABA
germination day 3 [%]
D
cotyledon expansion day 6 [%]
E
Col-0
ost1-3
ost1-3/ GFP-HF
ost1-3/ OST1-HF
ost1-3/ OST1DA-HF
ost1-3/ OST1SA-HF
ost1-3/ OST1ΔC-HF
0 μM ABA
10 μM ABA
2 cm
F
0 μM ABA
10 μM ABA
root growth [%]
G
stomatal aperture [%]

Figure 1.

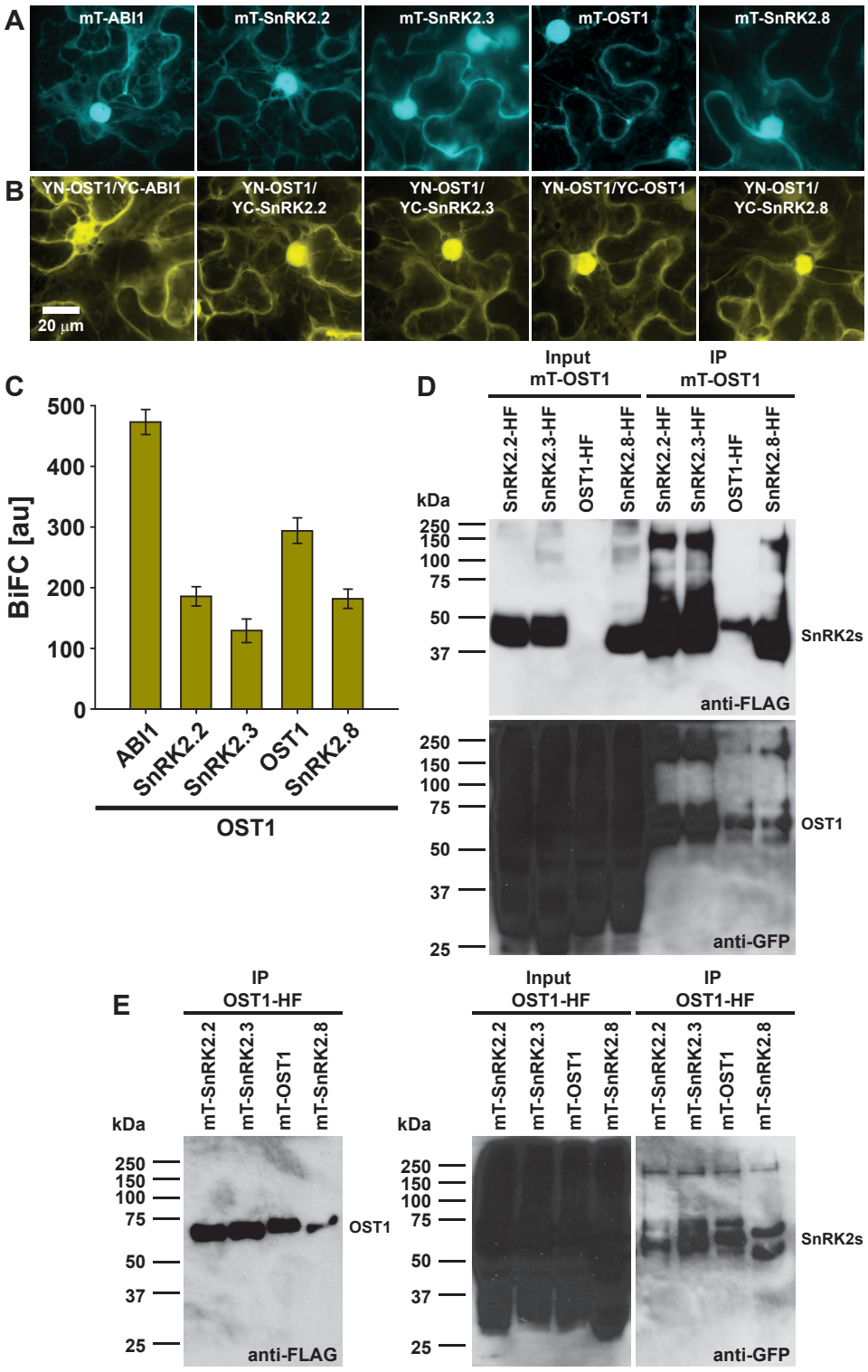
A
mT-ABI1
mT-SnRK2.2
mT-SnRK2.3
mT-OST1
mT-SnRK2.8
B
YN-OST1/YC-ABI1
YN-OST1/
YC-SnRK2.2
YN-OST1/
YC-SnRK2.3
YN-OST1/YC-OST1
YN-OST1/
YC-SnRK2.8
20 μm
C
BiFC [au]
500
400
300
200
100
0
ABI1
SnRK2.2
SnRK2.3
OST1
SnRK2.8
OST1
D
Input
mT-OST1
IP
mT-OST1
SnRK2.2-HF
SnRK2.3-HF
OST1-HF
SnRK2.8-HF
kDa
250
150
100
75
50
37
SnRK2s
anti-FLAG
250
150
100
75
50
37
25
OST1
anti-GFP
E
IP
OST1-HF
mT-SnRK2.2
mT-SnRK2.3
mT-OST1
mT-SnRK2.8
kDa
250
150
100
75
50
37
25
OST1
anti-FLAG
Input
OST1-HF
IP
OST1-HF
SnRK2s
anti-GFP

Figure 2.

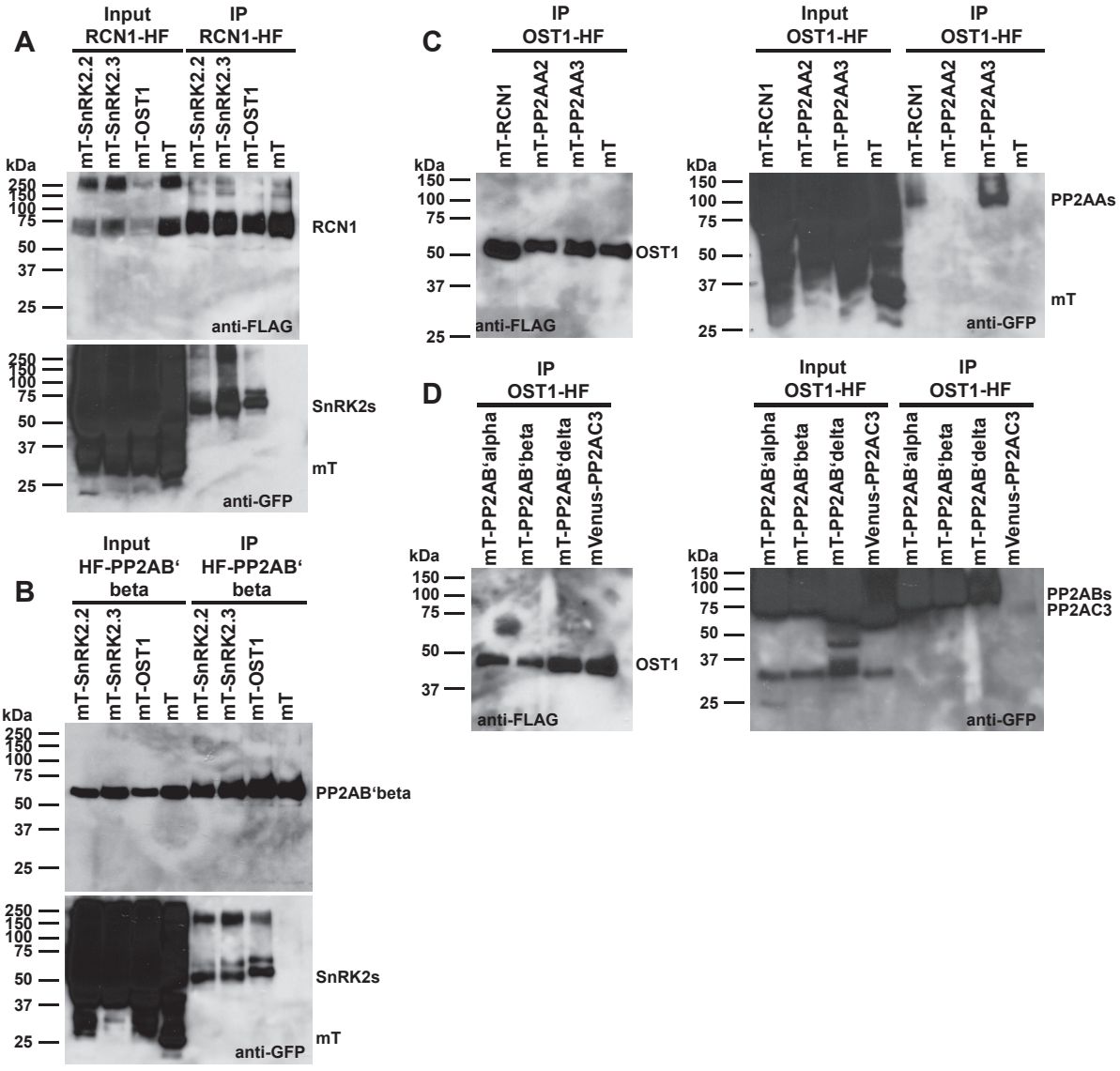
A
Input
RCN1-HF
IP
RCN1-HF
mT-SnRK2.2
mT-SnRK2.3
mT-OST1
mT
kDa
250
150
100
75
50
37
25
RCN1
anti-FLAG
SnRK2s
mT
anti-GFP
B
Input
HF-PP2AB‘
beta
IP
HF-PP2AB‘
beta
PP2AB‘beta
C
IP
OST1-HF
mT-RCN1
mT-PP2AA2
mT-PP2AA3
OST1
PP2AAs
D
mT-PP2AB‘alpha
mT-PP2AB‘beta
mT-PP2AB‘delta
mVenus-PP2AC3
PP2ABs
PP2AC3

Figure 3.

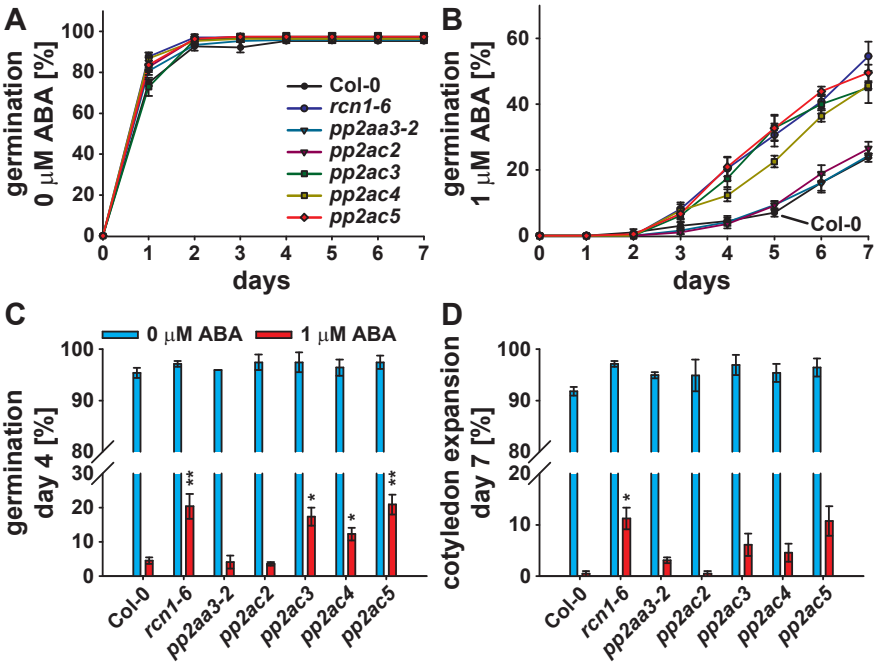
A
germination 0 μM ABA [%]
days
Col-0
rcn1-6
pp2aa3-2
pp2ac2
pp2ac3
pp2ac4
pp2ac5
B
germination 1 μM ABA [%]
days
Col-0
C
0 μM ABA
1 μM ABA
germination day 4 [%]
D
cotyledon expansion day 7 [%]

Figure 4.

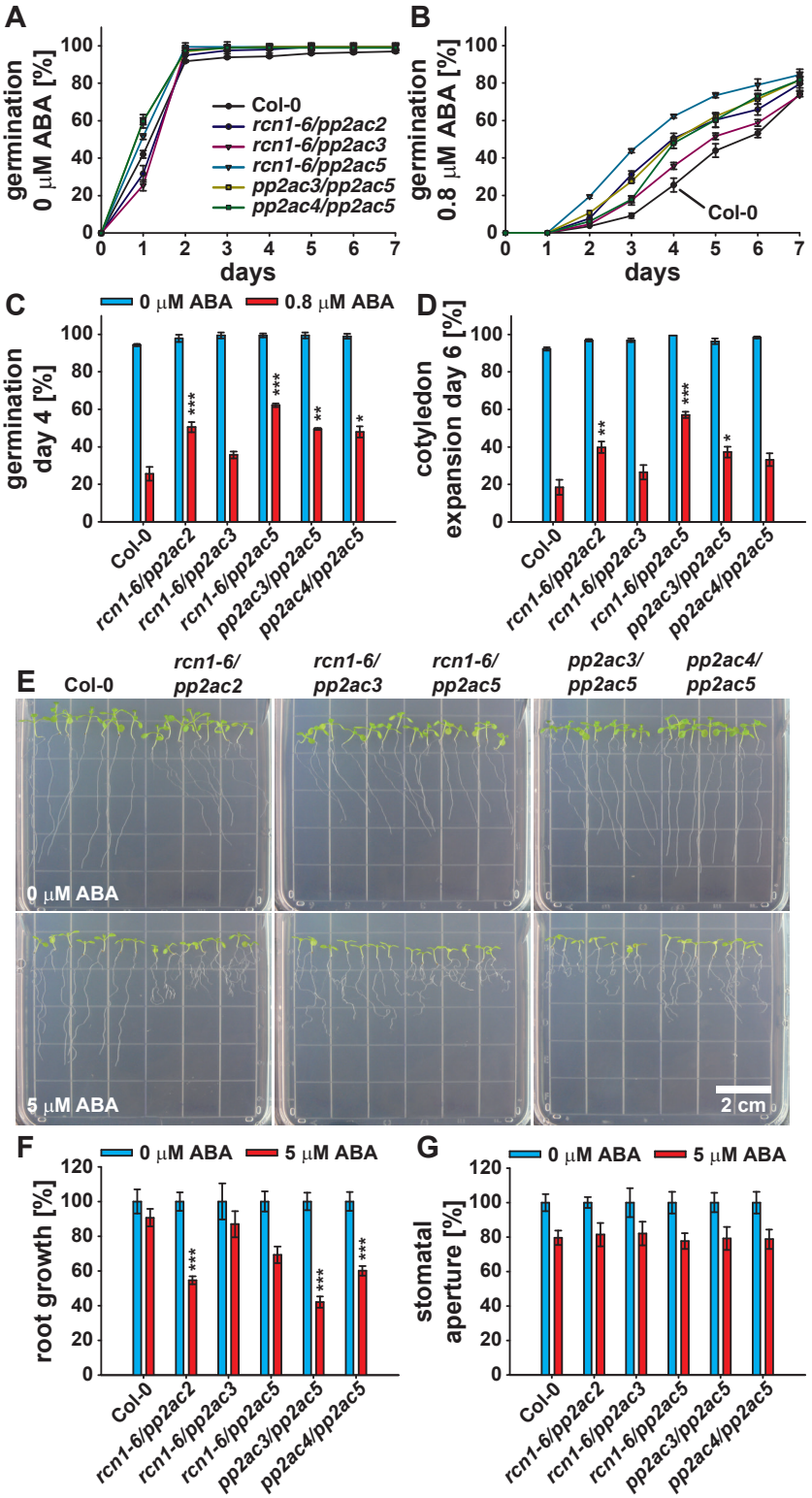
A
germination 0 μM ABA [%]
days
Col-0
rcn1-6/pp2ac2
rcn1-6/pp2ac3
rcn1-6/pp2ac5
pp2ac3/pp2ac5
pp2ac4/pp2ac5
B
germination 0.8 μM ABA [%]
days
Col-0
C
0 μM ABA
0.8 μM ABA
germination day 4 [%]
D
cotyledon expansion day 6 [%]
E
Col-0
rcn1-6/ pp2ac2
rcn1-6/ pp2ac3
rcn1-6/ pp2ac5
pp2ac3/ pp2ac5
pp2ac4/ pp2ac5
0 μM ABA
5 μM ABA
2 cm
F
0 μM ABA
5 μM ABA
root growth [%]
G
0 μM ABA
5 μM ABA
stomatal aperture [%]

Figure 5.

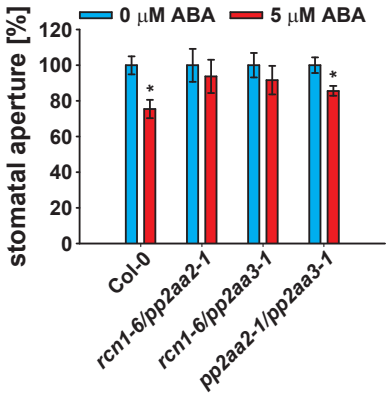
0 μM ABA
5 μM ABA
stomatal aperture [%]
120
100
80
60
40
20
0
*
*
Col-0
rcn1-6/pp2aa2-1
rcn1-6/pp2aa3-1
pp2aa2-1/pp2aa3-1

Figure 6.

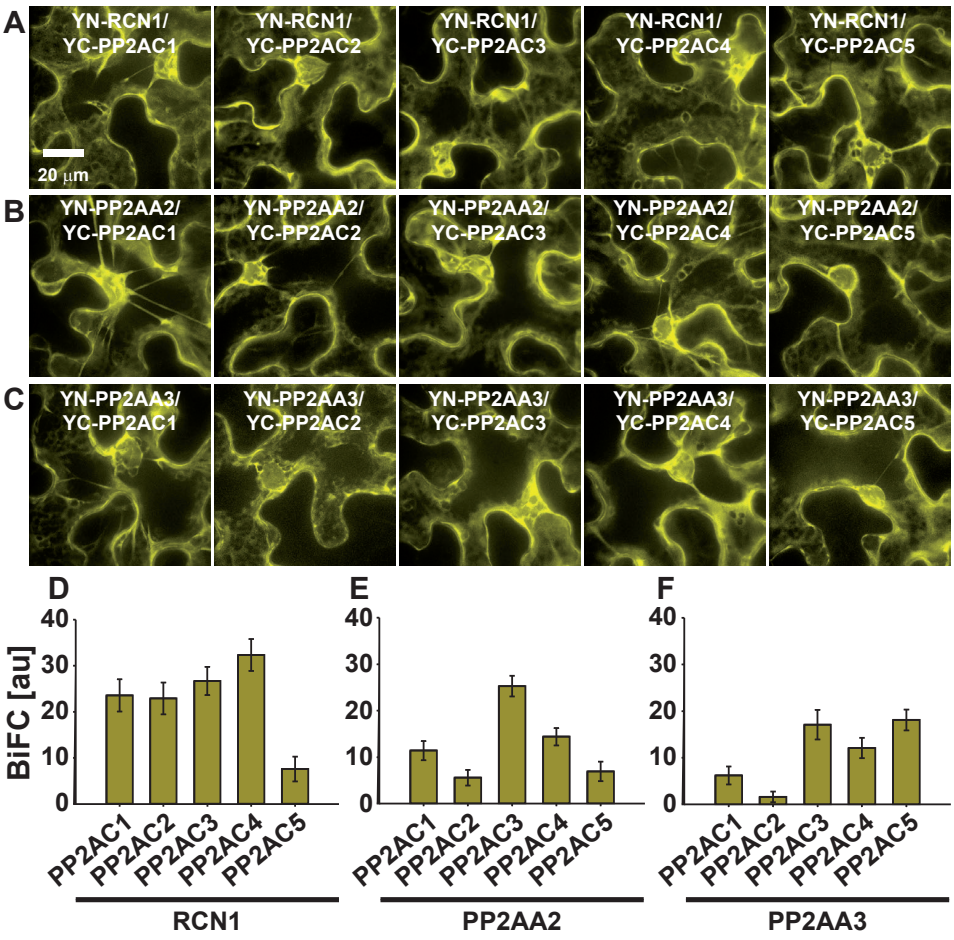
A
YN-RCN1/
YC-PP2AC1
YN-RCN1/
YC-PP2AC2
YN-RCN1/
YC-PP2AC3
YN-RCN1/
YC-PP2AC4
YN-RCN1/
YC-PP2AC5
20 μm
B
YN-PP2AA2/
YC-PP2AC1
YN-PP2AA2/
YC-PP2AC2
YN-PP2AA2/
YC-PP2AC3
YN-PP2AA2/
YC-PP2AC4
YN-PP2AA2/
YC-PP2AC5
C
YN-PP2AA3/
YC-PP2AC1
YN-PP2AA3/
YC-PP2AC2
YN-PP2AA3/
YC-PP2AC3
YN-PP2AA3/
YC-PP2AC4
YN-PP2AA3/
YC-PP2AC5
D
E
F
BiFC [au]
40
30
20
10
0
PP2AC1
PP2AC2
PP2AC3
PP2AC4
PP2AC5
RCN1
PP2AA2
PP2AA3

Figure 7.

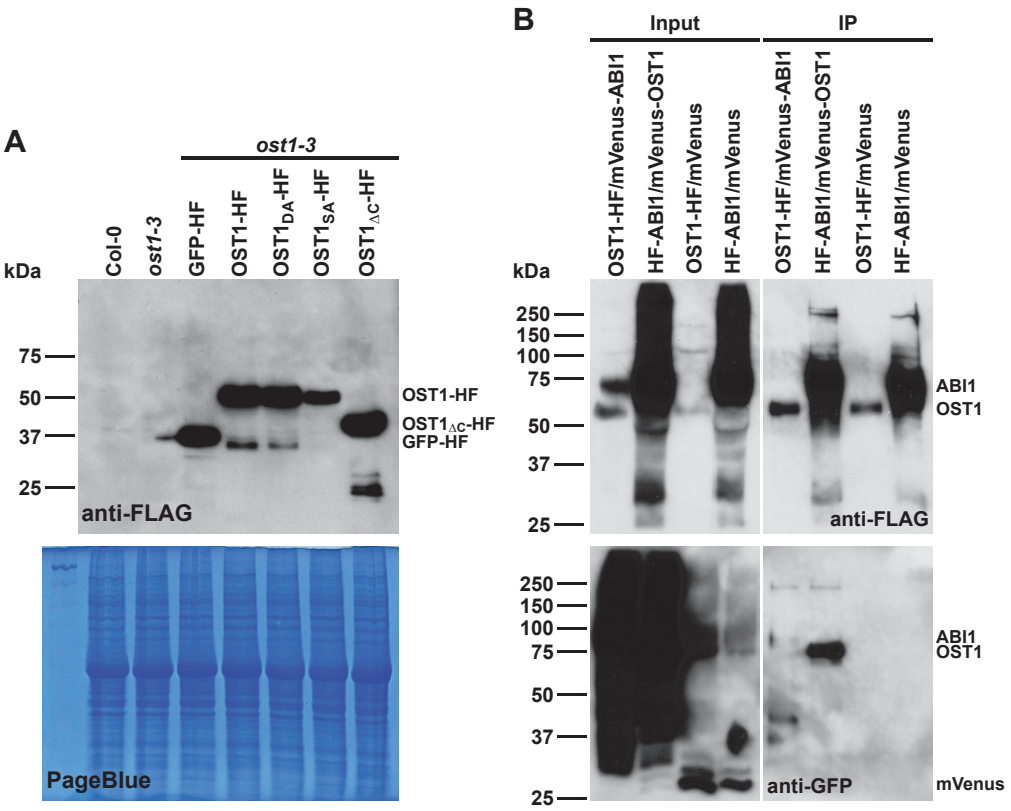

Supplemental Figure S1.

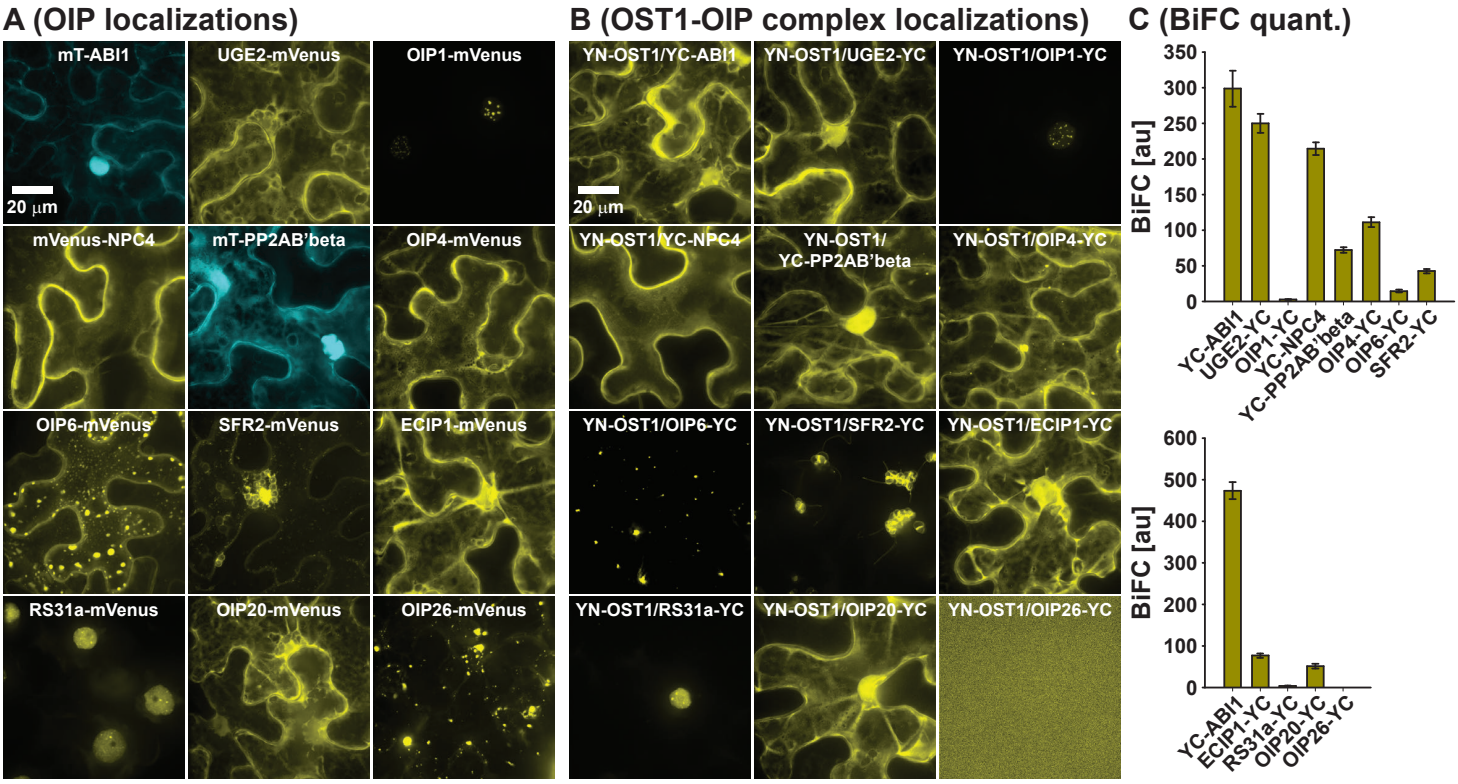

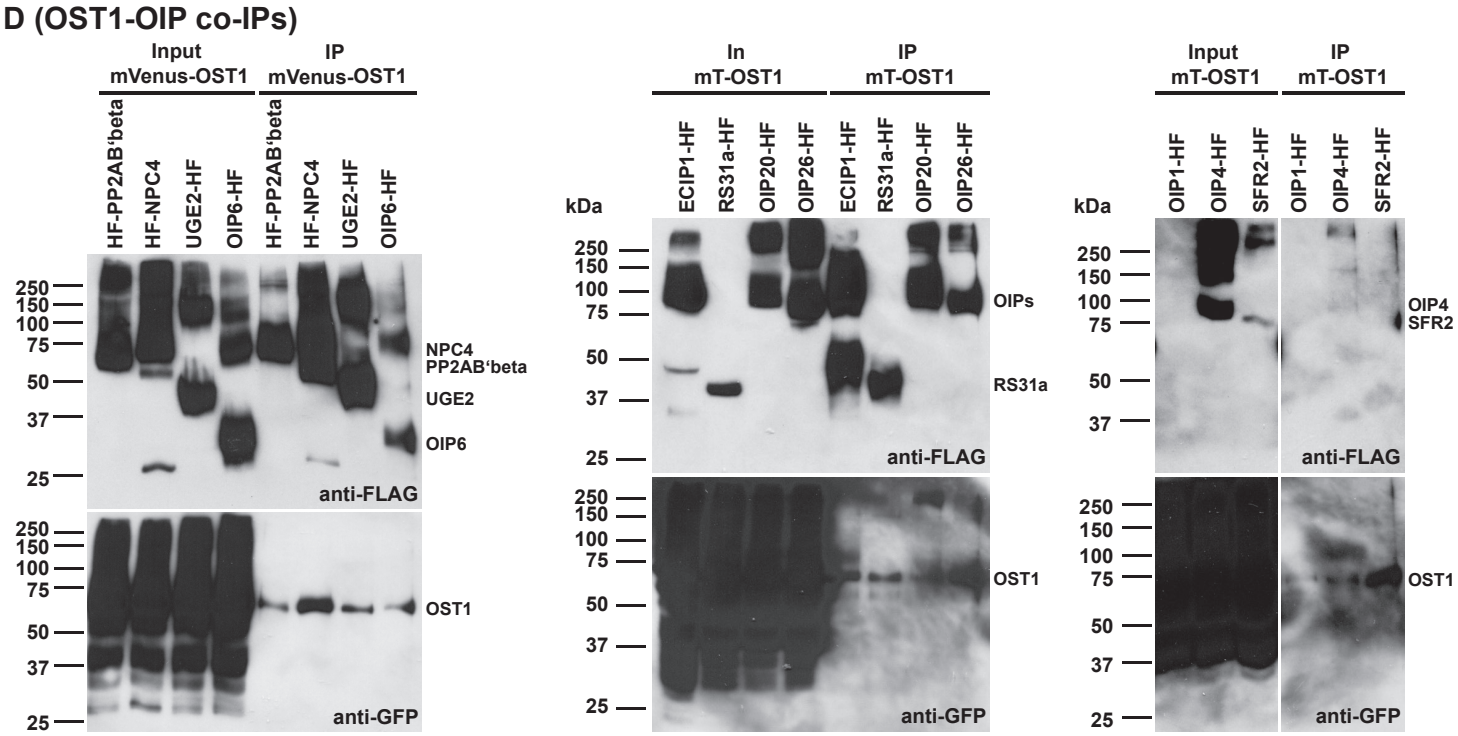

Supplemental Figure S2.

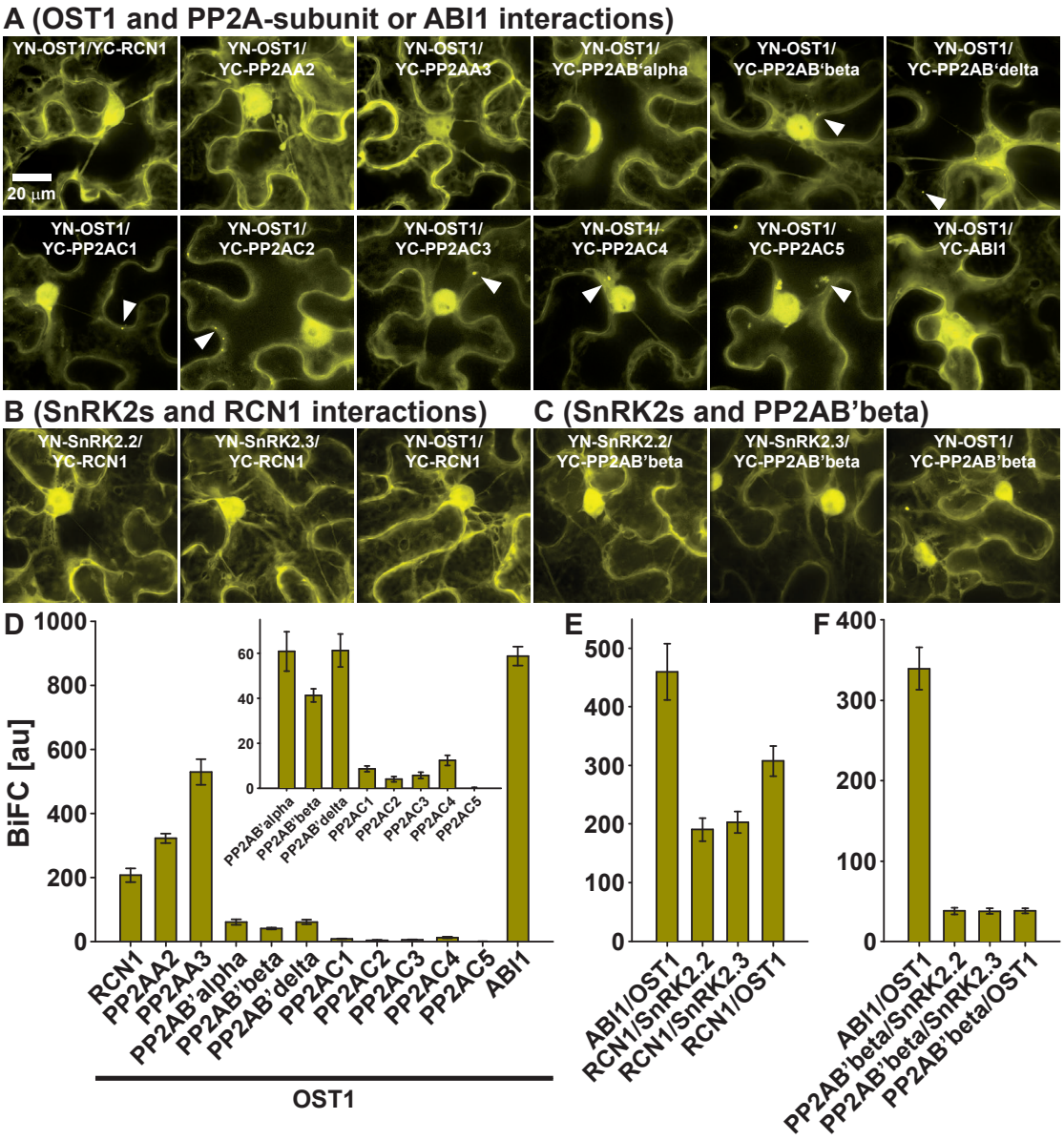

Supplemental Figure S3.

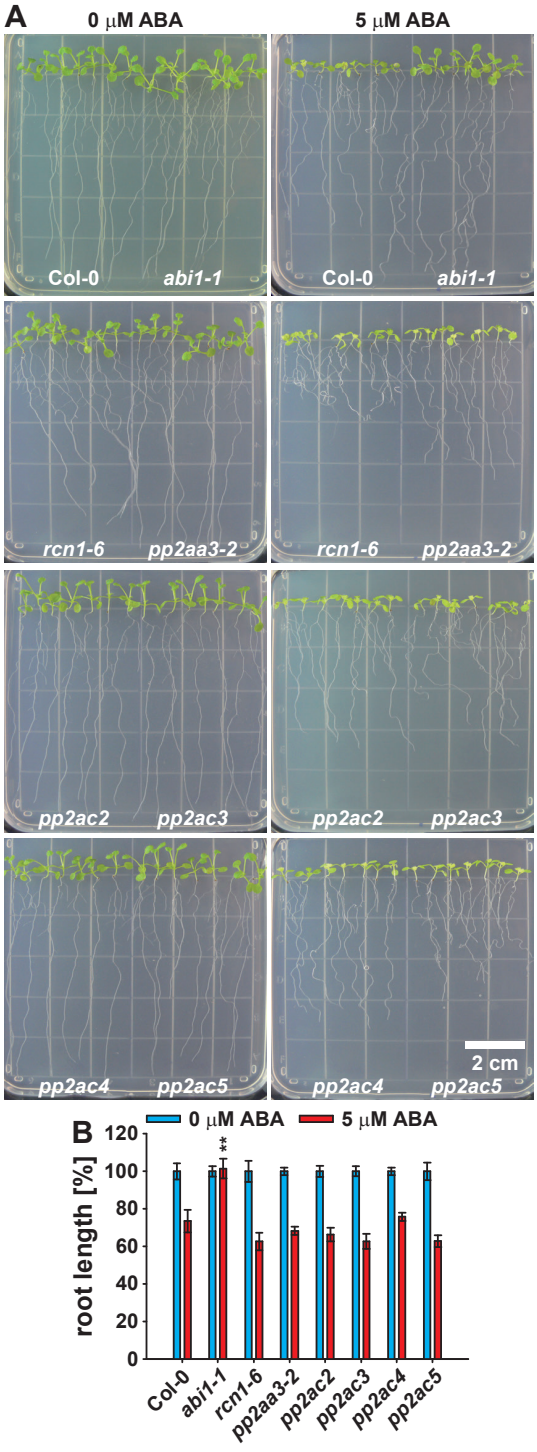

Supplemental Figure S4.

Supplemental Figure S5.

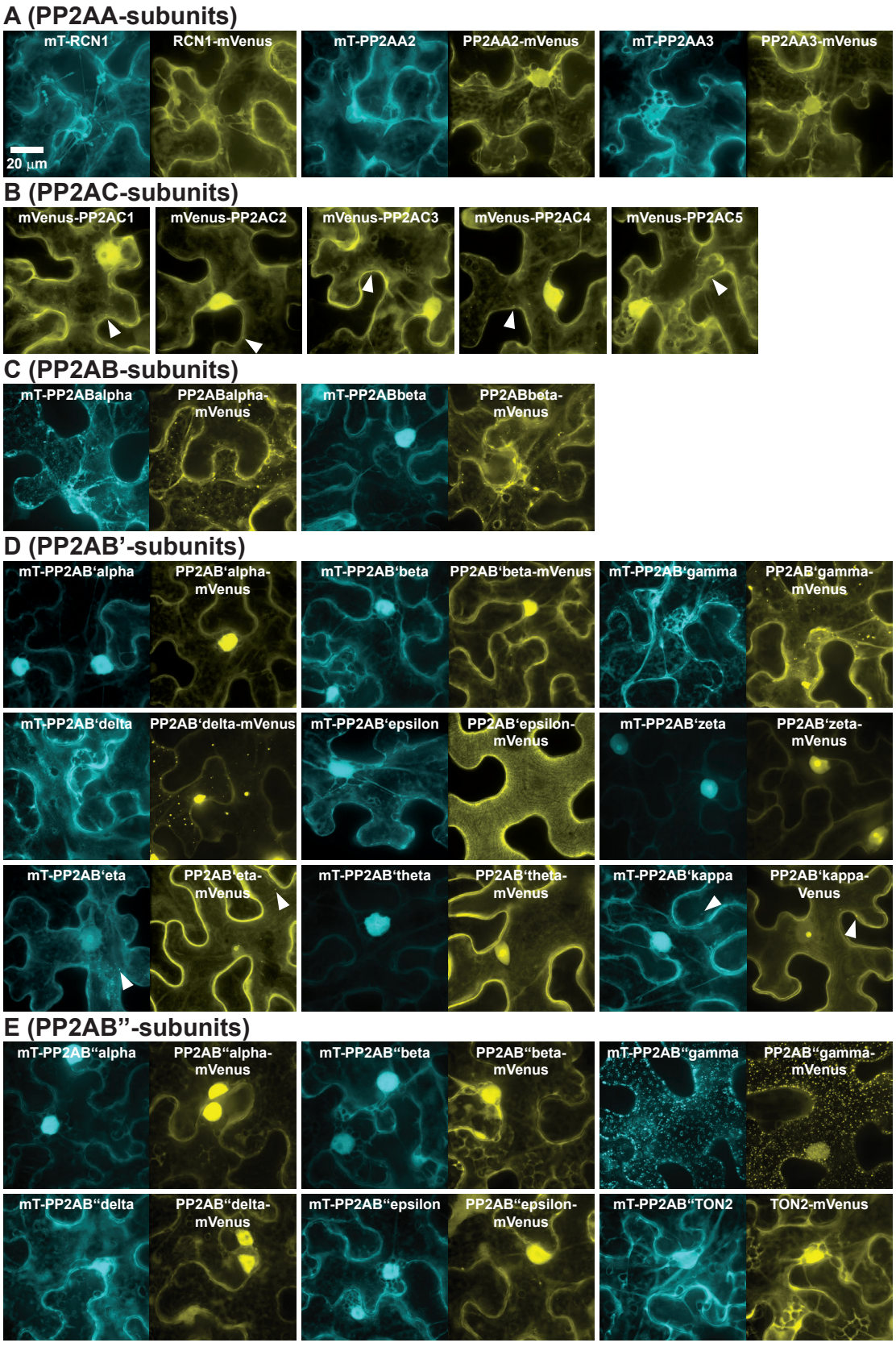

Supplemental Figure S6.

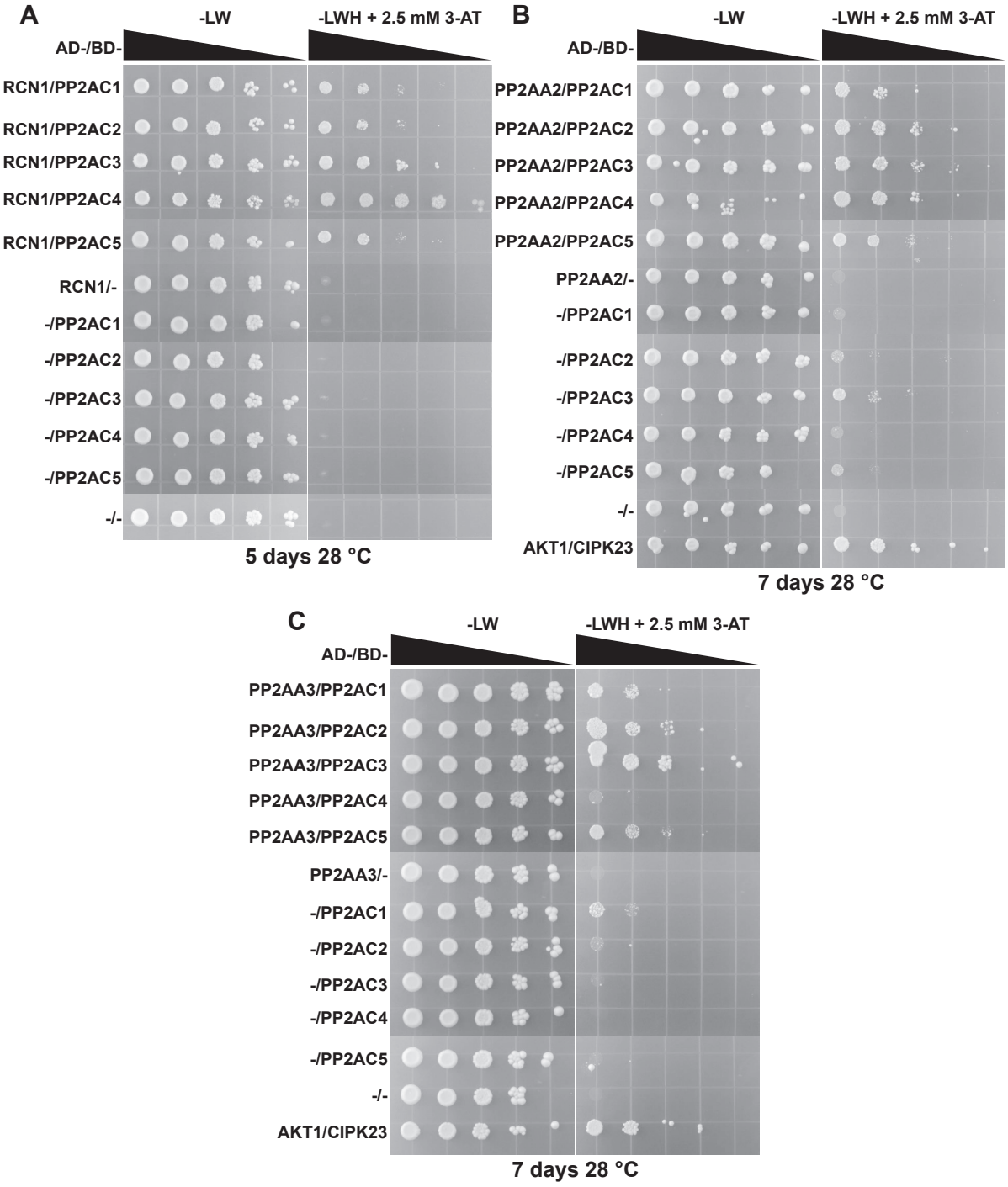

Supplemental Figure S7.